Journal of Research of the National Bureau of Standards Vol. 47, No. 5, November 1951 Research Paper 2259

Mass Spectra of Some Organo-Lead and Organo-Mercury Compounds

Vernon H. Dibeler and Fred L. Mohler

Mass spectra of tetramethyl and tetraethyl lead and of dimethyl, diethyl, and di-*n*-butyl mercury were obtained with a Consolidated 21–102 mass spectrometer. Monoisotopic spectra were calculated by using the isotopic abundance derived from each spectrum. A variation in the lead isotope abundance was observed in the commercially available lead alkyls. No variation was observed among the mercury alkyls and good agreement was obtained with previously published measurements on mercury vapor. There was no indication of voltage discrimination. The mass spectra of the lead alkyls are qualitatively similar. The principal portion of the total ionization is contributed by the dissociation of one and three alkyl groups. Ions resulting from the dissociation of one or more hydrogen atoms are small, as are the hydrocarbon ions. Hydrides and hydrocarbon ions resulting from intramolecular rearrangement were observed. The principal part of total ionization in the mercury alkyl spectra was contributed by hydrocarbon ions. Hydrides and other rearrangement peaks were observed. A preliminary experiment on a leaded gasoline, using a model 21–103 spectrometer, indicated that sensitivity is sufficient to analyze for a few hundredths of a mole percent of tetraethyl lead with a precision of about 2 percent of the value.

1. Introduction

In recent years hydrocarbons have been an important subject of fundamental and applied research [1][1] in mass spectrometry, as well as the principal subject of the systematic accumulation of mass spectral data [2]. It is surprising, however, that very little has been reported on the mass spectra of organometallic compounds in spite of the interesting properties and commercial importance of some of these materials.

The volatile alkyl compounds of many of the elements, including zinc, germanium, tin, and lead were used by Aston [3] in his early studies of the isotopic constitution of the elements. No details of the mass spectra were reported, but it was subsequently shown by various investigators that corrections as to the identity and abundance of the isotopes so obtained were necessary because of the presence of hydrides in the mass spectra.

More recently, Hipple and Stevenson [4] studied the ionization by electron impact of methyl and ethyl radicals formed in the mass spectrometer by the thermal decomposition of tetramethyl and tetraethyl lead. They did not report the complete mass spectra of the undecomposed molecules but observed that in both cases the molecule ion abundance was almost immeasurably small. A rough measurement using 15-v electrons and an ion source at about room temperature showed the trimethyl lead ion to be about 50 times as abundant as the tetramethyl lead ion. No similar measurement was given for tetraethyl lead.

There have been a number of mass spectrometric studies of the isotopic abundance of lead obtained from various natural and commercial sources. Nier [5] has demonstrated a wide variation in the isotopic abundance of leads obtained from virgin ores. Lead obtained from commercial sources, sometimes called "common lead", may be expected to show much less variation than the natural ores because it is a mixture from many sources. However, one would not expect isotopic ratios to be accurately constant in compounds made at different times or in different places. Recent investigators have measured lead isotopes by using inorganic lead halides, which preclude the formation of hydrides but present technical difficulties not encountered in the use of the relatively volatile alkyl compounds.

Isotopic analyses of mercury have usually been made by using the vapor of the element [6, 7]. Experimental difficulties again result from the low vapor pressure of the element and from the possibility of amalgamation with interior parts of the mass spectrometer. No measurable variation in the natural abundance of the mercury isotopes has been reported.

It is the purpose of this paper to give a complete description of the mass spectra of several related organometallic compounds and to demonstrate the applicability of these molecules to isotopic analysis. A discussion is also given concerning the dissociation processes of these molecules.

2. Experimental Details

Mass spectra were obtained by using a Consolidated 21–102 mass spectrometer with the resolving power increased to about 1-in 350. Liquid samples were introduced by means of a micropipet through a porous glass disk covered with liquid gallium. The pressure of the expanded vapors was measured with a micromanometer [8]. Spectra were obtained by varying the ion accelerating voltage. Each complete spectrum required two magnetic field settings: 0.535 amp for the mass range 12 to 90, and 1.320 amp for the mass range 48 to 350. The correlation

[1] Figures in brackets indicate the literature references at the end of this paper.

of the two mass ranges was made by the comparison of peak heights in the overlapping mass range.

The preliminary test of the analysis of a leaded gasoline of known composition [2] was made after the above instrument was modified to a model 21–103. The total pressure of the sample introduced was measured with the micromamometer. The partial pressure of the lead tetraethyl was calculated from the observed ion current of the $Pb(C_2H_5)^+$ ion and the previously measured sensitivity (ion current per unit of pressure) of this ion.

The tetramethyl and tetraethyl lead were obtained from the Ethyl Corp. Portions of the liquid samples were removed from the shipping containers and vacuum distilled without rectification into Pyrex ampoules, sealed in vacuum and protected from light until used. The tetramethyl lead (sample number 133.7–XP–3) was received sometime in 1947 and was considered to be of high purity. An estimated 0.1 mole percent of tetramethyl tin was the only impurity observed. The tetraethyl lead was received about the same time. Total impurities were estimated less than 2 mole percent and ascribed principally to ethyl chloride.

Dimethyl, diethyl, and di-*n*-butyl mercury were obtained from the Eastman Kodak Co. These were stored in vacuum in the same manner as the lead compounds. They were not as pure as the lead compounds and contained unknown small amounts of oxygenated molecules, alkyl halides, and possibly hydrocarbons. Impurities with vapor pressures considerably different from that of the alkyl mercury compounds were removed in the process of distilling the samples into the storage ampoules.

3. Results

Table 1 gives the principal part of the polyisotopic spectrum of tetramethyl lead for 70-v electrons. The contributions of ions containing C^{13} atoms have been subtracted. The abundances of the ions are relative to the most abundant ion of mass 253. Doubly charged ions appearing at masses 118, 118.5, 119, 125.5, 126, and 126.5 are omitted from the table. Their abundance was 0.1 percent or less of the maximum peak. One metastable transition peak was observed with an apparent mass of 196.6 and a relative abundance of 0.22 percent. It was attributed to the delayed dissociation: $(253^+) \rightarrow (223^+)+30$. The sensitivity of the 253 peak—attributed to the $Pb^{208}C_3H_9^+$ ion—was about 0.7 times the sensitivity of the 43 peak of *n*-butane under similar conditions.

TABLE 1. *Polyisotopic spectrum of tetramethyl lead for 70-v electrons*

m/e	Relative intensities	m/e	Relative intensities
12	0.32	230	0.02
13	.75	231	.09
14	2.59	232	.09
15	12.2	233	.17
16	0.25	234	.66
		235	.35
204	1.65	236	13.1
205	0.15	237	10.6
206	33.2	238	24.9
207	28.5	239	0.25
208	66.2		
209	5.73	248	.03
		249	2.56
216	0.03	250	0.50
217	.08	251	52.4
218	.62	252	41.2
219	3.98	253	100.0
220	5.13	254	0.31
221	49.6		
222	40.3	266	.10
223	85.3	267	.08
224	0.40	268	.21

[2] Sample obtained from the Bureau's Engine Fuel Section.

In order to compare the relative probabilities of the various dissociation processes in tetramethyl lead, it is first necessary to calculate the monoisotopic spectrum. This is possible if the relative abundances of the lead isotopes are known. For reasons that will be apparent in the following pages the isotopic abundances must be computed from the same mass spectrum. From the spectrum in the mass range 204 to 209 (table 1) it is obvious that hydride ions are present in addition to the atom ions. An approximation of the hydride abundance is given by the ratio 209/208; namely, 5.73/66.2=0.087. No dihydride was observed, and it is estimated that the ratio PbH_2^+/Pb^+ is less than 0.002. Therefore, the approximate monohydride contribution to mass 208 is calculated from the 207 peak as $28.5\times0.087=2.2$. Thus the more accurate PbH^+/Pb^+ ratio is given by 5.73/64.0=0.090. Using this ratio, the hydride contributions were calculated and subtracted from the 207 and 208 peaks. The mole percentages of the Pb^{204}, Pb^{206}, Pb^{207}, and Pb^{208} ions were computed. The first row of table 2 gives the mean values thus obtained for tetramethyl lead from four independent spectra. The mean deviation expressed in this and following tables is merely an indication of the reproducibility of the data. The estimated accuracy is 1 percent of the value for the principal isotopes and 5 percent for the rare isotope. Also included in table 2 are the isotopic abundance values for "common" lead reported by White and Cameron [9] and the extreme abundance values for lead ores reported by Nier [5].

The mean values for the isotopic abundance observed in tetramethyl lead were used in computing the monoisotopic spectrum, starting at the heavy-mass end of each ion group, by computing the contribution of each isotopic ion to the total ion peaks as illustrated by table 3. Columns 1 and 2 repeat

TABLE 2. *Mole percentage of lead isotopes*

Mass	204	206	207	208
$Pb(CH_3)_4$	1.31	26.79	20.55	51.35
Mean deviation	±.02	±.04	±.04	±.08
$Pb(C_2H_5)_4$	1.36	25.42	21.11	52.10
Mean deviation	±.01	±.05	±.02	±.03
White and Cameron [9]; $PbCl_2$, "common lead"	1.37	25.15	21.11	52.38
Nier [5]; PbI_2, Galena, Ivigtut, Greenland	1.55	22.51	22.60	53.34
Galena, Joplin, Mo	1.23	27.52	19.81	51.43

the $Pb(CH_3)^+$ portion of the polyisotopic spectrum given in table 1. The ion at mass 224 is entirely the result of $HPb^{208}CH_3^+$ ions. The abundance of this ion (0.40) times the relative abundances of the lead isotopes (obtained from table 2) gives the contributions of the isotopic ions[3] listed in column 3, table 3. The calculated contribution of the $HPb^{207}CH_3^+$ ion (0.16) subtracted from the observed 223 peak (85.3) gives the abundance of the $Pb^{208}CH_3^+$ ion (85.14). Again the relative abundance values of the lead isotopes are used to calculate the contributions of the isotopic $PbCH_3^+$ ions listed in column 4. Similarly, the contributions of the $PbCH_2^+$, $PbCH^+$, and PbC^+ ions are obtained and listed in the columns indicated. In this case, there are four checks on the accuracy of the calculation at masses 216, 217, 218, and 219. Column 8 shows the differences between the sums of the computed contributions and the observed abundances of these four peaks. The agreement is entirely satisfactory, since errors are cumulative and some deviations are expected on the small peaks.

TABLE 3. *Calculation of the* $Pb(CH_3)^+$ *portion of the monoisotopic spectrum of tetramethyl lead for 70-v electrons*

m/e	"poly" spectrum	$PbCH_4$	$PbCH_3$	$PbCH_2$	PbCH	PbC	Δ
216	0.03	.....	.....	.....	.....	0.02	0.01
217	.08	.....	.....	.....	0.07	.....	.01
218	.62	.....	.....	0.15	.....	.45	.02
219	3.98	.....	2.17	.....	1.45	.35	.01
220	5.13	0.01	.....	3.14	1.11	.87	.....
221	49.6	.....	44.42	2.41	2.71	.....	.....
222	40.3	.21	34.07	6.02	.....	.....	.....
223	85.3	.16	85.14	.....	.....	.....	.....
224	.40	.40	.....	.....	.....	.....	.....
Total ionization		0.78	165.80	11.72	5.40	1.69	.....

The total ionization of the isotopic ions is given at the bottom of the appropriate columns. Similar calculations were made for the Pb^+, the $Pb(CH_3)_2^+$ and the $Pb(CH_3)_3^+$ regions (the small peaks in the $Pb(CH_3)_4^+$ region were summed directly.) The summation values were normalized relative to the most abundant ion, $Pb(CH_3)_3^+$. These values appear in columns 2 and 5 of table 4. The abundance of the hydrocarbon ions was also normalized relative to the $Pb(CH_3)_3^+$ ion and is included in this table. Similar calculations on data obtained with 50-v electrons differed only in that the ratio $PbH^+/Pb^+ = 0.094$ was used to compute the abundance of the lead isotopes.

In tetraethyl lead, the ratio PbH^+/Pb^+ was 0.88 and 0.95, respectively, for 70- and 50-v electrons as determined from the polyisotopic spectra. No dihydride was observed, and it is estimated that the ratio PbH_2^+/Pb^+ was less than 0.002. The mean mole percentages of the lead isotopes determined for tetraethyl lead are given in the second row of table 2. The monoisotopic spectrum for 70-v electrons calculated as described above appears in columns 3 and 6 of table 4. Twelve small peaks of doubtful origin in the mass range 69 to 101 have been omitted. These were all considerably less than 1 percent of the maximum peak.

[3] "Isotopic ions" are defined as ions identical in specie and number of constituent atoms but differing in the isotopic weight of one or more of the constituent atoms.

TABLE 4. *Monoisotopic spectra of tetramethyl and tetraethyl lead for 70-v electrons*

Ion	Relative intensities		Ion	Relative intensities	
	$Pb(CH_3)_4$	$Pb(C_2H_5)_4$		$Pb(CH_3)_4$	$Pb(C_2H_5)_4$
C	0.16	0.04	PbC	0.87	0.03
CH	.39	.05	PbCH	2.78	.22
CH_2	1.33	.14	$PbCH_2$	6.03	.62
CH_3	6.27	.27	$PbCH_3$	85.3	.18
CH_4	.13	.02	$PbCH_4$	.37	.....
C_2	.....	.03	PbC_2	.03	.03
C_2H	.....	.09	PbC_2H	.14	.55
C_2H_2	.09	.97	PbC_2H_2	.05	1.69
C_2H_3	.24	3.95	PbC_2H_3	.....	.38
C_2H_4	.15	1.13	PbC_2H_4	.55	100.0
C_2H_5	.09	2.44	PbC_2H_5	24.8	.62
C_2H_6	.....	.05	PbC_2H_6	.25	.....
C_3H_2	.....	.03	PbC_2H_7	.....	.38
C_3H_3	.....	.16	PbC_3H_3	1.07	.....
C_3H_4	.....	.03	PbC_3H_4	100.0	.....
C_3H_5	.....	.54	PbC_3H_{10}	.33	.....
C_3H_6	.....	.16			
C_3H_7	.....	.50	PbC_4H_3	.....	.22
			PbC_4H_{10}	.....	14.3
C_4H_3	.....	.03	PbC_4H_{11}	.....	3.12
C_4H_5	.....	.05	PbC_4H_{12}	.20	.....
C_4H_7	.....	.11			
C_4H_8	.....	.14	PbC_5H_{11}	.....	.14
C_4H_9	.....	.73	PbC_5H_{15}	.....	71.8
C_4H_{10}	.....	.04	PbC_5H_{16}	.....	.51
Pb	64.0	44.8	PbC_6H_{19}	.....	.10
PbH	5.74	39.7	PbC_7H_{20}	.....	.27

In the tetramethyl lead, the ratio PbH^+/Pb^+ was 0.88 and 0.95, respectively, for 70- and 50-v electrons as determined from the polyisotopic spectra. No dihydride was observed, and it is estimated that the ratio PbH_2^+/Pb^+ was less than 0.002. The mean mole percentages of the lead isotopes determined for tetramethyl lead are given in the second row of table 2. The monoisotopic spectrum for 70-v electrons calculated as described above appears in columns 3 and 6 of table 4. Twelve small peaks of doubtful origin in the mass range 69 to 101 have been omitted. These were all considerably less than 1 percent of the maximum peak.

Three peaks due to metastable transitions were also omitted. These were observed to have apparent masses of 190.4, 211.2, and 239.9 with abundances of 0.21, 0.20, and 0.25 percent, respectively, of the maximum peak. They were ascribed to the transitions $(295^+) \rightarrow (266^+) + 29$, $(266^+) \rightarrow (237^+) + 29$, and $(295^+) \rightarrow (237^+) + 58$. No doubly charged ions were observed. The sensitivity of the maximum peak relative to the *n*-butane maximum peak was 1.26 at 50 v.

Monoisotopic spectra of dimethyl, diethyl, and di-*n*-butyl mercury were calculated from the polyisotopic spectra by the method used for the lead compounds. Monohydrides of the atom ions were observed in each case, and a dihydride was apparent in diethylmercury. The ratio HgH^+/Hg^+ was 0.117, 0.215, and 0.04, respectively, for the methyl, ethyl, and butyl compounds at 70 v. The ratio was 0.118, 0.225, and 0.04 for 50-v electrons. In diethyl mercury the dihydride ratio HgH_2^+/Hg^+ was 0.01 for both 50- and 70-v, and was estimated to be less than 0.003 for the other two compounds. Using the appropriate ratios, the mole percentages of the mercury isotopes were calculated as before. The mean values and the mean deviations for each of the compounds are given in table 5. The isotopic abundance of mercury reported by Hibbs [6] and by Nier [7] are included for comparison.

In the computation of the monoisotopic spectra of the mercury alkyls, larger errors appeared in the mercury-hydrocarbon portion of the spectrum than appeared in the case of the lead alkyls. This was

TABLE 5. *Mole percentage of mercury isotopes*

	Mass	196	198	199	200	201	202	204
$Hg(CH_3)_2$		0.17	10.05	16.88	23.12	13.12	29.78	6.87
Mean deviation		±.01	±.02	±.03	±.04	±.02	±.06	±.04
$Hg(C_2H_5)_2$		.18	10.05	16.86	23.19	13.05	29.79	6.91
Mean deviation		±.0	±.08	±.02	±.09	±.08	±.09	±.05
$Hg(n\text{-}C_4H_9)_2$		.16	10.04	16.86	23.06	13.15	29.86	6.89
Mean deviation		±.04	±.07	±.03	±.08	±.07	±.01	±.05
Hibbs [6]; Hg vapor		.16	10.02	16.92	23.10	13.22	29.72	6.84
Nier [7]; Hg vapor		.146	10.02	16.84	23.13	13.22	29.80	6.85

undoubtedly the result of the increase in the number of isotopes, and the fact that a major portion of the total ionization in the mercury alkyls was contributed by hydrocarbon ions. For the latter reason, four additional runs were made on dimethyl mercury at pressures up to three times the normal operating pressure of the mass spectrometer. The HgH^+/Hg^+ ratio was unchanged, and no dihydride was observed. The isotopic abundance ratios were within the average deviations given for dimethyl mercury in table 5.

The major portions of the monoisotopic spectra of the three mercury alkyls are given in table 6 for 70-v electrons. The ion intensities are relative to the most abundant ion containing mercury since this is a more convenient basis for comparison. A number of peaks due to double ionization, metastable transition, and rearrangement are omitted from the table. Some of these are described below.

No metastable transitions were observed in dimethyl mercury. The only doubly charged ions, Hg^{++}, were less than 0.5 percent of the $HgCH_3^+$ peak.

TABLE 6.—*Portions of the monoisotopic spectra of dimethyl, diethyl and di-n-butylmercury for 70-v electrons*

Ion	Relative intensities			Ion	Relative intensities		
	Hg $(CH_3)_2$	Hg $(C_2H_5)_2$	Hg $(C_4H_9)_2$		Hg $(CH_3)_2$	Hg $(C_2H_5)_2$	Hg $(C_4H_9)_2$
C	2.90	0.4	1.2	C_3H_{10}			5.4
CH	5.11	.6	1.6	C_3H_{11}			11
CH_2	22.9	3.2	5.7	C_3H_{12}			2.0
CH_3	110	4.3	25				
CH_4		.08	.6	C_4H_{13}			14
C_2	.09	.2	.3	C_4H_{17}			.1
C_2H	.36	.3	2.1	C_4H_{18}			2.3
C_2H_2	3.93	23	32				
C_2H_3	14.3	113	215	Hg	41.8	68	100
C_2H_4	6.19	44	126	HgH	4.80	14	5.1
C_2H_5	7.36	380	415	HgH_2		.7	
C_2H_6	.20		1.4				
C_3			.6	HgC	2.81		
C_3H		.4	4.7	HgCH	5.93	.5	1.5
C_3H_2		.6	10	$HgCH_2$	13.7	6.2	3.4
C_3H_3		2.5	107	$HgCH_3$	100.0	2.8	.8
C_3H_4		.2	14	$HgCH_4$	.44		
C_3H_5		4.7	401				
C_3H_6		.7	41	HgC_2H_4		13	18
C_3H_7		9.2	166	HgC_2H_5	1.36	100	13
				HgC_2H_6	40.2	12	
C_4			.5	HgC_4H_9		1.5	9.7
C_4H		.08	2.8	HgC_4H_{10}		83	1.7
C_4H_2		.2	11				
C_4H_3		.2	11	HgC_4H_{12}			1.8
C_4H_4		.08	3.6	HgC_4H_{14}			3.4
C_4H_5		.2	15				
C_4H_6		.08	5.4	HgC_4H_{17}			2.4
C_4H_7		.4	47	HgC_4H_{18}			51
C_4H_8		.3	121				
C_4H_9		.4	616				
C_4H_{10}		3.1					

The sensitivity of the CH_3^+ ion relative to the sensitivity of the *n*-butane 43 peak was 1.1 at 70 v.

In diethyl mercury the one metastable transition resulted in an ion with an apparent mass of 25.1 and an abundance of 0.3 percent relative to the $HgC_2H_5^+$ peak. The sensitivity of the $C_2H_5^+$ ion relative to the 43 peak of *n*-butane was 1.9 at 70 v.

Three metastable transition peaks were observed in dibutyl mercury with apparent masses of 37.1, 29.5, and 25.1 and respective percentage abundances of 0.4, 1.4, and 0.4 relative to the Hg^+ ion. These were attributed to the transitions: $(41^+)\rightarrow(39^+)+2$, $(57^+)\rightarrow(41^+)+16$, and $(29^+)\rightarrow(27^+)+2$. Doubly charged ions, $C_4H_9^{+\,+}$, $C_4H_8^{+\,+}$, and Hg^{++} were observed with the respective percentage abundances 1.2, 0.2, and 2.9 relative to the Hg^+ ion. The sensitivity of the $C_4H_9^+$ ion was of the order of 10 times the sensitivity of the 43 peak in *n*-butane.

4. Discussion

4.1. Isotope Assay

The precision of the isotope abundance measurements of lead using the tetramethyl and tetraethyl compounds is indicated by the mean deviation given in table 2. An uncertainty of 1 percent in the mole percentages of the principal isotopes and 5 percent in the rare isotope is principally the result of errors in the recording system. The small residuals in the calculations illustrated by table 3 indicate a high order of accuracy in the correction for hydrides and the computation of the isotopic abundance.

The abundances obtained using the tetraethyl lead are in good agreement with the values reported by White and Cameron for "common" lead chloride. The abundance values obtained for the tetramethyl compound differ from the values for tetraethyl lead by an amount greater than the uncertainty in the two measurements. They are more nearly in agreement with the values reported by Nier for lead obtained from galena of Joplin, Mo. Differences like this are to be expected, as commercial lead will usually be a mixture of leads from many sources but sometimes lead from one source will predominate.

Both the tetramethyl and the tetraethyl lead appear to be suitable compounds for the isotopic assay of the element. [4] The higher vapor pressure of the tetramethyl lead is an advantage in the speedy removal of samples from the reservoir. Unlike the inorganic lead halides, conventional precautions for pumping out the lead alkyls are all that is required to prevent memory effects. Inlet systems without lubricated stopcocks are expected to be superior in this respect to the sample handling system used in this research.

The precision of the isotopic abundance measurements of mercury using dimethyl, diethyl, and dibutyl mercury is indicated by the mean deviations given in table 5. The estimated uncertainty in the abundance of the principal isotopes is 1 percent of the value. The uncertainty in the rare isotope is

[4] After this paper was written, Collins, Freeman, and Wilson [12] reported the use of lead tetramethyl for mass spectrometric analyses in the isotopic lead method for the determination of geological ages.

about 10 percent of the value. The agreement between the values obtained by using the mercury alkyls is very good, and they agree well with values obtained by Hibbs and by Nier, using mercury vapor. The consistency of the results for three very different molecules shows that the correction for the contributions of the hydride ions can be made with precision. It also shows that in these measurements made with different instruments and techniques there is no evidence of instrumental selectivity for ions of different mass. As our measurements were made by electrostatic scanning, any selectivity would tend to make the heavier isotope peak too small. Hibbs used magnetic scanning, which is not subject to this effect, whereas Nier calibrated for discriminative effects with carefully made synthetic isotope mixtures of A^{36} and A^{40}.

Schaeffer [10] has recently published data showing large discrimination effects in a 60° mass spectrometer when the isotopes of krypton were measured using electrostatic scanning. The present results with mercury confirm previous evidence that in the 180° Consolidated mass spectrometer this discrimination is negligible for most isotope measurements. Berry [11] has also demonstrated this to be the case over a wide range of ion-accelerating voltage when the ions are formed with little kinetic energy.

4.2. Dissociation Probabilities

The mass spectrum of tetramethyl lead is like that of 2,2-dimethylpropane [2] in several respects. The relative abundance of the molecule ion is small, and the most probable dissociation is the loss of one methyl group. However, the large abundance of the Pb^+ ion (fortunate from the standpoint of isotopic assay) illustrates a marked difference resulting from the substitution of a heavy metal atom for the central carbon atom of the hydrocarbon.

The ratio $Pb(CH_3)_3^+/Pb(CH_3)_4^+$ observed in this research is about ten times that reported by Hipple and Stevenson [4]. This is to be expected, however, since the ion source used by Hipple and Stevenson operated at nearly room temperature compared to the operating temperature of 285°C for the source used in this study.

The relative probabilities of dissociating one and three methyl groups are nearly equal, whereas the probability of dissociating two methyl groups is much smaller. Ion peaks resulting from the dissociation of one or more hydrogen atoms from the lead-methyl groups are small, as are the hydrocarbon peaks. This results in a comparatively simple spectrum, with the $Pb(CH_3)_3^+$ and the $Pb(CH_3)^+$ ions being the principal contributors to the total ionization.

The ions PbH, $HPbCH_3$, $HPb(CH_3)_2$, and $HPb(CH_3)_3$ involve a rearrangement of H atoms in the ionization process. The very small hydrocarbon peaks containing two carbon atoms also involve a rearrangement of two methyl groups in the ionization process. The relative intensities of the latter ions indicate that they are not the result of a hydrocarbon impurity.

Except for the low abundance of the molecule ion, which is almost always associated with this type of symmetry, the mass spectrum of tetraethyl lead is quite unlike that of its carbon analog, 3,3-diethylpentane [2]. It is, however, qualitatively similar to the tetramethly lead spectrum. The relative probabilities of dissociating one and three ethyl groups is reversed, the latter being the more probable in the tetraethyl compound. As in tetramethyl lead, a relatively simple spectrum is obtained with the $Pb(C_2H_5)^+$ and the $Pb(C_2H_5)_3^+$ ions contributing the major portion of the total ionization. The abundance of fragment ions involving dissociation of hydrogen atoms or methyl radicals is relatively small.

As in tetramethyl lead we find fragment ions containing one additional H atom. These are PbH $HPbC_2H_5$, $HPb(C_2H_5)_2$, and $HPb(C_2H_5)_3$; and the first and third are much more abundant than the analogous ions in the tetramethyl spectrum. The presence of hydrocarbon ions containing three and four carbon atoms indicates a rearrangement of ethyl radicals in the ionization process analogous to the formation of C_2 ions from methyl radicals in the tetramethyl spectrum. However, unidentified trace impurities may contribute to these peaks.

The mass spectra of the three mercury alkyls are significantly different from the lead alkyls in several respects. A large fraction of the total ionization in each case is contributed by the hydrocarbon ions, the maximum peaks in each case being the hydrocarbon ions, CH_3^+, $C_2H_5^+$, or $C_4H_9^+$. Also, the abundance of the molecule ions is of the same order of magnitude as that of the base peak. This is a distinct difference between the mercury and the lead compounds.

As in the lead alkyls, monohydrides of the metal ions were observed. A dihydride, HgH_2^+ was observed in the case of diethylmercury only. A number of spectra of dimethyl-mercury obtained over a range of pressures up to three times the normal operating pressure of the mass spectrometer showed that the ratio HgH^+/Hg^+ was constant. This is evidence that the metal hydride is formed by intramolecular rearrangement rather than by recombination. The abundance of the hydrides in the mercury-alkyl portions of the spectra was less accurately measured but also appeared to be constant over the pressure range. Identification of some of these ions is uncertain, particularly in the dibutyl mercury because of the low relative abundance of the mercury alkyl groups. The low abundance of $HgC_4H_9^+$ in the dibutyl spectrum is unexpected, for in this respect it is unlike the other two compounds.

In addition to the hydrides, hydrocarbon peaks involving rearrangements are observed in all three spectra. As in the lead compounds, methyl, ethyl, and butyl radicals apparently rearrange to form C_2, C_4, and C_8 hydrocarbons, respectively. However, identification is uncertain because of the small size of the peaks and the possible contributions of suspected hydrocarbon impurities.

4.3. Chemical Analysis

The sensitivity of the most abundant ions in tetramethyl lead and tetraethyl lead is of the same order of magnitude as the sensitivity of the most abundant ion in most hydrocarbons. A commercial gasoline commonly contains a few hundredths of a mole percent of tetraethyl lead. Consequently, the peaks corresponding to the $PbC_2H_5^+$ ion will be a few hundredths of a percent of the maximum hydrocarbon peak. The 21–102 Consolidated mass spectrometer has a sensitivity of about 0.01 percent of the maximum peak, and this is scarcely adequate for quantitative measurements. The new 21–103 instrument, however, has about 10 times this sensitivity. A preliminary test with a 21–103 instrument on a gasoline containing 2.5 ml of tetraethyl lead per gallon, or about 0.045 mole percent, gave $PbC_2H_5^+$ peaks that could be measured with a precision of about 2 percent. Further investigation of this point is under way in this laboratory. Instruments made by the General Electric Co. and by the Metropolitan Vickers Co. have comparable sensitivity and are probably of equal value for such analyses.

5. References

[1] Mass spectrometry, a review by J. A. Hipple and M. Shepherd, Anal. Chem. **21,** 32 (1949).
[2] API Tables of Mass Spectral Data (Carnegie Institute of Technology, Pittsburgh, Pa., 1948).
[3] F. W. Aston, Mass spectra and isotopes, 2d ed. (Longmans, Green and Co., New York, N. Y.).
[4] J. A. Hipple and D. P. Stevenson, Phys. Rev. **63,** 121 (1943).
[5] A. O. Nier, R. W. Thompson, and B. F. Murphey, Phys. Rev. **60,** 112 (1941).
[6] R. F. Hibbs, USAEC unclassified report Y–472.
[7] A. O. Nier, Phys. Rev. **79,** 450 (1950).
[8] V. H. Dibeler and F. Cordero, J. Research NBS **46,** 1 (1951) RP2167.
[9] J. R. White and A. E. Cameron, Phys. Rev. **74,** 991 (1948).
[10] A. O. Schaeffer, J. Chem. Phys. **18,** 1681L (1950).
[11] C. E. Berry, Phys. Rev. **78,** 597 (1950).
[12] C. B. Collins, J. R. Freeman, and J. T. Wilson, Phys. Rev. **82,** 966 (1951).

Washington, May 3, 1951

Journal of Research of the National Bureau of Standards Vol. 47, No. 5, November 1951 Research Paper 2260

Resolution of the Dissociation Constants of *d*-Tartaric Acid from 0° to 50° C*

Roger G. Bates and Richard G. Canham

The ratio of the first thermodynamic dissociation constant, K_1, of tartaric acid to the second, K_2, is only 20 to 23 at temperatures between 0° and 50° C. The two dissociative steps therefore overlap to a considerable extent. The greater the amount of overlapping, the more difficult it is to resolve the two equilibria and to determine each individual dissociation constant.

Electromotive-force measurements of the cell

$$\mathrm{Pt;\ H_2\ (g,\ 1\ atm),}\ d\text{-tartrate solution, Cl}^-\text{, AgCl; Ag}$$

were made at intervals of five degrees from 0° to 50° C. Thirty-two tartrate solutions were studied. All but 5 of the 22 solutions of series 1 were composed of sodium hydrogen tartrate, sodium tartrate, and sodium chloride in the molar proportions 1:3:1. The other 17 contained sodium hydrogen tartrate, sodium tartrate, and potassium chloride in the molar proportions 1:1.3411:0.5853. The 10 solutions of series 2 were 1:1 mixtures of sodium hydrogen tartrate and sodium chloride.

The calculation of the second dissociation constant by the conventional method requires not only a knowledge of the concentration of hydrogen ion but also that of the free tartaric acid formed as a result of the overlapping. Neither can ordinarily be evaluated exactly from the emf. However, the 1:3 buffer ratio of series 1 reduced the hydrogen-ion concentration and at the same time lowered the ratio of the concentrations of tartaric acid and hydrogen tartrate ion to about 0.03. Hence, an adequate correction for the amount of acid could be made with an approximate value of the first dissociation constant. However, it is impossible to lower the K_2 correction for the determination of K_1 without increasing the hydrogen-ion concentration. Accordingly, a method developed earlier, utilizing emf data for solutions of the acid salt (series 2), was employed. Thus the hydrogen-ion concentration was kept relatively low, and the emf became a function of the product of K_1 and K_2 rather than substantially independent of K_2.

The two dissociation constants of tartaric acid from 0° to 50° C are given by the equations

$$-\log K_1 = 1525.59/T - 6.6558 + 0.015336T$$

and

$$-\log K_2 = 1765.35/T - 7.3015 + 0.019276T,$$

where T is the temperature in degrees K. The standard thermodynamic quantities for the two dissociation steps were calculated.

1. Introduction

Although tartaric acid and its salts have been widely used as constituents of buffer solutions for the regulation of acidity [1, 2],[1] little accurate information on the strengths of the two acidic groups as a function of temperature is available. This neglect is due, in part at least, to the complex composition of solutions containing these substances. The ratio of the first thermodynamic dissociation constant, K_1, of tartaric acid to the second, K_2, is only 20 to 23 at temperatures between 0° and 50° C. Hence, the two dissociative steps "overlap" to such an extent that appreciable amounts of molecular tartaric acid and both the primary and secondary tartrate ions exist simultaneously in tartrate buffer solutions. The concentrations of all three tartrate species must be established in order to calculate accurate values of either constant.

The second dissociation constant was calculated from data for the electromotive force of cells of the type

$$\mathrm{Pt;\ H_2\ (g,\ 1\ atm),}\ d\text{-tartrate solution, Cl}^-\text{, AgCl; Ag}$$

by what can be termed the conventional method [3, 4, 5]. All but five of the 22 solutions of series 1 were composed of sodium hydrogen *d*-tartrate, sodium *d*-tartrate, and sodium chloride in the molar proportions 1:3:1. The rest of the solutions of series 1 contained sodium hydrogen *d*-tartrate, sodium *d*-tartrate, and potassium chloride in the proportions 1:1.3411:0.5853. The computation of $\log K_2$ from the data for these 22 buffer solutions requires, in addition to the stoichiometric molalities of the three components, a knowledge of the concentration of hydrogen ion and also that of the molecular tartaric acid formed as a result of overlapping of the dissociative steps. Neither of these quantities can ordinarily be evaluated exactly from the emf. However, the 1:3 buffer ratio of most of the solutions of series 1 kept the hydrogen-ion concentration reasonably low and at the same time reduced the ratio of the concentrations of tartaric

* Presented before the Twelfth International Congress of Pure and Applied Chemistry at New York City (Sept. 11, 1951).

[1] Figures in brackets indicate the literature references at the end of this paper.

acid and hydrogen tartrate ion to about 0.03. Hence, an adequate correction for the amount of tartaric acid present could be made with an approximate value of the first dissociation constant.

Unfortunately, a similar application of the conventional method to the determination of the first dissociation constant is not as successful. Any attempt to minimize the concentration of bivalent tartrate ion inevitably increases the concentration of hydrogen ion. Thus the advantage gained on the one hand is offset by a parallel disadvantage on the other. In order to facilitate the separation of the constants for overlapping equilibria, the senior author suggested in 1948 [6] the use of emf data for cells containing aqueous mixtures of the acid salt, in this case sodium hydrogen tartrate, with a soluble chloride. The relationship between the electromotive force of the cell and the product of the two overlapping constants was developed. Together with the data of experiments such as series 1 designed for the determination of K_2, it is possible to obtain consistent values of K_1K_2 by a short series of approximations. Thus, no attempt is made to minimize both the K_2 correction and the hydrogen-ion concentration. Instead, the latter is kept fairly low in all of the solutions, and the emf of the cells from which K_1 is determined becomes a function of the product of K_1 and K_2 rather than substantially independent of K_2, a condition the conventional method seeks to achieve. On the other hand, experimental errors in the measurement of the emf have twice as large an effect upon the final value of K_1 determined in this way as upon that determined by the conventional method. Nevertheless, this new approach is of particular advantage when the primary object is to determine K_2 and when economy of time and effort is a factor. Further measurements by the conventional method serve to establish K_1 accurately once the value of K_2 has been fixed.

The 10 solutions of series 2 were 1:1 mixtures of sodium hydrogen tartrate and sodium chloride. By analysis of the data for series 1 and 2, apparent values of log K_2 and 1/2 log K_1K_2 at intervals of 5 deg from 0° to 50° C were calculated. The true thermodynamic dissociation constants were obtained by extrapolation of the apparent values to infinite dilution. The second dissociation constant and its temperature coefficient were used to compute the changes of free energy, heat content, entropy, and heat capacity for the dissociation of hydrogen tartrate ion in the standard state from 10° to 40° C. These quantities were also computed for the first dissociation step at 25° C.

2. Experimental Procedures and Results

Each cell contained two hydrogen electrodes and two silver–silver-chloride electrodes. At least two values of the emf, E, were therefore obtained for each

TABLE 1. pwH *of tartrate-chloride solutions from 0° to 50° C*

m_{NaHTar}	Temperature, °C										
	0	5	10	15	20	25	30	35	40	45	50
	Series 1a. NaHTar:Na_2Tar:NaCl=1:3:1										
0.05200	4.6184	4.5961	4.5765	4.5621	4.5513	4.5416	4.5367	4.5343	4.5375	4.5403	4.5464
.04983	4.6218	4.5991	4.5795	4.5649	4.5528	4.5461	4.5403	4.5392	4.5397	4.5449	4.5503
.04502	4.6277	4.6030	4.5812	4.5676	4.5501	4.5514	4.5436	4.5408	4.5456	4.5520	4.5588
.04161	4.6327	4.6101	4.5915	4.5771	4.5662	4.5581	4.5533	4.5527	4.5537	4.5585	4.5640
.03976	4.6367	4.6144	4.5955	4.5809	4.5695	4.5637	4.5561	4.5564	4.5569	4.5619	4.5664
.03903	4.6417	4.6195	4.6013	4.5874	4.5763	4.5671	4.5642	4.5629	4.5641	4.5683	4.5740
.03103	4.6491	4.6294	4.6120	4.5983	4.5875	4.5762	4.5746	4.5739	4.5735	4.5792	4.5879
.03010	4.6546	4.6331	4.6143	4.6004	4.5895	4.5834	4.5776	4.5773	4.5787	4.5844	4.5910
.02986	4.6548	4.6323	4.6138	4.5997	4.5878	4.5819	4.5758	4.5735	4.5751	4.5822	4.5898
.02700	4.6620	4.6397	4.6221	4.6084	4.5974	4.5899	4.5846	4.5828	4.5855	4.5910	4.5975
.02058	4.6768	4.6555	4.6381	4.6254	4.6166	4.6086	4.6034	4.6016	4.6017	4.6087	4.6165
.02012	4.6796	4.6585	4.6404	4.6277	4.6165	4.6102	4.6048	4.6021	4.6065	4.6103	4.6178
.019077	4.6821	4.6607	4.6427	4.6295	4.6192	4.6127	4.6078	4.6075	4.6092	4.6152	4.6233
.011993	4.7116	4.6924	4.6733	4.6629	4.6524	4.6448	4.6408	4.6393	4.6418	4.6474	4.6566
.010218	4.7228	4.7031	4.6858	4.6728	4.6628	4.6547	4.6523	4.6516	4.6534	4.6596	4.6701
.010183	4.7263	4.7039	4.6880	4.6753	4.6653	4.6576	4.6553	4.6551	4.6550	4.6631	4.6721
.008016	4.7319	4.7113	4.6944	4.6817	4.6712	4.6638	4.6604	4.6602	4.6625	4.6699	4.6773
	Series 1b. NaHTar:Na_2Tar:KCl=1:1.3411:0.5853										
0.03276	4.3773	4.3587	4.3406	4.3287	4.3136	4.3075	4.3022	4.3020	4.3039	4.3093	4.3162
.02732	4.3895	4.3664	4.3478	4.3362	4.3253	4.3195	4.3144	4.3144	4.3160	4.3208	4.3287
.02175	4.4022	4.3790	4.3617	4.3495	4.3381	4.3338	4.3267	4.3258	4.3276	4.3327	4.3396
.016300	4.4191	4.3985	4.3799	4.3683	4.3575	4.3515	4.3478	4.3476	4.3492	4.3541	4.3620
.010582	4.4448	4.4229	4.4052	4.3938	4.3835	4.3769	4.3724	4.3739	4.3755	4.3809	4.3897
	Series 2. NaHTar:NaCl=1:1										
0.06000	3.6517	3.6311	3.6134	3.6002	3.5889	3.5794	3.5739	3.5724	3.5717	3.5751	3.5804
.05000	.....	.....	.....	.....	3.5976	3.5908	3.5849	3.5829	3.5815	3.5854	3.5896
.04488	3.6654	3.6452	3.6277	3.6149	3.6038	3.5955	3.5901	3.5878	3.5872	3.5899	3.5953
.04000	3.6710	3.6505	3.6324	3.6198	3.6066	3.6014	3.5955	3.5928	3.5927	3.5975	3.6022
.03485	3.6816	3.6630	3.6428	3.6290	3.6168	3.6098	3.6040	3.6014	3.6014	3.6051	3.6110
.03026	3.6856	3.6650	3.6475	3.6341	3.6222	3.6153	3.6078	3.6063	3.6066	3.6105	3.6155
.02543	3.6923	3.6742	3.6570	3.6434	3.6323	3.6241	3.6181	3.6161	3.6155	3.6191	3.6239
.02011	3.7079	3.6967	3.6908	3.6561	3.6447	3.6369	3.6303	3.6287	3.6285	3.6332	3.6376
.015041	3.7205	3.6986	3.6823	3.6694	3.6586	3.6520	3.6475	3.6464	3.6465	3.6506	3.6564
.010043	3.7447	3.7244	3.7074	3.6948	3.6840	3.6749	3.6714	3.6709	3.6706	3.6753	3.6802

cell solution. These were averaged, and the corresponding values of the quantity pwH were computed by the equation [2]

$$\text{pwH} \equiv -\log (f_{\text{H}} f_{\text{Cl}} m_{\text{H}}) = (E - E^\circ)\boldsymbol{F}/(2.3026\ RT) + \log m_{\text{Cl}}, \quad (1)$$

where m is molality; f is the activity coefficient on the scale of molality; E° is the standard potential [3] of the cell; $\boldsymbol{F}$ is the faraday, 96,496 abs coulombs equiv^{-1} [9]; R is the gas constant, 8.3144 abs j deg^{-1} mole^{-1} [9]; and T is the absolute temperature, $T = t$ (°C) + 273.16. The values of pwH are summarized in table 1. As eq 1 shows, pwH is a physically defined property of each buffered chloride solution.

Fifteen of the aqueous tartrate-chloride mixtures that made up series 1a and 1b were prepared by the addition of the appropriate weights of sodium hydrogen tartrate and bromide-free sodium chloride (or potassium chloride) to a carbonate-free solution of sodium hydroxide. The remaining seven were prepared from sodium chloride and the anhydrous primary and secondary sodium tartrates. These two tartrate salts were purified by two crystallizations from water. The sodium hydrogen tartrate was dried at 50° in a vacuum oven and was found to assay 99.98 percent by titration with standard alkali to the endpoint of phenolphthalein. The same solution of alkali was used for the titration and for the preparation of the cell solutions. The secondary sodium tartrate was dried to the anhydrous condition in air at 150°. Three samples of the dry salt were ashed in platinum in a muffle furnace at temperatures near 800°. The weight of residue, assumed to be sodium carbonate, was 99.94 percent of the theoretical.

Solutions of the purified sodium hydrogen tartrate and sodium tartrate were strongly dextrorotatory. The dissociation constants of the dextro, levo, and *dl* forms of tartaric acid appear to be identical, but the meso acid is somewhat weaker than the other three forms [10].

The solutions were freed of dissolved air by passage of nitrogen. Details of the procedure followed in making the hydrogen electrodes, in filling the cells, and in measuring the emf have been set forth in an earlier article [11]. The design of the cells [5] and the method of preparing the silver–silver-chloride electrodes [12] have also been described elsewhere.

3. Calculation of the Dissociation Constants

As indicated in an earlier section, neither dissociation constant of an overlapping pair can be obtained independently of the other. However, to resolve the two constants it is sufficient that equations for K_1K_2 and for K_2 in terms of the same unknowns be set up and solved simultaneously or by successive approximations. This approach has been used to determine the second dissociation constant of succinic acid accurately and the first constant approximately [11]. Its application was described in some detail and will not be repeated in its entirety for tartaric acid.

3.1. Calculation of K_2 from pwH (series 1)

If m_1 represents the stoichiometric molality of sodium hydrogen tartrate and m_2 that of sodium tartrate, the formal expression for the relation between the pwH of the mixtures of series 1 and the second dissociation constant, K_2, of tartaric acid is

$$-\log K_2' \equiv -\log K_2 - \beta\mu = \text{pwH} - \log \frac{m_2 + m_{\text{H}} + m_{\text{H}_2\text{Tar}}}{m_1 - m_{\text{H}} - 2m_{\text{H}_2\text{Tar}}} + \frac{2A\sqrt{\mu}}{1 + Ba^*\sqrt{\mu}}, \quad (2)$$

where K_2' is the "apparent" value of K_2, μ is the ionic strength, β and a^* are adjustable parameters, A and B are constants of the Debye-Hückel theory [13], and H_2Tar is written for tartaric acid (COOH-CHOH-CHOH-COOH). If $f_{\text{H}} f_{\text{H Tar}^-} m_{\text{H}} / f_{\text{H}_2\text{Tar}}$ is taken equal to $f_{\text{H}} f_{\text{Cl}} m_{\text{H}}$, that is, to 1/(antilog pwH), a reasonable assumption for dilute solutions, the concentration of free (molecular) tartaric acid is given by

$$-m_{\text{H}_2\text{Tar}} = (m_1 - m_{\text{H}})/(2 + K_1 \text{ antilog pwH}) \quad (3)$$

and the ionic strength by

$$\mu = m_1 + 3m_2 + m_{\text{Cl}} + 2m_{\text{H}} + m_{\text{H}_2\text{Tar}}. \quad (4)$$

Unfortunately, the hydrogen-ion concentration, m_{H}, can only be established approximately, as the activity coefficients needed to compute it from pwH (compare eq 1) are not known. The apparent or inexact concentration of hydrogen ion, m_{H}', is obtained by use of the Debye-Hückel equation with a reasonable value of the ion-size parameter, a^*:[4]

$$-\log m_{\text{H}}' = \text{pwH} - 2A\sqrt{\mu}/(1 + Ba^*\sqrt{\mu}). \quad (5)$$

The uncertainty in a^* (and hence in m_{H}') is of little importance when the hydrogen-ion concentration is much smaller than m_1 or m_2 but limits the accuracy with which the dissociation constant of moderately strong acids such as the first step of phosphoric acid can be obtained [14]. Evidently m_{H}' approaches the true m_{H} at low values of the ionic strength. Inasmuch as the thermodynamic dissociation constants are obtained by an extrapolation procedure, m_{H}' can be used for m_{H} when the dissociation constant is 10^{-3} or smaller without perceptible effect on the result.

3.2. K_1K_2 from pwH (series 2)

The formal relationship between $(K_1K_2)'$, the apparent value of K_1K_2 calculated with estimated

[2] In the equations of the following sections, the charges of the hydrogen and chloride ions will not be indicated. Furthermore, the term "hydrogen ion" will be understood to embrace all forms of this ion, hydrated or unhydrated.

[3] E° is obtained from the experimental data of Harned and Ehlers [7]. Values of E° and $2.3026\ RT/\boldsymbol{F}$ in absolute volts are listed in reference [8].

[4] As m_{H} is so small, the choice of a^* has little influence on the result. Values of 5.5 and 6 were chosen, for these furnished the best straight-line plots of log K_2' with respect to ionic strength when used in eq 2.

activity coefficients, and pwH for the solutions of series 2 is written [6]

$$-1/2 \log (K_1K_2)' = \text{pwH} - 1/2 \log \frac{m_{H_2Tar} + m_H}{m_{H_2Tar}} + \frac{A\sqrt{\mu}}{1+Ba^*\sqrt{\mu}}. \quad (6)$$

If m_1 is the molality of sodium hydrogen tartrate and also that of sodium chloride, the ionic strength of the solutions of series 2 is

$$\mu = 2m_1 + 2m_H + m_{H_2Tar} \quad (7)$$

The concentration of molecular tartaric acid, m_{H_2Tar}, is given by eq 3. The apparent hydrogen-ion concentration, m'_H, was computed by eq 5 with $a^*=4$ and used for m_H in eq 6 and 7. A value of 4 was also used for a^* in eq 6. A choice of 6 instead of 4 for a^* (eq 5) altered the second term on the right of eq 6 by only 0.0003.

3.3. Resolution of K_1 and K_2

The two constants were resolved as follows: The ionic strength of the solutions of series 1 was first estimated, m'_H computed (eq 5), and $-\log K'_2$ obtained (eq 2) neglecting m_{H_2Tar}. Extrapolation of the results to zero ionic strength then furnished a first approximation to K_2. Next, an estimated value of K_1 was employed in eq 3 to compute the approximate m_{H_2Tar} and, from this, the approximate ionic strength and m'_H in the solutions of series 2. A value of K_1K_2 was obtained by use of eq 6 and subsequent extrapolation to zero ionic strength, and K_1K_2 was divided by the first value of K_2 to obtain a first measure of K_1. The latter was then used in eq 3 to obtain m_{H_2Tar} and, hence, the ionic strength of series 1 solutions needed for the second approximation. After the dissociation constants at 0°, 25°, and 50° had been established, interpolation furnished reasonably accurate estimates of the various quantities at the intermediate temperatures and simplified the computations considerably.

The extrapolation of log K'_2 for the 22 solutions of series 1 to zero ionic strength at 0°, 25°, and 50° is shown in figure 1. The circles represent data for series 1a and the dots for series 1b. Figure 2 shows the determination of log K_1K_2 at the same temperatures. In both cases, the lines were drawn by inspection. The final values of log K_1, log K_2, and 1/2 log K_1K_2 are summarized in tables 2 and 3. The accuracy of log K_2 is thought to be about ± 0.003 and that of log K_1 about ± 0.006.

TABLE 2. *Log K_2 and K_2 from 0° to 50° C*

Temperature (°C)	$-\log K_2$	$K_2 \times 10^3$	Temperature (°C)	$-\log K_2$	$K_2 \times 10^3$
0	4.426	3.75	25	4.366	4.31
5	4.407	3.92	30	4.365	4.32
10	4.391	4.06	35	4.367	4.30
15	4.381	4.16	40	4.372	4.25
20	4.372	4.25	45	4.380	4.17
			50	4.391	4.06

TABLE 3. *Log K_1K_2 and log K_1 from 0° to 50° C*

Temperature (°C)	$-1/2 \log K_1K_2$	$-\log K_1$	Temperature (°C)	$-1/2 \log K_1K_2$	$-\log K_1$
0	3.772	3.118	25	3.701	3.036
5	3.751	3.095	30	3.695	3.025
10	3.733	3.075	35	3.693	3.019
15	3.719	3.057	40	3.695	3.018
20	3.708	3.044	45	3.700	3.020
			50	3.709	3.021

Some of the more recent determinations of the dissociation constants of *d*-tartaric acid are summarized in table 4. As a result, no doubt, of the difficulty of resolving equilibria that overlap so extensively, these values show very little uniformity. Several of the emf determinations were based upon the analysis of pH-titration curves plotted from data for cells with the hydrogen or quinhydrone electrode and the calomel reference electrode. Jones and Soper [10] used the same cell as was used in this investigation. They computed m_H by an equation similar to eq 5 and used the values thus

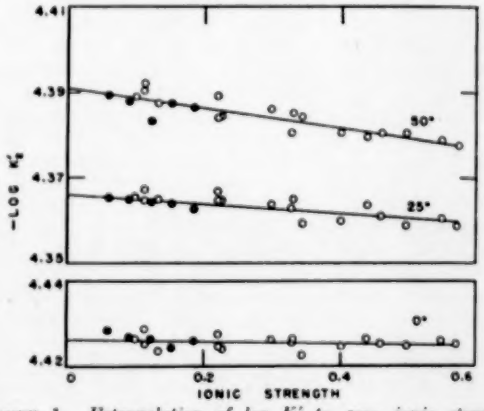

FIGURE 1. *Extrapolation of log K'_2 to zero ionic strength at 0°, 25°, and 50°.*

Circles represent data of series 1a; dots represent those of series 1b.

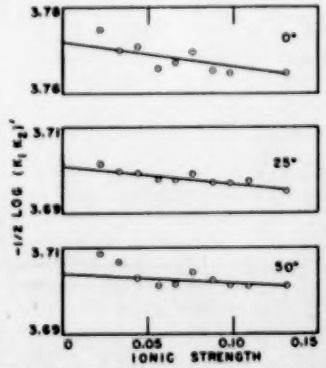

FIGURE 2. *Extrapolation of $-1/2 \log (K_1K_2)'$ to zero ionic strength at 0°, 25°, and 50°.*

Data of series 2.

TABLE 4. *Summary of determinations of log K_1 and log K_2 for d-tartaric acid*

Reference	Temperature (°C)	$-\log K_1$	$-\log K_2$	Method
[15]	20	3.05	4.13	emf
[16]	18	3.91	4.55	Conductance, sucrose inversion.
[17]	18	2.99	4.02	emf
[18]	25	.....	4.29	Solubility.
[19]	25	.....	4.40	Rate of decomposition of diazoacetic ester.
[20]	16.8	2.93	.....	emf, KCl added.
	17.6	.....	4.23	
[21]	18	3.62	4.55	emf
[22]	20	3.04	4.40	Do.
[10]	25	2.98	4.34	Do.
	50	2.94	4.39	
	74	3.01	4.51	
[23]	20	2.98	4.39	Do.
This investigation	0	3.12	4.426	Do.
	25	3.04	4.366	
	50	3.02	4.391	

obtained to calculate the dissociation constants in much the same manner as pH measurements had been used by earlier investigators.

The values of log K_1 and log K_2 at the 11 temperatures were fitted to the following equation by the method of least squares:

$$-\log K = A/T + B + CT, \tag{8}$$

where T is the temperature in degrees K. The constants of eq 8 for the first and second steps are

	A	B	C
First dissociation	1525.59	−6.6558	0.015336
Second dissociation	1765.35	−7.3015	.019276

The average difference between the "observed" log K and that calculated by eq 8 is 0.0008 for log K_1 and 0.0005 for log K_2.

In figure 3, $-\log K_1$, $-\log K_2$, and $-\frac{1}{2}\log K_1K_2$ are plotted as a function of temperature, and each of these quantities is seen to pass through a minimum in the experimental temperature range. It was shown in an earlier paper [24] that the absolute temperature, T_{min}, at which the minimum is reached can be readily calculated from the constants of eq 8:[5]

$$T_{min} = \sqrt{A/C}.$$

Hence, T_{min} is found to be 42.2° C for $-\log K_1$ and 29.5° C for $-\log K_2$.

4. Thermodynamic Quantities

By application of familiar thermodynamic formulas, the dissociation constants and their changes with temperature yield values of the changes of free energy, heat content, entropy, and heat capacity that would take place if 1 mole of tartaric acid or hydrogen tartrate ion were to dissociate completely

[5] The square-root sign has been omitted from the right side of eq 20, reference [24].

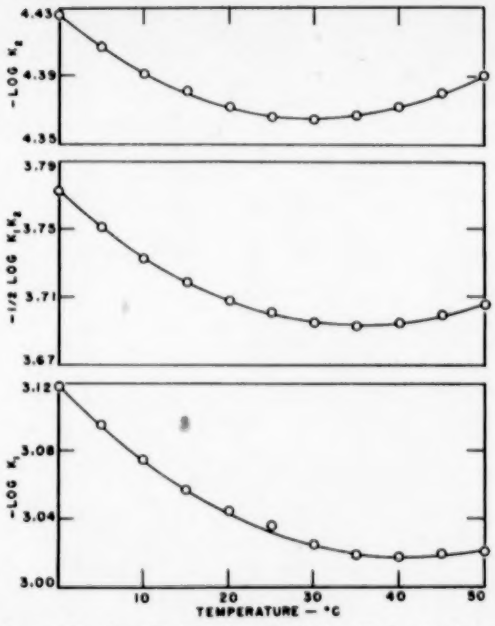

FIGURE 3. *Log K_1, log K_2, and $\frac{1}{2}$ log K_1K_2 plotted as a function of temperature.*

under conditions obtaining in the standard state for aqueous solutions. These quantities, which are designated ΔF°, ΔH°, ΔS°, and ΔC_p°, respectively, correspond to the processes

$$H_2Tar = H^+ + HTar^- \tag{10}$$

and

$$HTar^- = H^+ + Tar^= \tag{11}$$

when unit activity of both reactants and products is maintained at all times. Inasmuch as overlapping of the two steps prevents either process from achieving completion without involvement of the other, these thermodynamic functions can only be used in practice when a detailed analysis of the solution has been made. They are, nevertheless, of some theoretical interest.

In terms of the constants A, B, and C of eq 8, the formulas for the four thermodynamic quantities are

$$\Delta F^\circ = -2.3026\ RT \log K, \tag{12}$$

$$\Delta H^\circ = 2.3026\ R(A - CT^2), \tag{13}$$

$$\Delta S^\circ = 2.3026\ R(-B - 2CT), \tag{14}$$

$$\Delta C_p^\circ = 2.3026R(-2CT). \tag{15}$$

With the use of $R = 8.3144$ j deg^{-1} mole^{-1}, these quantities were obtained in joules. The accuracy of the quantities derived from the first or second derivatives of log K with respect to temperature is greater near

the middle of the experimental temperature range than at the ends. Hence, $\Delta H°$, $\Delta S°$, and $\Delta C_p°$ were computed only for the range 10° to 40° C. In view of the lower accuracy of log K_1, the thermodynamic quantities were computed for the first dissociation step only at 25° C. The results are summarized in table 5.

TABLE 5. *Thermodynamic quantities for the dissociation of tartaric acid and hydrogen tartrate ion*

Temperature	$\Delta F°$	$\Delta H°$	$\Delta S°$	$\Delta C_p°$
	Tartaric acid (eq 10)			
°C	*j mole*$^{-1}$	*j mole*$^{-1}$	*j deg*$^{-1}$ *mole*$^{-1}$	*j deg*$^{-1}$ *mol*$^{-1}$
25	17,330	3,100	−47.7	−170
	Hydrogen tartrate ion (eq 11)			
0	23,150	.....	.....	.....
5	23,470	.....	.....	.....
10	23,800	4,210	−69.2	−209
15	24,170	3,150	−72.9	−213
20	24,540	2,080	−76.6	−216
25	24,920	980	−80.3	−220
30	25,330	−120	−84.0	−224
35	25,760	−1,250	−87.7	−227
40	26,210	−2,390	−91.4	−231
45	26,680	.....	.....	.....
50	27,170	.....	.....	.....

5. References

[1] D. I. Hitchcock and A. C. Taylor, J. Am. Chem. Soc. **59,** 1812 (1937).

[2] J. J. Lingane, Anal. Chem. **19,** 810 (1947).

[3] H. S. Harned and R. W. Ehlers, J. Am. Chem. Soc. 54 1350 (1932).

[4] W. J. Hamer, J. O. Burton, and S. F. Acree, J. Research NBS **24,** 269 (1940) RP1284.

[5] R. G. Bates and S. F. Acree, J. Research NBS **30,** 129 (1943) RP1524.

[6] R. G. Bates, J. Am. Chem. Soc. **70,** 1579 (1948).

[7] H. S. Harned and R. W. Ehlers, J. Am. Chem. Soc. **55,** 2179 (1933).

[8] R. G. Bates and G. D. Pinching, J. Research NBS **42,** 419 (1949) RP1982.

[9] J. W. DuMond and E. R. Cohen, Rev. Modern Phys. **20,** 82 (1948).

[10] I. Jones and F. G. Soper, J. Chem. Soc. 1836 (1934).

[11] G. D. Pinching and R. G. Bates, J. Research NBS **45,** 322 (1950) RP2142.

[12] R. G. Bates, G. D. Pinching, and E. R. Smith, J. Research NBS **45,** 418 (1950) RP2153.

[13] G. G. Manov, R. G. Bates, W. J. Hamer, and S. F. Acree, J. Am. Chem. Soc. **65,** 1765 (1943).

[14] R. G. Bates, J. Research NBS **47,** 127 (1951) RP2236.

[15] F. Auerbach and E. Smolczyk, Z. physik. Chem. **110,** 65 (1924).

[16] T. Paul, Z. physik. Chem. **110,** 417 (1924).

[17] H. T. S. Britton, J. Chem. Soc. **127,** 1896 (1925).

[18] E. Larsson, Z. anorg. allgem. Chem. **155, 247** (1926).

[19] M. Duboux and J. Frommelt, J. chim. phys. **24,** 245 (1927).

[20] R. Kuhn and T. Wagner-Jauregg, Ber. **61,** 483 (1928).

[21] I. M. Kolthoff and W. Bosch, Rec. trav. chim. **47,** 861 (1928).

[22] F. L. Hahn and R. Klockmann, Z. physik. Chem. **A571,** 206 (1931).

[23] H. Bode and K. Peterson, Ber. **71B,** 871 (1938).

[24] G. D. Pinching and R. G. Bates, J. Research NBS **45,** 444 (1950) RP2156.

WASHINGTON April 27, 1951

Journal of Research of the National Bureau of Standards Vol. 47, No. 5, November 1951 Research Paper 2261

Effect of SO_3 on the Alkali Compounds of Portland Cement Clinker[1]

Terry F. Newkirk[2]

This investigation shows that the compound $Na_2O.8CaO.3Al_2O_3$, which is known to be one of the forms in which Na_2O may occur in portland cement clinker, is unstable at clinkering temperatures in the presence of SO_3. This compound reacts with SO_3 to form Na_2SO_4 and $3CaO.Al_2O_3$. Any excess of Na_2O will remain as $Na_2O.8CaO.3Al_2O_3$, become a constituent of the clinker glass, or enter into solid solution with one of the other clinker components.

In clinker compositions containing both soda and potash together with SO_3, an alkali-sulfate phase is produced that contains both of the alkalies. For molecular ratios R_2O/SO_3 greater than unity, a preferential reaction of the SO_3 with K_2O is indicated. Empirical relationships between the alkalies and the SO_3 of the cement mixture indicate that the alkalies first combine with the SO_3 in the approximate molecular ratio $K_2O/Na_2O=3$ to the extent that the composition limits of the mixture permit. The composition of the alkali-sulfate phase for mixtures of varying soda-potash contents with R_2O/SO_3 molecular ratios equal to 1, 2, and 3 have been determined. Equations are developed for calculating the approximate composition of the alkali sulfate and the potential phase composition of clinker-type mixtures having other R_2O/SO_3 ratios.

1. Introduction

Portland cement clinker contains, in addition to the major constituent oxides of calcium, aluminum, and silicon, small quantities of other oxides that occur in the raw materials. The alkalies Na_2O and K_2O have a particular interest because of their unfavorable reaction with certain types of aggregate used in concrete, and during the burning process these minor oxides affect the temperature at which the first liquid forms and the nature and quantity of the phases that ultimately constitute the clinker. The nature and quantity of these phases determine, for the most part, the physical and chemical properties of the cement. Small amounts of the alkalies may have an effect on the phase relations in the cement clinker of a magnitude not commensurate with their low concentration in the mixture.

The nature of the alkali-bearing phases has been studied by various investigators [1, 2, 3] [3] with mixtures containing CaO, Al_2O_3, SiO_2, and either Na_2O or K_2O. They recognized, however, that acidic oxides such as SO_3 and TiO_2, when present, may react with the alkalies during the burning process to produce new phases.

Taylor [3] found that, for mixtures approximating portland cement compositions and composed of K_2O, CaO, Al_2O_3, SiO_2, Fe_2O_3, and MgO, the stable compound of potash is $K_2O.23CaO.12SiO_2$. He reported, however, [4] that this compound is unstable when heated in the presence of SO_3, the reaction being represented by the equation,

$$K_2O.23CaO.12SiO_2+CaSO_4=12(2CaO.SiO_2)+K_2SO_4.$$

He found molten potassium sulfate to be immiscible with the clinker liquid, to show no tendency to react with the components of mixtures containing $3CaO.SiO_2$, $2CaO.SiO_2$, $3CaO.Al_2O_3$, $4CaO.Al_2O_3.Fe_2O_3$, and MgO and to crystallize readily upon cooling. In 11 out of 19 commercial clinkers subjected to microscopic examination, he found the phase identified as potassium sulfate.

In a few subsequent experiments, Taylor [5] observed that a solid solution of sodium and potassium sulfates appeared upon heating certain mixtures of Na_2SO_4, $K_2O.CaO.SiO_2$ and $2CaO.SiO_2$. As in the case of the potassium compound, he found sodium sulfate to be essentially immiscible with the clinker melt. A phase identified as K_2SO_4 occurred in several Na_2O-K_2O-CaO-SiO_2-SO_3 mixtures of high K_2O/Na_2O and K_2O/CaO ratios. The manner in which the soda was combined in these mixtures was not determined.

Eubank [6] made a preliminary investigation of the clinker phases produced upon heating mixes containing Na_2O and combinations of Na_2O and K_2O together with SO_3. As a result of microscopic studies of quenched and slowly cooled charges, he found that the compound $Na_2O.8CaO.3Al_2O_3$ is decomposed by heating with calcium sulfate in the range 1,300° to 1,470°.[4] Charges containing equimolar quantities of these two compounds were found to consist only of $3CaO.Al_2O_3$ and Na_2SO_4 after heat treatment, indicating complete reaction. The alkali sulfate produced in the reaction was found to be stable in the presence of $3CaO.SiO_2$, $2CaO.SiO_2$, $3CaO.Al_2O_3$, and $4CaO.Al_2O_3.Fe_2O_3$. Indications were obtained that if a solid solution of Na_2O and Fe_2O_3 in $2CaO.SiO_2$ was prepared, the Na_2O was not removed from this solution by heating it with $CaSO_4$. Some of Eubank's mixes also contained K_2O either as $K_2O.23CaO.12SiO_2$ or as K_2SO_4 in addition to the soda compounds. Studies of these mixtures were inconclusive, due to

[1] In portland cement terminology, the sulfur in clinker is usually referred to as SO_3 and is ordinarily reported as such in clinker analyses. For convenience, this terminology is utilized throughout this paper, and SO_3 is treated as one of the primary components in a multi-component system.

[2] Research Associate at the National Bureau of Standards, representing the Portland Cement Association.

[3] Figures in brackets indicate the literature references at the end of this paper.

[4] All temperatures are in deg. C.

the difficulty in distinguishing between certain of the compounds having practically identical optical properties. This made it evident that any further work on this subject would require the application of a different experimental method.

Portland cement clinker ordinarily contains both soda and potash as well as SO_3. It was necessary, therefore, to study further the effect of SO_3 on the alkali compounds of clinker containing both soda and potash. This study has provided a basis for the development of equations for approximating the potential phase composition of portland cement clinker containing known quantities of K_2O, Na_2O, and SO_3. This information represents one more advance in our understanding of the formation of clinker, by means of which we may better define and control its constitution and behavior.

2. Experimental Method

2.1. Phase Analysis of Mixtures

A few CaO-Al_2O_3-SiO_2-SO_3 mixtures to which had been added one or both of the alkali oxides were studied by the familiar quenching technique [7]. The quenched (or in a few cases slow-cooled) charges were crushed and examined in index oils under the petrographic microscope. After equilibrium was established in these mixtures at clinkering temperatures, the entire quantity of SO_3 (never more than equivalent to the alkalies) was found to be combined with soda or potash. In mixtures containing both alkalies, this sulfate consisted either of a single solid solution of Na_2SO_4 and K_2SO_4 or of an intimate mixture of two sulfate phases, depending upon the conditions of cooling. Excess Na_2O and K_2O remained as $Na_2O.8CaO.3Al_2O_3$ and $K_2O.23CaO.12SiO_2$, respectively. Consequently, it appeared that the determination of the relative amounts of sodium and potassium sulfates formed by heating each mixture would provide data for including the sulfates in calculations of the potential phase composition of portland cement clinker from its oxide composition.

Several methods for determining the composition of the alkali sulfate were investigated. These included chemical analysis of water extracts, chemical analysis of concentrates obtained by sedimentation or centrifugation, correlation of the refractive index of the sulfate with its composition, and correlation of the characteristic temperatures of phase changes in the alkali sulfate with its composition. The last method was selected as the most reliable for the purpose at hand, the temperatures being determined by thermal analysis.

Preliminary thermal analyses of several mixtures of $3CaO.Al_2O_3$, $2CaO.SiO_2$, and either K_2SO_4 or Na_2SO_4, after these mixtures had been preheated at 1,400° for 30 minutes, confirmed the findings of Taylor and Eubank that the alkali sulfate was essentially immiscible with the other components. It was therefore possible to determine the liquidus temperature or the temperature of characteristic inversions of the alkali-sulfate phase in each mixture without fear of errors due to miscibility. The temperatures of these phase changes were correlated with corresponding temperatures on a phase diagram for the binary system Na_2SO_4-K_2SO_4. The approximate composition of the sulfate phase was then determined directly from the diagram.

Nacken [8] prior to 1907 studied the binary system Na_2SO_4-K_2SO_4 by means of cooling curves. A portion of this work was repeated by the author employing both direct and differential heating curves. The phase diagram that resulted was used in determining the composition of the sulfate in the K_2O-Na_2O-CaO-Al_2O_3-SiO_2-SO_3 mixtures. This procedure served as a calibration of the method, since the same equipment and technique were employed with all mixtures.

2.2. Equipment and Raw Materials

A Leeds and Northrup "Speedomax" two-point recording potentiometer was used to record on a single chart both the differential and direct heating curves produced by the test charge undergoing thermal analysis. Since the alkali sulfate in many instances comprised only about 3 percent of the weight of the test charge, the differential emf was preamplified by a Leeds and Northrup low-level direct-current amplifier. With this arrangement, differential peaks of from 1½ to 2 in. were produced by the melting of as little as 3 percent of the immiscible sulfate phase. Background "noise" was negligible even at the highest amplification. The temperature of the vertical tube furnace was raised automatically by a motor-driven variable transformer at a rate of approximately 10 deg per minute.

Platinum-10 percent rhodium thermocouples were used with an external ice-bath cold junction. These couples were calibrated periodically against an NBS-certified thermocouple and also with chemically pure salts as auxiliary standards.

The alumina and dehydrated silica gel used in preparing the mixtures were of greater than 99.9-percent purity. The other raw materials met the ACS specifications for chemical reagents.

2.3. Preparation of Mixtures

Thirteen mixtures having different Na_2SO_4-K_2SO_4 ratios were prepared for use in a limited study of the system Na_2SO_4-K_2SO_4. After weighing, the two sulfates were ground together in an agate mortar to pass a No. 200 sieve and thoroughly mixed. The mixtures were placed in covered platinum crucibles and heated in an electric muffle furnace for 10 minutes at a temperature near 1,200°, at which temperature the charge was completely melted. Each melt was stirred with a platinum-covered ceramic rod, after which the charge was cooled, crushed, screened and mixed. After a second similar treatment, the charges were ready for the thermal analyses, which served to define the pure binary system.

Hundred-gram quantities of the compounds $Na_2O.8CaO.3Al_2O_3$ and $K_2O.23CaO.12SiO_2$ were pre-

pared and ground to pass a No. 200 sieve for use in making the mixtures of those compounds with calcium sulfate. The finely ground raw materials ($CaCO_3$, K_2CO_3, Na_2CO_3, Al_2O_3, SiO_2), which contained an excess of the alkalies to compensate for volatilization during heating, were ground in an agate mortar and subjected to repeated cycles of 1-hour burning, grinding, screening, and mixing. This was continued until microscopic observation and flame-photometer analysis indicated that the charges consisted of the desired compounds with only occasional traces of impurities. The $Na_2O.8CaO.3Al_2O_3$ mix was burned at 1,350° and the $K_2O.23CaO.12SiO_2$ at 1,450°. All burns and thermal analyses were carried out in platinum—3½ percent rhodium containers. An average of six burns was required for each compound, since both compounds are difficult to prepare, requiring repeated cycles of heating, grinding, screening, and mixing to secure complete reaction. A slight amount of the alkali may remain uncombined, even though the theoretical alkali content of the pure $K_2O.23CaO.12SiO_2$ or $Na_2O.8CaO.3Al_2O_3$ is closely approximated and microscopic examination shows the material to consist essentially of the desired compound.

Ten-gram quantities were usually made of the final mixtures of $Na_2O.8CaO.3Al_2O_3$, $K_2O.23CaO.12SiO_2$, and $CaSO_4$. The desired quantities of these compounds were weighed on an analytical balance, thoroughly mixed, and ground in an agate mortar to pass a No. 200 sieve. The mixtures were then heated in a muffle at about 1,400° for 30 minutes. They were removed, ground as before, mixed, and given a second similar heat treatment. Representative samples of each charge were observed under the petrographic microscope. Some of the charges required additional heatings before equilibrium was attained.

In all, 72 mixes representing 51 different compositions were prepared and studied. Thermal analyses were made of all of these mixes and of a number of single compounds.

3. Results

3.1. The System Na_2SO_4–K_2SO_4

A diagram of the binary system Na_2SO_4-K_2SO_4 as developed in the present investigation appears as figure 1. No attempt has been made to identify the low-temperature phases or to develop the details of the phase relationships in the portion below the continuous solid-solution region, as this was beyond the scope and purpose of this investigation. Points representing temperatures of phase changes as obtained by thermal analyses of the mixes have been plotted in this lower region as an aid to future investigations of this system. Further small breaks in the thermal analysis curves obtained while employing the highest amplication range of the direct-current amplifier suggest the possibility of even greater complexity in the low-temperature region. Additional phase changes might have been indicated in this region for the other compositions had the highest amplification been employed in each case.

It appears that the low-temperature phase relations in this system may be somewhat more complex than those reported by Nacken [8].

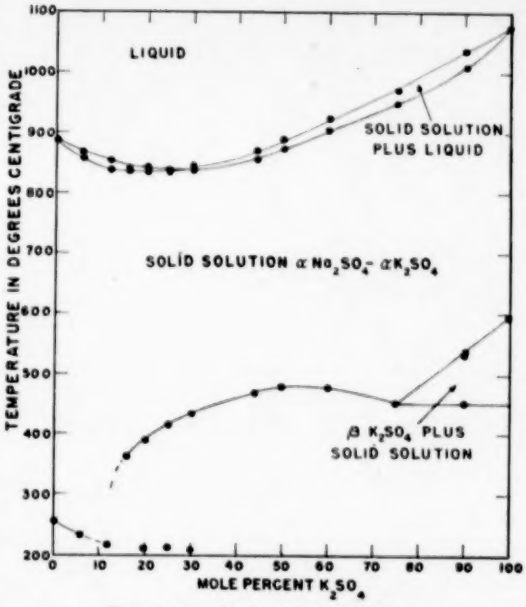

FIGURE 1. *System* Na_2SO_4-K_2SO_4.

The continuous solid-solution region in this diagram was found to correspond to a single phase of uniaxial negative optical character, having refractive indices somewhat higher than those of the low-temperature forms.

The compositions of the mixtures investigated in this system, together with the temperatures of their phase changes, are given in table 1.

TABLE 1. *Summary of thermal analysis data for the system* K_2SO_4–Na_2SO_4

Mix compositions	Temperature corresponding to differential peak		
	Solid transitions	Solidus	Liquidus
Mole percent K_2SO_4	°C	°C	°C
0	238		888
6	232	857	869
12	227	840	852
16	363	838	840
20	211	835	841
	391		
25	215	835	840
	244		
	415		
30	207	838	846
	432		
44	235	856	870
	469		
50	480	873	888
60	478	905	923
75	452	950	973
90	454	1,012	1,037
	532		
100	595		1,076

3,2. Reaction of $Na_2O.8CaO.3Al_2O_3$ with $CaSO_4$

Charges composed of equimolar quantities of $Na_2O.8CaO.3Al_2O_3$ and $CaSO_4$ (mix 2, table 2) after quenching from above 1,400° contained only $3CaO.Al_2O_3$ and Na_2SO_4. The sulfate appeared as a very finely divided phase of low birefringence surrounding the grains of $3CaO.Al_2O_3$. A mixture of $3CaO.Al_2O_3$ and Na_2SO_4 in the proportions that would result from the complete reaction between equimolar quantities of $Na_2O.8CaO.3Al_2O_3$ and $CaSO_4$ showed the same phases after quenching from above 1,400°. Differential thermal analyses of these mixtures after preliminary heating at 1,400° showed definite peaks at a temperature corresponding closely to the melting point of Na_2SO_4. The lower diagram in figure 2 is a reproduction of the curves obtained with chemically pure Na_2SO_4. The upper diagram is a similar reproduction of the curves for mixture 2 after preheating. The correspondence in the temperature of the two peaks is evident. Similar peaks were obtained in the thermal-analysis curves for mixes 37 and 38 (table 2), which consisted of $Na_2O.8CaO.3Al_2O_3$–$CaSO_4$ mixtures having Na_2O/SO_3 molar ratios of 2 and 3, respectively.

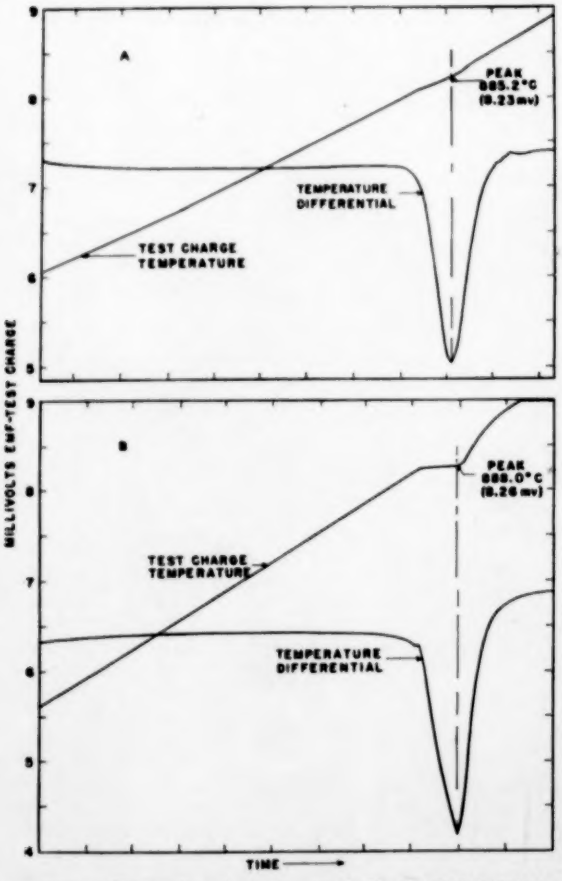

FIGURE 2. *Thermal analysis curves: A,* $Na_2O.8CaO.3Al_2O_3$+$CaSO_4$ *(reaction products after preheating at 1,400° C); B,* Na_2SO_4.

The differential curves were obtained with different amplifier settings, and therefore their ordinates are not comparable.

TABLE 2. *Thermal analysis data*

Mix number	Composition of alkali in total mixture	Significant solid inversion temperature	Liquidus temperature	R_2SO_4 composition
		Series $R_2O/SO_3=1$		
	Mole fraction of K_2O *in* $R_2O(K_x)$	°C	°C	*Mole fraction of* $K_2SO_4(K_x)$
4	1.00	.....	1,061	0.965
35	.95	.....	1,036	.900
34	.85	.....	1,011	.842
32	.65	.....	924	.610
16	.50	.....	902	.544
51	.373	.....	860	.385
31	.35	.....	853	.375
30	.25	.....	842	.270
29	.10	208	864	.081
2	0	.....	885	.017
		Series $R_2O/SO_3=2$		
36	1.00	.....	1,060	0.962
26	.95	.....	1,043	.917
24	.85	.....	994	.796
18	.75	.....	981	.765
27	.65	.....	973	.745
7	.50	.....	953	.720
17	.25	480	874	≈.460 to .500
28	.10	208	831	≈.195
37	0	388	882	.025
		Series $R_2O/SO_3=3$		
47	1.00	.....	1,060	0.963
46	.95	.....	1,038	.904
45	.85	.....	994	.795
44	.75	.....	986	.780
43	.65	.....	983	.770
42	.50	.....	972	.745
41	.35	.....	968	.734
40	.25	.....	940	.653
39	.10	420	830	≈.262
38	0	.....	882	.025

≈ Determined from solid inversion temperature.

3.3. Reaction of $K_2O.23CaO.12SiO_2$ with $CaSO_4$

In agreement with the work previously reported by Taylor [4], $K_2O.23CaO.12SiO_2$ was found to react with $CaSO_4$ in an equimolar ratio upon heating mixtures of those compounds in the region of clinkering temperatures. The observed reaction products after quenching the mixture from 900° were β-$2CaO.SiO_2$, γ-$2CaO.SiO_2$ and K_2SO_4.

Preheated mixtures of $K_2O.23CaO.12SiO_2$ and $CaSO_4$ having molecular ratios K_2O/SO_3, of 1, 2, and 3 (4, 36, and 47, respectively, table 2) showed an endothermic transformation in the region of the K_2SO_4 melting point during thermal analysis. The temperature of this transformation was somewhat lower than that for pure potassium sulfate. This is believed to be due to the solution by the K_2SO_4 of a small amount of K_2O, which remained uncombined in the preparation of the $K_2O.23CaO.12SiO_2$.

3.4 Reaction of Combinations of $Na_2O.8CaO.3Al_2O_3$ and $K_2O.23CaO.12SiO_2$ with $CaSO_4$

The reaction that takes place upon heating mixtures of $Na_2O.8CaO.3Al_2O_3$, $K_2O.23CaO.12SiO_2$, and $CaSO_4$ was studied with 23 different compositions. These mixtures represented three series of compositions having R_2O/SO_3 molecular ratios of 1, 2, and 3. Each series of constant R_2O/SO_3 ratio consisted in turn of a number of preparations with different K_2O/Na_2O ratios.

The charges, after a preheating treatment at 1,400°, were examined with a petrographic microscope and then subjected to thermal analysis. A quantitative phase analysis by microscopic means was not practicable, since the charges contained considerable fine-grained material, much of which consisted of different phases having similar optical properties. However, in general, these charges were found to consist of β-$2CaO.SiO_2$, together with some γ-$2CaO.SiO_2$, $3CaO.Al_2O_3$, and a very finely divided alkali-sulfate phase of low birefringence. Mixtures having R_2O/SO_3 ratios of 2 and 3 contained, in addition, one or both of the compounds $Na_2O.8CaO.3Al_2O_3$ and $K_2O.23CaO.12SiO_2$. All of the mixtures exhibited an endothermic effect in the Na_2SO_4-K_2SO_4 melting range. The temperature at which this phenomenon occurred varied with the composition of the sulfate, and therefore with that of the mixture (table 2).

A charge composed of equimolar quantities of $Na_2O.8CaO.3Al_2O_3$ and $K_2O.23CaO.12SiO_2$ and containing no $CaSO_4$ did not exhibit any thermal effect in the Na_2SO_4-K_2SO_4 melting range. No appreciable change in the phase composition was observed after heating this mixture at 1,400° for 1 hour although a slight loss in the birefringence of the $Na_2O.8CaO.3Al_2O_3$ was noted. This may have been due to the loss of part of the soda by volatilization.

The composition of the sulfate phase produced by the reaction of $K_2O.23CaO.12SiO_2$ and $Na_2O.8CaO.3Al_2O_3$ with $CaSO_4$ was determined for each of the mixtures of these compounds, as described in section 2 by associating the temperature of phase changes of the alkali-sulfate in the mixtures with the phase-equilibrium diagram of figure 1, assuming complete insolubility of the clinker components in the sulfate phase.

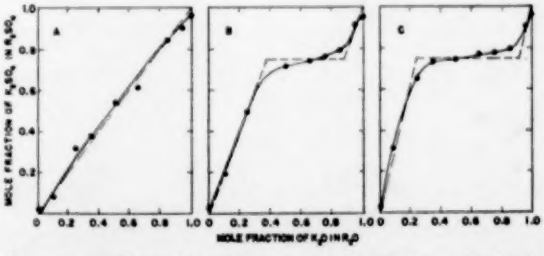

FIGURE 3. *Relationship between the composition of the alkali and that of the alkali sulfate in cement clinker for mixtures with molecular ratios: A,* $R_2O/SO_3=1$; *B,* $R_2O/SO_3=2$; *C,* $R_2O/SO_3=3$.

The relationship between the compositions of the mixtures of $K_2O.23CaO.12SiO_2$, $Na_2O.8CaO.3Al_2O_3$, and $CaSO_4$ of three different R_2O/SO_3 and varying Na_2O/K_2O ratios, and the compositions of the alkali-sulfate phases resulting from the reaction of these compounds upon heating at 1,400°, are shown in the three diagrams of figure 3 by solid lines in the experimental curves represented. The dashed lines on which calculations are based are discussed in section 4.

4. Derivation of Equations for Calculating the Alkali-Sulfate Composition in Clinker Mixtures

4.1. Mixtures with Molecular Ratio $R_2O/SO_3 \leq 1$.

Figure 3,A, illustrates the relationship between the mole fraction of K_2O in the total alkali (R_2O) of clinker-type mixtures having a molecular ratio $R_2O/SO_3=1$ and the mole fraction of potassium sulfate in the alkali sulfate (R_2SO_4). Mixtures with $R_2O/SO_3=1$ contained sufficient SO_3 to react with the entire quantity of both soda and potash. Inasmuch as the empirical relationship is nearly a linear one, it appears that the reaction approached completion. Thus for mixtures having a molecular ratio $R_2O/SO_3=1$, the ratio K_2O/Na_2O in the sulfate is the same as that in the entire clinker mixture. Since the reason for this condition is the complete conversion of the alkalies to sulfates, the same rule may be expected to apply for mixtures having R_2O/SO_3 ratios less than unity.

If we let K_s=mole fraction of K_2SO_4 in the alkali sulfate, and K_c=mole fraction of K_2O in the total alkali (R_2O) of the clinker, then $K_s=K_c$.

4.2. Mixtures with Molecular Ratios $R_2O/SO_3>1$.

The composition relationship for mixtures that do not contain sufficient SO_3 to combine with the entire quantity of both alkalies, that is, those in which $R_2O/SO_3>1$, was found to be more complex than that in the previous example.

In figure 3,B, mixtures having a molecular ratio $R_2O/SO_3=2$ are represented. This curve is considerably different in form from the previous one. In mixtures in which the mole fraction, K_2O/R_2O is 0.35 or less, the fraction of K_2SO_4 in the sulfate is about twice that of K_2O in the total alkali of the mixture. Above this value, the composition of the sulfate remains practically constant until the mole fraction, K_2O/R_2O reaches 0.85, after which the K_2SO_4 content of the sulfate increases rapidly until it consists of pure K_2SO_4.

Figure 3,C, shows a similar curve for mixtures having a molecular ratio $R_2O/SO_3=3$. This curve is of the same general shape as the previous one, the primary difference being in the slope of the first portion of the curve. Mixtures with the molecular ratio of 3 have a mole fraction of K_2SO_4 in the sulfate approximately three times that of the K_2O in the total alkali up to K_2O contents approaching

0.30 mole fraction of the total alkali. The composition of this sulfate again remains practically constant near 0.75 mole fraction K_2SO_4 until the alkali of the mixture becomes nearly pure K_2O, whereupon the K_2SO_4 content of the sulfate increases rapidly until only K_2SO_4 is present.

In deriving equations from these data for convenient calculation of the composition of the alkali sulfate formed in cement mixtures, it was found convenient to assume that the $CaSO_4$ always reacts with excess $Na_2O.8CaO.3Al_2O_3$ and $K_2O.23CaO.12SiO_2$ in such a manner as to form continuously a sulfate of constant composition as long as all three reactants are available. The composition of this sulfate may be expressed by a particular mole fraction of potassium sulfate, K_{s1}.

Let r=number of moles of R_2O in the clinker per mole of SO_3. Since K_s=mole fraction of K_2SO_4 in the alkali sulfate (i. e., the number of moles of K_2SO_4 per mole of alkali sulfate), and K_c=mole fraction of K_2O in the alkalies of the clinker, then $1-K_s$=the mole fraction of Na_2SO_4 in the alkali sulfate, and $1-K_c$=the mole fraction of Na_2O in the alkalies of the clinker.

As SO_3 reacts with alkalies to form the alkali-sulfate phase with $K_s=K_{s1}$, it removes K_{s1} mole of K_2O and $(1-K_{s1})$ mole of Na_2O for every mole of SO_3. There are present, however, rK_c moles of K_2O and $r(1-K_c)$ moles of Na_2O for every mole of SO_3. Therefore, if K_2O is the first of the three oxides to reach depletion,

$$rK_c<K_{s1}, \text{ or } K_c<\frac{K_{s1}}{r}. \quad (1)$$

If SO_3 is the first to reach depletion,

$$rK_c>K_{s1}, \text{ and } r(1-K_c)>(1-K_{s1}),$$

or,

$$\frac{K_{s1}}{r}<K_c<\frac{K_{s1}+(r-1)}{r}. \quad (2)$$

If Na_2O is the first to reach depletion,

$$r(1-K_c)<(1-K_{s1}), \text{ or } K_c>\frac{K_{s1}+(r-1)}{r}. \quad (3)$$

Within the range of composition represented by eq. 1, there will be in the sulfate phase rK_c moles of K_2O for every mole of SO_3, and therefore

$$K_s=rK_c. \quad (4)$$

Within the range specified by (2) it will be true, as mentioned above, that

$$K_s=K_{s1}. \quad (5)$$

Within the range specified by (3), there will be in the sulfate phase $r(1-K_c)$ moles of Na_2O, and therefore $1-r(1-K_c)$ moles of K_2O per mole of alkali sulfate. Thus

$$K_s=1-r(1-K_c). \quad (6)$$

These equations appear in table 3, together with convenient weight formulas for r and K_c.

In order that the approximate composition of the alkali sulfate may be readily calculated for any clinker mixture from its oxide composition, the value of K_{s1} must be stated. Since this value corresponds to the horizontal portion of the curves in figure 3, B and C, it is readily found to be 0.75 ± 0.04. Composition curves based on this value of K_{s1} and calculated by means of equations derived in the foregoing discussion have been constructed for three series of K_2O-Na_2O-CaO-Al_2O_3-SiO_2-SO_3 mixtures having R_2O/SO_3 molecular ratios (r values) of 1, 2, and 3. These appear as dashed lines in figure 3 for comparison with the experimental curves, which appear as solid lines. The two sets of curves are in reasonable agreement for each of the three molecular ratios. Consequently the composition of the sulfate phase in clinkers having other r values of the same order as those studied may be approximated by using the equations in table 3.

TABLE 3.—*Procedure for calculatng the approximate composition of the alkali sulfate in portland cement clinker*

1. Calculate r (the R_2O/SO_3 molecular ratio in the cement mixture)

$$r=\frac{0.8500\ K_2O+1.2915\ Na_2O}{SO_3}.$$

2. Calculate K_c (the mole fraction of K_2O in the total alkali of the cement mixture)

$$K_c=\frac{0.8500\ K_2O}{r\ (SO_3)}.$$

The formulas for the oxides in these two equations represent the weight percentages of these oxides in the clinker.

3. Calculate K_s (the mole fraction of K_2SO_4 in the sulfate) using the appropriate equation below as determined by the values for r and K_c:

	If r is greater than 1.0—		
If r is equal to or less than 1.0, use the equation $K_s=K_c$	and K_c lies between 0 and $0.75/r$, use the equation $K_s=rK_c$	and K_c is equal to or lies between $0.75/r$ and $(r-0.25)/r$ use the equation $K_s=0.75$	and K_c lies between $(r-0.25)/r$ and 1.0, use the equation $K_s=1-r(1-K_c)$

For clinkers in which the R_2O/SO_3 ratio is high, the amount of sulfate must be low, since the total alkali in the clinker rarely exceeds 1½ percent. The amount of the sulfate phase then approaches a negligible quantity; thus a high degree of accuracy is not required in determining the composition of this sulfate phase.

5. Discussion

It appears from the results of this and earlier studies that when mixtures approximating portland cement compositions contain SO_3, the alkalies in these mixtures will react with the SO_3 during the burning process to produce an alkali-sulfate phase. The present investigation confirms that this alkali-sulfate is immiscible with the primary clinker melt and stable in the presence of the major clinker components.

Cement mixtures containing only K_2O as the alkali, together with SO_3, will, after burning, have the available SO_3 combined with the K_2O as the compound K_2SO_4, which will appear in the form of crystals in the clinker. In the event that more K_2O is present than the quantity required to combine with the available SO_3, this K_2O will become a constituent of the clinker glass or, if cooling is sufficiently slow, may appear as the compound $K_2O.23CaO.12SiO_2$.

If a cement mixture contains only Na_2O as the alkali, this oxide will combine with the available SO_3 to form Na_2SO_4, which will appear as finely divided crystals in the clinker unless cooling has been extremely rapid. Soda in excess of that required to combine with the SO_3 will become a constituent of the glass or may enter into solid solution with $2CaO.SiO_2$ or one of the other clinker components. If cooling were sufficiently slow, some of the excess soda might appear in the form of the compound $Na_2O.8CaO.3Al_2O_3$.

When both the alkalies, K_2O and Na_2O are present in cement mixtures together with SO_3, they react at clinkering temperatures to form a separate liquid phase, which changes to a single solid solution on cooling. This solid solution is stable above a temperature that varies from 400° to 600°, depending on the sulfate composition.

The sulfate phase has a constant composition if both $Na_2O.8CaO.3Al_2O_3$ and $K_2O.23CaO.12SiO_2$ are present at crystalline equilibrium. Under these conditions the mole fraction of K_2SO_4 in the sulfate is 0.75 ± 0.04.

It is evident that the reaction of a portion of each of the alkalies with SO_3 during the burning of portland cement clinker will affect the final phase composition of the clinker. The formation of K_2SO_4 and Na_2SO_4 will greatly reduce the potential quantity of $K_2O.23CaO.12SiO_2$ and $Na_2O.8CaO.3Al_2O_3$, which would otherwise be formed in the event of complete equilibrium crystallization. This in turn regulates the quantity of $3CaO.SiO_2$, $2CaO.SiO_2$, and $3CaO.Al_2O_3$ appearing in the clinker.

Equations that take into account the effect of SO_3 on the potential phase composition of K_2O-Na_2O-CaO-Al_2O_3-SiO_2-Fe_2O_3-SO_3 mixtures approximating the composition of portland cement clinker have been derived in the manner of Dahl [9]. These equations, in the convenient weight percentage form, appear in table 4. The application of the equations in table 4(B) (for those mixtures having R_2O/SO_3 molecular ratios greater than 1.0) requires the preliminary calculation of the value of K_s, the mole fraction of K_2SO_4 in the sulfate, for the mixture as outlined in table 3. This numerical value of K_s, together with the weight percentage of each of the oxides in the clinker is then substituted in the equations in table 4(B).

This preliminary calculation is unnecessary if the given mixture has an R_2O/SO_3 molecular ratio equal to or less than 1.0, inasmuch as the equations in table 4 (A) apply directly to this case.

The use of the equations in tables 3 and 4 should be of assistance in controlling the composition of the cement and in regulating burning processes to produce clinker of the desired phase composition.

TABLE 4. *Equations for the calculation of the potential phase composition of clinker-type mixtures, assuming complete equilibrium crystallization to yield only the compounds indicated*

The formulas represent weight percentages of the corresponding compounds in the mixtures. In using the equations in part B (those for mixtures having R_2O/SO_3 molecular ratios greater than 1.0) the value of K_s should be calculated by the method outlined in table 3.

A. Mixtures having R_2O/SO_3 molecular ratios equal to or less than 1.0	
$3CaO.SiO_2$	$=4.0710\ CaO-7.6024\ SiO_2-6.7187\ Al_2O_3-1.4297\ Fe_2O_3+3.0820\ Na_2O+2.4238\ K_2O-2.8516\ SO_3$
$2CaO.SiO_2$	$=8.6024\ SiO_2+5.0830\ Al_2O_3+1.0784\ Fe_2O_3-2.7780\ Na_2O-1.8284\ K_2O+2.1511\ SO_3-3.0710\ CaO$
$3CaO.Al_2O_3$	$=2.6504\ Al_2O_3-1.6918\ Fe_2O_3$
$4CaO.Al_2O_3.Fe_2O_3$	$=3.0430\ Fe_2O_3$
$CaSO_4$	$=1.7005\ SO_3-2.1960\ Na_2O-1.4453\ K_2O$
Na_2SO_4	$=2.2914\ Na_2O$
K_2SO_4	$=1.8500\ K_2O$
B. Mixtures having R_2O/SO_3 molecular ratios greater than 1.0	
$3CaO.SiO_2$	$=4.0710\ CaO-7.6024\ SiO_2-1.4297\ Fe_2O_3-6.7187\ Al_2O_3+2.4238\ K_2O+3.0826\ Na_2O-2.8516\ SO_3$
$2CaO.SiO_2$	$=8.6024\ SiO_2+1.0784\ Fe_2O_3+5.0883\ Al_2O_3-23.769\ K_2O-2.7780\ Na_2O+2.1511\ (12K_s+1)\ SO_3-3.0710\ CaO$
$3CaO.Al_2O_3$	$=2.6504\ Al_2O_3-13.075\ Na_2O+10.123\ (1-K_s)\ SO_3-1.6918\ Fe_2O_3$
$4CaO.Al_2O_3.Fe_2O_3$	$=3.0430\ Fe_2O_3$
$K_2O.23CaO.12SiO_2$	$=22.345\ K_2O-26.288\ K_s\ (SO_3)$
$Na_2O.8CaO.3Al_2O_3$	$=13.170\ Na_2O-10.197\ (1-K_s)\ SO_3$
K_2SO_4	$=2.1764\ K_s\ (SO_3)$
Na_2SO_4	$=1.7743\ (1-K_s)\ SO_3$

The mixtures that have been the subject of investigation were designed to furnish data on the stability of the alkali compounds $K_2O.23CaO.12SiO_2$ and $Na_2O.8CaO.3Al_2O_3$ in the presence of SO_3 and on the equilibrium products resulting from heating mixtures of these components. These mixtures, while not in themselves of portland cement clinker composition, were composed of the primary components present in commercial clinker. Furthermore, the phases that appeared in the mixtures after equilibrium was attained were among those commonly found in commercial clinker. These factors provide the basis for applying the experimental data to portland cement technology.

It should be noted that other acidic oxides such as P_2O_5 or TiO_2 when present in the clinker may enter into reaction with the alkalies and otherwise alter the phase relations. The potential phase composition given in table 4 will then be affected. Likewise, the details of the phase relationships in the senary system K_2O-Na_2O-CaO-Al_2O_3-SiO_2-Fe_2O_3 are as yet unknown, although a study of this system is being implemented. It has been determined on the basis of microscopic examination of quenched charges containing $Na_2O.8CaO.3Al_2O_3$ and $K_2O.23CaO.12SiO_2$, that these two compounds are stable when heated together below 1,500°. These compounds have consequently been included in the list of compounds in table 4 (B). It is recognized, however, that a certain amount of solid solution may occur between them and the others that have been included in the potential phase composition. It is further recognized that changes in table 4 may be

necessitated as a result of the detailed study of pertinent portions of the indicated senary system.

The author expresses his appreciation for the assistance of Louis A. Dahl, Senior Research Mathematician of the Portland Cement Association, in the derivation of the equations appearing in this paper.

6. References

[1] L. T. Brownmiller and R. H. Bogue, Am. J. Sci. **23,** 501 (1932); PCAF Paper 25.

[2] K. T. Greene and R. H. Bogue, J. Research NBS **36,** 187 (1946) RP1699; PCAF Paper 47.

[3] W. C. Taylor, J. Research NBS **27,** 311 (1941) RP1421; PCAF Paper 40.

[4] W. C. Taylor, J. Research NBS **29,** 437 (1942) RP1512; PCAF Paper 43.

[5] W. C. Taylor, Unpublished PCAF Report (Jan. 20, 1944).

[6] W. R. Eubank, Unpublished PCAF Report (May 3, 1948).

[7] R. H. Bogue, The chemistry of portland cement, p. 229 (Reinhold Publishing Corp., New York, N. Y. (1947).

[8] Richard Nacken, Neues Jahrbuch für Mineralogie, Geologie, und Palaontologie **24,** part 1 (1907).

9] Louis A. Dahl, J. Phys. Coll. Chem. **52,** 698 (1948); PCAF Paper 51.

WASHINGTON, October 3, 1950.

Journal of Research of the National Bureau of Standards Vol. 47, No. 5, November 1951 Research Paper 2262

Resin Bonding of Offset Papers Containing Mineral Fillers

Martin J. O'Leary, Bourdon W. Scribner, and Joshua K. Missimer

Papermaking studies at the National Bureau of Standards have shown that melamine-formaldehyde resin used as a binding agent in offset lithographic papers containing no mineral fillers has the beneficial effects of improved printing quality, decrease in the beating time of the fibers, and large increase in permissible content of hardwood fibers. The last is desirable for the conservation of the scarcer softwood fibers.

The previous work has shown that as little as 1½ hours of beating gives satisfactory results with the usual 50 percent of hardwood fibers increased to 75 percent, when 1 to 3 percent of melamine resin is added.

Further investigation has been made to determine whether these beneficial effects occur when the mineral fillers, clay and titanium dioxide, are used. With 1½ hours of beating of a fiber furnish consisting of 75 percent of soda pulp (hardwood fibers) and 25 percent of sulfite pulp (softwood fibers) 15 percent of clay made the papers too soft for lithographic papers, lowering all of their desirable physical properties. The addition of the melamine resin had little or no beneficial effect on these papers. However, with a 50-percent-sulfite, 50-percent-soda, 15-percent-clay furnish, the physical properties were improved by the addition of 3 percent of melamine resin, resulting in good lithographic papers. The clay retention was lowered slightly by the addition of 3 percent of melamine resin, and more so with 1 percent of melamine resin. When the stock was given 5½ hours of beating, the melamine resin was of assistance in producing improved lithographic papers made from 75 percent of soda pulp and 25 percent of sulfite pulp.

When 3 percent of titanium dioxide was added to both 50-percent soda, 50-percent sulfite, and 75-percent soda, 25-percent sulfite furnishes with 5½ hours of beating and 1 or 3 percent of melamine resin added, satisfactory offset papers were produced. The retention of the titanium dioxide was decreased somewhat by the resin.

As reported in an earlier publication, the retention of both fillers was improved by using an excess of aluminum sulfate and adjusting the stock to the desired pH with sodium carbonate.

1. Introduction

Previous investigations in the paper mill of the National Bureau of Standards on the use of melamine-formaldehyde resin as a binding agent in offset papers, have shown that the resin imparted better printing quality, decreased the beating time required for the fibers, and permitted the use of a greatly increased proportion of hardwood fibers in the papers. As little as 1½ hours of beating gave satisfactory results with the usual 50 percent of the short, weak hardwood fibers increased to 75 percent. [1, 2][1] The use of the larger content of hardwood fibers is desirable for the conservation of the scarcer softwood fibers.

In the previous work, no mineral filler was used. This is a desirable component because it fills the interstices between the fibers of paper and imparts a better finish and higher opacity, all of which are favorable for improved printing quality. This article gives the results of an investigation of the influence of mineral fillers on the beneficial effects of the binding resin, and the effect of the resin on the retention of the fillers in the paper.

2. Experimental Papermaking Equipment

The papermaking equipment at the Bureau is semicommercial in size and is adapted to the experimental manufacture of papers under conditions that simulate those of typical industrial plants. Detailed description and photographs of the essential equipment are contained in previous publications [3, 4].

The equipment used in this work consisted essentially of a 50-lb beater with a copper-lined wooden tub and manganese-bronze bars and plate; a jordan refiner with bars of bronze and steel alloy; a four-plate, flat screen and a 29-in. fourdrinier papermaking machine with a wire 33 ft in length; two presses; nine 15-in. dryers; a machine calender stack of seven rolls; a reel; a supercalender with 5 rolls; 3 steel rolls; 2 cotton rolls; and a 38-in. trimmer.

3. Papermaking Raw Materials

Different percentages of the following commercial pulps were used in this study: (1) Bleached sulfite, made by cooking Eastern spruce wood, a softwood, in a solution or calcium bisulfite. This is a relatively standard quality of pulp such as is commonly used for offset paper. (2) Bleached soda, a filler pulp produced by cooking poplar wood, a hardwood, in a strong solution of caustic soda. This is an unusually strong soda pulp for a short fibered stock.

The chemical characteristics of the pulps used are shown in table 1.

The fillers were 15 percent of clay and 3 percent of titanium dioxide. Their chemical compositions are given in table 2. The fillers were mixed with water and screened through an 80-mesh wire to remove dirt or foreign ingredients.

[1] Figures in brackets indicate the literature references at the end of this paper.

TABLE 1. *Test data on pulp used in experimental papers*

Kind of pulp	Alpha cellulose [a]	Beta cellulose [a]	Gamma cellulose [a]	Pentosans	Copper number	Ash [b]	Natural resin [b]	Acidity (glass electrode), hot water extraction
	%	%	%	%		%	%	
Sulfite	85.2	3.5	11.3	3.5	1.4	0.20	0.42	pH 6.6
Soda	79.7	17.7	2.6	15.3	1.5	1.80	.38	8.4

[a] Based on total cellulose.
[b] Oven dry basis.

TABLE 2. *Composition of fillers used*

Fillers	Loss at 105° C	Further loss on ignition	SiO_2	Fe_2O_3	Al_2O_3	TiO_2
	%	%	%	%	%	%
Clay	0.3	13.8	45.3	0.2	38.8	1.8
Titanium dioxide	None	.15	None	None	None	98.2

The retention of the fillers in the paper was determined by the formula

$$\text{Retention}=\frac{0.94B(100-C-A)}{A(100-C-B)},$$

in which

A = percentage of ash in oven-dry stock going to machine;
B = percentage of ash in oven-dry paper at reel;
C = percentage of oven-dry filler lost on ignition.

One-percent rosin size precipitated with aluminum sulfate was used on all the runs.

Melamine-formaldehyde resin 607 of the American Cyanamid Co. was used as the binding agent.

All percentages of materials added to the pulp are based on the oven-dry (110° C) weight of the pulp.

4. Manufacturing Procedure

Fifty pounds of fibers was furnished to the beater in each instance. When clay was added, the fibers were 85 percent, and the clay was 15 percent of the furnish, making a total of 58.8 lb in the beater.

When titanium dioxide was used, 97 percent of the furnish was fibers and 3 percent titanium dioxide, making a total of 51.55 lb.

An excess of alum was used when a filler was furnished to the beater, because it was found in the study of experimental manufacture of paper for war maps [5], that by adding an excess of alum and then adjusting the pH with sodium carbonate, the retention of the pigment was increased resulting in a decided improvement in the opacity of the paper. A minimum and a medium beating time were used. A detailed description of the roll setting may be found in a previous publication on offset papers [6].

With the minimum beating time, 1½ hours, the stock received a mixing just long enough to thoroughly separate the fibers and give fillers, size, and alum a good mixing. Such treatment does not develop strength in the paper.

With the medium beating time, 5½ hours, the stock received a light brushing for ½ hour. This treatment slightly frays out the fibers, causing them to interlace better in forming a sheet of paper. It also makes the surface a little harder, which helps to minimize fuzz.

A longer beating time creates a gelatinous substance on the fibers. It also makes a hard, brittle sheet of paper. The more gelatinous substance that is combined with the finished paper, the more the paper will expand when it becomes wet and contract when it dries. This expansion and contraction of the paper cause misregister in offset lithographic printing.

The beaten stock was dropped to the chest and pumped in a continuous stream through the stuff box into the jordan.

The stuff box is divided into three compartments: one section receives the stock from the pump; the second compartment has a gate that regulates the desired amount of stock delivered to the machine per hour; the third section receives the surplus stock, which then returns to the machine chest.

The jordan was used only for mixing the fibers with the same setting for all runs.

From the jordan the stock drains into a fan pump and is mixed with the white water from the paper machine. The mixture is then pumped to a riffle box that contains several baffle boards. The stock flows over these baffle boards, and the heavy particles, such as sand, metal, etc., settle to the bottom of the box. From the riffle box the stock flows through a screen with slots cut 0.018 in., thence to the headbox onto the wire.

Melamine-formaldehyde resin was added in the form of a colloidal solution, made by dissolving the powdered resin in warm water acidified with hydrochloric acid.

The formula used in this study was submitted in 1943 by the American Cyanamid Co.

> 39 pounds of 20° Be hydrochloric acid is added to 50 gallons of water and heated to 140° F; 100 pounds of melamine resin 607 is added slowly to the acid solution while stirring; the resin solution is added to cold water to make a total volume of 100 gallons.

The resin was added at the screen hopper, after the stock had left the screens and before the head box. There are two reasons for adding the resin at this particular place; first, melamine resin has an affinity for dirt, therefore, it should be added at a point after the dirt has been removed; second, melamine resin should have the minimum amount of agitation to obtain the maximum efficiency of wet strength in the paper, but should be added at a point where the resin will have time to obtain uniform distribution in the stock before it flows onto the wire. The temperature of the stock was maintained at 90° ±2 deg F. One percent of rosin size was used in each of the papers. It was precipitated with papermaker's alum, $Al_2(SO_4)_3$, which was used to control the pH of the stock.

The finish imparted by the small machine calenders was low, therefore a light supercalendering of the paper was necessary, so that the finish would be comparable to that of commercial papers.

5. Testing

All physical and chemical tests of the pulps and papers were made in accordance with the standard methods of The Technical Association of the Pulp and Paper Industry.[3]

The pH of mill waters at the beater, stuff box, and head box was determined with a glass electrode.

6. Interpretation and Discussion of Test Data

To enable the reader to interpret the graphs more clearly, a dividing line has been drawn through the graphs. All test results above the line are considered good and all those below the line, poor.

Some of the important tests are the pick, expansion, oil penetration, opacity, curl, tear, bursting strength, and folding endurance. It is impossible to develop a paper whose characteristics are good in all respects. In order to develop a paper with a low curl, low expansion, and a low oil penetration time, which are essential in lithographic papers, the process usually adversely affects the strength and pick. A low pick causes much trouble in lithographic printing because the printing blanket picks bunches of fibers from the paper and in a short time the blanket and plate fill up, necessitating a shutdown to clean the press. According to Robert F. Reed and James J. Spevecak [7], "Bond strength is measured by the wax pick test, and a pick of six or better is generally conceded to be necessary". Using this statement as a base, a wax pick of 6A was placed on the line; therefore, any pick test shown above the line will be considered good, and any test shown below the line, poor.

The pick, bursting strength, and folding endurance correlate. When the pick increases, the bursting strength and folding endurance increase also, and vice versa. An average was taken of the bursting strength, tensile strength, tearing strength, and folding endurance for the six papers in table 3 having a pick of 6A, and the average values were placed on the line also. They are comparable to those of book papers when clay is used. The other values on the median line are based on the previous investigations of offset papers by the Bureau [8].

7. Results of Tests

The test data for the experimental papers are given in table 3 and shown graphically in the figures.

Figure 1 shows the results obtained with a furnish of 75 percent of strong soda pulp and 25 percent of Eastern sulfite pulp; beating time was 1½ hours. This furnish, with melamine added, was found satisfactory in the previous work. Fifteen percent of clay, an amount normally used for offset papers, softened the paper and adversely affected the desirable physical properties of folding endurance, pick, and bursting and tensile strengths. Also, the clay resulted in lint or fuzz on the wire side of the paper, the side next to the paper machine wire. The fuzz and the pick correlate—the lower the pick, the more

[3] Available from the Association headquarters at 122 East Forty Second Street, New York 17, N. Y.

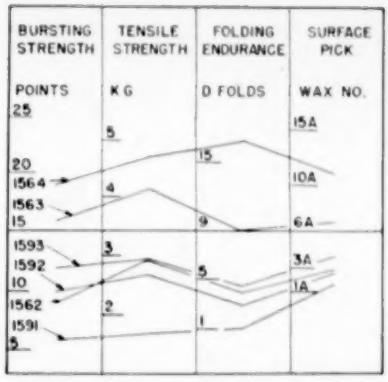

FIGURE 1. *Effects of melamine resin on physical properties of papers containing clay filler*

Pulp: 75-percent soda, 25-percent sulfite; beating time 1½ hours.
1562, No M, no clay; 1564, 3% M, no clay; 1592, 1% M, 15% clay
1563, 1% M, no clay; 1591, No M, 15% clay; 1593, 3% M, 15% clay

fuzz occurs on the paper. The cause of fuzz, in most cases, is a free under-beaten stock. This gives the paper a soft surface. The greater part of the surface friction is on the wire side, and this friction causes the loosely bound fibers to fluff up on that side. The clay has the same effect on the paper in these respects as unbeaten free stock.

The addition of 3 percent of melamine resin in the absence of clay (run 1564) increased the bursting strength 100 percent, folding endurance 300 percent, tensile strength 55 percent, and the pick about 300 percent, compared to paper made without resin and clay (run 1562). However, the paper made with 15 percent of clay and 3 percent of melamine resin (run 1593) had physical properties comparable to those of the paper made without resin and clay (run 1562). Papers with such low physical properties would not be suitable for lithographic papers because of the tacky ink that is used in lithographic printing. The blanket would pick bunches of fibers from the paper, and in a short time the blanket and plate would be filled up, necessitating a shutdown to clean the press. The clay had little effect on the tear. The retention of clay was lowered considerably with 1 percent of the resin (run 1592) but only slightly when 3 percent was used (run 1593).

Figure 2 shows the results for a series of papers made with 50 percent of strong soda pulp and 50 percent of Eastern sulfite pulp with a beating time of 1½ hours. Comparing the clay-free papers (runs 1540, 1560, and 1561) with the corresponding papers made with 15 percent of clay (runs 1594, 1595, and 1596), the tests show that the clay again had a deleterious effect. However, the 3 percent of melamine resin (run 1596) strengthened the paper containing the clay to a degree that made it satisfactory for lithographic printing, as it had good pick, low expansion, low oil penetration time, low curl, and good bursting strength. The paper made with 15 percent of clay required 1 percent of melamine resin (run 1595) to bring the physical properties

TABLE 3. *Comparative data on effect of melamine-formaldehyde resin on offset papers containing mineral fillers* [a]

Run	Beating time	Beater furnish: Pulp	Beater furnish: Filler: Kind	Beater furnish: Filler: Amount	Beater furnish: Melamine resin	Retention of resin	Basis weight, 25×40 inches (500 sheets)	Thickness	Bursting strength	Folding endurance (double folds) MIT (tension 1 kg): Machine	Folding endurance (double folds) MIT (tension 1 kg): Cross	Tensile strength: Machine	Tensile strength: Cross	Tearing resistance: Machine	Tearing resistance: Cross	Expansivity (15% change in relative humidity): Machine	Expansivity (15% change in relative humidity): Cross	Opacity (contrast ratio)	Smoothness (Bekk)	Pick (Dennison wax)	Oil penetration	Air permeability	Curl	Acidity (hot water) extraction	Ash in beater stock	Ash in paper	Retention of filler
	hr			%	%	%	*lb*	*in.*	*Pt*			*kg*	*kg*	*g*	*g*	%	%	%	*sec*	*No.*	*sec*	*sec*	*deg*	pH	%	%	%
1562	1½	25% bleached sulfite, 75% bleached strong soda.	None				53.2	0.0034	9	4	4	3.3	2.5	47	49	0.05	0.12	91	148	3A	36	32	32	5.0			
1563	1½	do	do		1	81	54.0	.0033	16	10	8	4.8	3.5	46	47	.05	.13	90	147	7A	36	38	33	5.1			
1564	1½	do	do		3	84	54.3	.0033	19	18	16	5.4	4.0	46	44	.05	.14	89	151	11A	38	46	35	5.1			
1591	1½	do	Clay[b]	15			52.4	.0034	6	1	1	2.1	1.3	45	45	.05	.12	91	114	−2A	27	21	22	4.9	14.0	11.4	74
1592	1½	do	do	15	1	75	54.5	.0031	10	4	2	3.3	2.1	42	50	.05	.13	91	258	3A	36	48	30	4.6	13.9	10.7	69
1593	1½	do	do	15	3	70	54.2	.0034	12	5	4	3.4	2.4	43	44	.05	.13	91	180	4A	33	43	30	4.7	13.6	11.1	72
1540	1½	50% bleached sulfite, 50% bleached strong soda.	None				54.8	.0040	12	6	4	3.7	2.6	61	63	.05	.13	88	64	3A	34	22	31	4.5			
1560	1½	do	do		1	93	54.4	.0036	17	15	12	4.7	3.3	57	58	.06	.14	87	79	10A	28	29	36	5.2			
1561	1½	do	do		3	70	53.6	.0031	20	29	21	5.9	3.8	46	44	.06	.15	87	166	11A	41	48	43	4.8			
1594	1½	do	Clay	15			54.6	.0032	9	3	2	2.7	1.7	53	60	.05	.10	89	254	2A	40	42	28	5.2	13.6	11.0	74
1595	1½	do	do	15	1	83	52.5	.0031	11	6	3	3.3	2.0	48	56	.05	.13	89	178	3A	31	38	25	4.8	13.9	10.0	64
1596	1½	do	do	15	3	74	54.6	.0032	14	10	8	4.1	2.7	46	49	.05	.15	90	235	7A	40	60	34	4.7	13.4	10.6	72
1621	5½	do	None				55.4	.0039	16	12	8	4.9	2.9	63	61	.05	.14	88	58	3A	44	35	36	4.2			
1622	5½	do	do		1	81	54.3	.0037	21	38	22	6.3	3.8	52	51	.06	.16	87	73	10A	38	41	44	4.6			
1623	5½	do	do		3	77	52.8	.0035	24	63	38	6.7	4.3	48	45	.07	.17	86	59	11A	43	43	43	4.5			
1616	5½	do	Clay	15			54.8	.0034	11	5	4	3.9	2.1	53	58	.05	.15	90	163	2A	49	65	41	4.3	14.0	12.2	78
1617	5½	do	do	15	1	73	54.7	.0036	14	9	5	4.1	2.4	50	55	.05	.15	90	83	6A	48	54	41	4.4	14.6	11.7	72
1599	5½	do	do	15	3	73	53.8	.0031	17	16	11	5.2	3.0	42	40	.06	.16	90	164	8A	65	82	46	4.7	15.7	12.3	70
1605	5½	do	TiO_2[c]	3			53.2	.0034	16	12	6	5.1	2.7	48	51	.06	.17	91	111	6A	50	58	56	4.6	4.2	4.3	95
1620	5½	do	TiO_2	3	1	75	54.9	.0036	19	24	14	5.9	3.3	51	53	.05	.16	91	75	7A	61	58	42	4.2	4.4	4.0	84
1607	5½	do	TiO_2	3	3	67	53.5	.0035	22	34	21	6.3	3.9	44	44	.06	.17	92	90	11A	45	68	53	4.5	4.7	4.0	79
1624	5½	25% bleached sulfite, 75% bleached strong soda.	None				54.1	.0039	12	6	4	4.2	2.5	58	59	.06	.15	89	59	2A	31	21	32	4.2			
1625	5½	do	do		1	75	53.8	.0038	19	15	10	4.9	3.4	56	54	.07	.15	89	54	6A	29	22	34	4.3			
1626	5½	do	do		3	76	56.1	.0039	22	27	21	5.9	4.3	52	47	.07	.16	90	49	9A	31	26	35	4.7			
1618	5½	do	Clay	15			54.9	.0036	10	3	2	3.3	1.9	47	49	.05	.14	92	111	3A	41	44	37	4.3	14.4	12.5	80
1619	5½	do	do	15	1	86	54.9	.0034	13	6	4	4.0	2.4	51	52	.05	.14	92	165	6A	55	65	43	4.4	14.6	11.9	74
1598	5½	do	do	15	3	78	52.9	.0030	15	8	6	4.5	2.7	35	37	.06	.18	90	182	7A	48	72	61	5.3	14.7	12.1	75
1608	5½	do	TiO_2	3			53.6	.0038	14	7	4	4.2	2.7	46	50	.06	.18	94	103	5A	42	46	52	4.6	4.9	4.7	89
1609	5½	do	TiO_2	3	1	75	53.9	.0037	17	12	8	5.7	3.3	43	40	.06	.17	93	89	6A	49	51	49	4.5	4.9	4.5	85
1610	5½	do	TiO_2	3	3	70	55.1	.0037	19	16	10	5.8	3.5	42	42	.07	.18	94	80	8A	51	56	44	4.7	5.0	4.2	78

[a] All physical tests made under condition of 50-percent relative humidity and 73°F., by the Standard Methods of the Technical Association of the Pulp and Paper Industry.

[b] Beater furnish for each run with clay was 85 percent fibers and 15 percent clay.

[c] Beater furnish for each run with TiO_2 was 97 percent fibers and 3 percent TiO_2.

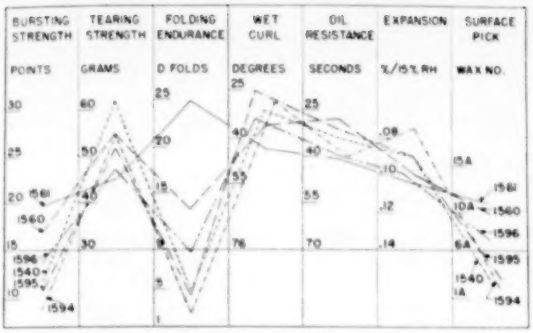

FIGURE 2. *Effects of melamine resin on physical properties of papers containing clay filler.*

Pulp: 50-percent soda, 50-percent sulfite; beating time, 1½ hours.

1540, No M, no clay
1560, 1% M, no clay
1561, 3% M, no clay
1594, No M, 15% clay
1595, 1% M, 15% clay
1596, 3% M, 15% clay

up to those of the paper made without clay and resin (run 1540).

The melamine resin had an adverse effect on the tearing resistance in this series of papers (fig. 2). The retention of clay was about the same as in the preceding series.

To offset the low physical properties caused by the addition of clay, fibers of the remaining runs were given the medium beating of 5½ hours with a light brushing. In runs using 15 percent of clay without resin with 50-percent sulfite, 50-percent soda and 25-percent sulfite, 75-percent soda furnishes, the 5½-hours beating did not improve the physical properties to any appreciable extent. The clay retention was increased somewhat.

Figure 3 shows a comparison of the effects of the 1½ (run 1595) and 5½ (run 1617) hours of beating for papers made with 50 percent of sulfite pulp, 50 percent of soda pulp, 15 percent of clay, and 1 percent of melamine resin. The figure shows that even with 5½ hours beating the paper would be on the borderline for a good lithographic paper. However, the advantages of the latter paper were a 100-percent improvement in the wax pick and a minimum of fuzz. Figure 4 shows that the addition of 3 percent of melamine resin (run 1599) made a good lithographic paper with improved physical properties compared to those of papers made with 1 percent of melamine resin (run 1617) or no resin (run 1616). The retention of clay was better than that of the preceding two series, figures 1 and 2.

Figure 5 shows comparison tests of 5½ hours of beating time, 75-percent soda, 25-percent sulfite, using a filler.

Figure 6 shows the results for papers made with 25 percent of sulfite pulp, 75 percent of soda pulp, 3 percent of titanium dioxide, and 0 (run 1608), 1 (run 1609), and 3 (run 1610) percent, respectively, of melamine resin; beating time was 5½ hours. The physical properties of the resin-free paper (run 1608) were below average for a good lithographic paper, but the retention of the titanium dioxide was high. The melamine resin improved the physical properties in

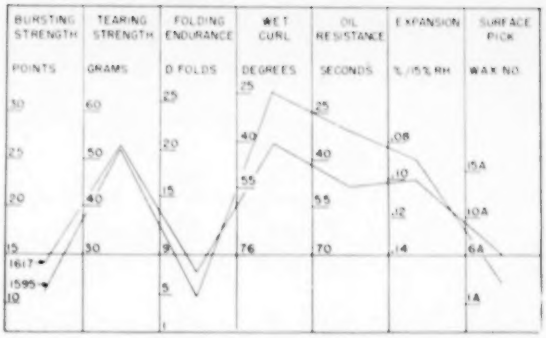

FIGURE 3. *Comparison of effects of beating times of 1½ and 5½ hours.*

15-percent clay, 1-percent melamine resin; pulp: 50-percent soda, 50-percent sulfite.

1595, beating time, 1½ hours
1617, beating time, 5½ hours

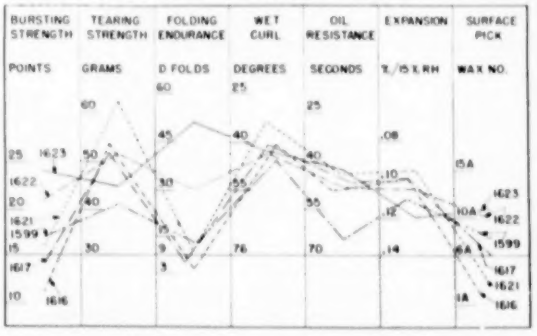

FIGURE 4. *Effects of melamine resin on physical properties of papers containing clay filler.*

Pulp: 50-percent soda, 50-percent sulfite; beating time: 5½ hours.

1621, No M, no clay
1622, 1% M, no clay
1623, 3% M, no clay
1616, No M, 15% clay
1617, 1% M, 15% clay
1599, 3% M, 15% clay

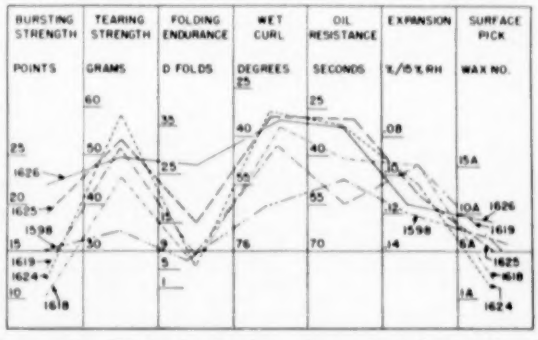

FIGURE 5.—*Effects of melamine resin on physical properties of paper containing clay filler.*

Pulp: 75-percent soda, 25-percent sulfite; beating time: 5½ hours.

1624, No M, no clay
1625, 1% M, no clay
1626, 3% M, no clay
1618, No M, 15% clay
1619, 1% M, 15% clay
1598, 3% M, 15% clay

both runs and made these papers satisfactory lithographic papers with good folding endurance, bursting strength, tensile strength, and wax pick. The melamine resin again had an adverse effect on the retention of the filler. As the amount of resin

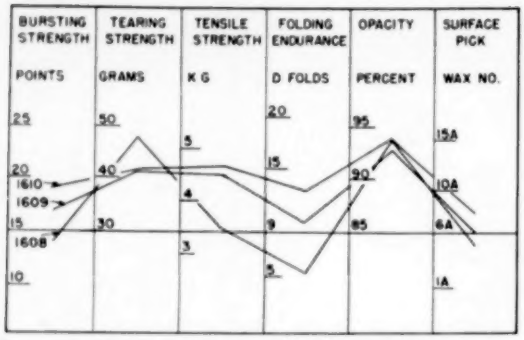

FIGURE 6. *Effects of melamine resin on physical properties of papers containing titanium dioxide filler.*

Pulp: 75-percent soda, 25-percent sulfite; beating time: 5½ hours.
1608, no M, 3% TiO_2
1609, 1% M, 3% TiO_2
1610, 3% M, 3% TiO_2

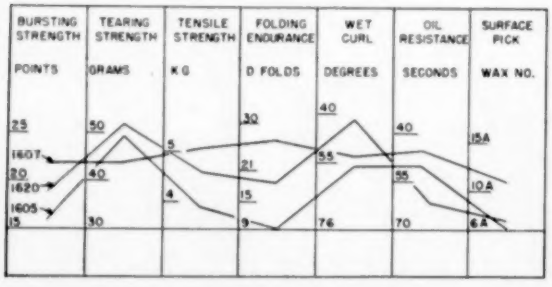

FIGURE 7. *Effects of melamine resin on physical properties of papers containing titanium dioxide filler.*

Pulp: 50-percent soda, 50-percent sulfite, beating time: 5½ hours.
1605, No M, 3% TiO_2
1620, 1% M, 3% TiO_2
1607, 3% M, 3% TiO_2

was increased, the retention of filler decreased inversely; however, the opacity was not affected.

Figure 7 shows the results for papers made with 50 percent of sulfite pulp, 50 percent of soda pulp, 3 percent of titanium dioxide, and 0 (run 1605), 1 (run 1620), and 3 (run 1607) percent, respectively, of melamine resin; beating time was 5½ hours. All three runs made good lithographic papers. The paper with 3 percent of melamine resin meets all the requirements of good lithographic papers, having high folding endurance, bursting strength, tensile strength, and pick number, and a low oil penetration time and curl.

8. Summary

When a beating time of 1½ hours was employed, 15 percent of clay had an adverse effect on the desirable physical properties of papers made with 75 percent of soda pulp and 25 percent of sulfite pulp; the addition of 3 percent of melamine resin did not result in the production of satisfactory papers. The clay weakened the paper, and made it softer, therefore fuzzier. The latter condition would cause trouble on the lithographic printing presses, filling the printing blanket and plate and thus necessitating frequent shutdowns to clean the press. However, when equal parts of soda and sulfite pulps were used, satisfactory papers resulted when 3 percent of melamine resin was used. The retention of clay was lowered considerably when 1 percent of melamine resin was used, but only slightly with 3 percent of the resin.

When the beating time was increased to 5½ hours, satisfactory papers were obtained from both 75-percent-soda, 25-percent-sulfite and 50-percent-soda, 50-percent-sulfite furnishes, containing 15 percent of clay and 3 percent of melamine resin. Also, the clay retention was improved somewhat.

When 3 percent of titanium dioxide was used as filler, good lithographic papers were obtained from both 75-percent-soda, 25-percent-sulfite and 50-percent-soda, 50-percent-sulfite furnishes, containing 1 and 3 percent, respectively, of melamine resin with 5½-hour beating time. The retention of the titanium dioxide decreased inversely as the melamine resin increased. The titanium dioxide improved the opacity considerably.

The authors are indebted to Thelma L. Worksman, Ruth E. Dowden, and Alice A. Padgett for the tests of the experimental papers, and to James J. Erving for assistance in the papermaking.

This investigation and the previous investigations dealing with offset papers were conducted with the counsel of an advisory committee of technicians of the papermaking and printing industries, under the chairmanship of R. F. Reed, Research Consultant, Lithographic Technical Foundation.

9. References

[1] Charles G. Weber, Merle B. Shaw, Martin J. O'Leary, and Joshua K. Missimer, Resin bonding and strength development in offset papers, J. Research NBS **40,** 427 (1948) RP1887.

[2] Bourdon W. Scribner, Merle B. Shaw, Martin J. O'Leary, and Joshua K. Missimer, Resin bonding of hardwood fibers in offset paper, J. Research NBS **45,** 208 (1950) RP2126.

[3] M. B. Shaw, Equipment and research work of the Bureau of Standards paper mill, Paper Trade J. **89,** No. 19, 60 (1929).

[4] Merle B. Shaw and Martin J. O'Leary, Study of the effects of fiber components on the stability of book papers, J. Research NBS **17,** 859 (1936) RP949.

[5] Charles G. Weber and Merle B. Shaw, Experimental manufacture of paper for war maps, J. Research NBS **37,** 328 (1946) RP1751.

[6] Charles G. Weber, Merle B. Shaw, Martin J. O'Leary, and Joshua K. Missimer, Resin bonding and strength development in offset papers, J. Research NBS **40,** 429 (1948) RP1887.

[7] Robert F. Reed and James J. Spevecak, Offset papers, Nat. Lithographer **56,** No. 6, 46 (June 1949).

[8] Charles G. Weber, Merle B. Shaw, Martin N. Geib, and Martin J. O'Leary, An experimental study of beater practice in the manufacture of offset papers, J. Research NBS **30,** 267 (1943) RP1532.

WASHINGTON, April 30, 1951.

Journal of Research of the National Bureau of Standards Vol. 47, No. 5, November 1951 Research Paper 2263

A Method for Corn-Sirup Analysis Involving Selective Adsorption

Emma J. McDonald and Roger E. Perry, Jr.

A chromatographic method is described for the separation of corn sirups into dextrose, maltose, and dextrin fractions. The sample is adsorbed on a Darco column; separation of the components is effected by using water, a 5-percent-ethanol-in-water solution and a 15-percent-ethanol-in-water solution as eluting media. Pressure is used to increase the flow rate.

1. Introduction

The separation of carbohydrate mixtures on columns of carbon has received wide application in the isolation and purification of sugars during the past 5 years.[1] Tiselius [1],[2] using charcoal as an adsorbent, separated mixtures containing glucose and lactose, glucose and sucrose, and maltose and sucrose by elution with 0.5-percent phenol or 0.5-percent ephedrine. Claesson [2] separated mixtures of glucose, sucrose, and raffinose by a similar procedure. Montgomery, Weakley, and Hilbert [3] isolated 6-[α-D-glucopyranosyl]-D-glucose by chromatographic adsorption on Darco and selective elution of the enzymatic hydrolyzate of starch. As eluting agents these authors used water to remove the glucose and 0.5-percent phenol to remove the disaccharide. Whistler and Durso [4] reported the selective elution of mono-, di-, and trisaccharides from Darco columns by means of water and water-ethanol mixtures. Selective adsorption and elution permit isolation of the individual sugars of a carbohydrate mixture.

The extensive use of sugar mixtures in food products has resulted in an increasing demand for more accurate and more rapid analytical methods in this field. Hydrol, the molasses of the dextrose industry; lactose, sucrose, and dextrose mixtures as found in infant foods, and liquid sugars of the sucrose industry are typical of these products.

The methods that are available for the analysis of corn sirups are unsuitable both because of the time required to carry them out and the unsatisfactory results obtained. These methods are based on the selective fermentation of dextrose in the presence of maltose and dextrins, or the selective reduction of a copper acetate solution by dextrose. The advantage offered by the procedure reported in this paper is that the dextrose and maltose are isolated and can then be determined as pure sugars. This separation of the sirup into its components is rapidly accomplished by passing the eluting agents through the column under 30 to 50 pounds of pressure. Satisfactory separation of dextrose, maltose, and dextrins can be accomplished in approximately 1½ hours.

[1] A general discussion of the selective adsorption of sugars and their derivatives is given in Chromatography of sugars and related substances by W. W. Binkley and M. L. Wolfrom, Scientific Report Series No. 10 (Sugar Research Foundation, Inc., New York, N. Y., 1948).

[2] Figures in brackets indicate the literature references at the end of this paper.

2. Experimental Details

The columns are Pyrex tubing of 34-mm inside diameter (fig. 1). One standard length of glass (120 cm) holds a column of adsorbent 200 mm high, together with 900 ml of solution. One end of the tube is drawn down to a nipple about 3 cm long and 8 mm in diameter. To the other end is sealed a short length of Pyrex pipe, flanged on its free end. Connection to the pressure system is made with aluminum flanges sold by the manufacturer for use with Pyrex piping. One flange fits around the end of the column, and the other grips a piece of brass stock machined to the proper size and taper; through it is fed the one-quarter-in. copper tubing that connects to the reducing valve of the tank of nitrogen. A gasket of Koroseal separates the glass and brass surfaces at the joint. The copper tubing system is equipped with such valves as may be desirable for proper control of pressure. For simultaneous operation of the two columns it has been found convenient to have a cutoff

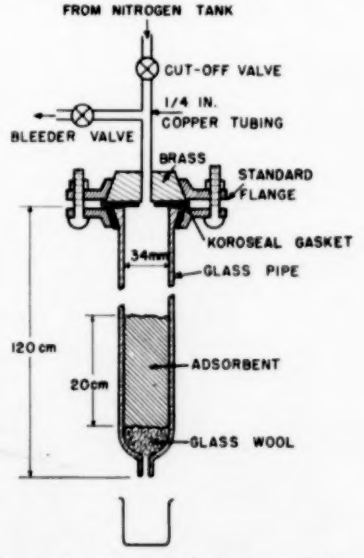

FIGURE 1.—*Diagram of column assembly.*

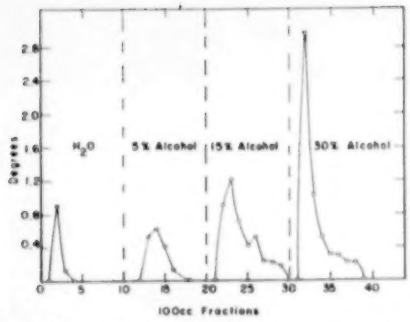

FIGURE 2. *Polarimetric analysis of a corn sirup.*

valve and a bleeder valve for each column. Since as much as 50 lb/in.^{2} of pressure is applied, the columns are incased in an easily applied shield of split copper tubing.

To fill the column a glass wool plug is placed at the bottom, and the tip of the column is then immersed in water so that the plug is thoroughly wet. This prevents the carbon particles from running through the glass wool during filling of the column. The adsorbent, composed of equal weights of Darco [3] 60 (analytical grade) and Celite, is then poured into the column to a height of about one and one half times that desired for operation. It is packed by tapping lightly. The copper casing is then put in place, and connection to the pressure system is made. The column is washed with 2 or 3 liters of water. When the water level reaches that of the adsorbent, the pressure is released and the sugar sample added.

The sample to be analyzed is dissolved in 20 to 50 ml of water and added to the column. After the walls have been washed free of any adhering sugar solution, sufficient time is allowed for the level of the solution to reach that of the adsorbent; this may be accomplished either with or without increased pressure. About 900 ml, or one column, of water is then added. In preliminary experiments 100-ml samples of the eluted solution are collected and the optical rotation of the individual fractions taken. This locates the fractions where dextrose, and subsequently maltose, may be expected to appear. Six hundred milliliters has been found adequate for removal of the dextrose; the remaining 300 ml acts as a safety factor. Figure 2 is illustrative of such a run. Pressure is then released from the column, 900 ml of 5-percent ethanol [4] is added, and the maltose is separated from the dextrins. The dextrins are then removed with more concentrated alcohol solution. Fifteen- and 30-percent alcohol fractions were collected in some experiments; however, a single fraction for dextrins seems sufficient. Upon completion of the run the column is cleaned with 95-percent alcohol; this has been found to remove all traces of carbohydrates. The alcohol is then washed out by a column length of water, and the apparatus is ready for the next run.

As a general procedure it is desirable to collect the entire amount of each eluate in a single fraction, evaporate it under diminished pressure to a volume that can be made up to 100 ml, and make duplicate determinations on aliquot portions. This permits fewer analyses on a given fraction and larger quantities of sugar in each determination.

3. Results

A series of analyses of dextrose-maltose mixtures of known composition was made in order to ascertain the accuracy of the method. The recovery of sugar obtained in these determinations is given in table 1. It was found that the percentage recovery was not effected when pressures up to 50 lb/in.^{2} were used to increase the rate of flow of the eluting agents; higher pressures were not investigated. It is suggested that a correction factor be determined by analyzing a known dextrose-maltose mixture under the same experimental conditions that are to be used for the sirup analysis. This factor will be in the range of 3 percent of the weight of each sugar and will be a function of the individual column and the eluting agent.

Paper chromatographs indicated that the dextrose, maltose, and dextrin fractions as separated were not contaminated with the other sugars present in the dextrose-maltose mixtures or sirups. The chromatographs were run by the method described by Partridge [5]. The solvent consisted of ethyl acetate 250, pyridine 70, and water 85 parts by volume. The chromatographs were run 16 to 24 hours on Whatman No. 1 filter paper. Ammoniacal silver nitrate solution was sprayed on the air-dried paper to indicate the position of the sugars.

TABLE 1. *Separation of dextrose-maltose mixtures on Darco*

Method of analysis	Dextrose			Maltose		
	Present	Found	Recovery	Present	Found	Recovery
	g	*g*	*Pct.*	*g*	*g*	*Pct.*
Polarization	{0.5021	0.4803	95.66	0.5010	0.4781	95.4
	{1.0004	.9606	96.02	1.0040	.9458	94.2
Average			95.7			94.8
Munson and Walker reducing sugar method.	{.6082	.5801	95.39	.6416	.6323	98.55
	{.3410[5]	.3229	94.68	.3502	.3393	96.03
	{.2736	.2748	100.40	.4450	.4353	97.82
	{.2736	.2608	95.35	.4450	.4275	96.07
Average			96.45			97.12

After separation of the sugars on the column, analyses of the respective fractions were made either by direct polarization or by Munson and Walker's reducing sugar method. There appears to be no relation between the size of the sample and the percentage recovery, showing that all samples are within the loading capacity of the column. In general, it may be said that the reducing sugar method is the more accurate means of analysis.

[3] Darco is a vegetable carbon manufactured by the Darco Corp., New York, N. Y. Celite is a diatomaceous earth product manufactured by Johns Manville Corp., New York, N. Y.

[4] 5.2 ml of 95-percent alcohol per 100 ml of solution.

Here an error of ±0.3 percent is to be expected, while in the case of polarimetric analysis an error of ±0.05 degrees in reading the polarimeter appears as an error of 1.7 percent in the determination of 0.5 g of dextrose in 100 ml of solution (4-dm polarimeter tube).

When cocoanut char was used in place of Darco, it was found that the dextrose was removed quantitatively by 5-percent aqueous alcohol and the maltose by 10-percent alcohol. However, when samples of corn sirups were introduced, the maltose and dextrins were not sharply separated. Further studies with eluting agents are required with this char. Norit also requires 5-percent alcohol to remove the dextrose, and here again the separation is not sharp when sirups are introduced.

Six corn sirups were separated on Darco columns, the final analysis being made by both Munson and Walker's method and by use of a polarimeter. Their dextrose equivalents, as determined by Lane and Eynon's method, ranged from 30.6 to 80.7 based on total solids. The dextrins are reported as dextrose equivalents in the reducing sugar procedure, and in degrees of rotation per gram of sirup in the polarization analysis; it is not to be expected that the results obtained by the two methods of analysis will be interconvertible. It is noteworthy that the dextrins possess considerable reducing power when Fehling solution is used as in the method of Munson and Walker. The results of the analysis of the six sirups are summarized in table 2.

TABLE 2. *Corn sirup analysis by use of Darco-Celite columns*

Sirup	Dextrose equivalents based on whole sirup	Method of sugar analysis					
		Munson and Walker			Polarimeter		
		Dextrose	Maltose	Dextrins (as dextrose)	Dextrose	Maltose	Dextrins
		Percent [a]	*Percent*	*Percent*	*Percent*	*Percent*	*Degrees per g of sirup*
1	24.3	.....	.....	.....	4.8	2.9	.....
2	32.5	14.7	11.7	10.8	16.6	10.3	.....
		14.8	11.95	7.9	16.5	8.8	.....
		14.5	13.95	.....	13.4	9.2	.....
		14.6	11.7	.....	.....	.....	.....
3	33.5	15.1	13.7	10.9	17.0	16.6	4.6
4	45.5	26.9	16.3	9.5	27.3	14.6	3.5
		26.9	16.4	9.3	.....	.....	.....
		27.2	16.6	7.9	.....	.....	.....
		27.4	15.4	8.8	.....	.....	.....
5	48.1	30.6	17.6	.....	30.0	17.5	3.1
		30.1	16.6	.....	.....	.....	.....
6	61.3	56.7	14.4	.....	56.4	13.4	1.0

[a] All percentages are based on whole sirup.

Sirups of different concentration may be compared by graphs similar to those in figures 3 and 4, since these results are based on samples containing 1 gram of dry substance.[5] The direct rotation of each fraction after concentration to 100 ml is represented on the ordinate of figure 3. Such a graph gives an over-all picture of a sirup and is of value for comparison purposes in the consideration of different products. The percentage content of dextrose and

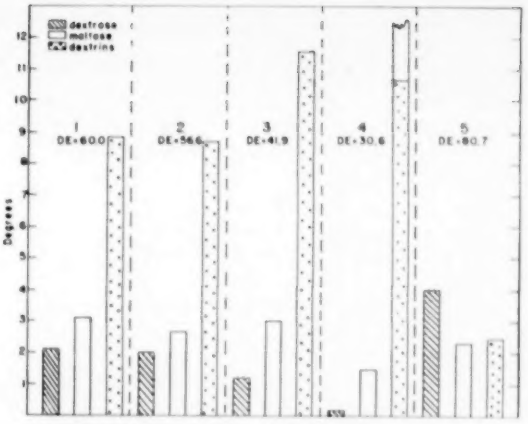

FIGURE 3. *Polarimetric analysis of five corn sirups.*

Direct rotation of 1 g of dry substance in 100 ml of solution. DE indicates dextrose equivalent.

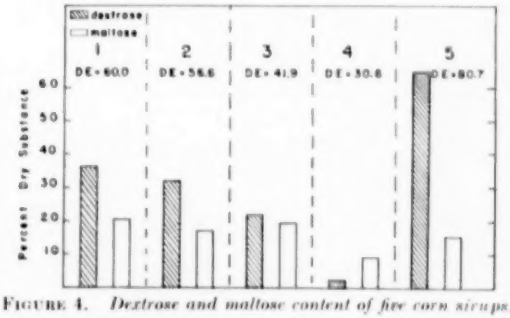

FIGURE 4. *Dextrose and maltose content of five corn sirups.*

DE indicates dextrose equivalent.

maltose as shown in figure 4 is based upon reducing-sugar analysis. Dextrins are not included in the figure since they can not be determined directly.

In order to compare the proposed method with the most accurate procedure available, sirup 4, table 2, was also analyzed by a method used by F. W. Zerban,[6] who has kindly made the following description available:

> The total reducing power of the original sirup is determined by means of Fehling solution, and the result expressed as glucose. The reducing power is again determined in the residue after fermentation with baker's yeast, against Fehling solution and also against the Steinhoff copper acetate reagent; the results are expressed as glucose. The difference between the results with Fehling solution, before and after fermentation, gives the sum of glucose and maltose hydrate, expressed as glucose (1st approximation). The glucose originally present in the sirup is determined by Steinhoff's copper acetate reagent, and corrected for the apparent glucose found in the unfermentable residue by the same method. This corrected glucose is then deducted from the sum of glucose and maltose hydrate, expressed as glucose found in the 1st approximation. This gives the maltose hydrate, expressed as glucose (1st approximation). It is converted into maltose hydrate on the basis of the

[5] We express our appreciation to C. F. Snyder for the dry substance analyses.

[6] F. W. Zerban, New York Sugar Trade Laboratory (unpublished results).

reducing ratio of glucose to maltose hydrate, and the glucose is corrected for the reducing power of the maltose hydrate on the Steinhoff copper acetate reagent. The corrected glucose is subtracted from the sum of glucose and maltose hydrate expressed as glucose, previously found, and the approximations are repeated until there is no further change in the glucose and maltose values.

The composition of the sirup found by the two methods are:

Zerban's procedure	Dextrose, 27.0 percent. Maltose, 19.0 percent.
Darco-Celite column	Dextrose, 27.2 percent. Maltose, 16.2 percent. Dextrins, 8.9 percent.[a]

[a] Expressed as dextrose.

The two methods show good agreement for the dextrose content. It is evident that the dextrin portion contains an unfermentable fraction that has a reducing power equivalent to 8.9 percent of dextrose. Although this material does not interfere with the copper acetate reduction, it reduces Fehling solution, thereby causing the discrepancy in the maltose analyses.

If the alcohol concentration of the eluting agent is increased in several steps between 5 and 30 percent, the dextrins can be divided into triose, tetrose, and higher polysaccharides [6]. However for analytical purposes where time is important, it appears that the procedure here described gives the information that is necessary for characterizing a corn sirup. Studies are now in progress to extend the method to include sucrose and invert sugar in the mixtures.

4. References

[1] A. Tiselius, Kolloid Z. **105,** 101 (1943).
[2] S. Claesson, Arkiv. Kimi, Mineral Geol. **24A,** No. 16 (1947).
[3] E. Montgomery, F. B. Weakley, and G. E. Hilbert, J. Am. Chem. Soc. **71,** 1682 (1949).
[4] R. L. Whistler and F. Durso, J. Am. Chem. Soc. **72,** 677 (1950).
[5] S. M. Partridge, Biochem. J. **42,** 238 (1948).
[6] J. M. Bailey, W. J. Whelan, and S. Peat, J. Chem. Soc. (1950) 3692.

WASHINGTON, MAY 1, 1951

Journal of Research of the National Bureau of Standards Vol. 47, No. 5, November 1951 Research Paper 2264

Effect of Exposure to Soils on the Properties of Asbestos-Cement Pipe

Irving A. Denison and Melvin Romanoff

This report summarizes the results of study made on two varieties of asbestos-cement pipe involving the exposure to 15 different soils for periods up to 11 years. The soils range from well-aerated types deficient in water soluble salts to very poorly aerated ones containing high concentrations of soluble material. The effects of exposure to the soils on the mechanical and physical properties of asbestos-cement pipe are indicated by measurements of hydrostatic bursting pressure, crushing strength, water absorption, apparent specific gravity and by observations of the condition of the surface of the specimens removed. Bursting and crushing strengths of the pipe samples, after exposure, were without exception higher than the requirements of the Federal specifications for this class of material.

1. Introduction

The lack of information on the effect of exposure to different soil conditions on the properties of asbestos-cement pipe prompted the National Bureau of Standards to include two varieties of this material in its comprehensive field investigations of materials for underground construction including ferrous and nonferrous metals [1, 2].[1] The usual composition of asbestos-cement pipe is four parts of portland cement and one part of asbestos fibers, to which silica flour is sometimes added. In the manufacture of pipe, a felted asbestos-cement sheet, or lamination, is applied continuously to a revolving steel mandrel on which the material is compacted and finish-formed under heavy pressure rollers, after which the pipe is subjected to a curing operation. It is used in the United States for transporting water and sewage, farm irrigation, mine drainage, salt water disposal, and for handling industrial process liquids.

In 1937, 10 samples of 6-in. pipe, made by a process to be described, were installed at each of 15 test sites to provide for removal of two samples after each of five periods of exposure. Samples were removed from each site in 1939, 1941, 1946, and 1948 and returned to the laboratory for evaluation of the effect of underground exposure on the properties of the material. On the occasion of the removals in 1939, lengths of 4-in. pipe, manufactured by a slightly different process, were buried at the same sites. Two samples of this material were removed from each site after exposures of 2, 7, and 9 years. Because it was necessary to discontinue the tests at one site in 1946, six samples of the 6-in. pipe and 10 samples of the 4-in. pipe were removed from this location at that time. Two samples of the 6-in. pipe and four samples of the 4-in. pipe are currently exposed at each of the other 14 sites.

This report deals with the specimens that were removed after different periods of exposure, up to 11 years for the 6-in. specimens and up to 9 years for the 4-in. specimens. A brief discussion of the 2- and 4-year exposures of the 6-in. pipe only, was included in a Bureau circular on underground corrosion [3]. Final conclusions of this investigation will be deferred until the completion of examination of the remaining specimens still being exposed.

[1] Figures in brackets indicate the literature references at the end of this paper.

2. Properties of the Soils at the Test Sites

The test sites were selected as representative of a wide variety of soil conditions, as indicated by their chemical and physical properties (table 1). For example, the soils range from extreme acidity, pH 2.6 to high alkalinity, pH 9.4. Measurements of pH and total acidity were made on samples of soil shipped from the test sites in sealed containers to prevent drying. This precaution was taken to prevent aeration of certain poorly aerated soils because previous study had shown that oxidation of sulfides to sulfates caused a marked increase in acidity [4]. As a result, the pH values and total acidity of the soils in table 1 differ from previously reported values [5], which were determined after the soil samples had been dried and pulverized.

The texture of the soils and retentiveness of moisture are indicated relatively by values for the moisture equivalent, that is, the quantity of water retained by a previously saturated soil against a centrifugal force of 1,000 times gravity. Since the true specific gravities of the mineral portions of different soils vary only slightly, the apparent specific gravity, except in the case of organic soils, can be taken as a measure of compactness and hence as a relative measure of porosity. A soil having a very high moisture equivalent and a high specific gravity, such as Acadia clay (soil 51), may be considered to have a very fine texture, high moisture retention, and to be very dense, and impermeable to the flow of air and water. This is confirmed by the poor aeration or drainage of the soil as observed in the field. On the other hand, the sample of Hagerstown loam (soil 55), despite its rather high moisture equivalent (32 percent), is typical of a very porous and well aerated soil, as is indicated by the low apparent specific gravity, 1.49.

The electrical resistivities of the soils range from 62 ohm-cm, indicating a high concentration of soluble salts, to 17,800 ohm-cm, indicating the practical

TABLE 1. *Properties of the soils at the test sites*

Test sites			Aeration	Moisture equivalent	Apparent specific gravity	Resistivity at 60° F (15.6° C)	pH	Total acidity [a] (milligram equivalent per 100 g of soil)	Composition of water extract (milligram equivalent per 100 g of soil)						
Environment and soil type	Soil	Location							Na+K as Na	Ca	Mg	CO_3	HCO_3	Cl	SO_4
INORGANIC															
Oxidizing acid:				*Percent*		*Ohm-cm*									
Cecil clay loam	53	Atlanta, Ga	Good	33.7	1.60	17,800	4.8	5.1	.....	.....	.....	.....	.....	.....	.....
Hagerstown loam	55	Loch Raven, Md	do	32.0	1.49	5,210	5.8	10.9	.....	.....	.....	.....	.....	.....	.....
Susquehanna clay	62	Meridian, Miss	Fair	34.6	1.79	6,920	4.5	12.0	.....	.....	.....	.....	.....	.....	.....
Oxidizing, alkaline:															
Chino silt loam	65	Wilmington, Calif	Good	26.4	1.41	148	8.0	A	7.65	12.40	2.20	0.00	1.30	6.05	16.90
Mohave fine gravelly loam	66	Phoenix, Ariz	Fair	16.5	1.79	232	8.0	A	6.55	.51	.18	.00	.73	2.77	2.97
Reducing, acid:															
Acadia clay	54	Spindletop, Tex	Poor	47.1	2.07	190	6.2	13.2	10.27	15.55	5.03	.00	.56	5.75	22.00
Sharkey clay	61	New Orleans, La	do	30.8	1.78	943	6.8	4.9	.73	.68	.33	.00	.71	.10	.91
Reducing, alkaline:															
Docas clay	64	Cholame, Calif	Fair	41.1	1.88	62	7.5	A	28.10	2.29	.76	.00	.89	28.80	.26
Lake Charles clay	56	El Vista, Tex	Very poor.	28.7	2.03	406	7.1	5.1	3.12	.69	.47	.00	.80	1.59	3.04
Merced silt loam	70	Buttonwillow, Calif	Fair	24.7	1.69	278	9.4	A	8.38	.38	.22	.02	1.87	1.12	5.57
ORGANIC															
Reducing, acid:															
Carlisle muck	59	Kalamazoo, Mich	Very poor.	43.6	.....	1,660	5.6	12.6	1.03	3.08	2.70	.00	.00	3.47	1.04
Muck	58	New Orleans, La	Poor	57.8	1.43	712	4.8	15.0	2.03	2.23	1.29	.00	.00	.47	2.54
Rifle peat	60	Plymouth, Ohio	do	43.4	1.28	218	2.6	297.4	2.91	10.95	2.86	.00	.00	.00	56.70
Tidal marsh	63	Charleston, S. C	Very poor.	46.7	1.47	84	6.9	14.6	33.60	6.85	4.00	.00	.00	12.70	36.60
Cinders	67	Milwaukee, Wis	do	.....	.....	455	7.6	A	.77	3.03	.53	.00	.55	.08	2.89

[a] "A" indicates absence of acidity because of alkaline reaction.

absence of such salts (table 1). Other marked differences are indicated by the composition of the water-soluble material in the soils, as for example, the preponderance of chloride in soil 64 and of sulfate in soil 60.

The soils were classified according to type of environment, as indicated in table 1. The soils, excepting cinders, are placed in two main divisions depending on whether they are inorganic or organic. The inorganic soils are then divided into two groups according to their oxidizing or reducing nature. Finally, the soils within the groups are classified according to whether they were acid or alkaline. All of the organic soils were reducing and acid in reaction.

The wide differences in the conditions of exposure at the test sites are indicated in figure 1. Thus, aeration was good at site 55, fair at site 70, and very poor at sites 56 and 63. The manner in which the specimens were buried is shown in figure 1,D.

3. Description of the Materials

The two varieties of asbestos-cement pipe included in the field tests differ chiefly in method of manufacture. The 6-in. specimens buried in 1937 were fabricated from a thin slurry of portland cement and properly prepared asbestos fibers, which was picked up as a continuous sheet from the container vat on the wire screen surface of a partly immersed, rotating

FIGURE 1. *Test sites illustrating the environmental conditions to which specimens of asbestos-cement pipe were exposed.*

A, Site 56, Lake Charles clay at El Vista, Tex.; B, Site 70, Merced silt loam at Buttonwillow, Calif. C, Site 63, Tidal marsh at Charleston, S. C.; D, Site 55, Hagerstown loam at Loch Raven, Md.

cylinder mold. This sheet, ranging in thickness from 0.010 to 0.020 in., had a width equal to the full length of the pipe sections being manufactured. The sheet was transferred from the mold to an endless felt belt, carried forward over a vacuum chamber to remove excess water, and again transferred to a mandrel on which the pipe was formed continuously until the required wall thickness was attained under heavy compressive force exerted by a system of pressure rollers. The pressure applied during the process was not sufficient to cause any change in the chemical properties or structure of the portland cement.

The 4-in. specimens buried in 1939 were fabricated by essentially the same process, except that the mandrel was held in contact with the felt by compressing rollers. There were six felts, each about 10 in. wide. The mandrel was spiraled helically forward through the machine at the rate of about 1 in. per revolution, and the pipe was built up during this process.

When the required thickness was reached by either process, the seal between the mandrel and the pipe was released by the introduction of air between the mandrel surface and the pipe. This operation, necessarily carried out without the high pressures used while the pipe was being formed, added a small thickness of relatively uncompacted stock to the outside surface. This stock was in excess of the designed wall thickness and is known as the calendar layer. It was noted prior to exposing the specimens at the test sites that the calendar layer was slightly softer than the main body of the pipe.

After removal from the mandrel, the 6-in. pipe was cured by a high-pressure steam process in which heat and pressure were applied to the pipe in a moisture-saturated atmosphere. Silica flour was added to the slurry during the manufacture of these pipes to facilitate the chemical reactions resulting from steam curing. The 4-in. pipes were cured by submersion in water 2 to 3 weeks, the damp curing process ordinarily used for cement products, after which they were trimmed and machined.

According to the report of the Committee 716 of the American Concrete Institute [6], higher strength properties, more stabilized form, and increased resistance to sulfate are obtainable for masonry cement products with high-pressure steam curing than by the damp curing process. It states that while high strength developed in a few hours of steam curing is in part due to the acceleration of the normal process of hardening, a material contribution to strength comes from the reaction resulting in the formation of a hydrated calcium silicate from the lime and silica present. The more stabilized form of cement attributable to pressure steam curing results, in part, from the conversion (or partial conversion) of the amorphous calcium silicates to crystalline forms, which do not swell or shrink as much as do the amorphous forms with increase or decrease in moisture content. It also has been observed by the Committee that the series of compounds that are known as hydrogarnets, which result from steam curing of cement products, are very stable and highly resistant to the action of sulfate solutions.

The specimens buried in 1937, and for which data are reported for exposures up to 11 years, were cut from class 150 pipe designed to withstand a pressure of 150 lb/in.^{2}. The specimens were 12 in. in length, 6 in. in diameter, and had an average wall thickness of 0.72 $\pm$0.05 in. Near one end of each of the specimens was a hole, $\frac{3}{8}$ in. in diameter, which was used to hold an identification tag. The ends of the pipe were not sealed, and since it was the intent to limit exposure to the soil to the exterior surface, the interior surface and the ends were coated with a resinous varnish.

The specimens initially buried at the same test sites in 1939, and for which data are reported for exposures up to 9 years, were 4 in. in diameter, 15 in. long with an average wall thickness of 0.64 $\pm$0.09 in. The specimens were tapered 2½ inches from each end and closures were placed at the junction of the tapered and untapered portions to confine the action of the soil to the external surface. These sections were also cut from class 150 pipe.

4. Test Procedures

The specimens as periodically removed were returned to the laboratory for examination of their surfaces and for the determination of their respective hydrostatic bursting strengths, crushing strengths, water absorption, and apparent specific gravity. Five representative samples from each of the 4- and 6-in. "as manufactured" pipe, which were stored at the Bureau, were subjected to the same tests. In addition, a section from each length of pipe from which the 4-in. diameter specimens were cut was subjected to these tests by the manufacturer and the Pittsburgh Testing Laboratory in accordance with the same procedures employed at the Bureau. The determinations made on the unexposed samples were used as reference data in determining the effect of the various soils and periods of exposure on the pipe materials.

In order to simulate service conditions with respect to moisture, the 6-in. specimens were immersed in water for 48 hours before making the bursting and crushing tests. However, the 4-in. specimens were tested in the air-dry condition because the reference samples had been tested in this condition. In this connection, it may be noted that saturation with water reduces the strength of asbestos-cement pipe from 10 to 20 percent [7]. The details of the procedures employed in evaluating the properties of the exposed and unexposed samples of asbestos-cement follow.

4.1. Surface Condition

The depth of softening of the surface was estimated in a semiquantitative manner by scratching or scraping the external surface, allowing for the original condition of the outermost or calendar layers.

967701—51——3

Based on these observations, the condition of the surface was classified according to the following categories: 0, hardening of the calendar layers; 1, surface unchanged; 2, softening to a maximum depth of 0.06 in.; 3, softening to a maximum depth of 0.15 in.

During the latter part of the investigation, quantitative measurements of the depth of affected surface layers of the exposed 6-in. diameter specimens were made by the Johns-Manville Research Center by a method recently developed by that laboratory [8]. A section of an exposed specimen was mounted in a precision lathe, and the surface layers, which had been softened by contact with the soil, were removed by grinding under carefully controlled conditions. The grinding operation was continued until the measured hardness was equal to that of unexposed reference asbestos-cement pipe. The thickness of the softened layer was then taken as the difference in thickness between the original and residual wall, as measured with a micrometer or by recording the movement of the graduated compound cross feed of the lathe. In measuring the hardness of the specimen, a cut was made with a tool so designed that the width of the cut varied with the applied load and hardness according to the formula.

$$\text{Hardness number} = \frac{\text{Applied load (g)} \times 1000}{\text{Width of cut (mm)} \times 0.1}.$$

Preliminary evaluation of softening of the specimens developed during 9 years of exposure was made on a single stave cut from each specimen, 4 in. along the length of the pipe and 2 in. in width. However, the determinations of softening of the specimens exposed for 11 years were made on four staves cut at random from each specimen.

4.2. Hydrostatic Bursting Pressure

The 4-in. specimens were prepared for the hydrostatic bursting tests by removing the closures and the tapered ends, the length of the specimens being thereby reduced to 11 in. The 6-in. specimens required no alteration in their shape or size. The tests were made on only one specimen for each exposure period from each of the test sites, except as noted in the footnote appended to table 2.

The apparatus (fig. 2) for determining the bursting strength was provided with internally fitting rubber gasketed heads to close the ends of the pipe and so designed that the pipe was not subjected to end compression during the test. A vent arrangement for expelling air entrapped in the pipe during test was provided at one of the heads. The opposite head was equipped with a water and pressure inlet, the pressure being provided from a high-pressure hand pump. Backing up of the pressure into the inlet line was prevented by use of suitable check valves.

After filling the pipe with water, the entrapped air was allowed to escape and the pressure was increased at the rate of approximately (10 lb/in.^{2})/sec

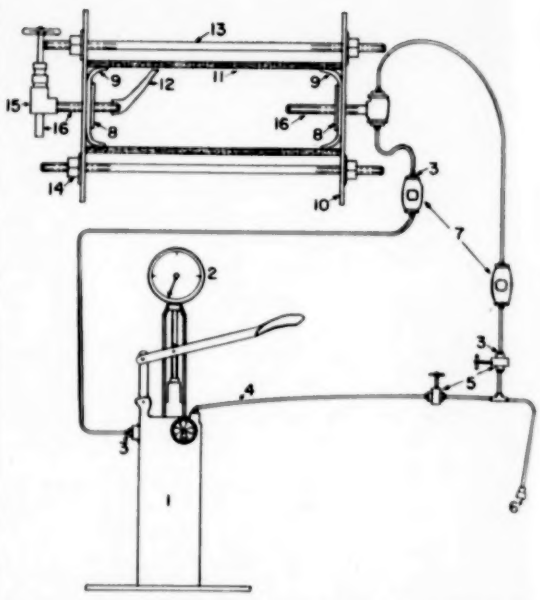

FIGURE 2. *Arrangement of apparatus for hydrostatic bursting tests.*

1, Hand-operated hydraulic pump; 2, pressure gage; 3, ½-in. pipe thread connector with 7/16-in. compression screw for connection to ¼-in. copper tubing; 4, ¼-in. copper tubing; 5, ¼-in. needle valve; 6, ¾- to ½-in. reducer for connection to main water supply; 7, ¼-in. high pressure check valves; 8, steel disks, 2½ or 4½ in. in diameter, which screws on the ¾-in. threaded pipe to hold the rubber gaskets in place; 9, 4- or 6-in. rubber gaskets for testing the appropriate size of pipe; 10, steel plates, 9 by 9 by ½ in.; 11, asbestos cement pipe specimen under test, approximately 12 in. in length; 12, overflow or air vent; 13, ½-in. diameter steel rods, threaded on both ends; 14, ½-in. nut with washer; 15, ½-in. needle valve for expelling air; 16, ½-in. threaded pipe.

until the pipe failed. The pressure gage employed was calibrated before and after the tests for each exposure period, and the bursting pressures shown in tables 2 through 5 are values obtained after applying the correction factor. The corresponding maximum tensile stress values were calculated from the respective bursting pressures.

The minimum, or average, wall thickness along the fracture as well as the location and character of failure of each specimen were noted. Many specimens failed initially by splitting out of a section of the pipe at one end, following which a crack propagated from a point on this fracture along the entire length of the specimen. The others failed by cracking in one or two places simultaneously along the entire length of the specimen. In all but a few cases a crack passed through the hole, which was located near one end of the 6-in. diameter pipe to hold the identification tag. In the few cases where the crack did not pass through the hole, the bursting pressure values were not noticeably greater than those of the other specimens.

Direct comparison between the bursting pressures of the exposed and unexposed specimens is not valid unless the variations of wall thickness and diameter are taken into account. This was accomplished by computing the maximum tensile strength according

TABLE 2. *Hydrostatic bursting and crushing strength of air-dry specimens of 4-in. asbestos-cement pipe after exposure to soils* [a]

Soil		Exposure	Bursting strength			Crushing strength [b]		
No.	Type		Identification of pipe from which specimen was cut [c]	Bursting pressure	Maximum tensile strength	Identification of pipe from which specimen was cut [c]	Crushing load	Modulus of rupture
		Years		*lb/in.²*	*lb/in.²*		*lb/linear ft*	*lb/in.²*
51	Acadia clay	7.0	P	1,300	5,210	U	10,930	11,560
			I	1,075	4,360	T	13,080	10,510
			Q	775	3,550	P	13,080	12,030
			O	825	3,600	V	12,470	10,620
			L	1,075	4,290	K	12,740	11,010
53	Cecil clay loam	1.9	C	1,050	4,070	T	10,030	8,350
		6.8	S	1,150	5,000	E	11,440	9,720
		9.1	V	1,245	4,890	S	10,060	10,890
55	Hagerstown loam	2.0	S	1,000	4,120	G	12,930	11,190
		7.1	O	1,000	4,560	J	13,240	11,510
		9.1	C	885	3,680	F	16,080	11,030
56	Lake Charles clay	1.9	T	1,250	4,750	H	12,400	9,030
		6.8	N	1,200	4,720	F	16,660	12,650
		9.1	N	950	3,970	J	12,310	10,700
58	Muck	1.9	V	1,275	5,060	R	11,340	8,820
		6.8	I	1,425	5,500	K	13,910	12,280
		9.1	J	1,290	5,000	T	13,180	10,280
59	Carlisle muck	1.9	U	1,350	5,610	Q	7,730	8,660
		7.0	N	1,200	4,860	B	13,120	11,350
		9.0	C	1,000	4,040	S	9,980	9,440
60	Riffe peat	1.9	M	1,250	4,690	H	12,860	8,680
		7.0	G	1,375	5,490	D	8,500	7,510
		9.0	A	950	3,950	B	10,530	8,170
61	Sharkey clay	1.9	E	1,375	5,490	A	7,990	9,940
		6.8	H	1,350	4,850	U	12,710	11,770
		9.1	W	1,100	4,110	Q	10,330	10,230
62	Susquehanna clay	1.9	O	800	3,680	P	10,440	9,360
		6.8	Q	975	3,950	C	12,730	11,340
		9.1	L	1,195	4,740	W	12,750	9,170
63	Tidal marsh	1.9	L	1,125	4,350	H	14,410	9,630
		6.7	E	1,200	4,830	E	12,860	10,780
		9.0	U	1,100	4,440	L	12,160	10,580
64	Docas clay	1.9	J	1,400	5,530	G	12,330	10,440
		6.9	I	1,125	4,590	S	13,760	11,730
		9.1	J	1,340	5,330	L	13,460	12,450
65	Chino silt loam	1.9	K	1,100	4,460	M	12,900	9,780
		6.9	Q	1,075	4,320	D	10,090	9,540
		9.1	U	1,195	4,710	B	16,630	12,880
66	Mohave fine gravelly loam	1.9	D	1,100	4,410	P	11,190	9,910
		6.9	I	1,350	5,420	T	14,180	10,510
		9.1	E	1,245	4,860	T	12,460	9,560
67	Cinders	1.9	O	800	3,560	A	9,570	9,850
		7.0	R	1,325	4,840	F	12,210	9,560
		9.0	S	1,245	4,870	Q	8,010	7,970
70	Merced silt loam	1.9	F	1,425	5,420	P	11,310	10,000
		6.9	M	1,375	5,140	D	8,260	8,230
		9.1	R	1,340	4,940	S	14,630	11,970

[a] Average dimensions—internal diameter, 3.99±0.05 in.; wall thickness, 0.63±0.10 in.; length of samples for crushing tests, 5.13+0.32 or −0.81 in.; length of samples for bursting tests, 11 in.

[b] Data are the average of two measurements made on one specimen.

[c] See table 3 for results of tests on reference (unexposed) specimens.

to the following modification of the Birnie [9] formula adapted to asbestos-cement pipe

$$f=\frac{P(d+1.7t)}{2t},$$

where

f=maximum tensile strength in pounds per square inch
P=bursting pressure at failure in pounds per square inch
d=internal diameter in inches
t=wall thickness in inches.

4.3. Crushing Strength

Determinations of crushing strength were made on lengths of pipe prepared by circumferentially cutting in half one specimen for each exposure period from each site. The values shown in tables 2 to 5 in each case are the averages of those obtained on two samples from each specimen. The tests were made according to the procedure described in Federal Specifications for asbestos-cement pipe [10], using the three-edge bearing method as illustrated in figure 3. The load was applied to one section at a rate of approximately 1,000 lb/min until failure

TABLE 3. *Mechanical and physical properties of unexposed specimens of air-dry asbestos-cement pipe 4 in. in diameter* [a]

Designation of original pipe from which section was cut	Bursting strength		Crushing strength		Water absorption	Apparent specific gravity
	Bursting pressure	Maximum tensile strength	Crushing load	Modulus of rupture		
	lb/in.²	*lb/in.²*	*lb/linear ft*	*lb/in.²*	*Percent*	
A	950	4,070	9,630	10,130	14.7	1.86
A [b]	1,000	4,330	10,570	10,760	13.6	1.84
B	1,120	4,440	11,770	9,410	14.1	1.86
B [b]	1,200	4,650	.....	.....	14.6	1.83
C	820	3,190	9,510	8,710	15.9	1.78
C [b]	.....	.....	10,270	8,710	15.0	1.81
C [b]	.....	.....	9,150	8,340	16.0	1.84
D	730	2,960	8,760	7,900	18.0	1.72
E	1,020	3,940	10,050	8,760	15.6	1.83
F	1,150	4,280	11,970	9,600	15.3	1.84
G	1,080	4,310	10,650	9,520	16.7	1.80
H	1,190	4,440	13,037	8,700	15.9	1.81
I	1,100	4,270	10,010	8,310	17.9	1.75
J	1,225	4,730	12,580	10,320	15.5	1.84
K	1,060	4,260	11,780	9,710	16.3	1.81
L	940	3,830	10,950	9,850	16.0	1.81
L [b]	1,100	4,570	.....	.....	15.6	1.83
M	1,100	4,100	11,760	8,670	16.5	1.81
N	950	3,730	12,120	9,200	16.1	1.80
N [b]	1,000	3,920	.....	.....	15.5	1.84
O	750	3,200	7,690	8,880	17.0	1.74
P	1,100	4,460	10,740	9,590	14.6	1.87
Q	790	3,360	8,390	8,110	16.3	1.78
R	1,000	3,720	9,050	8,360	15.9	1.79
S	1,050	4,260	11,100	8,470	13.5	1.85
T	1,100	4,280	9,850	8,140	13.1	1.84
U	1,000	4,110	11,240	8,950	13.9	1.87
V	1,050	4,120	9,600	7,460	14.5	1.83
W	750	2,860	9,910	8,450	14.6	1.81
W [b]	950	3,700	10,380	7,670	13.5	1.85

[a] Average dimensions—internal diameter, 3.99±0.05 in.; wall thickness, 0.64±0.09 in.; length of samples for crushing tests, 4.13+0.75 or −0.18 in.; length of samples for bursting tests, 11 in.

[b] Measurements made by the National Bureau of Standards. Measurements on the other reference specimens were made by the Pittsburgh Testing Laboratories and the research laboratories of the manufacturer.

TABLE 4. *Hydrostatic bursting and crushing strength of water-saturated 6-in. asbestos-cement pipe after exposure to soils* [a]

Soil		Exposure	Bursting strength [b]		Crushing strength [c]	
No.	Type		Bursting pressure	Maximum tensile strength	Crushing load	Modulus of rupture
		Years	*lb/in.²*	*lb/in.²*	*lb/linear ft*	*lb/in.²*
51	Acadia clay	2.1	995	4,980	12,440	10,770
		[d] 9.0	1,025	5,130	10,170	9,800
53	Cecil clay loam	2.1	1,140	5,460	14,150	13,630
		4.0	1,010	5,080	10,840	10,970
		8.9	950	4,860	11,120	11,630
		11.2	1,000	4,860	13,480	13,340
55	Hagerstown loam	1.9	1,085	5,400	12,130	12,560
		3.9	1,100	5,450	12,870	13,030
		9.0	1,150	5,820	10,290	9,880
		11.0	910	4,420	13,180	11,450
56	Lake Charles clay	2.1	995	5,070	13,140	13,010
		4.0	1,050	5,100	12,560	12,810
		8.9	1,050	5,410	9,260	9,650
		11.1	935	4,600	10,500	10,990
58	Muck	2.1	1,140	5,560	12,760	12,570
		4.0	925	4,630	12,260	11,230
		8.9	.....	.....	7,850	9,240
		11.2	855	4,520	9,220	9,390
59	Carlisle muck	2.1	1,255	6,070	12,050	12,260
		4.0	1,215	6,340	11,730	11,540
		9.1	1,125	5,830	11,540	10,530
		11.1	1,100	5,300	11,300	10,900

TABLE 4. *Hydrostatic bursting and crushing strength of water-saturated 6-in. asbestos-cement pipe after exposure to soils* [a]—Continued

Soil		Exposure	Bursting strength [b]		Crushing strength [c]	
No.	Type		Bursting pressure	Maximum tensile strength	Crushing load	Modulus of rupture
		Years	*lb/in.²*	*lb/in.²*	*lb/linear ft*	*lb/in.²*
60	Rifle peat	2.1	1,010	5,080	12,120	11,970
		4.0	1,165	5,770	12,120	11,330
		9.1	1,125	5,760	9,920	10,020
		11.1	1,050	5,220	9,790	9,410
61	Sharkey clay	2.1	1,205	6,040	14,930	13,960
		4.0	1,095	5,330	9,690	10,710
		8.9	975	4,870	9,990	9,600
		11.2	1,000	4,760	9,420	9,530
62	Susquehanna clay	2.1	1,095	5,410	15,650	14,460
		4.0	1,125	5,700	12,980	12,840
		8.9	900	4,570	10,080	10,860
		11.2	1,125	5,450	12,700	12,630
63	Tidal marsh	2.1	1,175	5,620	17,370	14,680
		4.0	1,170	5,570	14,980	14,820
		8.9	775	4,290	11,430	10,960
		11.2	1,000	4,940	12,720	11,960
64	Docas clay	2.1	1,100	5,810	14,410	13,900
		4.0	1,150	5,570	15,290	14,290
		9.0	750	3,930	11,750	11,930
		11.2	1,195	5,890	11,600	10,650
65	Chino silt loam	2.1	935	4,800	15,980	15,750
		4.0	1,070	5,420	13,160	12,300
		9.0	975	4,900	11,080	11,290
		11.2	1,125	5,400	13,650	12,640
66	Mohave fine gravelly loam	2.1	1,215	5,820	14,500	13,900
		4.0	1,240	6,210	13,080	14,170
		9.0	1,075	5,470	11,110	10,710
		11.2	1,100	5,400	.....	.....
67	Cinders	2.1	1,030	5,100	15,620	14,680
		4.0	1,105	5,410	11,140	11,320
		9.0	675	3,570	11,275	11,430
		11.1	940	4,680	9,700	9,840
70	Merced silt loam	2.1	1,155	5,720	13,180	13,380
		4.0	1,285	6,020	14,260	13,330
		11.2	1,025	5,220	12,790	12,730

[a] Average dimensions—internal diameter, 5.93±0.07 in.; wall thickness, 0.72±0.05 in.; length of samples for crushing tests, 5.86±.013 in.; length of samples for bursting tests, 12 in.

[b] Data are for one specimen only except as noted.

[c] Data are for two specimens only except as noted.

[d] Average of measurements on four specimens.

TABLE 5. *Mechanical and physical properties of unexposed specimens of water-saturated asbestos-cement pipe 6 in. in diameter* [a]

Specimen	Bursting pressure	Maximum tensile strength	Crushing load	Modulus of rupture	Water absorption	Apparent specific gravity
	lb/in.²	*lb/in.²*	*lb/linear ft*	*lb/in.²*	*Percent*	
1	995	5,010	.....	.....	9.6	1.81
2	940	4,670	.....	.....	10.9	1.88
3	970	4,750	.....	.....	10.0	1.93
4a	.....	.....	9,940	10,160	9.6	1.92
4b	.....	.....	10,270	10,470	9.1	1.90
5a	.....	.....	11,840	11,660	9.6	1.90
5b	.....	.....	10,530	10,300	9.8	1.93
Average	990	4,810	10,640	10,660	9.8	1.90

[a] Average dimensions: internal diameter, 5.94±0.03 in.; wall thickness, 0.71±0.01 in.; length of samples for crushing tests, 5.81±0.23 in.; length of samples for bursting tests, 12 in.

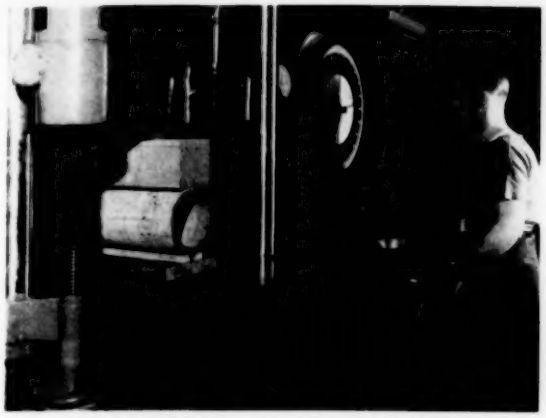

FIGURE 3. *Determination of crushing strength of section of asbestos-cement pipe.*

occurred and similarly applied to the other section of the same specimen rotated through 90°.

In order to take into account the normal dimensional variations in comparing the crushing strengths of the exposed and unexposed specimens, the modulus of rupture of the individual specimens was calculated from the values of crushing strength according to the formula given below. This formula, which is used generally in the asbestos-cement industry, is obtained by combining the standard ASTM formulas for crushing tests for application to the three-edge bearing method.

$$f=\frac{0.9P(d+t)}{Lt^2},$$

where

f = modulus of rupture in pounds per square inch
P = load to produce failure in pounds
d = internal diameter in inches
t = wall thickness in inches
L = length in inches.

4.4. Water Absorption and Apparent Specific Gravity

After completion of the bursting and crushing tests, samples, approximately 4 in. in length and 2 in. in width, were cut from sound sections of the tested specimens for water absorption and apparent specific gravity determinations. Air-dried samples were immersed in water for 24 hours and weighed in water and in air, respectively. The specimens then were dried at 105° C until a constant weight was obtained. The percentage of moisture absorbed and the apparent specific gravity were calculated as follows:

Water absorption (in percent)=

$$\frac{(\text{wet weight in air})-(\text{dry weight})}{\text{dry weight}}\times 100,$$

Apparent specific gravity=

$$\frac{\text{dry weight}}{(\text{wet weight in air})-(\text{wet weight in water})}.$$

5. Results

5.1. Hydrostatic Bursting Pressure and Crushing Strength

The results of hydraulic bursting pressure and crushing strength tests, which were made on the 4-in. specimens after exposure at the test sites for three periods, are given in table 2. Corresponding data for the reference specimens, together with values for water absorption and apparent specific gravity, are given in table 3. The letter symbols identifying the particular pipe from which the specimens were cut, permit comparison of the strengths of the exposed and unexposed specimens with a minimum of error due to normal variability of the material. As was previously noted, these measurements were made on the specimens in the air-dry condition.

The values for bursting pressure and crushing strength of the 6-in. specimens exposed at the test sites for four periods and the properties of the reference specimens are given in tables 4 and 5, respectively. Unlike the determinations made on the 4-in. pipe, these were made on water-saturated specimens. Because the particular pipes from which the 6-in. specimens were cut were not identified it is necessary to make use of the average values given in table 5 in evaluating the effects of exposure to the soils.

The data for the exposed specimens of 4- and 6-in. pipe, recorded in tables 2 and 4, show that for the maximum exposures of 9 and 11 years the bursting and crushing strengths of the specimens were without exception much higher than the requirements of the Federal Specifications for this class of material.

Federal Specifications for asbestos-cement pipe [10] require that the pipe be tested under hydrostatic pressure of two and one-half times the maximum working pressure for the given class of pipe. For example, samples of pipe of class 150 are required to withstand a hydraulic pressure of 375 lb/in^2. The specifications also require that pipe sections tested by the three-edge bearing method shall not fail until the crushing load exceeds 4,600 lb/linear ft. for 6-in. pipe and 5,000 lb/linear foot for 4-in. pipe of class 150.

The effect of exposure to the various soils is seen to somewhat better advantage in figure 4, in which the differences in maximum tensile stress and modulus of rupture of the 4-in. specimens are plotted against the duration of exposure. These curves reveal definite maxima, which indicate that the increase in strength associated with the curing process is followed by a slight decrease, the magnitude of which is probably associated with the properties of the soil. Whether the indicated trends persist for greater periods of exposure or whether the reduction in strength tends to level off with time will, of course, be brought out by the data for longer exposures.

Table 5 contains the results of bursting pressure and crushing-strength tests on the unexposed 6-in.

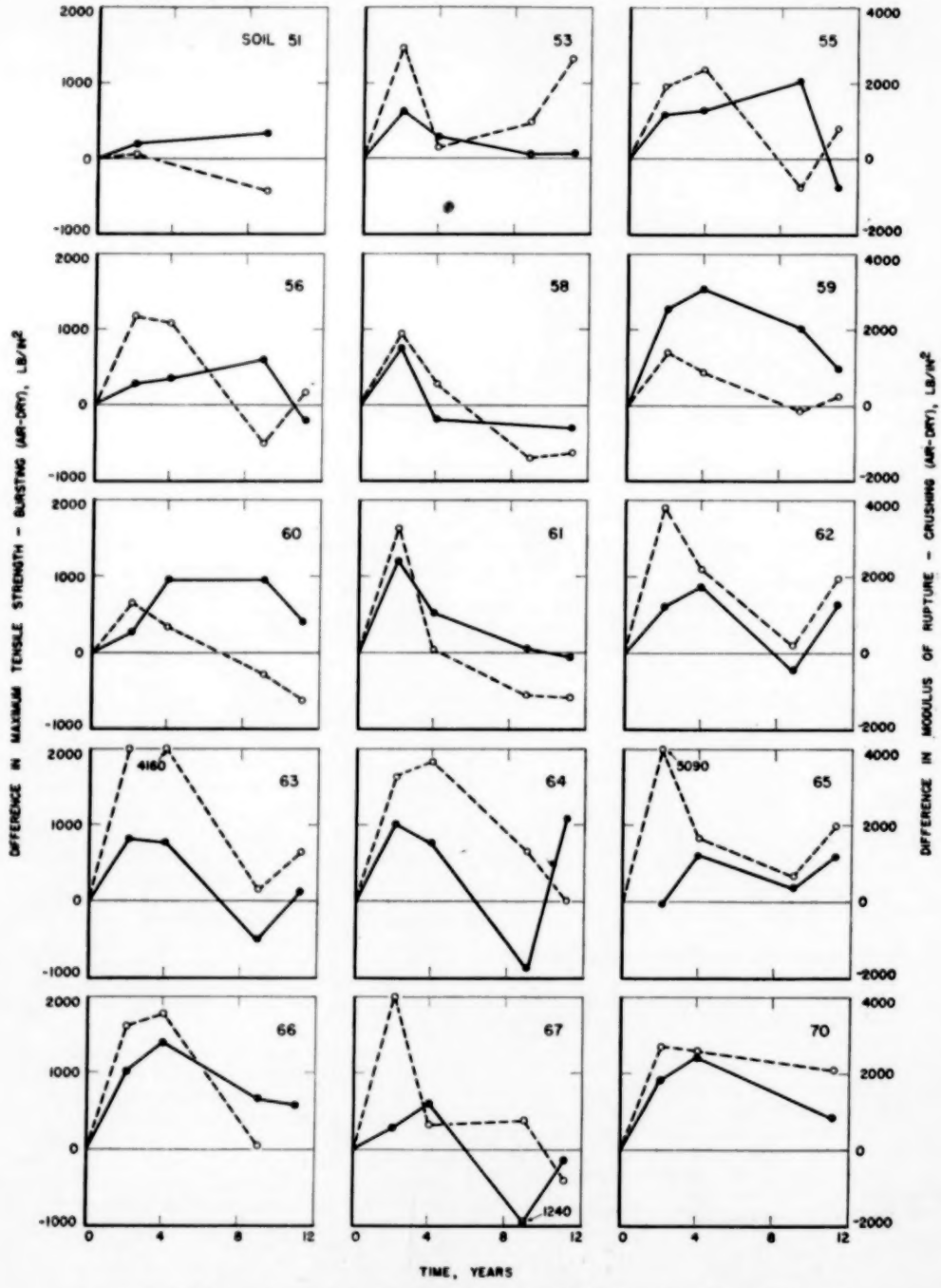

FIGURE 4. *Differences in maximum tensile strength and modulus of rupture between unexposed specimens of 4-in. pipe and similar specimens exposed for different periods.*

●——●, Maximum tensile stress; ○——○, modulus of rupture.

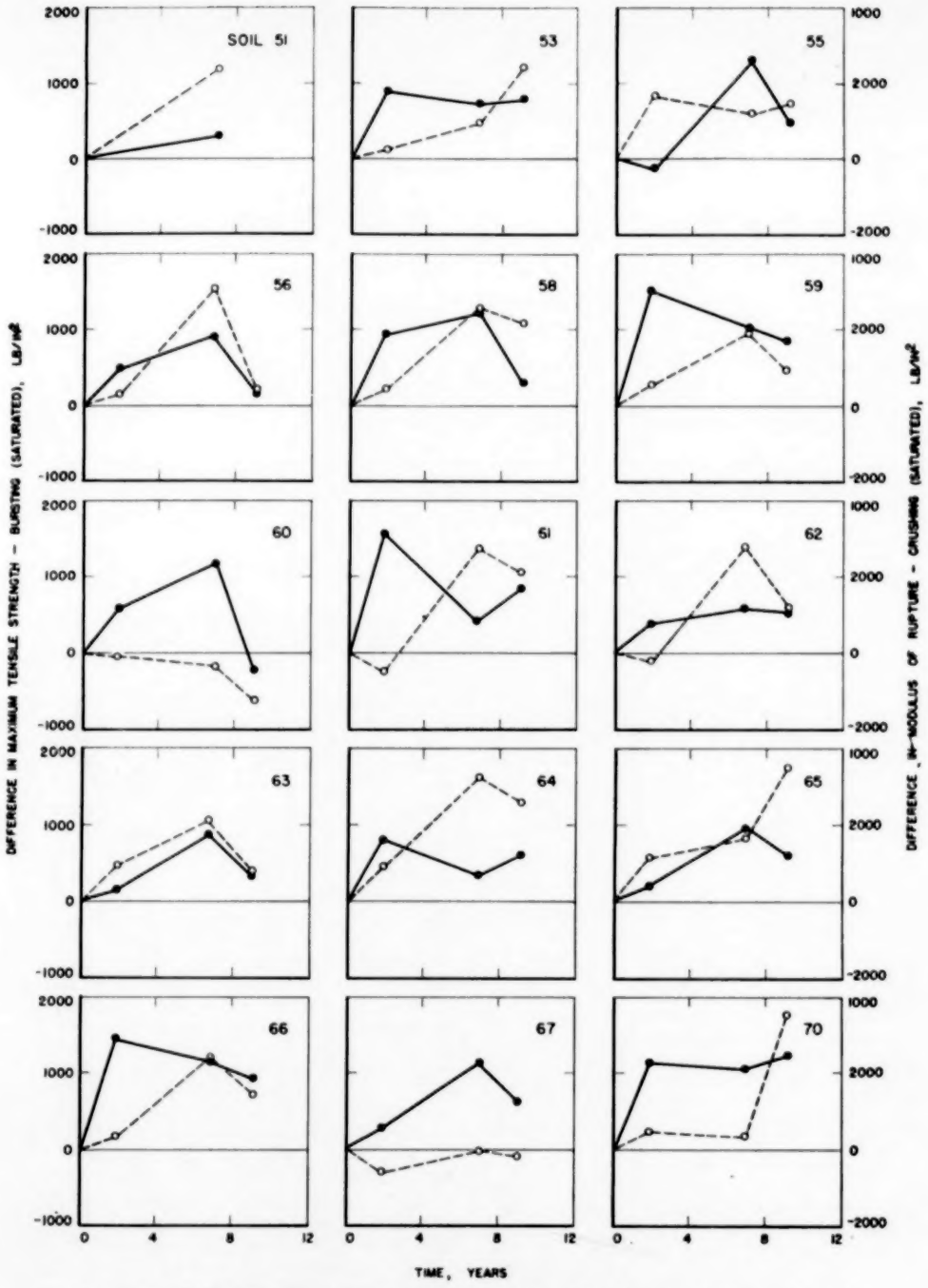

FIGURE 5. *Differences in maximum tensile strength and modulus of rupture between unexposed specimens of 6-in. pipe and similar specimens exposed for different periods.*

●——●, Maximum tensile stress; ○——○, modulus of rupture.

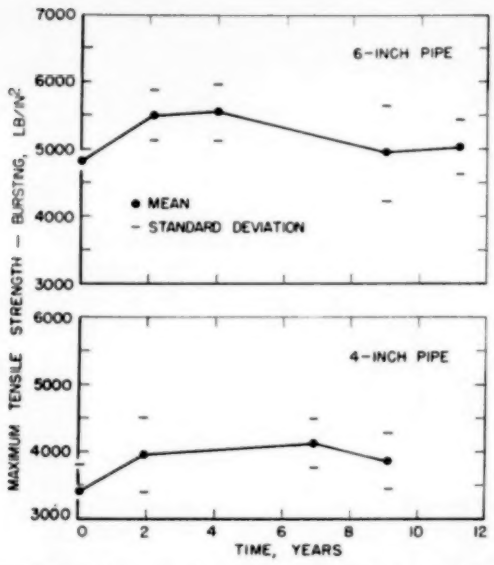

FIGURE 6. *Average maximum tensile strength of 4- and 6-in. asbestos-cement pipe in 14 soils for various periods of exposure.*

Data for both materials are based on the saturated condition.

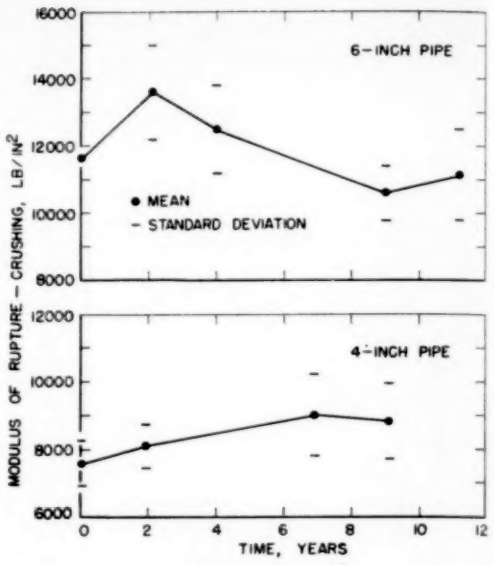

FIGURE 7. *Average modulus of rupture of the 4- and 6-in. asbestos-cement pipe in 14 soils for various periods of exposure.*

Data for both materials are based on the saturated condition.

specimens, together with the corresponding derived values for maximum tensile strength and modulus of rupture. As previously stated, unexposed specimens cut from the same lengths of 6-in. pipe were not available. Consequently, the effect of exposure to the soils on the strengths of the 6-in. specimens was evaluated with reference to the average values for the maximum tensile stress and modulus of rupture of the unexposed specimens recorded in table 5.

Like the curves for the 4-in. specimens, those in figure 5 are characterized by maxima, followed by slight reductions in strength with increasing exposure. However, no consistent trend toward progressive reduction in strength with duration of exposure is indicated.

In order to observe to somewhat better advantage the general behavior of asbestos-cement pipe exposed to soils, the values for maximum tensile strength and modulus of rupture of the 4- and 6-in. specimens in all of the soils were separately averaged for each period of exposure. The averages and the standard deviations [2] about these averages for each exposure period are shown graphically in figures 6 and 7. In preparing these figures, the data for the 4-in. specimens were adjusted to the water-saturated condition by reducing the values for maximum tensile strength and modulus of rupture by 15 percent, the average loss in strength resulting from saturation [7]. The data for the 6-in. specimens show a characteristic increase in strength during the initial period of exposure, followed by a slight decrease during the remaining periods. The 4-in. specimens, on the other hand, increased in strength over the greater period of exposure, tending to decrease only after relatively long exposure. Except in the case of the data for the modulus of rupture for the 6-in. pipe, the mean values of the exposed specimens are greater than the values for the unexposed specimens.

This difference in reaching maximum strength of the 4- and 6-in. specimens can be accounted for on the basis of the difference in the method of curing the two classes of material. As previously stated, the 4-in. specimens were water cured, whereas the 6-in. specimens were steam cured. Reference had been made to the fact that steam curing of concrete masonry products results in the development of the maximum strength in a relatively short time [6] as compared with the usual method of water curing. Consequently, it would be expected that the maximum strength of the 6-in. steam-cured specimens would be manifested relatively soon after exposure, and this effect is indicated by the data. The relatively flat curves at somewhat lower levels of strength of the 4-in. specimens are consistant with the anticipated behavior of water-cured cement products.

The curves shown in figures 6 and 7 indicate somewhat greater average strength of the 6-in. specimens throughout the maximum period for which data are available. Because of the differences in dimensions, composition of cement, and in the method of fabrication of the two varieties of pipe, the difference in strength cannot be ascribed solely to the different processes of curing.

[2] With normally distributed data, approximately 95% of the values would theoretically be within an interval of plus or minus two times the standard deviation about the mean.

5.2. Water Absorption, Apparent Specific Gravity, and Condition of Surface

The results of the determinations of water absorption and apparent specific gravity, which were made on the 4-in. specimens after exposure to the soils, and a description of the condition of the surfaces of the specimens are given in table 6. The differences between the amounts of water absorbed by the exposed and unexposed specimens given in the table show that almost without exception the specimens that had been dried and immersed in water after exposure to the soils for the periods indicated absorbed less water than the reference specimens. The data further show that in many cases the specimens that had been exposed for 7 years absorbed less water than the specimens that had been exposed for 2 and 9 years, respectively. Gain in apparent specific gravity tends to follow reduction in moisture absorption, the changes in both properties being greatest during the intermediate period of exposure. The occurrence of these maxima are undoubtedly associated with the curing process.

Softening of the surface of the specimens beneath the calendar layers was appreciable only at sites 60 (Rifle peat) and 67 (cinders). Even in these soils, the softening probably should be regarded as superficial, the maximum depth of softening being no greater than 0.15 in. The alkaline soils, 74, 65, 66, and 70, however, produced a reverse effect, the original porous and relatively soft external layers of the specimens exposed to all of these soils having been converted to a material of considerable hardness.

The effect of exposure to the soils on the water absorption capacity and the apparent specific gravity of the 6-in. specimens is indicated in table 7. In the absence of reference specimens cut from the same lengths of pipe as the exposed specimens, evaluation of the effect of exposure on water absorption and apparent specific gravity is necessarily limited to comparison of the values of these properties for the individual exposed specimens with the average values for the group of reference specimens (table 5). There is a general decrease in water absorption during one or more of the earlier periods of exposure. In general this effect persisted for the maximum exposure in

TABLE 6. *Water absorption, apparent specific gravity, and condition of the surface of 4-in. asbestos-cement pipe after exposure to soils*[a]

Soil	Exposure	Identification of pipe from which specimen was cut [a]	Water absorption	Apparent specific gravity	Difference from unexposed: Water absorption	Difference from unexposed: Apparent specific gravity	Condition of surface [b]
	Years		*Percent*		*Percent*		
		P	9.2	1.94	−5.4	0.06	2
		I	13.4	1.82	−4.5	.07	2
		Q	11.7	1.87	−4.6	.09	2
51	7.0	O	11.6	1.85	−5.4	.11	2
		L	11.6	1.89	−4.2	.07	2
		V	9.8	1.92	−4.4	.07	2
		T	10.3	1.90	−2.8	.06	2
		K	9.7	1.92	−6.6	.11	2
Avg					−4.7	.08	2
53	1.9	C	14.4	1.76	−1.2	−.05	1
	6.8	S	9.0	1.94	−4.5	.09	1
		E	9.4	1.94	−6.2	.11	1
	9.1	V	12.2	1.86	−2.3	.03	1
		S	10.3	1.92	−3.2	.07	1
55	2.0	S	11.4	1.78	−2.1	−.07	1
	7.1	O	13.2	1.82	−3.8	.08	1
		J	7.4	1.99	−8.1	.15	1
	9.1	C	14.0	1.80	−1.6	.01	1
		F	10.2	1.93	−5.1	.09	1
56	1.9	T	12.7	1.84	− .4	.00	1
	6.8	N	10.9	1.88	−4.9	.06	2
		F	8.0	1.99	−7.3	.15	2
	9.1	N	13.8	1.83	−2.0	.01	2
		J	11.6	1.91	−3.9	.07	2
58	1.9	V	12.9	1.84	−1.6	.01	3
	6.8	I	11.3	1.85	−6.6	.10	2
		K	9.5	1.94	−6.8	.13	2
	9.1	J	11.6	1.90	−3.9	.06	2
		T	12.2	1.85	− .9	.01	2
59	1.9	U	12.0	1.89	−1.9	.02	2
	7.0	N	11.5	1.90	−4.3	.08	2
		B	9.3	1.95	−5.1	.11	2
	9.0	C	16.1	1.76	.5	−.05	2
		S	14.1	1.83	.6	−.02	2
60	1.9	M	14.8	1.79	−1.7	−.02	3
	7.0	G	13.1	1.84	−3.6	.04	3
		D	10.1	1.74	−1.9	.02	3
	9.0	A	12.4	1.90	−1.8	.05	3
		B	15.8	1.79	1.4	−.05	3
61	1.9	E	13.8	1.85	−1.8	.02	1
	6.8	H	9.0	1.92	−6.9	.11	2
		U	9.3	1.94	−4.6	.07	2
	9.1	W	12.2	1.85	−1.8	.02	2
		Q	12.4	1.85	−3.9	.07	2
62	1.9	O	12.3	1.80	−4.7	.06	1
	6.8	Q	9.8	1.89	−6.5	.11	1
		C	9.8	1.92	−5.8	.11	1
	9.1	L	11.8	1.89	−4.0	.07	1
		W	10.7	1.88	−3.3	.05	1
63	1.9	L	11.7	1.88	−4.1	.06	1
	6.7	E	9.8	1.94	−5.8	.11	1
		E	9.4	1.94	−6.2	.11	1
	9.0	U	11.1	1.91	−2.8	.04	1
		L	11.8	1.88	−4.0	.06	1
64	1.9	J	10.8	1.91	−4.7	.07	1
	6.9	I	10.9	1.89	−7.0	.14	0
		S	6.3	2.02	−7.2	.17	0
	9.1	J	9.1	1.96	−6.4	.12	0
		L	9.4	1.92	−6.4	.10	0
65	1.9	K	11.6	1.85	−4.7	.04	1
	6.9	Q	9.4	1.91	−6.9	.13	0
		D	13.4	1.82	−4.6	.10	0
	9.1	U	10.9	1.92	−3.0	.05	0
		B	9.5	1.95	−4.9	.11	0
66	1.9	D	14.6	1.80	−3.4	.08	1
	6.9	I	9.7	1.91	−8.2	.16	0
		T	7.4	1.98	−5.7	.14	0
	9.1	E	10.6	1.93	−5.0	.10	0
		T	10.2	1.91	−2.9	.07	0
67	1.9	O	12.7	1.80	−4.3	.06	2
	7.0	R	12.1	1.85	−3.8	.06	3
		F	9.3	1.94	−6.0	.10	3
	9.0	S	12.7	1.85	−.8	.00	3
		Q	17.1	1.72	.8	−.06	3
70	1.9	F	10.4	1.90	−4.9	.06	1
	6.9	M	8.9	1.93	−7.6	.12	0
		D	10.5	1.86	−7.5	.14	0
	9.1	R	11.3	1.89	−4.6	.10	0
		S	9.7	1.93	−3.8	.08	0

[a] See table 3 for results of tests on reference (unexposed) specimens.
[b] Condition of surface: 0, hardening of calendar layer; 1, surface unchanged; 2, softening to maximum depth of 0.06 in.; 3, softening to maximum depth of 0.15 in.

TABLE 7. *Water absorption, apparent specific gravity, and condition of surface of 6-in. asbestos-cement pipe after exposure to soils* [a]

Soil	Exposure	Water absorption	Apparent specific gravity	Condition of surface [b]	Maximum depth of softening [c]
	Years	*Percent*			*in.*
51	2.1	8.1	1.89	2	
		6.5	1.90	2	
	9.0	10.6	1.85	2	0.24
		11.2	1.87	2	
53	2.1	11.4	1.83	1	
		5.8	1.93	1	
	4.0	7.5	1.84	1	
		7.1	1.91	1	
	8.9	7.4	1.98	1	.011
		6.8	2.02	1	
	11.2	9.0	1.86	1	.024
		7.4	1.95	1	
55	1.9	10.0	1.87	1	
		9.9	1.82	1	
	3.9	10.8	1.77	1	
		9.1	1.85	1	
	9.0	11.0	1.86	1	.017
		6.7	1.99	1	
	11.0	10.8	1.82	1	.060
		11.4	1.78	1	
56	2.1	6.0	2.00	1	
		5.2	1.94	1	
	4.0	9.1	1.84	2	
		6.7	1.87	2	
	8.9	6.3	1.97	2	.020
		8.7	1.94	2	
	11.1	10.3	1.90	2	.043
		11.0	1.91	2	
58	2.1	12.6	1.76	2	
		7.2	1.89	2	
	4.0	5.8	1.90	2	
	8.9	7.7	1.88	2	
		7.6	1.88	2	.021
	11.2	14.4	1.77	2	.048
		13.1	1.85	2	
59	2.1	7.7	1.93	2	
		9.7	1.85	2	
	4.0	8.7	1.89	2	
		9.4	1.85	2	
	9.1	12.5	1.94	2	.035
		15.0	1.76	2	
	11.1	14.2	1.82	2	.043
		16.8	1.75	2	
60	2.1	11.8	1.76	3	
		8.0	1.84	3	
	4.0	9.5	1.85	3	
		8.2	1.90	3	
	9.1	18.8	1.69	3	.110
		18.2	1.76	3	
	11.1	18.1	1.75	3	.126
		18.7	1.72	3	
61	2.1	6.6	1.92	1	
		6.2	1.90	1	
	4.0	5.0	1.94	1	
		5.2	1.98	1	
	8.9	12.5	1.82	2	.024
		11.8	1.81	2	
	11.2	11.9	1.88	2	.056
		14.7	1.82	2	
62	2.1	5.6	1.97	1	
		6.2	1.93	1	
	4.0	13.9	1.78	1	
		6.2	1.90	1	
	8.9	12.2	1.95	2	.025
		9.5	1.88	2	
	11.2	11.6	1.89	2	.029
		9.9	1.91	2	
63	2.1	12.0	1.84	1	
		8.8	1.83	1	
	4.0	9.7	1.88	1	
		5.7	1.92	1	
	8.9	9.7	1.78	0	.013
		6.6	1.94	0	
	11.2	12.3	1.88	1	.022
		14.1	1.84	1	
64	2.1	7.2	1.98	1	
		5.4	1.94	1	
	4.0	5.0	1.94	0	
		4.0	1.98	0	
	9.0	5.0	2.08	0	.010
		4.8	2.03	0	
	11.2	4.3	1.89	0	.028
		7.3	1.86	0	
65	2.1	8.3	1.76	1	
		5.6	1.92	1	
	4.0	8.2	1.84	1	
		4.4	1.94	1	
	9.0	5.4	1.95	0	.021
		5.2	2.01	0	
	11.2	7.2	1.91	0	.029
		5.7	1.92	0	
66	2.1	7.5	1.93	1	
		4.5	1.96	1	
	4.0	5.8	1.88	0	
		6.6	1.88	0	
	9.0	12.1	1.81	0	.013
		8.5	1.95	0	
	11.2	8.9	1.94	0	[d] .019
67	2.1	8.5	1.86	2	
		5.8	1.94	2	
	4.0	11.0	1.82	3	
		6.8	1.88	3	
	9.0	12.6	1.80	3	.042
		11.4	1.90	3	
	11.1	15.3	1.79	3	.101
		15.6	1.80	3	
70	2.1	12.5	1.80	0	
		5.6	1.92	0	
	4.0	7.0	1.84	0	
		4.5	2.00	0	
	11.2	4.0	1.94	0	.033
		8.8	1.83	0	

[a] See table 5 for results of the tests on reference (unexposed) specimens.
[b] Condition of surface: 0, hardening of calendar layer; 1, surface unchanged; 2, softening to maximum depth of 0.06 in.; 3, softening to maximum depth of 0.15 in.
[c] Exposure 9 years—average of single measurements on each of two specimens. Exposure 11 years—average of the maximum of four measurements on each of two specimens.
[d] One specimen only.

the alkaline soils (64, 65, and 70), but in several of the other soils, notably 58, 59, 60, 61 and 67, the amounts of water absorbed by the specimens exposed for the longer periods were greater than the average of the reference specimens.

In order to determine whether the increased amounts of water absorbed by the specimens in these soils was confined to the surface layers or whether it had penetrated to greater depths, the surfaces of the test pieces from the 11-year exposures were removed by machining to a depth of one-quarter in., and the measurement of water absorption repeated. The data summarized in table 8, indicate that in three of the soils, 59, 61, and 63, at least as much water was absorbed in the body of the specimen as was absorbed by the surface to a depth of one-quarter in. In the other three soils, 58, 60, and 67, more water was absorbed in the surface layers than in the body of the material, but the quantity of water absorbed by the material as a whole was nevertheless considerable.

The condition of the surface of the 6-in. specimens indicated in table 7 in the column headed "condition of surface" shows good agreement with the corresponding data for the 4-in. specimens given in table

TABLE 8. *Distribution of absorbed water in 6-in. specimens (in percent)*

Soil	58		59		60		61		63		67	
Specimen	a	b	a	b	a	b	a	b	a	b	a	b
Increase in water absorption over average of unexposed specimens	4.6	3.3	4.4	7.0	8.3	8.9	2.1	4.9	2.5	4.3	5.5	5.8
Water absorption of specimens with original surface	14.4	13.1	14.2	16.8	18.1	18.7	11.9	14.7	12.3	14.1	15.3	15.6
Water absorption of specimens with surface removed	13.1	10.9	14.3	16.5	13.3	15.7	12.4	15.3	12.9	14.3	14.1	13.7
Difference between specimens with original surface and specimen with surface removed	−1.3	−2.2	+.1	−.3	−4.8	−3.0	+.5	+.6	+.6	+.2	−1.2	−1.9

6. The maximum softening of both groups occurred in soil 60, and both groups exhibited marked hardening of the surface in the alkaline soils.

In addition to the semiquantitative data on the condition of the surface recorded in table 7, precise measurements of the maximum depth of softening are given for the specimens [3] after exposure for 9 and for 11 years, approximately. Although these data indicate a general tendency for the depth of softening to increase with time, the maximum softening has been small (less than 0.15 in.) in relation to the wall thickness of the specimens (approximately 0.7 in.).

6. Summary

This report summarizes the results of measurements of the mechanical and physical properties of two varieties of asbestos-cement pipe after exposure to 15 different soils for a maximum period of 11 years. Measurements of hydrostatic bursting pressure and crushing strength showed that the maximum strength of asbestos-cement pipe was not attained until several years of exposure underground. Bursting and crushing strengths of the pipe samples, after exposure, were without exception higher than the requirements of the Federal Specifications for this class of material.

There was no definite correlation between strength and length of exposure indicated by the data for the different soil environments.

It is noteworthy that asbestos-cement pipe showed no appreciable deterioration in soils despite the known detrimental effect of high acidity, alkalinity, and high concentrations of sulfate ions toward concrete products.

Superficial softening occurred in some soils, but the depth of the softened layer was less than 0.15 in. Absorption of water was not confined to the softened layer but progressed beneath these layers. Although the measurements of softening, water absorption, and apparent specific gravity might be taken to indicate incipient deterioration of asbestos-cement pipe in some soils, in general the data for hydrostatic bursting pressure and crushing strength do not indicate actual loss in strength.

[3] The measurements of maximum depth of softening were provided through the courtesy of the Johns-Manville Research Center.

The field tests described in this paper were initiated, installed, and, until 1946, were conducted by K. H. Logan. The measurements for the more recent removals were made by Warren P. Dettmers, who also assisted in other capacities. The authors acknowledge the material assistance received from the Johns-Manville Co. and the Keasbey-Mattison Co.

7. References

[1] Irving A. Denison and Melvin Romanoff, J. Research NBS **44,** 47 (1950) RP2057.
[2] Irving A. Denison and Melvin Romanoff, J. Research NBS **44,** 259 (1950) RP2077.
[3] Kirk H. Logan, Underground corrosion, NBS Circular C450 (1945).
[4] Melvin Romanoff, J. Research NBS **34,** 227 (1945) RP1639.
[5] Kirk H. Logan and Melvin Romanoff, J. Research NBS **33,** 145 (1944) RP1602.
[6] Report of the Committee 716, Proc. Am. Concrete Inst. **40,** 409 (1944).
[7] Clyde R. Hutchcroft, Physical and chemical characteristics of asbestos-cement pipe, Fifth NBS Soil Corrosion Conference (1943) unpublished.
[8] Report No. 425–145, Johns-Manville Research Center, Manville, N. J. (unpublished).
[9] George B. Haven and George W. Swett, The design of steam boilers and pressure vessels, p. 62 (John Wiley and Sons, Inc., New York, N. Y., 1923).
[10] Federal Specifications for Pipe: Asbestos-cement, SS-P-351 (1942).

WASHINGTON, March 27, 1951

Journal of Research of the National Bureau of Standards Vol. 47, No. 5, November 1951 Research Paper 2265

Photometric Determination of Copper in Iron and Steel with Diethyldithiocarbamate

John L. Hague, Eric D. Brown, and Harry A. Bright

A method is described for the direct photometric determination of copper in steel and iron. An 0.1- to 0.25-gram sample is dissolved in diluted nitric acid, and a sulfuric-phosphoric-perchloric acid mixture is added. The solution is evaporated to fumes of sulfuric acid, diluted, and the sodium salt of dimethylglyoxime or ethylenediaminetetraacetic acid added as a complexing reagent. The copper diethyldithiocarbamate complex is then formed, and extracted with butyl acetate. The butyl acetate extract is washed with diluted sulfuric acid, and the absorbancy of the copper complex is measured at 560 to 600 millimicrons. An accuracy of about 0.005 percent of copper or better is indicated for steels containing 0.05 to 0.25 percent of copper, and of about 0.001 percent of copper for steels containing less than 0.05 percent of copper.

1. Introduction

Due to the increasing use of alloyed steel-scrap during the last decade, many of the residual elements in irons and steels have accumulated to the point where control and specification analyses are frequently required. One of the residual elements that is not removed in the usual steel-making processes is copper. Umpire determinations of copper in steel are generally made by the sulfide-oxide, sulfide-electrolytic, or the thiosulfate-iodide method [1, 10].[1] While these methods yield accurate values when properly used, they require considerable manipulative ability and time. Attention has therefore been directed to the development of rapid photometric procedures for this determination.

One of the reagents frequently used for the photometric determination of copper is sodium diethyldithiocarbamate [3], the absorbancy of the copper carbamate complex being measured directly or after extraction with an organic solvent. Whereas a number of elements react with this reagent [4, 5, 9], most of these elements are either not present ordinarily in steel and iron, or suitable conditions can be chosen to reduce or eliminate their interferences. For example, Haddock and Evers [6] have shown that ferric iron does not react with diethyldithiocarbamate in ammoniacal citrate solution, and a number of procedures have been developed on this basis for the photometric determination of copper in ferrous metals [8, 12, 13]

The procedures described in this paper are the result of a study to adjust conditions so that a large variety of ferrous materials can be handled directly without filtrations or aliquoting operations, and at the same time to retain an accuracy acceptable for umpire analyses.

Perhaps the chief difficulty encountered in using this reagent in the determination of copper is the fact that nickel also reacts. The use of dimethylglyoxime [2] to complex nickel and cobalt is not completely satisfactory because the nickel glyoxime is also partially extracted and must be separated previous to the extraction. During the course of the present work, it was found that washing the butyl acetate extract with a dilute sulfuric acid solution removed the nickel glyoxime and stabilized the copper carbamate color. This technique provided a satisfactory method for the analysis of alloys containing up to 4 percent of nickel. The ethylenediaminetetraacetate ion has been shown [11] to form a useful complex with nickel and is employed in the procedure for high-nickel alloys.

The essential operations in the new procedures reported are as follows:

The sample is dissolved in dilute nitric acid or a mixture of nitric and hydrochloric acids. A sulfuric-phosphoric-perchloric acid mixture is added and the solution evaporated to fumes of sulfuric acid. The use of the sulfuric-phosphoric acid mixture provides for the complete solution of tungsten tool-steels. The solution is diluted and, after the addition of citric acid, is made slightly ammoniacal. The sodium salt of dimethylglyoxime or ethylenediaminetetraacetic acid is added as a complexing reagent, and sodium diethyldithiocarbamate is added to form the copper complex. The copper complex is extracted with butyl acetate, and the butyl acetate extract washed with dilute sulfuric acid. The absorbancy of the copper diethyldithiocarbamate complex in the butyl acetate layer is measured at 560 to 600 mμ, and the amount of copper is read from a calibration curve or from a table. A single determination can be completed in approximately 30 minutes, and a set of eight determinations can be completed in about 2 hours.

2. Apparatus

Colorimeter. An Evelyn type of colorimeter, filters, voltage stabilizer, and galvanometer as manufactured by the Rubicon Co. were used for most of the quantitative measurements reported in this paper. Matched test tubes (22 by 175 mm) were used as absorption cells.

[1] Figures in brackets indicate the literature references at the end of this paper.

3. Reagents

Sulfuric-phosphoric-perchloric acid mixture for fuming. To 200 ml of dilute sulfuric acid (1+1),[2] add 100 ml of water, 100 ml of phosphoric acid (85%), and 50 ml of perchloric acid (70%). Dilute to 500 ml with water and mix thoroughly.

Citric acid solution (250 g/liter). Dissolve 125 g of citric acid in about 250 ml of water, add 10 ml of dilute sulfuric acid (1+1), and dilute to 500 ml.

Sodium dimethylglyoxime solution (10g/liter). Dissolve 5 g of sodium dimethylglyoxime octahydrate in 500 ml of water.

Disodium ethylenediaminetetraacetate solution (40 g/liter). Dissolve 20 g of disodium ethylenediaminetetraacetate dihydrate [3] in 400 ml of water, and dilute to 500 ml.

Butyl acetate. A technical grade low in alcohols is satisfactory. Some lots of butyl acetate contain copper, and it may be necessary to wash the butyl acetate with dilute sulfuric acid (5+95) before use. The washed reagent may be dried over anhydrous sodium sulfate.

4. Procedures

Carbon and alloy steels containing less than 4 percent of nickel or cobalt. Transfer 0.100 g of the sample [4] to a 125-ml Erlenmeyer flask, add 10 ml of dilute nitric acid (1+3),[5] and heat until the sample dissolves. Add 10 ml of the "fuming acid" mixture, boil until brown fumes have been expelled, evaporate to fumes, and fume vigorously to remove the perchloric acid. Cool, add 10 ml of water, and boil to remove chlorine. Cool and add 10 ml of water and 10 ml of the citric acid solution. Neutralize to litmus with ammonium hydroxide, cooling if necessary, and add 2 to 3 ml of ammonium hydroxide in excess.

Cool the solution to room temperature and transfer it to a 125-ml separatory funnel. Wash the flask with two 5-ml portions of water and transfer the washings to the funnel. Add 15 ml of the dimethylglyoxime solution, shake for 10 to 15 seconds, add 10 ml of sodium diethyldithiocarbamate solution, and shake again for 10 to 15 seconds. Pipet exactly 20 ml of butyl acetate into the funnel, shake for 30 seconds, and cool in running water for about 2 to 3 minutes. Repeat the shaking for 15 seconds, cool, and allow the layers to separate.

Drain off completely the lower aqueous layer [6] and discard it. Add 25 ml of dilute sulfuric acid (5+95) to the funnel, shake for 15 seconds, and cool in running water. Repeat the shaking, allow the layers to separate, then drain off the aqueous layer and discard it. Transfer the butyl acetate extract to a test tube and stopper the tube.

Transfer a portion of the butyl acetate extract to a 2-cm absorption tube or cell and measure the absorbancy, using a narrow-band filter centered between 560 to 600 mμ. Use either butyl acetate or the blank solution to set the zero. Determine the percentage of copper from a calibration curve or table prepared from data obtained from synthetic solutions containing known amounts of copper and carried through all steps of the procedure. Correct the value obtained for a reagent blank, if the blank solution is not used as the "zero" solution.

Nickel, nickel-chromium, or nickel-chromium-cobalt alloys. Transfer 0.100 g of the sample to a 125-ml Erlenmeyer flask, add 10 ml of dilute nitric acid (1+3)[7] and heat until the sample dissolves. Add 10 ml of the fuming acid mixture, evaporate to fumes,[8] and fume vigorously to remove all perchloric acid. Cool, add 10 ml of water, and boil to remove chlorine. Cool and add 10 ml of water and 10 ml of citric acid solution. Neutralize to litmus with ammonium hydroxide,[9] cooling if necessary, and add 3 to 5 ml in excess.

Add 15 ml of the ethylenediaminetetraacetate solution to the warm test solution and cool to room temperature or lower. Transfer the solution to a 125-ml separatory funnel. Wash the flask with two 5-ml portions of water and transfer the washings to the funnel. Add 10 ml of the carbamate solution and complete the determination as described above. Since the copper carbamate color is somewhat slow in extracting from the "versene"-complexed solution, the shaking periods should be somewhat longer, 30 to 60 seconds.

[2] This denotes 1 volume of concentrated sulfuric acid, sp gr 1.84, diluted with 1 volume of water. Dilute nitric acid (1+3) denotes 1 volume of nitric acid, sp gr 1.42, diluted with 3 volumes of water. If no dilution is specified, the concentrated reagent is meant.

[3] An "analytical reagent" grade of this chemical is produced by the Bersworth Chemical Co., Framingham, Mass., under the trade name Di Sodium Versenate.

[4] A sample weighing 0.250 g can be used if the copper content is less than 0.05%.

[5] For high-chromium materials also add 2 ml of hydrochloric acid. Troublesome amounts of silicon can be eliminated by adding 1 or 2 drops (0.05 ml) of hydrofluoric acid.

[6] The aqueous layer must be completely drained, or the iron complex will decompose in the acid wash-solution and form an interfering color.

[7] Most high-chromium alloys will dissolve in nitric-hydrochloric acid mixtures. For these alloys use 5 ml of aqua regia—a mixture of three parts of hydrochloric acid and 1 part of nitric acid.

[8] Some nickel or cobalt salts precipitate at this point but will redissolve during the vigorous fuming.

[9] Approximately 15 ml of ammonium hydroxide is required to neutralize the acid, and as much as 10 ml in excess does no harm.

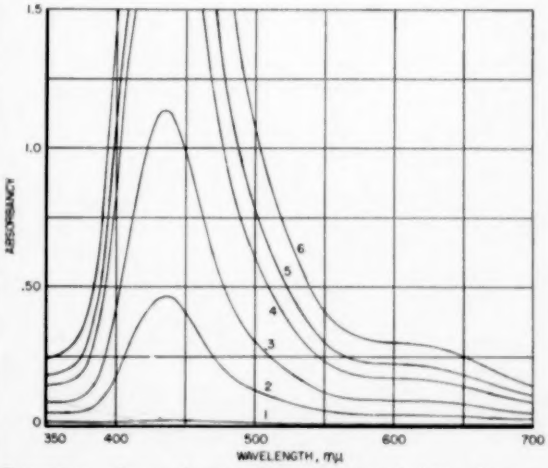

FIGURE 1. *Curves showing absorption characteristics of copper diethyldithiocarbamate.*

1, Blank; 2, 0.04-percent copper; 3, 0.10-percent copper; 4, 0.20-percent copper 5, 0.26-percent copper; 6, 0.36-percent copper. Cell length, 10.03 mm.

5. Results and Discussion

Calibration curves and tables were prepared in the usual manner [7] from data obtained by carrying known amounts of copper through all steps of the procedures and correcting to a zero absorbancy-zero concentration basis by appropriate blanks. The calibration curves obtained for the two procedures are identical within an experimental error of 1 to 2 percent and obey Beer's Law. Parallel experiments in the presence of iron (added as high-purity iron containing less than 0.0005% of copper) indicate that iron does not inhibit the extraction of the copper carbamate complex. The absorbing characteristics of the copper complex are shown in figure 1, which shows the absorbancy measurements obtained by John H. Gould with a Cary recording spectrophotometer on one of the series of solutions used in calibrating the procedure.

The values obtained on a group of ferrous metals by the procedure for carbon and alloy steels low in nickel content (<4%) are shown in table 1. As will be noticed, most of the average values are within 0.002 to 0.003 percent of the certificate value. A systematic trend toward values lower than the average certificate values is exhibited in the low-copper range. These lower values are probably due to the difficulties in the older procedures of completely separating copper from the other sulfide-forming elements, such as tin, arsenic, molybdenum, and the like, commonly present in ferrous materials and to the fact that rigorous blank corrections were run on all determinations.

Separate experiments on 0.25- and 0.50-g samples

TABLE 1. *Results obtained for copper by the procedure recommended for carbon and alloy steels (<4% Ni)*

NBS Standard sample	Copper					Weight of sample	Type of steel
	Certificate value	Found	Difference	Range	No. of determinations		
CARBON STEELS							
	Percent	*Percent*	*Percent*	*Percent*		*g*	
9d	0.009	0.0053	−0.0037	0.0052 to 0.0054	3	0.500	Bessemer
				0.0053	1	.250	
8f	.009	.0074	−.0016	.0074 to .0075	3	.500	Do.
				0.0074	1	.250	
22c	.011	.0091	−.0019	.0091 to .0093	3	.500	Do.
				0.0090	1	.250	
8g	.019	.0190	.....	.0189 to .0190	3	.500	Do.
				0.0192	1	.250	
120a	.021	.0184	−.0026	.0180 to .0186	3	.250	Sulfur-bearing.
13d	.022	.0205	−.0015	.0198 to .0212	3	.250	BOH 0.6% C.
14c	.025	.0236	−.0014	.0234 to .0237	3	.250	BOH 0.8% C.
10e	.032	.0318	−.0002	.0312 to .0322	4	.250	Bessemer.
55c	.040	.0394	−.0006	.0390 to .0404	6	.250	Open hearth iron.
15d	.054	.052	−.002	0.052	3	.100	BOH 0.1% C.
16c	.060	.061	+.001	.061 to .062	3	.100	BOH 1.0% C.
51a	.082	.082	.....	0.082	3	.100	Electric.
13e	.103	.098	−.005	.097 to .100	6	.100	BOH 0.6% C.
11e	.105	.105	.....	.104 to .107	6	.100	BOH 0.2% C.
20e	.111	.109	−.002	0.109	3	.100	AOH 0.4% C.
19e	.166	.166	.....	.166 to .167	3	.100	AOH 0.2% C.
34a	.222	.222	.....	.221 to .222	3	.100	AOH 0.8% C.
35a	.267	.262	−.005	.260 to .264	3	.100	AOH 1.0% C.
ALLOY STEELS							
130	0.017	0.018	+0.001	0.0174 to 0.0192	4	0.250	Lead-bearing
133	.061	.060	−.001	.059 to .063	4	.100	14 Cr; 0.6 Mo
73a	.080	.081	+.001	.078 to .083	4	.100	14 Cr
30d	.092	.090	−.002	.089 to .091	4	.100	Cr-V (SAE 6135)
153	.099	.100	+.001	.099 to .100	3	.100	Mo-W-Cr-V-Co
170	.102	.102	.....	.100 to .107	6	.100	Titanium-bearing
50b	.110	.114	+.004	0.114	3	.100	W-Cr-V
132	.149	.149	.....	.148 to .150	3	.100	Mo-W-Cr-V
159	.181	.181	.....	.179 to .181	3	.100	0.09 Ag—1 Cr
NICKEL STEELS							
111b	0.028	0.0248	−0.0032	0.0222 to 0.0272	9	0.250	1.75% nickel
33c	.031	.026	−.005	0.026	2	.250	3.28% nickel
		.0312	+.0002	.0310 to .0313	3	.100	
111a	.079	.079	.....	.078 to .079	4	.100	1.75% nickel
111	.122	.122	.....	.115 to .127	3	.100	1.75% nickel
101c	.124	.094	−.030	.085 to .102	4	.100	9.0% nickel
		.124	.....	0.124	2	.050	
CAST IRONS							
122b	0.047	0.050	+0.003	0.0495 to 0.0504	3	0.100	Car-wheel
107a	.105	.104	−.001	.103 to .106	3	.100	Nickel-molybdenum
4g	.240	.246	+.006	.241 to .250	3	.100	

TABLE 2. *Results obtained for copper by the procedure recommended for materials high in nickel content*

NBS Standard sample	Copper					Weight of sample	Type of alloy
	Certificate value	Found	Difference	Range	No. of determinations		
	Percent	*Percent*	*Percent*	*Percent*		*g*	
33c	0.031	0.0297	−0.0013	0.0297 to 0.0300	4	0.250	3.3% Ni steel
160		.013		0.013	4	.100	80 Ni-20 Cr
161	.04	.040		.039 to .041	4	.100	64 Ni-17 Cr-15 Fe
121a	.085	.086	+.001	.085 to .088	4	.100	11 Ni-19 Cr-0.4 Ti steel
126a	.092	.088	−.004	.087 to .090	4	.100	36 Ni steel
126	.097	.094	−.003	.094 to .095	4	.100	36 Ni steel
153	.099	.098	−.001	.097 to .099	4	.100	Mo-W-Cr-V-Co tool steel
50b	.110	.114	+.004	.114 to .115	4	.100	18W-4 Cr-1V steel
101c	.124	.120	−.004	.120 to .121	4	.100	18 Cr-9 Ni steel
121b	.124	.126	+.002	.125 to .128	4	.100	18 Cr-11 Ni-0.4 Ti steel
[a]159	.181	.186	+.005	.184 to .188	4	.100	0.09 Ag-1 Cr steel

[a] Extracts from this standard were slightly cloudy, presumably due to silver salts.

of high-purity iron indicated that amounts of copper up to 0.04 percent can be recovered in the presence of these quantities of iron to an accuracy of 0.0005 percent of copper. Blank corrections are very necessary, amounting to about 0.005 percent of copper on an 0.1-g sample basis using regular analytical reagents without purification. This figure can be reduced to 0.001 percent or less if appropriate steps of purification are used. The "blank" has proved in practice to be quite reproducible for any one lot of reagents.

The failure of the dimethylglyoxime procedure in the presence of more than moderate amounts of nickel is indicated by the low values obtained on the higher weight samples of NBS Standard Samples 33c and 101c, and is very likely caused by the occlusion or adsorption of the soluble copper glyoxime complex on the bulky nickel precipitate. Silver tends to give a cloudy extract, and the values reported for the silver-bearing steel, Standard Sample 159, are those obtained on centrifuged extracts, in order to eliminate this difficulty.

The results obtained by the procedure for ferrous materials high in nickel content are given in table 2. As will be noticed, all of the average values are within 0.005 percent of the certificate value. Separate experiments run on copper alone, on copper and the ethylenediaminetetraacetate complex, and on copper, iron, and the complexing reagent indicate that these combinations in the concentrations specified do not materially affect the completion of the extraction of the copper carbamate. The reaction is a little slower in the presence of the ethylenediaminetetraacetate ion, and the time of shaking specified should not be shortened. Values given for the silver-bearing steel, Standard Sample 159, were obtained on extracts not centrifuged, and the high values reported are due to the slight turbidity of these extracts.

In all cases, the ammoniacal iron solution must be *completely drained* and *separated* from the butyl acetate extract, or the iron complexes will be partially decomposed and interfering colors will be extracted during the washing of the butyl acetate extract with the dilute sulfuric acid solution. While any possible difficulty could be taken care of by an intermediate ammoniacal citrate wash, the simpler procedure recommended has proved entirely satisfactory in practice.

Spectral curves showing the absorbing characteristics of extracts prepared from solutions containing nickel, cobalt, bismuth, lead, and silver are shown in figure 2. As will be seen, all of these elements, except silver, absorb least in the wavelength region recommended for measurement (560 to 600 mμ). The silver curve shows general absorption above 500 mμ, characteristic of turbid solutions. The nickel and cobalt interference is eliminated by the use of suitable complexing reagents. Interference from lead and silver in the amounts ordinarily present in steel is not serious, as is shown in table 1. Bismuth is not ordinarily added as an alloying element in steel, but a few experiments made on synthetic mixtures with iron indicate that at least 1 percent of bismuth may be present without causing significant interference. Residual amounts of tin and small amounts of platinum, such as might be introduced by operations in platinum containers, also do not interfere.

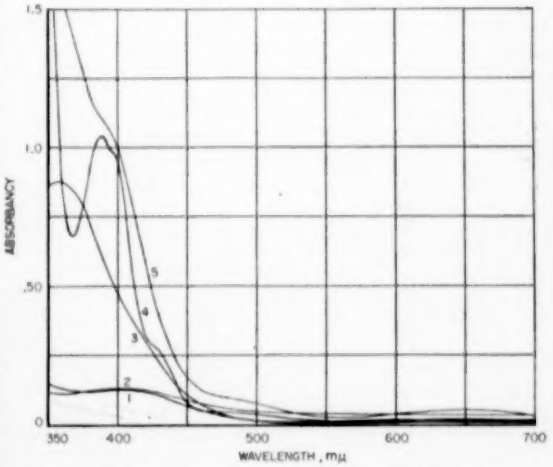

FIGURE 2. *Curves showing regions of absorption.*
1, Lead; 2, silver; 3, bismuth; 4, nickel; 5, cobalt.

Aside from the question of interferences, the absorbancy of the copper curves, figure 1, varies least with change in wavelength in the 600-mμ spectral region. This allows a filter photometer to be used in a routine manner under optimum conditions as regards requirements for spectral purity of the light used. As the high sensitivity of the copper reaction is also decreased, directly weighed samples of a practical size can be used, whereby the absolute amount of copper constituting the "blank" is reduced percentage-wise to a reasonable figure. This allows in everyday work the use of the usual quality of analytical reagents.

6. References

[1] ASTM Methods for chemical analysis of metals, Am. Soc. Testing Mat., pp. 97 to 100 (1950).

[2] L. I. Butler and H. O. Allen, J. Assoc. official Agr. Chem. **25,** 569 (1942).

[3] T. Callan and J. A. R. Henderson, Analyst **54,** 650 (1929).

[4] D. L. Drabkin, J. Assoc. official Agr. Chem. **22,** 320 (1939).

[5] K. Gleu and R. Schwab, Angew. Chem. **62,** 320 (1950).

[6] L. A. Haddock and N. Evers, Analyst **57,** 495 (1932).

[7] J. L. Hague, ASTM Proceedings **44,** 715 (1944).

[8] T. P. Hoar, Analyst **62,** 788 (1937).

[9] R. J. Lacoste, M. H. Earing, and S. E. Wiberly, Anal. Chem. **23,** 871 (1951).

[10] G. E. F. Lundell, J. I. Hoffman, and H. A. Bright, Chemical analysis of iron and steel, pp. 267 to 269. (John Wiley and Sons, Inc., New York, N. Y., 1931).

[11] V. Sedivec and V. Vasak, Collection Czechoslov. Chem. Comm. **15,** 260 (1950).

[12] S. D. Steele and L. Russell, Analyst **74,** 105 (1949).

[13] Arba Thomas, ASTM Proceedings **44,** 769 (1944).

Washington, August 7, 1951.

Journal of Research of the National Bureau of Standards Vol. 47, No. 5, November 1951 Research Paper 2266

Description and Analysis of the Second Spectrum of Chromium, Cr II

Carl C. Kiess

The analysis of Cr II presented in this paper is based on new wavelength measurements and estimated intensities, and on new observations of the Zeeman effect. Of approximately 2,100 lines listed in the tables, 89 percent have been classified as combinations of the levels of 48 even terms with levels of 51 odd terms. The even terms arise from the electron configurations $3d^5$, $3d^4\,4s$, and $3d^3\,4s^2$, the odd terms from the configuration $3d^4\,4p$. No odd terms from the configuration $3d^3\,4s\,4p$ have been established. High even terms from the excited configurations $3d^4\,4d$ and $3d^4\,5s$ have been found that form Rydberg series with terms from the low even configurations. From them an ionization potential of 16.49 electron volts has been derived for the work required to convert a singly ionized Cr atom in the $a\,^6S_{5/2}$ state to a doubly ionized atom in the $a\,^5D_0$ state. The terms of the $3d^3\,4s^2$ configuration lie high in the energy scale, and only a few relatively faint combinations between them and the odd terms have been found.

1. Introduction

The analysis of the second spectrum of chromium, presented in this paper, represents an attempt to classify its lines as completely as possible on the basis of present concepts of atomic structure. The work was started about 30 years ago and has been brought to its present status, from time to time, as new descriptive material for the spectrum became available. There are still some lines in the spectrum that resist classification; but at present it does not appear worth while to expend more time in order to identify them from existing data. The chief results of the investigation have been made known to those desiring them, as the work progressed, either through published notes or private communication, so that the main features of the analysis may be found in several well-known publications. But the new wavelength and Zeeman effect descriptions that have been made of the spectrum to improve and extend the analysis of the term-structure have not been published heretofore.

The inspiration for this work was found in the almost simultaneous discovery by Catalán [1] [1], by Frl. H. Gieseler [2], and by C. C. and H. K. Kiess [3], of complex groups of lines, called multiplets by Catalán, in the spectrum of neutral chromium. At that time the available data for an analysis of the chromium spark spectrum were those referred to by Kayser [4] in volumes 5 and 7 of the Handbuch der Spectroscopie; wavelengths by Exner and Haschek, by Eder and Valenta, and by Cooper; Zeeman patterns by Miller, by Purvis, by Babcock, and others; and some temperature classifications by King. These data were sufficient for a beginning of the analysis; but further progress was greatly aided by the new and unpublished Zeeman patterns that were made available to me by H. D. Babcock, of the Mt. Wilson Observatory.

The status of the analysis in 1930 was described in a short paper by the writer [5], listing the known terms of Cr I and Cr II. About the same time Krömer [6], and also Catalán [7], who had attacked the problem, made known their results, which were in substantial agreement with those worked out at the National Bureau of Standards. However, the growth of atomic theory during the decade from 1920 to 1930 gave insights into the problems of atomic spectra that indicated their scope and suggested lines of approach in unravelling them. One of the first-fruits of the application of theory to Cr II was the prediction and finding by Kiess and Laporte [8] of the $a\,^6S$ term as the ground state of the singly ionized chromium atom. In the light of the theoretical expectations it became apparent that further progress in the interpretation of Cr II demanded a more accurate and extensive description of it than was then in existence.

2. Experimental Procedure

The wavelengths and intensities listed in table 1 were derived from spectrograms made at the Bureau, at the Mt. Wilson Observatory, and at the Palmer Physical Laboratory of Princeton University. The first NBS observations were made with the Rowland concave grating ruled with 20,000 lines per inch. Owing to its low reflectance in the ultraviolet, this grating covered only the region above 2600 A, with a scale of 1.8 A/mm in the second order. Later, when a new concave grating with 30,000 lines per inch was received from R. W. Wood [9], the spectrum was resurveyed from 2000 A in the ultraviolet to 8500 A in the near infrared, with reciprocal dispersions of 1 and 2 A/mm, respectively, in the second and first orders. Supplementary spectrograms of the ultraviolet were obtained from 1950 to 2400 A with the Hilger E1 quartz-prism spectrograph, and from 2200 to 3100 A with another Hilger instrument, which carries a large 60°.Cornu prism in combination with a 30° reflecting prism in the E185 mounting.

The light sources were arcs and condensed sparks between metallic chromium electrodes in air or in enclosures through which air or other gases could be kept flowing at reduced pressures. The enclosed arc was a reproduction of that described and illustrated by H. D. Curtis [10]. The arcs were operated at 4 to 7 amp drawn from a 220-v direct-current circuit.

[1] Figures in brackets indicate the literature references at the end of this paper.

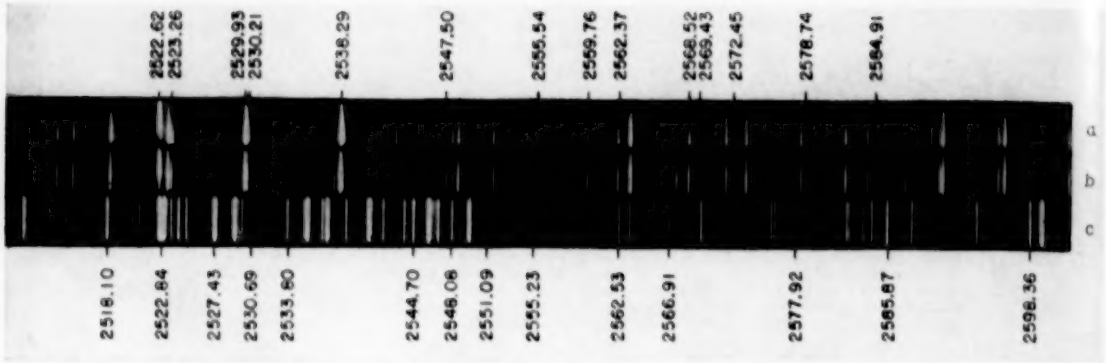

FIGURE 1. Cr II *lines at atmospheric and reduced pressures*: (*a*) *1 atm*; (*b*) *about ⅕ atm*; (*c*) Fe *arc spectrum*.

The sparks were supplied by discharges from a battery of condensers rated at 0.006μf and charged from the 30,000–v secondary coil of a transformer whose primary carried approximately 7 amp from a 110–v alternating-current circuit. Each exposure to the spark-in-air, with the Wood grating, was followed by an exposure to a condensed spark-discharge in the enclosure in which the pressure of the flowing gas was about ⅕ atm. The purpose of this procedure is to sharpen certain groups of lines that appear diffuse and asymetrically broadened toward longer waves in the spark at normal atmospheric pressure. Its effectiveness is illustrated in figure 1.

The spark chamber is illustrated in figure 2. The enclosure consists of two Pyrex 6 in. bowl-type lead-in insulators, which can be clamped against gaskets attached to the cast brass ring, *A*. In the removable cell, *B*, in the front of the ring, either glass or quartz windows may be inserted. On one side of the ring at *C* and *D* are the inlet and outlet valves to the high and low pressure lines, and at *E*, on the other side, is the pinion for separating the electrode holders. On the back of the ring at *F* is the sleeve by which it is attached to the vertical support along which it is raised and lowered. The connections to the electric circuit are through the binding posts at the small ends of the Pyrex bowls.

The spectrograms lent by A. S. King were obtained with the 15,000 lines-per-inch concave grating in the vertical Rowland mounting of the Mt. Wilson Observatory. They contain spectra of the arc and condensed spark in air covering the region from 3680 to 6600 A with a scale of 1.85 A/mm. The Princeton plates were made especially for this investigation by A. G. Shenstone with his vacuum spectrograph. This instrument carries a 2–m glass grating ruled by Wood with 30,000 lines per inch, and gives a dispersion of 4.2 A/mm. Light from arcs and sparks illuminated the full length of the slit so that some judgment of the ionization of the emitter of the lines might be formed from the distribution of intensity along the lines. The spectra extend from 1200 to 2200 A.

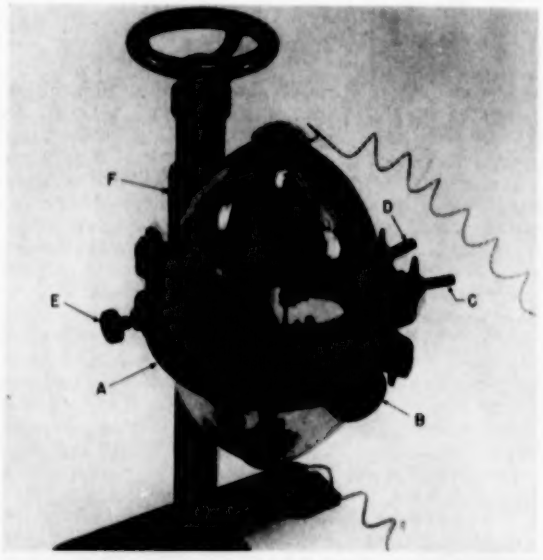

FIGURE 2. *Enclosed lamp for operating sparks between metal electrodes at atmospheric and reduced pressures.*

Babcock's published and unpublished Zeeman patterns were of inestimable value in the early stages of unravelling the chromium spectra. Yet as the analysis progressed, urgent need was felt for additional data of this kind, especially for fainter lines and those of shorter wavelength. When, therefore, the National Bureau of Standards acquired a large Weiss water-cooled magnet from the Société Genevoise, chromium was one of the first elements to be investigated. Fields of about 35,000 oersteds were attained in a gap of 5 mm between the ferro-cobalt poles when currents of 160 amp were flowing through the coils. The observations were recorded with the grating and prism spectrographs mentioned above and covered the wavelength range from 2300 to 6400 A. When the Zeeman program was begun at Massachusetts

Institute of Technology, a set of exposures to chromium was made, under the direction of G. R. Harrison, especially for this investigation; and later a supplementary set was made by W. F. Meggers.

3. Results

3.1. Wavelengths and Intensities

The wavelengths presented in the first column of table 1 were derived from measurements of the spectrograms described above. The tabulated values are means of two to eight determinations for all except a few of the lines. No line measured on only one spectrogram has been retained in the list unless its reality is verified from term-combinations. All the wavelengths in table 1 are air values. Although the wavelengths have been rounded off to the nearest 0.01 A, yet it is believed that their accuracy exceeds this limit, except for the wide and hazy lines. Wherever possible, for such lines, the wavelengths were determined from spectra of the low-pressure source. The wavelengths of diffuse lines observed only in the spark-in-air were corrected for the redward shift due to pressure. Wavelengths measured below 2000 A are vacuum values. The lines of Cr II in this region that have been classified are listed in table 2.

In the second column of the table are numbers and letters that indicate the strength and character of the lines. The letters have the following significance: d=double, g=ghost, h=hazy, diffuse, l=shaded toward longer waves, s=shaded toward shorter waves, w=wide, W=very wide. In the last column the symbol † following a Zeeman pattern means that it was measured only on NBS spectrograms, all the others having been measured on MIT plates. The letters indicate the type of shading in unresolved patterns, thus: A=◁▷, B=▷◁, C=△, D=□. The letter w, with subscripts, indicates different degrees of widening of unresolved p and n components that do not have distinctive shading.

The intensities assigned to the lines are visual estimates that seek to express their strengths relative to the weakest ones measurable, which are given intensity 1. Such estimates are only qualitatively comparable between one region of the spectrum and another, owing to differences in sensitivity of the various kinds of photographic plates used to record the spectra. Thus, lines in the yellow region should not be compared with those in the ultraviolet bearing the same intensity numbers. However, certain quantitative relationships have been found to exist between the intensity scales used in this work and A. S. King's [11] and the intensities measured photometrically by Allen and Hesthal [12]. For about 65 lines in eight Cr II multiplets the latter authors give measured intensities that are in very good agreement with the theoretical relative intensities calculated for *LS*-coupling. For about 50 percent of these lines comparisons with King's estimated intensities show that the square roots of the measured intensities are quite accurately 1.1 times the estimated values. This is in strict harmony with Russell's [13] finding "that King's estimated intensities are very nearly proportional to the square roots of the actual intensities."

King's estimates refer to the strengths with which the lines appear in arc excitation, whereas the estimates in table 1 refer to their strengths in condensed sparks. For the region common to the two investigations the intensity scale of table 1 has a wider range than King's. For 32 lines to which King assigns intensities 1 to 5 the corresponding numbers in the table are 17.5 times greater; for 26 of King's lines in the intensity group 6–10, the NBS values are 8.5 times greater; and for all of King's intensities above 10 the NBS values are 5.5 times greater.

3.2. Zeeman Effects

The magnetic patterns that have been measured on the NBS and MIT spectrograms are given in the last column of table 1. These results portray the magnetic behavior of the radiating atoms at two field strengths, namely, 35,000 and 76,000 oersteds. Only those patterns from the NBS plates are reported that do not appear or cannot be measured on the MIT spectrograms. The two sets of observations are in very good agreement for all lines for which they yield resolved patterns. And the same may be said with respect to Babcock's measurements and those published by Krömer.

From these patterns were derived the g-values given in tables 3 and 4 for the Cr II levels. The g's are very nearly those required by Landé's theory for *LS*-coupling, especially for the levels of the low terms. In the quartet terms from the $3d^5$ electron-configuration, however, the levels are separated by very small intervals, much less than their splittings in the magnetic fields used in this work, and they are partially inverted so that the algebraic sum of the intervals differs little from zero. The Zeeman patterns observed for lines involving these levels are badly distorted owing to Paschen-Back interactions. The patterns exhibit striking dissymmetries in the intensities of the components, and their complexity is increased by the presence of transitions forbidden by the selection rule for inner quantum numbers. Nevertheless, it has been possible to resolve these patterns by the procedure followed by Kiess and Shortley [14] for O I and N I and to derive the g-values listed in table 3 for the perturbed levels. The lines of table 1 so affected are designated by the symbol P–B. The details of their interpretation will be presented in a subsequent paper.

3.3. Term Structure of Cr II

The spectrum to be expected theoretically for the Cr^+ ion is similar to those of V I, Mn III, Fe IV, etc., which are characteristic of atoms and ions with 23 external electrons. All except five of these electrons are in closed groups. In the low and metastable states of the ion the five valence electrons

form the even configurations $3d^5$, $3d^4\,4s$, and $3d^3\,4s^2$. When the ion is excited these may be transformed into the odd configurations $3d^4\,4p$ and $3d^3\,4s\,4p$. Further excitation will produce, alternately, higher even and odd configurations whose terms form series with those from the lower configurations according to their parity. The terms belonging to these electron configurations, according to Hund's theory, are listed in table 5, and are valid for all spectra of the V I isoelectronic sequence. A similar but more extensive table in which the theoretical terms are coordinated with their limits is given as table 22 on page XXXVIII of the Introduction to volume 1 of "Atomic energy levels", Circular 467 of the National Bureau of Standards. The terms actually found are indicated by bold-face type in table 5, and their values are given in tables 3 and 4. No terms from the configuration $3d^3\,4s\,4p$ have as yet been found.

The correlation of the observed with the theoretical Cr II terms was achieved with the help of various guides. The terms of the $3d^5$ configuration, and the doublets of $3d^4\,4s$ that are derived from singlets, exhibit small separations, $\Delta\nu$, of only a few cm^{-1} between their component levels. With the quartet terms partial inversion occurs among the levels so that the algebraic sum of the $\Delta\nu$'s differs from zero by only a few wave number units. Some of the doublets are also inverted. On the other hand, the terms from the $3d^4\,4s$ and $3d^3\,4s^2$ configurations have wide level separations ranging from some tens to several hundred cm^{-1}. In some of the terms, however, the intervals are of the same order of magnitude for each of the configurations. This is particularly the case for terms with L-values greater than 2. In such cases the configuration assignments are those indicated by Laporte [15] for the d^5 configuration, by Laporte and Platt [16] for the d^4 and d^3 configurations, or by Racah [17] and coworkers, notably A. Schweitzer [18], in consideration of the interaction between the d^5 and $d^4\,s$ configurations.

It is to be noted that the terms assigned to $3d^3\,4s^2$ lie very high and give only weak combinations with some of the $3d^4\,4p$ terms. It is plausible that they could belong to the $3d^4\,4s$ configuration, but their positions in the term scale argue in favor of the assigned configuration.

3.4. Series and Ionization Potential

Among the terms of table 3 there are eight pairs that belong to Rydberg sequences. These are given in table 6. It is well known that limits calculated with a Rydberg formula for 2-member series are only approximately correct and do not give the best value for the ionization potential. In 1927 Russell [19] stated: "Experience shows that this value is usually nearly correct when the series is produced by the removal of an s electron, since in such series the Ritz correction is almost always small. Series involving changes in a d electron are usually very regular, except for the lowest term, when this involves the binding of the electron as part of an incomplete shell. In this case the energy of binding is considerably increased, and the application of a single Rydberg formula puts the limit a great deal too high". For this reason the five pairs of terms listed in table 6 as due to the migration of a d-electron have not been used to determine the ionization potential of Cr^+. Their representation by a Rydberg formula leads to rather erratic values for the series limit. On the other hand, the three pairs of terms due to the ns-electrons give the values 135,400, 134,500, and 137,500 cm^{-1}, respectively, for the distance between $^6S_{2½}$ of Cr II and $^5D_0$ of Cr III. The mean of these is only slightly less than 136,000 cm^{-1}, the value adopted tentatively for the ground state of Cr III. But evidence derived from other spectra in which series of three or more members are known indicates that this value also is too high.

To arrive at the true series limit, from which a correct value for the ionization potential may be derived, it is therefore necessary to apply corrections to the denominators of the Rydberg formula. These corrections can be determined accurately only in spectra in which three or more series members are represented by a Ritz formula, as illustrated by Shenstone [20], for example, in Cu II. For spectra with only two series members Russell [21] has shown, recently, that very close estimates of the Ritz corrections may be found by comparisons with spectra of neighboring elements. Thus, for Cr II the limit of 136,000 cm^{-1} given by the Rydberg formula is found to require a Ritz correction of $-2{,}940$ cm^{-1}, which gives 133,060 cm^{-1} for the distance between $a\,^6S_{2½}$ of Cr II and $a\,^5D_0$ of Cr III. This corresponds to an ionization potential of 16.49 v.

The work described would not have reached its present status without the friendly cooperation of various individuals. H. D. Babcock, of the Mt. Wilson Observatory, made available to me his unpublished Zeeman patterns of the chromium spectra. A. S. King, also of the Mt. Wilson Observatory, placed at my disposal his furnace observations of the ultraviolet spectra, in advance of publication, and some of his arc and spark spectrograms of the chromium spectra. Likewise, R. J. Lang, University of Alberta, sent me his unpublished list of chromium wavelengths in the far ultraviolet. Both G. R. Harrison, Massachusetts Institute of Technology, and W. F. Meggers, National Bureau of Standards, secured Zeeman effect observations with the high fields and high dispersion of the MIT magnet and spectrographs. Finally, W. H. Seaquist, B. H. Monish, and W. F. Hausstein of the Bureau gave valuable advice and suggestions on the design and construction of the enclosed spark lamp. It is a pleasure for me to express to each of them my appreciation for his contribution to this work.

TABLE 1. *Wavelengths of* Cr II *in air*

Wavelength	Intensity	Wave No.	Term combination	Zeeman effect
7311. 60	2	13673. 14	$c\ ^4D_{3\frac{1}{2}} - z\ ^4F^0_{4\frac{1}{2}}$	
6418. 87	20	15574. 77	$c\ ^4F_{4\frac{1}{2}} - x\ ^4F^0_{4\frac{1}{2}}$	(0.00)1.33†
6415. 60	2	15582. 71	$c\ ^4F_{4\frac{1}{2}} - x\ ^4F^0_{3\frac{1}{2}}$	
6358. 06	1	15723. 73	$b\ ^2P_{1\frac{1}{2}} - y\ ^2P^0_{0\frac{1}{2}}$	
6305. 61	15	15854. 52	$b\ ^2P_{1\frac{1}{2}} - y\ ^2P^0_{1\frac{1}{2}}$	(0.00)1.36†
6282. 92	6	15911. 77	$c\ ^4F_{3\frac{1}{2}} - x\ ^4F^0_{3\frac{1}{2}}$	
6274. 93	2	15932. 03	$c\ ^4F_{3\frac{1}{2}} - x\ ^4F^0_{4\frac{1}{2}}$	
6271. 84	15	15939. 88	$c\ ^4F_{3\frac{1}{2}} - x\ ^4F^0_{3\frac{1}{2}}$	(0.00)1.24†
6263. 22	6	15961. 82	$d\ ^2F_{2\frac{1}{2}} - z\ ^2D^0_{1\frac{1}{2}}$	
6239. 78	10	16021. 78	$c\ ^4D_{0\frac{1}{2}} - z\ ^4D^0_{0\frac{1}{2}}$	
6226. 67	8	16055. 52	$c\ ^4D_{1\frac{1}{2}} - z\ ^4D^0_{0\frac{1}{2}}$	
6208. 20	2	16103. 28	$c\ ^4D_{0\frac{1}{2}} - z\ ^4D^0_{1\frac{1}{2}}$	
6195. 17	15	16137. 15	$c\ ^4D_{1\frac{1}{2}} - z\ ^4D^0_{1\frac{1}{2}}$	
6181. 38	5	16173. 15	$e\ ^2G_{4\frac{1}{2}} - y\ ^2F^0_{3\frac{1}{2}}$	
6179. 17	35	16178. 94	$d\ ^2G_{3\frac{1}{2}} - z\ ^2H^0_{4\frac{1}{2}}$	(0.00)0.95†
6176. 95	15	16184. 75	$c\ ^4D_{2\frac{1}{2}} - z\ ^4D^0_{1\frac{1}{2}}$	
6168. 46	2	16207. 03	$c\ ^4F_{2\frac{1}{2}} - x\ ^4F^0_{2\frac{1}{2}}$	
6157. 80	7	16235. 08	$c\ ^4F_{2\frac{1}{2}} - x\ ^4F^0_{3\frac{1}{2}}$	
6147. 17	20	16263. 16	$c\ ^4D_{1\frac{1}{2}} - z\ ^4D^0_{2\frac{1}{2}}$	
6138. 77	10	16285. 41	$d\ ^2G_{3\frac{1}{2}} - z\ ^2F^0_{2\frac{1}{2}}$	(0.00)0.94†
6134. 38	2	16297. 06	$c\ ^4F_{1\frac{1}{2}} - x\ ^4F^0_{1\frac{1}{2}}$	
6129. 23	18	16310. 76	$c\ ^4D_{2\frac{1}{2}} - z\ ^4D^0_{2\frac{1}{2}}$	(0.00)1.38†
6116. 42	2	16344. 92	$d\ ^2F_{3\frac{1}{2}} - z\ ^2D^0_{2\frac{1}{2}}$	
6112. 27	3	16356. 02	$c\ ^4D_{3\frac{1}{2}} - z\ ^4D^0_{2\frac{1}{2}}$	
6089. 69	15	16416. 66	$d\ ^2G_{4\frac{1}{2}} - z\ ^2H^0_{3\frac{1}{2}}$	(0.00)1.07†
6081. 52	3	16438. 72	$d\ ^2G_{4\frac{1}{2}} - z\ ^2F^0_{3\frac{1}{2}}$	
6070. 10	2	16469. 64	$c\ ^4D_{2\frac{1}{2}} - z\ ^4D^0_{3\frac{1}{2}}$	
6069. 69	1	16470. 76	$c\ ^4F_{4\frac{1}{2}} - y\ ^2H^0_{3\frac{1}{2}}$	
6067. 99	7	16475. 37	$c\ ^4F_{4\frac{1}{2}} - y\ ^2H^0_{4\frac{1}{2}}$	
6053. 48	75	16514. 86	$c\ ^4D_{3\frac{1}{2}} - z\ ^4D^0_{3\frac{1}{2}}$	(0.00)1.42†
6040. 57	10	16550. 16		
5913. 86	12	16904. 76		
5895. 89	15	16956. 28	$c\ ^4F_{4\frac{1}{2}} - x\ ^4G^0_{5\frac{1}{2}}$	
5841. 88	12	17113. 04	$c\ ^4F_{3\frac{1}{2}} - x\ ^4G^0_{4\frac{1}{2}}$	
5827. 24	12	17156. 04	$c\ ^4F_{2\frac{1}{2}} - x\ ^4G^0_{3\frac{1}{2}}$	
5795. 28	2	17250. 65		
5790. 29	20	17265. 78	$c\ ^4F_{1\frac{1}{2}} - x\ ^4G^0_{2\frac{1}{2}}$	
5775. 81	4	17308. 80	$e\ ^2D_{2\frac{1}{2}} - w\ ^2F^0_{3\frac{1}{2}}$	
5685. 90	7	17582. 50	$d\ ^2G_{4\frac{1}{2}} - y\ ^2G^0_{5\frac{1}{2}}$	
5678. 44	20	17605. 60	$d\ ^2G_{3\frac{1}{2}} - y\ ^2G^0_{4\frac{1}{2}}$	(0.00)0.92†
5620. 68	30	17786. 52	$d\ ^2G_{4\frac{1}{2}} - y\ ^2G^0_{4\frac{1}{2}}$	(0.00)1.10†
5613. 18	10	17810. 28	$d\ ^2G_{3\frac{1}{2}} - y\ ^2G^0_{3\frac{1}{2}}$	
5542. 48	3	18037. 47		
5510. 71	20	18141. 46	$b\ ^4P_{2\frac{1}{2}} - z\ ^4P^0_{1\frac{1}{2}}$	(0.00*w*)1.42*A*†
5508. 63	30	18148. 30	$b\ ^4G_{3\frac{1}{2}} - z\ ^4F^0_{3\frac{1}{2}}$	(0.00)0.95
5503. 21	25	18166. 18	$b\ ^4G_{2\frac{1}{2}} - z\ ^4F^0_{1\frac{1}{2}}$	(0.00)0.78
5502. 07	40	18169. 94	$b\ ^4G_{4\frac{1}{2}} - z\ ^4F^0_{3\frac{1}{2}}$	(0.00)1.03*A*†
5497. 80	3	18184. 06	$b\ ^4P_{1\frac{1}{2}} - z\ ^4P^0_{2\frac{1}{2}}$	
5478. 37	50	18248. 55	$b\ ^4G_{5\frac{1}{2}} - z\ ^4F^0_{4\frac{1}{2}}$	(0.00*w*)1.10*A*†
5477. 80	2	18250. 45	$e\ ^2D_{1\frac{1}{2}} - x\ ^2P^0_{0\frac{1}{2}}$	
5477. 49	10	18251. 48	$b\ ^4G_{2\frac{1}{2}} - z\ ^4F^0_{2\frac{1}{2}}$	
5472. 60	12	18267. 79	$b\ ^4G_{3\frac{1}{2}} - z\ ^4F^0_{3\frac{1}{2}}$	
5455. 86	8	18323. 84	$b\ ^4G_{4\frac{1}{2}} - z\ ^4F^0_{3\frac{1}{2}}$	
5446. 77	10	18354. 42	$c\ ^4P_{1\frac{1}{2}} - w\ ^4D^0_{2\frac{1}{2}}$	
5420. 91	25	18441. 97	$b\ ^4P_{1\frac{1}{2}} - z\ ^4P^0_{0\frac{1}{2}}$	(0.56)**1.16,** 2.26†
5419. 38	2	18447. 18	$b\ ^4P_{0\frac{1}{2}} - z\ ^4P^0_{1\frac{1}{2}}$	
5414. 86	7	18462. 58	$c\ ^4P_{2\frac{1}{2}} - w\ ^4D^0_{3\frac{1}{2}}$	
5407. 62	25	18487. 30	$b\ ^4P_{2\frac{1}{2}} - z\ ^4P^0_{2\frac{1}{2}}$	(0.00)1.66†
5379. 80	6	18582. 90	$b\ ^2P_{1\frac{1}{2}} - x\ ^2P^0_{1\frac{1}{2}}$	

TABLE 1. *Wavelengths of* Cr II *in air*—Continued

Wavelength	Intensity	Wave No.	Term combination	Zeeman effect
5369.36	15	18619.03	$a\ ^4F_{4\frac{1}{2}} - z\ ^6D^0_{3\frac{1}{2}}$	
5368.09	7	18623.43	$a\ ^4F_{1\frac{1}{2}} - z\ ^6D^0_{2\frac{1}{2}}$	
5354.72	3	18669.93	$a\ ^4F_{3\frac{1}{2}} - z\ ^6D^0_{4\frac{1}{2}}$	
5346.54	5	18698.48	$b\ ^4P_{1\frac{1}{2}} - z\ ^4P^0_{1\frac{1}{2}}$	
5337.81	30	18729.08	$b\ ^4F_{2\frac{1}{2}} - z\ ^4F^0_{1\frac{1}{2}}$	(0.38)**0.74**, 1.34, **1.96**†
5334.89	50	18739.33	$b\ ^4F_{1\frac{1}{2}} - z\ ^4F^0_{1\frac{1}{2}}$	(0.00)0.42†
5318.38	15	18797.50	$b\ ^4P_{0\frac{1}{2}} - z\ ^4P^0_{0\frac{1}{2}}$	
5316.28	7	18804.93	$b\ ^2P_{1\frac{1}{2}} - x\ ^2D^0_{2\frac{1}{2}}$	
5313.61	40	18814.38	$b\ ^4F_{2\frac{1}{2}} - z\ ^4F^0_{2\frac{1}{2}}$	(0.00)1.06†
5310.73	30	18824.58	$b\ ^4F_{1\frac{1}{2}} - z\ ^4F^0_{2\frac{1}{2}}$	(0.27, 0.88) 0.80, 1.41, **2.02**†
5308.46	35	18832.63	$b\ ^4F_{2\frac{1}{2}} - z\ ^4F^0_{3\frac{1}{2}}$	(0.00*W*)1.72*B*†
5305.86	40	18841.85	$b\ ^4P_{2\frac{1}{2}} - z\ ^6D^0_{2\frac{1}{2}}$	(0.00*w*)1.66†
5280.08	30	18933.85	$b\ ^4F_{3\frac{1}{2}} - z\ ^4F^0_{3\frac{1}{2}}$	(0.00)1.35
5279.88	50	18934.57	$b\ ^4F_{4\frac{1}{2}} - z\ ^4F^0_{3\frac{1}{2}}$	(0.00*l*?)1.53*B*†
5274.99	75	18952.12	$b\ ^4F_{3\frac{1}{2}} - z\ ^4F^0_{3\frac{1}{2}}$	(0.00)1.28†
5249.43	20	19044.40	$b\ ^4P_{1\frac{1}{2}} - z\ ^4P^0_{2\frac{1}{2}}$	
5246.76	30	19054.09	$b\ ^4P_{0\frac{1}{2}} - z\ ^4P^0_{1\frac{1}{2}}$	(0.43)**1.41**, 2.26†
5237.35	100	19088.33	$b\ ^4F_{4\frac{1}{2}} - z\ ^4F^0_{4\frac{1}{2}}$	(0.00)1.34†
5232.54	20	19105.87	$b\ ^4F_{3\frac{1}{2}} - z\ ^4F^0_{4\frac{1}{2}}$	(0.00)1.61*w*†
5210.87	10	19185.33	$b\ ^4P_{1\frac{1}{2}} - z\ ^6D^0_{0\frac{1}{2}}$	(0.68)**0.93**, 2.52†
5202.60	3	19215.82	$d\ ^2F_{2\frac{1}{2}} - y\ ^2G^0_{3\frac{1}{2}}$	
5191.44	2	19257.13	$b\ ^4P_{1\frac{1}{2}} - z\ ^6D^0_{1\frac{1}{2}}$	
5188.91	1	19266.52	$d\ ^2F_{2\frac{1}{2}} - y\ ^2D^0_{2\frac{1}{2}}$	
5186.12	2	19276.88	$d\ ^2D_{1\frac{1}{2}} - z\ ^2D^0_{1\frac{1}{2}}$	
5153.50	20	19398.90	$b\ ^4P_{1\frac{1}{2}} - z\ ^6D^0_{2\frac{1}{2}}$	
5142.52	2	19440.32	$d\ ^2F_{3\frac{1}{2}} - y\ ^2G^0_{4\frac{1}{2}}$	
5137.09	7	19460.87	$c\ ^4P_{2\frac{1}{2}} - x\ ^4P^0_{2\frac{1}{2}}$	(0.00)1.64†
5121.10	2	19521.63		
5116.07	2	19540.82	$b\ ^4P_{0\frac{1}{2}} - z\ ^6D^0_{0\frac{1}{2}}$	
5110.45	2	19562.31	$c\ ^4F_{4\frac{1}{2}} - w\ ^4D^0_{3\frac{1}{2}}$	
5097.33	7	19612.66	$b\ ^4P_{0\frac{1}{2}} - z\ ^6D^0_{1\frac{1}{2}}$	(?)**1.51**, 2.20†
5091.14	2	19636.51	$c\ ^4P_{1\frac{1}{2}} - x\ ^4P^0_{1\frac{1}{2}}$	
5090.36	1	19639.52	$d\ ^2D_{1\frac{1}{2}} - z\ ^2D^0_{2\frac{1}{2}}$	
5085.70	4	19657.51	$d\ ^2D_{2\frac{1}{2}} - z\ ^2D^0_{2\frac{1}{2}}$	
5076.16	4	19694.46	$c\ ^4P_{2\frac{1}{2}} - x\ ^4P^0_{1\frac{1}{2}}$	
5031.28	3	19870.13	$c\ ^4F_{3\frac{1}{2}} - w\ ^4D^0_{2\frac{1}{2}}$	
5024.52	10	19896.87	$d\ ^2F_{2\frac{1}{2}} - y\ ^2F^0_{3\frac{1}{2}}$	(0.00)0.86†
4952.79	12	20185.06	$d\ ^2F_{3\frac{1}{2}} - y\ ^2F^0_{3\frac{1}{2}}$	(0.00)1.19†
4912.50	15	20350.57	$d\ ^2G_{3\frac{1}{2}} - x\ ^2G^0_{3\frac{1}{2}}$	(0.00)0.91†
4901.66	15	20395.58	$d\ ^2G_{4\frac{1}{2}} - x\ ^2G^0_{4\frac{1}{2}}$	(0.00)1.15†
4884.58	12	20466.89	$a\ ^4F_{2\frac{1}{2}} - z\ ^4F^0_{1\frac{1}{2}}$	(. . .?)0.12, **0.73**, 1.39, **2.05**
4876.41	20	20501.18	$a\ ^4F_{3\frac{1}{2}} - z\ ^4F^0_{2\frac{1}{2}}$	(0.00)1.64*B*†
4876.37	40	20501.49	$a\ ^4F_{1\frac{1}{2}} - z\ ^4F^0_{1\frac{1}{2}}$	(0.00)0.41
4864.31	60	20552.18	$a\ ^4F_{2\frac{1}{2}} - z\ ^4F^0_{3\frac{1}{2}}$	(0.00)1.04
4860.20	20	20569.56	$a\ ^4F_{4\frac{1}{2}} - z\ ^4F^0_{3\frac{1}{2}}$	(0.00)1.59*B*
4857.60	2	20580.57	$c\ ^4F_{4\frac{1}{2}} - w\ ^4F^0_{3\frac{1}{2}}$	
4856.18	20	20586.58	$a\ ^4F_{3\frac{1}{2}} - z\ ^4F^0_{4\frac{1}{2}}$	(?)0.74, 1.36, **2.04**†
4848.24	75	20620.30	$a\ ^4F_{3\frac{1}{2}} - z\ ^4F^0_{3\frac{1}{2}}$	(0.00)1.25
4836.22	25	20671.55	$a\ ^4F_{2\frac{1}{2}} - z\ ^4F^0_{3\frac{1}{2}}$	(?)1.71*B*†
4832.38	3	20687.97		
4824.12	100	20723.40	$a\ ^4F_{4\frac{1}{2}} - z\ ^4F^0_{4\frac{1}{2}}$	(0.00)1.34
4815.29	1	20761.40	$c\ ^2D_{1\frac{1}{2}} - w\ ^2D^0_{1\frac{1}{2}}$	
4812.34	25	20774.12	$a\ ^4F_{3\frac{1}{2}} - z\ ^4F^0_{4\frac{1}{2}}$	(0.00)1.63*B*†
4794.79	1	20850.16	$c\ ^2D_{2\frac{1}{2}} - w\ ^2D^0_{2\frac{1}{2}}$	
4793.09	2	20857.56	$c\ ^4F_{3\frac{1}{2}} - w\ ^4F^0_{3\frac{1}{2}}$	
4765.06	2	20980.25	$c\ ^2D_{1\frac{1}{2}} - z\ ^2D^0_{1\frac{1}{2}}$	
4761.40	2	20996.37	$c\ ^2D_{2\frac{1}{2}} - y\ ^2P^0_{1\frac{1}{2}}$	
4749.75	1	21047.87	$c\ ^4F_{2\frac{1}{2}} - w\ ^4F^0_{3\frac{1}{2}}$	
4715.12	3	21202.45	$c\ ^2D_{1\frac{1}{2}} - z\ ^2P^0_{0\frac{1}{2}}$	
4713.27	1	21210.78	$d\ ^2D_{1\frac{1}{2}} - z\ ^2F^0_{2\frac{1}{2}}$	

TABLE 1. *Wavelengths of* Cr II *in air*—Continued

Wavelength	Intensity	Wave No.	Term combination	Zeeman effect
4710.78	1	21221.99	$c\ ^4F_{1\frac{1}{2}} - w\ ^4F^\circ_{1\frac{1}{2}}$	
4697.61	3	21281.48	$c\ ^2D_{2\frac{1}{2}} - z\ ^2D^\circ_{2\frac{1}{2}}$	
4684.78	2	21339.76	$c\ ^2D_{2\frac{1}{2}} - z\ ^2P^\circ_{1\frac{1}{2}}$	
4634.10	40	21573.14	$b\ ^4F_{1\frac{1}{2}} - z\ ^4D^\circ_{0\frac{1}{2}}$	(0.24)0.24, **0.62**†
4618.82	50	21644.51	$b\ ^4F_{2\frac{1}{2}} - z\ ^4D^\circ_{1\frac{1}{2}}$	(0.00)0.82*A*†
4616.64	25	21654.73	$b\ ^4F_{1\frac{1}{2}} - z\ ^4D^\circ_{1\frac{1}{2}}$	(1.19) . . ., 0.79, 1.62†
4592.07	25	21770.59	$b\ ^4F_{2\frac{1}{2}} - z\ ^4D^\circ_{2\frac{1}{2}}$	(0.50, **0.86**)0.41, 0.82, **1.26**, 1.60, 1.90†
4589.89	4	21780.93	$b\ ^4F_{1\frac{1}{2}} - z\ ^4D^\circ_{2\frac{1}{2}}$	
4588.22	75	21788.86	$b\ ^4F_{3\frac{1}{2}} - z\ ^4D^\circ_{3\frac{1}{2}}$	(0.00, 0.18, 0.35) **0.90**, 1.09, 1.28, 1.48
4587.30	2	21793.23	$d\ ^2G_{4\frac{1}{2}} - x\ ^2F^\circ_{3\frac{1}{2}}$	
4572.84	2	21862.14	$c\ ^2D_{2\frac{1}{2}} - v\ ^2F^\circ_{3\frac{1}{2}}$	
4565.77	10	21895.99	$a\ ^2F_{3\frac{1}{2}} - z\ ^4D^\circ_{2\frac{1}{2}}$	(0.00) **0.51**, 0.78
4564.27	2	21903.19		
4558.66	100	21930.14	$b\ ^4F_{4\frac{1}{2}} - z\ ^4D^\circ_{3\frac{1}{2}}$	(0.00)1.07*A*†
4555.01	30	21947.72	$b\ ^4F_{3\frac{1}{2}} - z\ ^4D^\circ_{2\frac{1}{2}}$	(0.66)1.33*w*†
4546.63	2	21988.17		
4539.61	3	22022.17	$a\ ^2F_{2\frac{1}{2}} - z\ ^4D^\circ_{2\frac{1}{2}}$	
4515.83	4	22138.14	$d\ ^2G_{3\frac{1}{2}} - x\ ^2F^\circ_{2\frac{1}{2}}$	
4489.14	2	22269.76	$a\ ^2F_{3\frac{1}{2}} - z\ ^4D^\circ_{3\frac{1}{2}}$	
4465.77	5	22386.29	$d\ ^2G_{4\frac{1}{2}} - x\ ^2H^\circ_{5\frac{1}{2}}$	
4362.93	3	22913.96	$c\ ^2D_{1\frac{1}{2}} - z\ ^2F^\circ_{2\frac{1}{2}}$	
4341.09	10	23029.24	$c\ ^2D_{2\frac{1}{2}} - z\ ^2F^\circ_{3\frac{1}{2}}$	(0.00)1.13†
4308.81	3	23201.76		
4306.95	10	23211.78	$d\ ^2D_{1\frac{1}{2}} - y\ ^2F^\circ_{2\frac{1}{2}}$	(0.00)0.90†
4284.21	20	23334.98	$a\ ^4F_{1\frac{1}{2}} - z\ ^4D^\circ_{0\frac{1}{2}}$	(0.20)0.22, **0.63**†
4278.11	3*s*	23368.26	$b\ ^2D_{1\frac{1}{2}} - y\ ^4P^\circ_{1\frac{1}{2}}$	
4275.58	30	23382.08	$a\ ^4F_{2\frac{1}{2}} - z\ ^4D^\circ_{1\frac{1}{2}}$	(0.00)0.77
4269.29	10	23416.53	$a\ ^4F_{1\frac{1}{2}} - z\ ^4D^\circ_{1\frac{1}{2}}$	(1.24)0.00, **0.80**, 1.62†
4268.96	3	23418.34	$d\ ^2G_{3\frac{1}{2}} - w^2G^\circ_{3\frac{1}{2}}$	
4265.05	2	23439.81		
4261.92	30	23457.02	$a\ ^4F_{2\frac{1}{2}} - z\ ^4D^\circ_{2\frac{1}{2}}$	(0.00)1.00*A*
4256.17	5*l*, *d*?	23488.71	$d\ ^2G_{4\frac{1}{2}} - w^2G^\circ_{4\frac{1}{2}}$	(0.00)1.10
4252.63	10	23508.27	$a\ ^4F_{2\frac{1}{2}} - z\ ^4D^\circ_{3\frac{1}{2}}$	(0.62, **0.90**)0.56, 0.90, **1.23**, 1.62, 1.89†
4246.41	2	23542.70	$a\ ^4F_{1\frac{1}{2}} - z\ ^4D^\circ_{2\frac{1}{2}}$	
4245.12	2	23549.85		
4242.36	50	23565.17	$a\ ^4F_{4\frac{1}{2}} - z\ ^4D^\circ_{3\frac{1}{2}}$	(0.00)1.12*A*†
4233.26	18	23615.83	$a\ ^4F_{3\frac{1}{2}} - z\ ^4D^\circ_{3\frac{1}{2}}$	(0.63)1.36†
4229.81	1	23635.09	$b\ ^4P_{2\frac{1}{2}} - z\ ^4D^\circ_{1\frac{1}{2}}$	
4227.73	1	23646.72	$a\ ^8S_{3\frac{1}{2}} - y\ ^4D^\circ_{1\frac{1}{2}}$	
4224.85	25	23662.84	$b\ ^2D_{1\frac{1}{2}} - z\ ^2D^\circ_{1\frac{1}{2}}$	(0.08)0.86†
4222.00	3	23678.81	$c\ ^2D_{1\frac{1}{2}} - x\ ^4F^\circ_{1\frac{1}{2}}$	
4217.07	2	23706.49	$b\ ^4D_{1\frac{1}{2}} - z\ ^4P^\circ_{0\frac{1}{2}}$	
4215.76	2	23713.86	$b\ ^4D_{0\frac{1}{2}} - z\ ^4P^\circ_{0\frac{1}{2}}$	
4209.05	3	23751.66	$b\ ^2D_{2\frac{1}{2}} - z\ ^2D^\circ_{1\frac{1}{2}}$	
4207.36	4	23761.20	$b\ ^4P_{2\frac{1}{2}} - z\ ^4D^\circ_{2\frac{1}{2}}$	
4195.41	4	23828.88	$b\ ^2I_{6\frac{1}{2}} - z\ ^4H^\circ_{5\frac{1}{2}}$	(0.79)1.28†
4195.33	6	23829.34	$b\ ^2D_{2\frac{1}{2}} - y\ ^4P^\circ_{2\frac{1}{2}}$	(0.79)1.56†
4181.50	1	23908.15	$c\ ^2D_{2\frac{1}{2}} - y\ ^2D^\circ_{1\frac{1}{2}}$	
4179.43	12	23919.99	$b\ ^4P_{2\frac{1}{2}} - z\ ^4D^\circ_{3\frac{1}{2}}$	
4172.60	2	23959.14	$b\ ^4D_{2\frac{1}{2}} - z\ ^4P^\circ_{1\frac{1}{2}}$	
4171.92	3	23963.05	$b\ ^4D_{1\frac{1}{2}} - z\ ^4P^\circ_{1\frac{1}{2}}$	
4170.86	1	23969.14	$c\ ^2D_{1\frac{1}{2}} - y\ ^2D^\circ_{1\frac{1}{2}}$	
4170.65	1	23970.34	$b\ ^4D_{0\frac{1}{2}} - z\ ^4P^\circ_{1\frac{1}{2}}$	
4161.07	2	24025.53	$b\ ^2D_{1\frac{1}{2}} - z\ ^2D^\circ_{2\frac{1}{2}}$	
4151.00	5	24083.81	$b\ ^2D_{1\frac{1}{2}} - z\ ^2P^\circ_{1\frac{1}{2}}$	(0.58) 0.64, **0.92**, 1.25†
4145.77	25	24114.20	$b\ ^2D_{2\frac{1}{2}} - z\ ^2D^\circ_{2\frac{1}{2}}$	(0.00) 1.23†
4132.41	7	24192.16	$b\ ^4P_{1\frac{1}{2}} - z\ ^4D^\circ_{1\frac{1}{2}}$	(0.79) 0.89, **1.37**, 1.85†
4127.08	4	24223.40	$c\ ^2D_{2\frac{1}{2}} - y\ ^2D^\circ_{2\frac{1}{2}}$	
4116.65	2	24284.77	$c\ ^2D_{1\frac{1}{2}} - y\ ^2D^\circ_{2\frac{1}{2}}$	
4113.24	5	24304.90	$b\ ^4D_{2\frac{1}{2}} - z\ ^4P^\circ_{2\frac{1}{2}}$	

TABLE 1. *Wavelengths of* Cr II *in air*—Continued

Wavelength	Intensity	Wave No.	Term combination	Zeeman effect
4112. 58	1	24308. 80	$b\ ^4D_{1\frac{1}{2}} - z\ ^4P^0_{2\frac{1}{2}}$	
4111. 00	18	24318. 14	$b\ ^4P_{1\frac{1}{2}} - z\ ^4D^0_{3\frac{1}{2}}$ $b\ ^4D_{2\frac{1}{2}} - z\ ^4P^0_{2\frac{1}{2}}$	(**0.18,** 0.44) **0.89,** 1.16†
4098. 44	8	24392. 67	$b\ ^2D_{1\frac{1}{2}} - y\ ^4F^0_{1\frac{1}{2}}$	(0.53) 0.53, 0.81†
4089. 48	2	24446. 05	$b\ ^2D_{2\frac{1}{2}} - y\ ^4G^0_{2\frac{1}{2}}$	
4088. 88	1	24449. 70	$b\ ^4D_{1\frac{1}{2}} - z\ ^6D^0_{3\frac{1}{2}}$	
4087. 60	2	24457. 30	$b\ ^4D_{0\frac{1}{2}} - z\ ^6D^0_{1\frac{1}{2}}$	
4086. 14	8	24466. 09	$b\ ^4P_{0\frac{1}{2}} - z\ ^4D^0_{0\frac{1}{2}}$	(1.34) 1.35†
4082. 30	10	24489. 11	$b\ ^2D_{2\frac{1}{2}} - y\ ^4F^0_{3\frac{1}{2}}$	(0.38)/1.10†
4081. 21	1	24495. 65	$b\ ^2D_{2\frac{1}{2}} - y\ ^4F^0_{2\frac{1}{2}}$	
4077. 50	4	24517. 93	$b\ ^4D_{2\frac{1}{2}} - z\ ^6D^0_{1\frac{1}{2}}$	
4076. 87	3	24521. 72	$b\ ^4D_{1\frac{1}{2}} - z\ ^6D^0_{1\frac{1}{2}}$	
4072. 56	4	24547. 67	$b\ ^4P_{0\frac{1}{2}} - z\ ^4D^0_{1\frac{1}{2}}$	(0.74) **0.46,** · · ·†
4070. 88	10	24557. 80	$d\ ^2G_{4\frac{1}{2}} - w\ ^2F^0_{3\frac{1}{2}}$	(0.00) 1.08†
4056. 07	4	24647. 47	$c\ ^2D_{1\frac{1}{2}} - x\ ^4G^0_{2\frac{1}{2}}$	(0.00 *w*) 0.37 *A*†
4054. 10	8	24659. 45	$b\ ^4D_{2\frac{1}{2}} - z\ ^6D^0_{2\frac{1}{2}}$	
4053. 43	1	24663. 52	$b\ ^4D_{1\frac{1}{2}} - z\ ^6D^0_{2\frac{1}{2}}$	
4051. 96	12	24672. 47	$b\ ^4D_{2\frac{1}{2}} - z\ ^6D^0_{3\frac{1}{2}}$	(0.00 *w*) 1.16†
4049. 14	18	24689. 65	$d\ ^2G_{3\frac{1}{2}} - w\ ^2F^0_{3\frac{1}{2}}$	(0.00) 0.97†
4038. 02	25	24757. 64	$d\ ^2G_{4\frac{1}{2}} - w\ ^2H^0_{5\frac{1}{2}}$	(0.00) 1.06†
4022. 37	3	24853. 97	$c\ ^2D_{2\frac{1}{2}} - y\ ^2F^0_{2\frac{1}{2}}$	
4017. 96	3	24881. 24	$b\ ^2D_{1\frac{1}{2}} - x\ ^4D^0_{2\frac{1}{2}}$	
4012. 50	30	24915. 10	$c\ ^2D_{1\frac{1}{2}} - y\ ^2F^0_{1\frac{1}{2}}$	(0.00) 0.90†
4007. 55	2	24945. 88		
4003. 32	25	24972. 23	$d\ ^2G_{3\frac{1}{2}} - w\ ^2H^0_{4\frac{1}{2}}$	(0.00) 0.95†
4002. 48	5	24977. 47	$b\ ^2D_{2\frac{1}{2}} - x\ ^4D^0_{3\frac{1}{2}}$	(0.00) 0.73†
3979. 52	20	25121. 58	$c\ ^2D_{2\frac{1}{2}} - y\ ^2F^0_{3\frac{1}{2}}$	(0.00) 1.07†
3936. 95	1	25393. 21	$c\ ^2G_{4\frac{1}{2}} - z\ ^4I^0_{5\frac{1}{2}}$	
3935. 04	1	25405. 54	$c\ ^4D_{0\frac{1}{2}} - y\ ^4D^0_{0\frac{1}{2}}$	
3911. 32	3	25559. 60	$c\ ^2G_{4\frac{1}{2}} - z\ ^4G^0_{5\frac{1}{2}}$	(0.00) 1.11†
3909. 25	1	25573. 14	$c\ ^2G_{3\frac{1}{2}} - z\ ^4G^0_{3\frac{1}{2}}$	
3905. 64	25	25596. 77	$b\ ^2D_{1\frac{1}{2}} - z\ ^2F^0_{2\frac{1}{2}}$	(0.00) 0.94 *A*†
3895. 14	2	25665. 78	$c\ ^4D_{0\frac{1}{2}} - y\ ^4D^0_{1\frac{1}{2}}$	
3892. 15	4	25685. 49	$b\ ^2D_{2\frac{1}{2}} - z\ ^2F^0_{3\frac{1}{2}}$	
3866. 54	7	25855. 61	$c\ ^2G_{4\frac{1}{2}} - z\ ^2G^0_{4\frac{1}{2}}$	(0.00) 1.18†
3866. 01	5	25859. 16	$c\ ^2G_{3\frac{1}{2}} - z\ ^2G^0_{3\frac{1}{2}}$	
3865. 60	25	25861. 90	$b\ ^2D_{2\frac{1}{2}} - z\ ^2F^0_{3\frac{1}{2}}$	(0.00) 1.09†
3832. 40	1	26085. 94	$c\ ^4D_{1\frac{1}{2}} - y\ ^4D^0_{2\frac{1}{2}}$	
3813. 99	12	26211. 85	$d\ ^2F_{2\frac{1}{2}} - w\ ^2F^0_{3\frac{1}{2}}$	(0.00) 1.17†
3810. 74	3	26234. 20	$a\ ^2S_{0\frac{1}{2}} - z\ ^2D^0_{1\frac{1}{2}}$	
3801. 21	10	26299. 97	$d\ ^2F_{2\frac{1}{2}} - w\ ^2F^0_{3\frac{1}{2}}$	(0.00)0.86†
3783. 74	6	26421. 40		
3778. 70	6	26456. 64	$a\ ^2S_{0\frac{1}{2}} - z\ ^2P^0_{0\frac{1}{2}}$	(0.64)1.39†
3769. 32	1	26522. 48		
3766. 65	2	26541. 28	$b\ ^4D_{1\frac{1}{2}} - z\ ^4F^0_{1\frac{1}{2}}$	
3765. 61	8	26548. 61	$b\ ^4D_{0\frac{1}{2}} - z\ ^4F^0_{1\frac{1}{2}}$	(0.17)0.24, **0.58**†
3761. 90	8	26574. 79	$a\ ^4P_{0\frac{1}{2}} - z\ ^6P^0_{1\frac{1}{2}}$ $a\ ^4P_{1\frac{1}{2}} - z\ ^6P^0_{1\frac{1}{2}}$	P–B
3761. 68	7	26576. 34	$a\ ^4P_{2\frac{1}{2}} - z\ ^6P^0_{1\frac{1}{2}}$	P–B
3756. 55	3	26612. 63	$c\ ^2F_{2\frac{1}{2}} - y\ ^4F^0_{1\frac{1}{2}}$	
3755. 13	2	26622. 70	$b\ ^4D_{2\frac{1}{2}} - z\ ^4F^0_{2\frac{1}{2}}$	
3754. 59	20	26626. 53	$b\ ^4D_{1\frac{1}{2}} - z\ ^4F^0_{2\frac{1}{2}}$	(0.00)0.83†
3750. 99	1	26652. 02		
3750. 61	5	26654. 71	$b\ ^2D_{1\frac{1}{2}} - y\ ^2D^0_{1\frac{1}{2}}$ $a\ ^2S_{0\frac{1}{2}} - z\ ^2P^0_{1\frac{1}{2}}$	
3750. 56	7	26655. 14	$c\ ^4D_{2\frac{1}{2}} - y\ ^4D^0_{3\frac{1}{2}}$	(0.39)**0.82,** 1.61
3748. 68	7	26668. 50	$a\ ^4P_{2\frac{1}{2}} - z\ ^6P^0_{2\frac{1}{2}}$	
3738. 38	35	26741. 98	$c\ ^4D_{2\frac{1}{2}} - z\ ^4F^0_{3\frac{1}{2}}$	(**0.00,** 0.15, 0.30)**0.90,** 1.05, 1.21
3737. 55	10	26747. 92	$b\ ^2G_{3\frac{1}{2}} - z\ ^4G^0_{3\frac{1}{2}}$	(0.22)0.92†
3736. 56	1	26755. 00	$b\ ^4D_{3\frac{1}{2}} - z\ ^4F^0_{3\frac{1}{2}}$	
3735. 89	4	26759. 80	$d\ ^2D_{2\frac{1}{2}} - x\ ^2F^0_{2\frac{1}{2}}$	(0.00)0.96†
3727. 36	25	26821. 04	$b\ ^2G_{4\frac{1}{2}} - z\ ^4G^0_{4\frac{1}{2}}$	(0.00)1.12†
3723. 40	15	26849. 56	$c\ ^2F_{3\frac{1}{2}} - y\ ^4F^0_{3\frac{1}{2}}$	(**0.25,** 0.75, 1.19)**0.24,** 0.81†

TABLE 1. *Wavelengths of* Cr II *in air*—Continued

Wavelength	Intensity	Wave No.	Term combination	Zeeman effect
3715.44	20	26907.09	$c\ ^2F_{2½} - z\ ^2D^0_{1½}$	(0.00)0.82†
3715.18	25	26908.97	$b\ ^4D_{3½} - z\ ^4F^0_{4½}$	(0.00)1.10 *A*†
3712.95	45	26925.15	$a\ ^4P_{1½} - z\ ^4P^0_{½}$	P–B
3712.89	10	26925.56	$a\ ^4P_{0½} - z\ ^4P^0_{½}$	P–B
3711.29	7	26937.17	$e\ ^2D_{2½} - v\ ^2D^0_{3½}$	(0.00)1.05†
3707.57	1	26964.20	$a\ ^2S_{0½} - y\ ^4F^0_{1½}$	
3707.13	3	26967.40	$b\ ^2D_{1½} - y\ ^2D^0_{2½}$	
3704.89	5	26983.70	$c\ ^2D_{1½} - v\ ^2D^0_{1½}$	
3701.89	4	27005.57	$b\ ^2D_{2½} - y\ ^2G^0_{3½}$	
3698.01	35	27033.91	$b\ ^2G_{3½} - z\ ^2G^0_{3½}$	(0.00)0.91†
3696.79	10	27042.83		(**0.24,** 0.74)0.27†
3695.53	2	27052.05		
3694.98	4	27056.07	$b\ ^2D_{2½} - y\ ^2D^0_{2½}$	
3693.98	3	27063.40	$d\ ^2D_{1½} - x\ ^2F^0_{2½}$	
3686.68	20	27116.98	$b\ ^2G_{4½} - z\ ^2G^0_{4½}$	(0.00)1.13†
3684.25	25	27134.87	$c\ ^2F_{3½} - z\ ^2D^0_{2½}$	
3677.90	30	27181.72	$a\ ^4P_{1½} - z\ ^4P^0_{1½}$	P–B
3677.84	50	27182.16	$a\ ^4P_{0½} - z\ ^4P^0_{1½}$	P–B
3677.67	40	27183.39	$a\ ^4P_{2½} - z\ ^4P^0_{1½}$	P–B
3674.94	5	27203.61	$a\ ^4D_{3½} - z\ ^6F^0_{3½}$	
3664.95	30	27277.76	$b\ ^2I_{5½} - z\ ^2I^0_{5½}$	(0.00)0.93†
3661.44	3	27303.91	$b\ ^2I_{6½} - z\ ^2I^0_{5½}$	
3658.19	20	27328.16	$c\ ^2F_{2½} - z\ ^2P^0_{1½}$	(**0.15,** 0.38, 0.61)**0.35,** 0.61, 0.88†
3657.93	1	27330.11	$c\ ^2G_{3½} - z\ ^2D^0_{2½}$ $b\ ^2D_{1½} - x\ ^4G^0_{2½}$	
3651.68	12	27376.88	$a\ ^4D_{0½} - z\ ^6F^0_{1½}$ $b\ ^2P_{1½} - v\ ^2D^0_{2½}$	(**00.0***d*, 0.53)**1.08,** 1.60†
3650.37	40	27386.71	$b\ ^2I_{6½} - z\ ^2I^0_{6½}$	(**0.00**)1.10†
3649.69	7*w*	27391.81		
3647.40	8	27409.01	$a\ ^4D_{1½} - z\ ^6F^0_{2½}$	(**0.00**)1.44†
3644.70	10	27429.31	$a\ ^4D_{2½} - z\ ^6F^0_{3½}$	(**0.00**)1.43†
3643.22	10	27440.38	$a\ ^4D_{3½} - z\ ^6F^0_{4½}$	(**0.00**)1.45†
3634.04	10	27509.77	$c\ ^2G_{4½} - y\ ^4G^0_{5½}$	(**0.00**)1.05†
3631.70	40	27527.52	$a\ ^4P_{1½} - z\ ^4P^0_{2½}$	P–B
3631.49	50	27529.12	$a\ ^4P_{2½} - z\ ^4P^0_{2½}$	P–B
3622.44	1	27597.86	$b\ ^2D_{1½} - y\ ^2F^0_{2½}$	
3617.33	7	27636.85	$c\ ^2F_{2½} - y\ ^4F^0_{1½}$	(**0.17,** 0.54)0.71, 1.04, **1.36**†
3614.25	2	27660.40	$c\ ^2G_{3½} - y\ ^4G^0_{2½}$	
3613.33	15	27667.44	$a\ ^4P_{1½} - z\ ^6D^0_{½}$	P–B
3613.20	20	27668.44	$a\ ^4P_{0½} - z\ ^6D^0_{½}$	P–B
3608.66	3	27703.24	$c\ ^2G_{2½} - y\ ^4F^0_{2½}$	
3603.86	20	27740.14	$a\ ^4P_{1½} - z\ ^6D^0_{1½}$	P–B
3603.78	40	27740.75	$a\ ^4P_{0½} - z\ ^6D^0_{1½}$	P–B
3603.62	20	27741.99	$a\ ^4P_{2½} - z\ ^6D^0_{1½}$	P–B
3588.30	2	27860.43	$c\ ^4D_{0½} - y\ ^4P^0_{½}$	
3585.53	40	27881.95	$a\ ^4P_{1½} - z\ ^6D^0_{2½}$	P–B
3585.30	60	27883.74	$a\ ^4P_{2½} - z\ ^6D^0_{2½}$	P–B
3583.96	3	27894.16	$c\ ^4D_{1½} - y\ ^4P^0_{½}$	
3571.37	3	27992.50	$c\ ^4D_{1½} - y\ ^4P^0_{1½}$	
3566.37	1	28031.74	$b\ ^2F_{2½} - z\ ^4H^0_{3½}$	
3565.32	5	28039.99	$c\ ^4D_{2½} - y\ ^4P^0_{1½}$	(**0.17,** 0.47)**0.69,** 0.97†
3563.91	5	28051.09	$c\ ^2G_{4½} - x\ ^4D^0_{3½}$	
3552.42	2	28141.82	$b\ ^2H_{5½} - z\ ^4H^0_{5½}$	
3547.10	3	28184.02	$c\ ^2G_{3½} - x\ ^4D^0_{2½}$	
3540.23	2	28238.71	$b\ ^2H_{4½} - z\ ^4H^0_{3½}$	
3538.98	4	28248.68	$b\ ^2I_{5½} - z\ ^2H^0_{4½}$	
3538.47	1	28252.76	$c\ ^4D_{0½} - z\ ^2D^0_{1½}$	
3534.13	2	28287.45	$c\ ^4D_{1½} - z\ ^2D^0_{1½}$	
3529.73	2	28322.71	$b\ ^2H_{5½} - z\ ^4H^0_{4½}$	
3528.23	1	28334.75	$c\ ^4D_{2½} - z\ ^2D^0_{1½}$	
3522.13	7	28383.83	$c\ ^2D_{2½} - x\ ^2F^0_{3½}$	(0.00)1.08†

TABLE 1. *Wavelengths of* Cr II *in air*—Continued

Wavelength	Intensity	Wave No.	Term combination	Zeeman effect
3518.62	3	28412.14	$c\ ^4D_{2\frac{1}{2}} - y\ ^4P^0_{2\frac{1}{2}}$	
3513.03	10	28457.35	$c\ ^4D_{3\frac{1}{2}} - y\ ^4P^0_{2\frac{1}{2}}$	(0.00)1.30†
3511.83	35	28467.07	$a\ ^4D_{3\frac{1}{2}} - z\ ^4P^0_{3\frac{1}{2}}$	(**0.23,** 0.69, 1.13)**0.30,** 0.74, 1.20, 1.64, 2.11
3506.61	1	28509.45	$b\ ^2I_{5\frac{1}{2}} - z\ ^2H^0_{5\frac{1}{2}}$	
3503.35	3	28535.97	$b\ ^2I_{6\frac{1}{2}} - z\ ^2H^0_{5\frac{1}{2}}$	
3498.30	1	28577.17		
3495.54	20	28599.73	$c\ ^2F_{3\frac{1}{2}} - z\ ^2H^0_{4\frac{1}{2}}$	
3495.36	25	28601.20	$a\ ^4D_{2\frac{1}{2}} - z\ ^6P^0_{1\frac{1}{2}}$	(**0.51,** 1.51) — **0.14,** 0.86, 1.86, 2.87
3494.50	4	28608.24	$a\ ^4D_{3\frac{1}{2}} - z\ ^6P^0_{3\frac{1}{2}}$	
3489.44	2	28649.74	$c\ ^4D_{1\frac{1}{2}} - z\ ^2D^0_{2\frac{1}{2}}$ $c\ ^2D_{1\frac{1}{2}} - w\ ^2F^0_{2\frac{1}{2}}$	
3489.07	2	28652.76	$c\ ^2G_{4\frac{1}{2}} - z\ ^2H^0_{4\frac{1}{2}}$	
3484.14	20	28693.30	$a\ ^4D_{2\frac{1}{2}} - z\ ^6P^0_{2\frac{1}{2}}$	(0.27, 0.76, **1.28**)0.61, 1.13, **1.63,** 2.14, 2.65
3482.58	12	28706.16	$c\ ^2D_{2\frac{1}{2}} - x\ ^2F^0_{3\frac{1}{2}}$ $c\ ^2F_{3\frac{1}{2}} - z\ ^2F^0_{3\frac{1}{2}}$	(0.00w)1.40B†
3478.15	3	28742.72	$c\ ^4D_{3\frac{1}{2}} - z\ ^2D^0_{2\frac{1}{2}}$	
3475.12	20	28767.78	$c\ ^2D_{1\frac{1}{2}} - x\ ^2F^0_{2\frac{1}{2}}$ $a\ ^4D_{1\frac{1}{2}} - z\ ^6P^0_{1\frac{1}{2}}$	(0.58, 1.78)0.61, 1.79, 2.98†
3472.06	25	28793.13	$c\ ^2G_{3\frac{1}{2}} - z\ ^2H^0_{4\frac{1}{2}}$	(0.00 w_1D)0.64A
3466.25	2	28841.39	$c\ ^2F_{2\frac{1}{2}} - z\ ^2F^0_{2\frac{1}{2}}$ $b\ ^2F_{3\frac{1}{2}} - y\ ^4D^0_{3\frac{1}{2}}$	
3464.01	4	28860.04	$a\ ^4D_{1\frac{1}{2}} - z\ ^6P^0_{2\frac{1}{2}}$	
3462.71	6	28870.87	$a\ ^4D_{0\frac{1}{2}} - z\ ^6P^0_{1\frac{1}{2}}$	(1.18)1.15,**3.59**†
3461.28	3	28882.80	$c\ ^2F_{3\frac{1}{2}} - z\ ^2F^0_{3\frac{1}{2}}$	
3460.03	1	28893.24	$a\ ^2H_{5\frac{1}{2}} - z\ ^4H^0_{4\frac{1}{2}}$	
3459.28	25	28899.50	$c\ ^2G_{3\frac{1}{2}} - z\ ^2F^0_{3\frac{1}{2}}$	(0.00w_1D)1.30B
3457.61	30	28913.46	$c\ ^2G_{4\frac{1}{2}} - z\ ^2H^0_{5\frac{1}{2}}$	(0.00w)1.05w
3454.97	35	28935.55	$c\ ^2G_{4\frac{1}{2}} - z\ ^2F^0_{3\frac{1}{2}}$	(0.00)1.04†
3450.84	3	28970.18	$a\ ^2H_{4\frac{1}{2}} - z\ ^4H^0_{3\frac{1}{2}}$	
3449.28	1	28983.29	$c\ ^4D_{0\frac{1}{2}} - y\ ^4F^0_{1\frac{1}{2}}$	
3445.04	5	29018.95	$c\ ^2G_{4\frac{1}{2}} - y\ ^4H^0_{3\frac{1}{2}}$	
3444.34	4	29024.85	$c\ ^4D_{1\frac{1}{2}} - y\ ^4F^0_{2\frac{1}{2}}$	
3442.98	1	29036.32	$a\ ^2H_{5\frac{1}{2}} - z\ ^4H^0_{5\frac{1}{2}}$	
3438.46	1	29074.48	$c\ ^4D_{2\frac{1}{2}} - y\ ^4G^0_{3\frac{1}{2}}$	
3437.93	2	29078.95	$c\ ^4D_{2\frac{1}{2}} - y\ ^4F^0_{3\frac{1}{2}}$	
3433.29	75	29118.26	$a\ ^4D_{1\frac{1}{2}} - z\ ^4P^0_{0\frac{1}{2}}$	(0.82)**0.37,**2.03†
3430.42	3	29142.62	$a\ ^4P_{0\frac{1}{2}} - y\ ^4D^0_{0\frac{1}{2}}$	(0.31)0.38†
3429.90	1	29147.04	$a\ ^2G_{4\frac{1}{2}} - z\ ^4I^0_{5\frac{1}{2}}$	
3428.94	7	29155.20	$a\ ^2G_{3\frac{1}{2}} - z\ ^4G^0_{3\frac{1}{2}}$	(0.25)0.97†
3426.14	8	29179.10	$c\ ^4D_{3\frac{1}{2}} - y\ ^4F^0_{4\frac{1}{2}}$	(0.00w)1.05†
3422.73	125	29208.28	$a\ ^4D_{2\frac{1}{2}} - z\ ^4P^0_{1\frac{1}{2}}$	(**0.21,**0.65)**0.72,**1.16,1.59,2.02
3421.62	5	29217.57	$a\ ^2H_{4\frac{1}{2}} - z\ ^4H^0_{3\frac{1}{2}}$ $a\ ^2H_{5\frac{1}{2}} - z\ ^4H^0_{4\frac{1}{2}}$	
3421.19	75	29221.24	$a\ ^4D_{0\frac{1}{2}} - z\ ^4P^0_{0\frac{1}{2}}$	(1.40)1.40
3415.44	2	29270.44	$a\ ^2G_{4\frac{1}{2}} - z\ ^2G^0_{3\frac{1}{2}}$	
3410.53	3	29312.58	$b\ ^2G_{4\frac{1}{2}} - x\ ^4D^0_{3\frac{1}{2}}$	
3408.76	150	29327.80	$a\ ^4D_{2\frac{1}{2}} - z\ ^4P^0_{2\frac{1}{2}}$	(**0.10,**0.32,0.53)**0.90,**1.11,1.32,1.53,1.74,1.94
3405.13	2	29359.06	$b\ ^2G_{3\frac{1}{2}} - x\ ^4D^0_{2\frac{1}{2}}$	
3403.30	100	29374.85	$b\ ^4D_{1\frac{1}{2}} - z\ ^4D^0_{0\frac{1}{2}}$ $a\ ^4D_{1\frac{1}{2}} - z\ ^4P^0_{1\frac{1}{2}}$	(0.31,**0.91**)0.90,**1.49,**2.10
3402.43	25	29382.36	$b\ ^4D_{0\frac{1}{2}} - z\ ^4D^0_{0\frac{1}{2}}$	(0.00)0.00†
3400.08	2	29402.66	$a\ ^2P_{0\frac{1}{2}} - y\ ^4D^0_{1\frac{1}{2}}$	
3399.54	18	29407.34	$a\ ^2G_{4\frac{1}{2}} - z\ ^2G^0_{4\frac{1}{2}}$	(0.13)1.11w
3395.62	20	29441.28	$a\ ^2G_{3\frac{1}{2}} - z\ ^2G^0_{3\frac{1}{2}}$	(0.00w,d?)0.91w
3394.31	35	29452.64	$b\ ^4D_{2\frac{1}{2}} - z\ ^4D^0_{1\frac{1}{2}}$	(0.17)1.61†
3393.85	30	29456.64	$b\ ^4D_{1\frac{1}{2}} - z\ ^4D^0_{1\frac{1}{2}}$	(0.00)1.18†
3393.00	35	29464.02	$b\ ^4D_{0\frac{1}{2}} - z\ ^4D^0_{1\frac{1}{2}}$	(0.59)0.64,**1.78**†
3391.41	35	29477.73	$a\ ^4D_{0\frac{1}{2}} - z\ ^4P^0_{1\frac{1}{2}}$	(0.90)0.92,**2.73**†
3389.17	2	29498.18	$c\ ^4D_{1\frac{1}{2}} - x\ ^4D^0_{0\frac{1}{2}}$	
3387.95	3	29507.93	$c\ ^4D_{1\frac{1}{2}} - x\ ^4D^0_{1\frac{1}{2}}$	
3387.72	5	29509.94	$b\ ^2H_{5\frac{1}{2}} - z\ ^4I^0_{5\frac{1}{2}}$	

TABLE 1. *Wavelengths of* Cr II *in air*—Continued

Wavelength	Intensity	Wave No.	Term combination	Zeeman effect
3382.68	50	29553.90	$a\ ^4D_{2\frac{1}{2}} - z\ ^4P^0_{2\frac{1}{2}}$	(0.40,**0.65**)0.97,1.27,**1.50**,1.78,2.07†
3379.84	50	29578.74	$b\ ^4D_{2\frac{1}{2}} - z\ ^4D^0_{3\frac{1}{2}}$	(**0.00**)1.34†
3379.39	25	29582.67	$b\ ^4D_{1\frac{1}{2}} - z\ ^4D^0_{2\frac{1}{2}}$	(**0.00**,0.22)1.47,**1.63**†
3378.36	30	29591.69	$b\ ^4D_{3\frac{1}{2}} - z\ ^4D^0_{3\frac{1}{2}}$	(0.00)1.53†
3377.60	1	29598.35	$c\ ^4D_{3\frac{1}{2}} - x\ ^4D^0_{3\frac{1}{2}}$	
3377.36	5	29600.46	$d\ ^2F_{2\frac{1}{2}} - w\ ^2D^0_{1\frac{1}{2}}$	(0.00)0.92†
3376.71	5	29606.15	$c\ ^2F_{2\frac{1}{2}} - x\ ^4F^0_{1\frac{1}{2}}$ $c\ ^4D_{3\frac{1}{2}} - x\ ^4D^0_{3\frac{1}{2}}$	(0.00)1.52†
3376.62	4	29606.94	$b\ ^2H_{4\frac{1}{2}} - z\ ^4I^0_{5\frac{1}{2}}$	
3376.26	10	29610.10	$b\ ^2F_{3\frac{1}{2}} - z\ ^4I^0_{5\frac{1}{2}}$	(?)0.60*w*†
3374.99	3	29621.24	$c\ ^2F_{3\frac{1}{2}} - x\ ^4F^0_{4\frac{1}{2}}$	
3374.95	4	29621.59	$a\ ^4D_{3\frac{1}{2}} - z\ ^6D^0_{3\frac{1}{2}}$	(0.40*B*)1.88†
3373.08	3	29638.01		
3372.12	15	29646.45	$b\ ^2H_{4\frac{1}{2}} - z^*\ ^6G^0_{3\frac{1}{2}}$	(0.00*wD*)0.80*A*
3369.05	18	29673.46	$a\ ^2P_{1\frac{1}{2}} - z\ ^2S^0_{\frac{1}{2}}$	(0.31)**1.03**,1.62
3368.72	10	29676.37	$b\ ^2H_{3\frac{1}{2}} - z_-\ ^6G^0_{4\frac{1}{2}}$	(0.00)0.99
3368.04	150	29682.36	$a\ ^4D_{3\frac{1}{2}} - z\ ^6D^0_{3\frac{1}{2}}$	(**0.10**,0.30,0.51)**0.91**,1.14,1.33,1.54,1.72,1.92
3367.42	12	29687.83	$b\ ^2F_{3\frac{1}{2}} - z\ ^6G^0_{3\frac{1}{2}}$	(0.00)1.22*B*†
3364.67	7	29712.09		
3363.70	12	29720.66	$a\ ^4D_{1\frac{1}{2}} - z\ ^4P^0_{2\frac{1}{2}}$	(**0.22**, 0.66)1.20, 1.64, 209, **2.48**
3361.77	30*d*?	29737.72	$b\ ^4D_{2\frac{1}{2}} - z\ ^4D^0_{3\frac{1}{2}}$	
3360.30	100	29750.73	$b\ ^4D_{3\frac{1}{2}} - z\ ^4D^0_{3\frac{1}{2}}$	(0.00) 1.43
3358.49	75	29766.76	$a\ ^4D_{2\frac{1}{2}} - z\ ^6D^0_{1\frac{1}{2}}$	(**0.23**, 0.69)**0.69**, 1.15, 161, 2.05
3357.72	1	29773.59	$b\ ^2H_{4\frac{1}{2}} - z\ ^6G^0_{4\frac{1}{2}}$	
3357.39	40	29776.51	$b\ ^2F_{3\frac{1}{2}} - z\ ^6G^0_{3\frac{1}{2}}$	(0.00)1.09
3355.89	2*w*	29789.82	$z\ ^4D^0_{3\frac{1}{2}} - e\ ^4D_{3\frac{1}{2}}$	
3353.12	20	29814.43	$a\ ^4D_{3\frac{1}{2}} - z\ ^6D^0_{4\frac{1}{2}}$	(**0.06**, 0.19, 0.32, 0.44) . . . 1.89, **1.99**
3352.56	3*w*	29819.41	$z\ ^4D^0_{1\frac{1}{2}} - e\ ^4D_{1\frac{1}{2}}$	
3349.65	3	29845.32	$a\ ^4P_{1\frac{1}{2}} - z\ ^4F^0_{2\frac{1}{2}}$	
3349.34	6	29848.08	$a\ ^4D_{2\frac{1}{2}} - z\ ^6D^0_{2\frac{1}{2}}$	(0.26*w*)1.79, **2.09**†
3347.83	40	29861.54	$a\ ^4D_{1\frac{1}{2}} - z\ ^6D^0_{2\frac{1}{2}}$	(0.98)**0.23**, 2.17
3347.14	5*w*	29867.70	$z\ ^4D^0_{2\frac{1}{2}} - e\ ^4D_{2\frac{1}{2}}$	
3342.57	50	29908.53	$a\ ^4D_{2\frac{1}{2}} - z\ ^6D^0_{3\frac{1}{2}}$	(0.12, 0.42, **0.64**)0.98, 1.25, **1.50**, 176, 2.01
3341.97	5	29913.90	$b\ ^2G_{3\frac{1}{2}} - z\ ^2H^0_{4\frac{1}{2}}$	
3339.90	20	29932.44	$b\ ^2H_{4\frac{1}{2}} - z\ ^2G^0_{3\frac{1}{2}}$	(0.00)0.76
3339.81	50	29933.25	$a\ ^4D_{1\frac{1}{2}} - z\ ^6D^0_{1\frac{1}{2}}$	(0.32, **0.94**)0.94, **1.51**, 2.13
3338.89	10*w*, *l*	29941.49	$z\ ^4D^0_{3\frac{1}{2}} - e\ ^4D_{3\frac{1}{2}}$	(0.00)1.42†
3336.32	40	29964.56	$a\ ^4D_{4\frac{1}{2}} - z\ ^6D^0_{4\frac{1}{2}}$	(1.58)1.58
3336.16	2	29965.99	$a\ ^4P_{2\frac{1}{2}} - z\ ^4F^0_{3\frac{1}{2}}$	
3335.93	4	29968.06	$b\ ^2G_{3\frac{1}{2}} - z\ ^2H^0_{4\frac{1}{2}}$	
3335.45	30	29972.37	$b\ ^2H_{3\frac{1}{2}} - z\ ^2G^0_{4\frac{1}{2}}$	(0.00)0.99†
3335.27	40	29973.99	$b\ ^2F_{2\frac{1}{2}} - z\ ^2G^0_{3\frac{1}{2}}$	(0.00*w*)1.04*w*
3333.12	2*w*	29993.32	$z\ ^4D^0_{2\frac{1}{2}} - e\ ^4D_{2\frac{1}{2}}$	
3332.13	2	30002.23	$b\ ^2H_{3\frac{1}{2}} - z\ ^4G^0_{4\frac{1}{2}}$	
3330.98	1	30012.59	$b\ ^4G_{3\frac{1}{2}} - z\ ^4H^0_{4\frac{1}{2}}$	
3329.45	4	30026.38	$c\ ^2F_{3\frac{1}{2}} - y\ ^2G^0_{4\frac{1}{2}}$	
3328.34	25	30036.39	$a\ ^4D_{0\frac{1}{2}} - z\ ^6D^0_{1\frac{1}{2}}$	(0.91)0.91, **2.73**
3324.34	50	30072.54	$b\ ^2F_{3\frac{1}{2}} - z\ ^2G^0_{4\frac{1}{2}}$	(0.00)1.13
3324.09	20	30074.80	$b\ ^2G_{4\frac{1}{2}} - z\ ^2F^0_{3\frac{1}{2}}$	(0.00)0.92
3324.03	25	30075.34	$a\ ^4D_{1\frac{1}{2}} - z\ ^6D^0_{2\frac{1}{2}}$	(**0.21**, 0.66)142, 183, **2.26**
3323.52	8	30079.96	$b\ ^4G_{3\frac{1}{2}} - z\ ^4H^0_{3\frac{1}{2}}$	(0.66, **1.12**)0.97†
3322.69	12	30087.47	$b\ ^4G_{4\frac{1}{2}} - z\ ^4H^0_{4\frac{1}{2}}$	(0.76*B*)1.22†
3321.30	5*w*, *l*	30100.06	$z\ ^4D^0_{3\frac{1}{2}} - e\ ^4D_{3\frac{1}{2}}$	
3315.28	12	30154.72	$b\ ^4G_{3\frac{1}{2}} - z\ ^4H^0_{4\frac{1}{2}}$	(0.63*B*)1.13†
3314.57	35	30161.18	$c\ ^2F_{3\frac{1}{2}} - y\ ^2G^0_{3\frac{1}{2}}$	(0.00)0.98
3314.05	18	30165.91	$b\ ^2I_{5\frac{1}{2}} - y\ ^2H^0_{6\frac{1}{2}}$	(0.00*w*)0.38*A*†
3313.53	2	30170.64	$b\ ^2I_{5\frac{1}{2}} - y\ ^2H^0_{5\frac{1}{2}}$	
3313.07	20	30174.83	$b\ ^2G_{4\frac{1}{2}} - z\ ^2H^0_{5\frac{1}{2}}$	(0.00)1.13
3312.18	40	30182.94	$b\ ^4G_{2\frac{1}{2}} - z\ ^4H^0_{3\frac{1}{2}}$	(0.00*w*,*D*)0.89*w*
3311.91	40	30185.40	$b\ ^4G_{3\frac{1}{2}} - z\ ^4H^0_{4\frac{1}{2}}$	(0.00)0.94
3310.65	35	30196.89	$b\ ^2G_{4\frac{1}{2}} - z\ ^2F^0_{3\frac{1}{2}}$ $b\ ^2I_{6\frac{1}{2}} - y\ ^2H^0_{5\frac{1}{2}}$	(0.00*wD*)1.01*A*

TABLE 1. *Wavelengths of* Cr II *in air*—Continued

Wavelength	Intensity	Wave No.	Term combination	Zeeman effect
3308. 15	18	30219. 71	$c\ ^2G_{3½} - y\ ^2G^0_{3½}$	(0.27)0.95†
3307. 02	50	30230. 03	$b\ ^4G_{4½} - z\ ^4H^0_{3½}$	(0.00*wD*)0.96*A*
3306. 95	15	30230. 67	$c\ ^2F_{3½} - y\ ^2G^0_{4½}$	(0.00)1.38†
3304. 73	5	30250. 98	$b\ ^2G_{3½} - z\ ^2F^0_{3½}$	
3301. 21	15	30283. 23	$c\ ^2G_{4½} - y\ ^2G^0_{4½}$	(0.00)1.10
3295. 42	50	30336. 44	$b\ ^4G_{5½} - z\ ^4H^0_{4½}$	(0.00*wD*)1.02*A*
3294. 95	6	30340. 75	$d\ ^2D_{1½} - x\ ^2P^0_{1½}$	
3291. 75	40	30370. 26	$a\ ^2P_{0½} - z\ ^2S^0_{0½}$	(0.64)1.32
3291. 23	6	30375. 06		(0.00)1.41† [2.61
3288. 04	15	30404. 52	$d\ ^2D_{1½} - x\ ^2P^0_{0½}$ $a\ ^2H_{5½} - z\ ^4I^0_{5½}$	(**0.13**, 0.47, 0.81, 1.14, 1.48) . . . 1.62, 1.96, 2.29.
3286. 34	1	30420. 25	$b\ ^2D_{1½} - w\ ^4D^0_{0½}$	
3285. 95	20	30423. 85	$c\ ^2G_{3½} - y\ ^2G^0_{4½}$	(0.00*wD*)1.56*B*
3283. 04	20	30450. 83	$b\ ^2I_{5½} - x\ ^4G^0_{5½}$	(0.00*w*)0.52*A*†
3279. 54	5	30483. 33	$b\ ^2G_{3½} - y\ ^4H^0_{3½}$	(0.00)1.11†
3278. 78	2	30490. 39	$c\ ^4D_{3½} - z\ ^2F^0_{3½}$	
3276. 24	1	30514. 02	$b\ ^2D_{2½} - w\ ^4D^0_{1½}$	
3275. 91	10	30517. 10	$c\ ^2F_{3½} - y\ ^2H^0_{4½}$	(0.00)1.05†
3273. 19	3*w*	30542. 46		
3272. 87	4	30545. 45	$d\ ^2F_{2½} - v\ ^2F^0_{3½}$	(0.00)0.81†
3272. 73	1	30546. 76	$b\ ^2S_{0½} - y\ ^2P^0_{1½}$	
3271. 03	1	30562. 63	$d\ ^2D_{1½} - x\ ^2D^0_{2½}$	
3270. 13	40	30571. 04	$a\ ^2H_{5½} - z\ ^4G^0_{4½}$	(0.00*d*?)1.00*A*
3269. 76	15	30574. 50	$c\ ^2F_{2½} - x\ ^4G^0_{2½}$ $c\ ^2G_{4½} - y\ ^2H^0_{5½}$	(0.00)1.54†
3269. 10	30	30580. 67	$d\ ^2D_{2½} - x\ ^2D^0_{2½}$	(0.00)1.19
3268. 47	10 + *g*	30586. 57	$a\ ^2H_{4½} - z\ ^4I^0_{5½}$	(0.65). . . ?†
3266. 25	8	30607. 35	$b\ ^2G_{4½} - y\ ^4H^0_{5½}$ $a\ ^2H_{5½} - z\ ^4I^0_{5½}$	(0.00)1.17
3264. 26	35	30626. 01	$a\ ^2H_{4½} - z\ ^4G^0_{3½}$	(0.00*wD*)0.69*A*
3261. 88	4	30648. 36		
3261. 54	4	30651. 55	$b\ ^2I_{5½} - x\ ^4G^0_{5½}$	
3258. 76	30	30677. 70	$b\ ^2S_{0½} - y\ ^2P^0_{1½}$ $b\ ^2I_{6½} - x\ ^4G^0_{5½}$	(0.00w_3D)0.63*A*
3258. 00	3	30684. 86	$c\ ^2F_{2½} - x\ ^4G^0_{3½}$	
3255. 60	3	30707. 48	$c\ ^2F_{2½} - y\ ^2F^0_{2½}$	
3255. 30	15	30710. 31	$c\ ^2G_{3½} - y\ ^2H^0_{4½}$	(0.00)1.18†
3252. 49	25	30736. 84	$d\ ^2D_{1½} - x\ ^2D^0_{1½}$	(0.07)0.88
3250. 78	10	30753. 01	$a\ ^2H_{4½} - z\ ^4G^0_{4½}$	(0.94). . . ?†
3250. 59	1	30754. 80	$d\ ^2D_{2½} - x\ ^2D^0_{1½}$	
3249. 51	12	30765. 03	$d\ ^2F_{2½} - v\ ^2F^0_{3½}$	(0.00)1.15
3247. 33	8	30785. 68	$b\ ^2F_{2½} - y\ ^4P^0_{1½}$	(?)0.31*A*†
3247. 00	4	30788. 81	$a\ ^2H_{4½} - z\ ^4I^0_{4½}$	
3245. 29	5	30805. 03	$a\ ^2H_{5½} - z\ ^4I^0_{6½}$	
3241. 98	2	30836. 48		
3241. 37	4	30842. 28	$c\ ^2F_{2½} - y\ ^2F^0_{2½}$	
3240. 06	7	30854. 75	$c\ ^2G_{4½} - x\ ^4G^0_{4½}$	(0.31)1.10†
3238. 76	50	30867. 13	$a\ ^2H_{5½} - z\ ^2G^0_{4½}$	(0.00*d*?)0.96*A*
3238. 51	10	30869. 52	$b\ ^4F_{2½} - z\ ^4H^0_{3½}$	
3235. 24	4	30900. 72	$c\ ^2G_{3½} - y\ ^2F^0_{3½}$ $a\ ^2P_{1½} - y\ ^4P^0_{2½}$	
3234. 06	50	30911. 99	$a\ ^2H_{4½} - z\ ^2G^0_{3½}$	(0.00)0.92
3232. 38	2	30928. 06	$b\ ^4G_{3½} - y\ ^4D^0_{2½}$	
3231. 63	8	30935. 24	$b\ ^2G_{4½} - x\ ^4F^0_{4½}$	(0.93) . . . ?†
3230. 83	2	30942. 90	$b\ ^2G_{4½} - x\ ^4F^0_{3½}$	
3229. 88	10	30952. 00	$c\ ^4D_{0½} - x\ ^4F^0_{1½}$	(0.29)0.29,**0.92**
3229. 38	8	30956. 79	$b\ ^4F_{1½} - y\ ^4D^0_{0½}$	(0.00)0.84
3227. 48	3	30975. 01	$c\ ^2F_{2½} - y\ ^2F^0_{3½}$	
3226. 35	4	30985. 86	$c\ ^4D_{1½} - x\ ^4F^0_{1½}$	
3225. 44	8	30994. 60	$b\ ^4F_{4½} - z\ ^4H^0_{3½}$	

TABLE 1. *Wavelengths of* Cr II *in air*—Continued

Wavelength	Intensity	Wave No.	Term combination	Zeeman effect
3225. 38	12	30995. 18	$c\ ^2G_{2\frac{1}{2}} - x\ ^4G^0_{3\frac{1}{2}}$	(0.00wD)1.14w
3221. 39	1	31033. 57	$c\ ^4D_{2\frac{1}{2}} - x\ ^4F^0_{3\frac{1}{2}}$	
3219. 79	10	31048. 99	$a\ ^2H_{4\frac{1}{2}} - z\ ^2G^0_{3\frac{1}{2}}$	(0.76, **0.98**) . . . 1.28, 1.47
3219. 13	18	31055. 36	$c\ ^2G_{4\frac{1}{2}} - x\ ^4G^0_{3\frac{1}{2}}$	(0.00wD)1.37B
3217. 40	50	31072. 01	$a\ ^4G_{2\frac{1}{2}} - z\ ^4F^0_{1\frac{1}{2}}$	(0.00)0.80B†
3216. 55	20	31080. 27	$b\ ^2F_{2\frac{1}{2}} - z\ ^2D^0_{1\frac{1}{2}}$	(0.00)0.84
3213. 46	3	31110. 15	$c\ ^2F_{2\frac{1}{2}} - y\ ^2F^0_{3\frac{1}{2}}$	
3212. 90	18	31115. 57	$c\ ^4D^0_{1\frac{1}{2}} - x\ ^4F_{2\frac{1}{2}}$	(0.00)0.83†
3212. 52	20	31119. 25	$b\ ^2F_{3\frac{1}{2}} - y\ ^4P^0_{2\frac{1}{2}}$	(**0.19,** 0.57, 0.92) **0.19,** 0.57, 0.92
3211. 49	12	31129. 23	$e\ ^2G_{3\frac{1}{2}} - v\ ^2G^0_{3\frac{1}{2}}$	(0.00w)0.84†
3209. 19	50	31151. 57	$a\ ^4G_{3\frac{1}{2}} - z\ ^4F^0_{2\frac{1}{2}}$	P–B
3208. 60	20	31157. 29	$a\ ^4G_{2\frac{1}{2}} - z\ ^4F^0_{1\frac{1}{2}}$	P–B
3208. 01	8	31163. 00	$c\ ^4D_{2\frac{1}{2}} - x\ ^4F^0_{2\frac{1}{2}}$	(0.81)1.39†
3205. 35	2	31188. 85		
3205. 11	25	31191. 20	$c\ ^4D_{2\frac{1}{2}} - x\ ^4F^0_{3\frac{1}{2}}$	(**0.00,** 0.19, 0.35) **0.87,** 1.19
3203. 53	15	31206. 58	$b\ ^4F_{2\frac{1}{2}} - y\ ^4D^0_{1\frac{1}{2}}$	(0.00w)**0.76,**0.95†
3202. 51	15	31216. 52	$b\ ^2D_{2\frac{1}{2}} - x\ ^2F^0_{3\frac{1}{2}}$	(0.00w)1.07A
3202. 47	7	31216. 91	$b\ ^4F_{1\frac{1}{2}} - y\ ^4D^0_{1\frac{1}{2}}$	
3201. 26	25	31228. 70	$c\ ^4D_{3\frac{1}{2}} - x\ ^4F^0_{3\frac{1}{2}}$	(**0.07,** 0.21, 0.35) **0.85,** 1.07, 1.22, 1.36, 1.51, 1.63
3200. 44	10	31236. 71	$c\ ^4D_{3\frac{1}{2}} - x\ ^4F^0_{3\frac{1}{2}}$	(0.71B)1.18C†
3199. 86	10	31242. 37	$c\ ^4D_{0\frac{1}{2}} - y\ ^2D^0_{1\frac{1}{2}}$	(0.31)0.31,**0.91**
3198. 74	2	31253. 30		
3198. 00	15	31260. 54	$c\ ^2G_{4\frac{1}{2}} - x\ ^2G^0_{3\frac{1}{2}}$	(0.00)1.16†
3197. 08	75	31269. 48	$a\ ^4G_{4\frac{1}{2}} - z\ ^4F^0_{3\frac{1}{2}}$	P–B
3196. 93	20	31270. 99	$a\ ^4G_{2\frac{1}{2}} - z\ ^4F^0_{1\frac{1}{2}}$	P–B
3196. 39	5	31276. 31	$c\ ^4D_{1\frac{1}{2}} - y\ ^2D^0_{1\frac{1}{2}}$	
3196. 35	3	31276. 67	$a\ ^4G_{2\frac{1}{2}} - z\ ^4F^0_{2\frac{1}{2}}$	
3194. 62	10	31293. 61	$a\ ^2P_{1\frac{1}{2}} - z\ ^2D^0_{2\frac{1}{2}}$	(0.24, **0.67**)0.67, **1.11,** 1.55
3193. 41	2	31305. 47	$b\ ^4G_{4\frac{1}{2}} - y\ ^4D^0_{3\frac{1}{2}}$	
3190. 68	6	31332. 25	$b\ ^2D_{1\frac{1}{2}} - w\ ^4F^0_{2\frac{1}{2}}$	(0.00)1.13†
3189. 85	12	31340. 41	$b\ ^2G_{4\frac{1}{2}} - y\ ^2G^0_{3\frac{1}{2}}$	(**0.00,** 0.21, 0.46, 0.65) . . . **1.84**
3186. 75	18	31370. 89	$a\ ^2P_{1\frac{1}{2}} - y\ ^4P^0_{2\frac{1}{2}}$	(**0.09,** 0.28)1.41, 1.61, **1.78**
3184. 36	15	31394. 43	$b\ ^2G_{3\frac{1}{2}} - y\ ^2G^0_{3\frac{1}{2}}$	(0.00)0.90
3183. 33	40	31404. 59	$b\ ^2F_{2\frac{1}{2}} - z\ ^2D^0_{2\frac{1}{2}}$	(**0.00,** 0.16, 0.30)0.84 A
3181. 42	20	31423. 41	$a\ ^4G_{4\frac{1}{2}} - z\ ^4F^0_{4\frac{1}{2}}$	P–B
3180. 70	75	31430. 51	$a\ ^4G_{5\frac{1}{2}} - z\ ^4F^0_{4\frac{1}{2}}$	P–B
3179. 46	8	31442. 82	$b\ ^2F_{2\frac{1}{2}} - z\ ^2D^0_{2\frac{1}{2}}$	(0.62, **0.94**)1.25
3178. 80	7	31449. 34	$b\ ^2D_{1\frac{1}{2}} - x\ ^2F^0_{2\frac{1}{2}}$	(0.00 w_2D)1.05 w_2
3177. 90	1	31458. 25	$a\ ^2F_{2\frac{1}{2}} - y\ ^4D^0_{1\frac{1}{2}}$	
3177. 50	1	31462. 21		
3176. 60	4	31471. 12		
3173. 93	2w	31497. 60	$b\ ^2D_{1\frac{1}{2}} - x\ ^4P^0_{2\frac{1}{2}}$	
3173. 58	15	31501. 07	$b\ ^2F_{2\frac{1}{2}} - z\ ^2P^0_{1\frac{1}{2}}$	(**0.17,** 0.50)**0.34,** 0.69, 1.08
3172. 08	40	31515. 97	$a\ ^2P_{1\frac{1}{2}} - z\ ^2P^0_{0\frac{1}{2}}$	(0.27) 1.07, **1.60**
3170. 71	2	31529. 58		
3169. 86	2w, l	31538. 04	$b\ ^2D_{2\frac{1}{2}} - x\ ^2F^0_{3\frac{1}{2}}$	
3169. 20	25	31544. 61	$b\ ^2G_{4\frac{1}{2}} - y\ ^2G^0_{3\frac{1}{2}}$	(0.00)1.12
3168. 39	7	31552. 67		
3164. 48	1	31591. 66	$c\ ^4D_{1\frac{1}{2}} - y\ ^2D^0_{2\frac{1}{2}}$	
3164. 28	4	31593. 65	$b\ ^4F_{2\frac{1}{2}} - y\ ^4D^0_{2\frac{1}{2}}$	
3163. 93	10	31597. 15	$a\ ^2P_{0\frac{1}{2}} - y\ ^4P^0_{0\frac{1}{2}}$	(0.93) 1.62
3163. 37	3	31602. 74	$a\ ^2G_{4\frac{1}{2}} - x\ ^4D^0_{3\frac{1}{2}}$	
3162. 46	10	31611. 83	$b\ ^4F_{3\frac{1}{2}} - y\ ^4D^0_{2\frac{1}{2}}$	(0.00w)0.98 A†
3160. 11	5	31635. 34	$b\ ^4G_{2\frac{1}{2}} - z\ ^4G^0_{3\frac{1}{2}}$	(**0.21,** 0.62, 1.01)1.28, 1.61, **2.00**
3159. 86	3	31637. 84	$b\ ^4G_{4\frac{1}{2}} - z\ ^4G^0_{3\frac{1}{2}}$	
3159. 10	7	31645. 45	$a\ ^4D_{3\frac{1}{2}} - z\ ^4F^0_{3\frac{1}{2}}$	(**0.20,** 0.59, 1.00) . . . 2.03, **2.43**
3158. 03	10	31656. 17	$a\ ^2P_{1\frac{1}{2}} - z\ ^2D^0_{2\frac{1}{2}}$	(0.00w_2D)1.11A
3157. 52	2	31661. 29	$b\ ^2H_{5\frac{1}{2}} - y\ ^2G^0_{4\frac{1}{2}}$	(0.90) . . . ?†
3154. 10	3	31695. 62	$a\ ^2P_{0\frac{1}{2}} - y\ ^4P^0_{1\frac{1}{2}}$	(0.52)1.15, **2.12**†
3154. 04	3	31696. 22	$b\ ^4G_{3\frac{1}{2}} - x\ ^4I^0_{4\frac{1}{2}}$	(0.00d?)**0.00**w, 0.53†

TABLE 1. *Wavelengths of* Cr II *in air*—Continued

Wavelength	Intensity	Wave No.	Term combination	Zeeman effect
3152. 21	40	31714. 62	$a\ ^2P_{1\frac{1}{2}} - z\ ^2P^0_{1\frac{1}{2}}$	(0.21)1.11, **1.27**, 1.41
3150. 11	20	31735. 76	$b\ ^4G_{3\frac{1}{2}} - z\ ^4G^0_{3\frac{1}{2}}$	(0.10)0.98
3149. 82	20	31738. 68	$b\ ^4G_{2\frac{1}{2}} - z\ ^4G^0_{2\frac{1}{2}}$	(0.00)0.58
3149. 11	4	31745. 84	$b\ ^2F_{2\frac{1}{2}} - y\ ^4G^0_{3\frac{1}{2}}$	(0.00)1.31†
3147. 84	1	31758. 65	$b\ ^2H_{4\frac{1}{2}} - y\ ^4G^0_{3\frac{1}{2}}$	
3147. 22	50	31764. 90	$b\ ^4G_{4\frac{1}{2}} - z\ ^4G^0_{3\frac{1}{2}}$ $a\ ^4D_{3\frac{1}{2}} - z\ ^4F^0_{3\frac{1}{2}}$	(0.25, 0.46, **0.67**)0.96, 1.15, **1.34**, 1.52, **1.73**, 1.91
3145. 76	15	31779. 65	$b\ ^2F_{3\frac{1}{2}} - y\ ^4F^0_{3\frac{1}{2}}$	(0.00*d*?)1.29†
3145. 11	15	31786. 21	$b\ ^2F_{2\frac{1}{2}} - y\ ^4F^0_{2\frac{1}{2}}$ $a\ ^4D_{2\frac{1}{2}} - z\ ^4F^0_{1\frac{1}{2}}$	(**0.49**, 1.46)0.88, 1.84, **2.83**
3143. 90	7	31798. 45	$b\ ^2H_{5\frac{1}{2}} - z\ ^2I^0_{5\frac{1}{2}}$	(0.66) 1.15†
3143. 67	7	31800. 77	$b\ ^4G_{4\frac{1}{2}} - z\ ^4I^0_{5\frac{1}{2}}$	(0.00*w*)0.65†
3142. 97	8	31807. 85	$b\ ^2G_{3\frac{1}{2}} - x\ ^4G^0_{3\frac{1}{2}}$	(0.00*w*)1.35†
3142. 73	10	31810. 28	$b\ ^2F_{2\frac{1}{2}} - y\ ^4F^0_{3\frac{1}{2}}$	(**0.13**,0.43)0.74,1.00, **1.28**
3141. 80	4	31819. 70	$b\ ^2D_{2\frac{1}{2}} - x\ ^4P^0_{1\frac{1}{2}}$	
3140. 66	1	31831. 25	$b\ ^2G_{4\frac{1}{2}} - y\ ^2H^0_{5\frac{1}{2}}$	
3140. 21	25	31835. 81	$b\ ^2G_{4\frac{1}{2}} - y\ ^2H^0_{5\frac{1}{2}}$	
3139. 90	10	31838. 95	$b\ ^4G_{2\frac{1}{2}} - z\ ^4G^0_{3\frac{1}{2}}$	(**0.19**, 0.60, 0.97)1.54, **1.91**
3138. 21	7	31856. 10	$c\ ^2D_{2\frac{1}{2}} - u\ ^2D^0_{2\frac{1}{2}}$	
3137. 53	8	31863. 00	$b\ ^4G_{2\frac{1}{2}} - z\ ^4G^0_{2\frac{1}{2}}$	(0.00*w*)1.42†
3137. 44	2	31863. 92	$b\ ^2G_{4\frac{1}{2}} - x\ ^4G^0_{3\frac{1}{2}}$	
3137. 10	10	31867. 37	$b\ ^2D_{1\frac{1}{2}} - y\ ^2P^0_{0\frac{1}{2}}$	
3136. 68	45	31871. 64	$a\ ^4D_{2\frac{1}{2}} - z\ ^4F^0_{2\frac{1}{2}}$	(0.17, 0.50, **0.85**)0.51, 0.86, **1.19**, 1.54, 1.90
3135. 74	30	31881. 19	$b\ ^4H_{3\frac{1}{2}} - z\ ^2I^0_{3\frac{1}{2}}$	(0.00)0.96
3135. 34	20	31885. 26	$b\ ^2G_{3\frac{1}{2}} - y\ ^2H^0_{4\frac{1}{2}}$	(**0.09**, 0.31, 0.49)0.78, 0.96, 1.18, **1.42**
3134. 33	25	31895. 53	$b\ ^2H_{4\frac{1}{2}} - z\ ^2I^0_{5\frac{1}{2}}$	(0.00)0.98
3132. 05	100	31918. 75	$a\ ^4D_{2\frac{1}{2}} - z\ ^4F^0_{2\frac{1}{2}}$	(0.00 w_3D)0.99*A*
3131. 53	5	31924. 05	$b\ ^4G_{4\frac{1}{2}} - z\ ^2G^0_{3\frac{1}{2}}$ $b\ ^4G_{3\frac{1}{2}} - z\ ^4I^0_{3\frac{1}{2}}$	
3130. 55	7	31934. 04	$b\ ^2D_{2\frac{1}{2}} - x\ ^4P^0_{2\frac{1}{2}}$	(0.38)**0.38**, 1.16
3128. 69	40	31953. 03	$a\ ^4D_{1\frac{1}{2}} - z\ ^4F^0_{1\frac{1}{2}}$	(0.40, **1.21**)0.00, **0.80**, 1.62
3128. 08	4	31959. 26		
3125. 79	5	31982. 67	$c\ ^2D_{2\frac{1}{2}} - x\ ^2P^0_{1\frac{1}{2}}$	
3125. 46	7	31986. 04	$b\ ^4G_{2\frac{1}{2}} - z\ ^2G^0_{4\frac{1}{2}}$	(0.00)1.81 *B*†
3125. 02	60	31990. 55	$a\ ^2P_{0\frac{1}{2}} - z\ ^2D^0_{1\frac{1}{2}}$	
3124. 94	40	31991. 37	$a\ ^4D_{2\frac{1}{2}} - z\ ^4F^0_{3\frac{1}{2}}$	(**0.08**, 0.20, 0.35)**0.89**, 1.03, 1.16, 1.31, 1.45, 1.58
3124. 23	3	31998. 64	$b\ ^2D_{1\frac{1}{2}} - y\ ^2P^0_{1\frac{1}{2}}$	
3122. 59	30	32015. 44	$b\ ^4G_{3\frac{1}{2}} - z\ ^4G^0_{3\frac{1}{2}}$	(0.00)1.26
3121. 95	7	32022. 00	$b\ ^4G_{2\frac{1}{2}} - z\ ^2G^0_{3\frac{1}{2}}$	(0.30)0.92†
3121. 83	10	32023. 24	$a\ ^2P_{1\frac{1}{2}} - y\ ^4F^0_{1\frac{1}{2}}$	(1.19)0.00*d*?, **0.94**, 1.75†
3121. 21	6	32029. 60	$e\ ^2D_{1\frac{1}{2}} - u\ ^2D^0_{1\frac{1}{2}}$	(0.00)0.80
3121. 04	8	32031. 34	$a\ ^2P_{1\frac{1}{2}} - y\ ^4F^0_{2\frac{1}{2}}$	
3120. 36	75	32038. 32	$a\ ^4D_{1\frac{1}{2}} - z\ ^4F^0_{2\frac{1}{2}}$	(**0.09**, 0.27)**0.77**, 0.95, 1.11, 1.28
3118. 64	60	32055. 99	$a\ ^4D_{0\frac{1}{2}} - z\ ^4F^0_{1\frac{1}{2}}$	(0.21)0.21, **0.62**
3118. 14	10	32061. 13	$b\ ^4G_{4\frac{1}{2}} - z\ ^2G^0_{4\frac{1}{2}}$	(0.17)1.11
3117. 28	15	32069. 98	$b\ ^4F_{4\frac{1}{2}} - y\ ^4D^0_{3\frac{1}{2}}$	(0.10 *A*)1.02 *w A*
3116. 75	20	32075. 43	$b\ ^2G_{3\frac{1}{2}} - y\ ^2F^0_{3\frac{1}{2}}$	(0.00 *w*)0.97 *B*
3115. 65	20	32086. 76	$b\ ^2D_{2\frac{1}{2}} - y\ ^2P^0_{1\frac{1}{2}}$ $b\ ^4F_{3\frac{1}{2}} - y\ ^4D^0_{3\frac{1}{2}}$	(**0.09**, 0.25)**0.95**, 1.11, 1.29
3115. 27	12	32090. 67	$b\ ^4G_{4\frac{1}{2}} - z\ ^4G^0_{3\frac{1}{2}}$	(0.00 w_3 *D*)1.68 *B*
3113. 59	5	32107. 98	$c\ ^2D_{1\frac{1}{2}} - x\ ^2P^0_{0\frac{1}{2}}$	(0.00)0.92†
3113. 17	3	32112. 31	$c\ ^4D_{2\frac{1}{2}} - x\ ^4G^0_{3\frac{1}{2}}$	
3111. 94	15	32125. 00	$b\ ^4G_{3\frac{1}{2}} - z\ ^2G^0_{3\frac{1}{2}}$	(**0.16**, 0.50, 0.83)0.44, 0.76, 1.08, 1.40, **1.72**
3108. 98	3	32155. 59		
3108. 65	10	32159. 01	$b\ ^4G_{3\frac{1}{2}} - z\ ^4G^0_{3\frac{1}{2}}$	(**0.88**, 0.23, 0.35, 0.51) 1.53m **1.64**
3107. 57	50	32170. 18	$b\ ^2G_{3\frac{1}{2}} - x\ ^4G^0_{3\frac{1}{2}}$	(**0.06**, 0.20, 0.33, 0.48) 1.55 *B*
3104. 29	3	32204. 17	$a\ ^2G_{4\frac{1}{2}} - z\ ^2H^0_{5\frac{1}{2}}$	
3103. 47	30	32212. 68	$a\ ^2P_{0\frac{1}{2}} - z\ ^2P^0_{1\frac{1}{2}}$	(0.08)0.73
3102. 55	3	32222. 23	$c\ ^4D_{3\frac{1}{2}} - y\ ^2F^0_{2\frac{1}{2}}$	

TABLE 1. *Wavelengths of* Cr II *in air*—Continued

Wavelength	Intensity	Wave No.	Term combination	Zeeman effect
3099.88	2	32249.98	$a\ ^2D_{2\frac{1}{2}} - z\ ^4H^0_{3\frac{1}{2}}$	
3098.88	4	32260.39	$b\ ^2F_{3\frac{1}{2}} - x\ ^4D^0_{2\frac{1}{2}}$	
3098.16	18	32267.89	$b\ ^2F_{3\frac{1}{2}} - x\ ^4D^0_{3\frac{1}{2}}$	(0.88)1.30†
3096.11	35	32289.25	$b\ ^2G_{4\frac{1}{2}} - y\ ^2F^0_{3\frac{1}{2}}$	(0.00)1.07
3095.48	12	32295.82	$b\ ^2P_{1\frac{1}{2}} - u\ ^2D^0_{2\frac{1}{2}}$	(0.00 *w*)1.11†
3095.20	3	32298.74	$b\ ^2F_{2\frac{1}{2}} - x\ ^4D^0_{2\frac{1}{2}}$	
3094.93	10	32301.56	$b\ ^2F_{3\frac{1}{2}} - x\ ^4D^0_{1\frac{1}{2}}$ $b\ ^4F_{3\frac{1}{2}} - z\ ^4G^0_{3\frac{1}{2}}$	
3093.97	15	32311.58	$b\ ^4F_{1\frac{1}{2}} - z\ ^4G^0_{2\frac{1}{2}}$	(0.00 *d*?)0.72†
3093.47	40	32316.80	$b\ ^2G_{4\frac{1}{2}} - x\ ^4G^0_{5\frac{1}{2}}$	(0.00 w_2 *D*)1.39 *B*
3093.17	3	32319.94	$b\ ^4F_{3\frac{1}{2}} - z\ ^4G^0_{2\frac{1}{2}}$	
3090.91	2*w*	32343.57	$b\ ^2G_{3\frac{1}{2}} - y\ ^2F^0_{3\frac{1}{2}}$	
3089.72	1	32356.03	$d\ ^2G_{4\frac{1}{2}} - u\ ^2F^0_{3\frac{1}{2}}$	
3087.90	20	32375.10	$a\ ^2G_{3\frac{1}{2}} - z\ ^2H^0_{4\frac{1}{2}}$	(0.00)0.96
3085.35	10	32401.85	$b\ ^4F_{2\frac{1}{2}} - z\ ^4G^0_{3\frac{1}{2}}$	(.00)0.95†
3084.45	15	32411.31	$a\ ^2P_{0\frac{1}{2}} - z\ ^2P^0_{1\frac{1}{2}}$	(0.27)0.94, **1.46**
3083.61	10	32420.14	$b\ ^4F_{3\frac{1}{2}} - z\ ^4G^0_{3\frac{1}{2}}$	(0.79 *B*)1.09 *C*†
3083.04	3	32426.13	$b\ ^2P_{1\frac{1}{2}} - u\ ^2D^0_{1\frac{1}{2}}$	
3080.23	4*w*	32455.71		
3079.34	15	32465.09	$a\ ^2G_{4\frac{1}{2}} - z\ ^2H^0_{5\frac{1}{2}}$	(0.00)1.07
3077.78	25	32481.54	$a\ ^2G_{3\frac{1}{2}} - z\ ^2F^0_{3\frac{1}{2}}$	(0.00)0.91
3077.59	5	32483.55	$a\ ^4F_{2\frac{1}{2}} - z\ ^4H^0_{3\frac{1}{2}}$	
3077.24	18	32487.25	$a\ ^4F_{4\frac{1}{2}} - z\ ^4H^0_{5\frac{1}{2}}$ $a\ ^2G_{4\frac{1}{2}} - z\ ^2F^0_{3\frac{1}{2}}$	(0.00w_3D)1.00w_2
3074.90	3	32511.97	$a\ ^2P_{1\frac{1}{2}} - x\ ^4D^0_{2\frac{1}{2}}$	
3074.67	3	32514.40	$a\ ^2P_{1\frac{1}{2}} - x\ ^4D^0_{1\frac{1}{2}}$	
3073.24	15	32529.53	$b\ ^4F_{4\frac{1}{2}} - z\ ^4G^0_{4\frac{1}{2}}$	(0.85*B*)1.28 *C*†
3072.47	8	32537.68	$a\ ^4F_{3\frac{1}{2}} - z\ ^4H^0_{4\frac{1}{2}}$	(0.00*w*)0.00*w*
3072.19	2	32540.64	$a\ ^2H_{5\frac{1}{2}} - y\ ^4G^0_{4\frac{1}{2}}$	
3071.85	3*w*	32544.24		
3071.57	7	32547.21	$b\ ^4F_{3\frac{1}{2}} - z\ ^4G^0_{4\frac{1}{2}}$	(0.00)0.83†
3071.02	2	32553.04	$a\ ^2F_{2\frac{1}{2}} - z\ ^4G^0_{2\frac{1}{2}}$	
3069.02	1	32574.25		
3067.18	20	32593.79	$a\ ^4P_{0\frac{1}{2}} - z\ ^4D^0_{0\frac{1}{2}}$ $a\ ^4P_{1\frac{1}{2}} - z\ ^4D^0_{0\frac{1}{2}}$	P–B
3064.32	3*w*, *l*	32624.22	$z\ ^4F^0_{1\frac{1}{2}} - e\ ^4D_{0\frac{1}{2}}$	
3063.82	7	32629.54	$a\ ^4F_{4\frac{1}{2}} - z\ ^4H^0_{5\frac{1}{2}}$	(**0.10**, 0.30, 0.50)**0.24**, 0.44, 0.64
3063.25	6	32635.61	$a\ ^2H_{5\frac{1}{2}} - y\ ^4F^0_{4\frac{1}{2}}$	
3062.02	5*w*, *l*	32648.72	$z\ ^4F^0_{2\frac{1}{2}} - e\ ^4D_{1\frac{1}{2}}$	(0.00)1.12†
3061.58	8	32653.41	$a\ ^2F_{2\frac{1}{2}} - z\ ^4G^0_{3\frac{1}{2}}$	(0.00)1.01†
3059.53	25	32675.29	$a\ ^4P_{0\frac{1}{2}} - z\ ^4D^0_{1\frac{1}{2}}$ $a\ ^4P_{1\frac{1}{2}} - z\ ^4D^0_{1\frac{1}{2}}$	P–B
3059.38	10	32676.89	$a\ ^4P_{2\frac{1}{2}} - z\ ^4D^0_{1\frac{1}{2}}$	P–B
3058.36	12	32687.79	$b\ ^4F_{2\frac{1}{2}} - z\ ^2G^0_{3\frac{1}{2}}$	(0.00)0.68†
3057.86	12	32693.13	$a\ ^2H_{5\frac{1}{2}} - z\ ^2I^0_{6\frac{1}{2}}$	(0.78*B*)0.92*C*†
3056.66	8*w*, *l*	32705.97	$z\ ^4F^0_{3\frac{1}{2}} - e\ ^4D_{2\frac{1}{2}}$ $b\ ^4F_{3\frac{1}{2}} - z\ ^2G^0_{3\frac{1}{2}}$	(0.00*w*)1.01*w*†
3056.20	3	32710.89	$a\ ^2D_{2\frac{1}{2}} - y\ ^4D^0_{1\frac{1}{2}}$	
3055.44	15	32719.03	$a\ ^4F_{1\frac{1}{2}} - y\ ^4D^0_{0\frac{1}{2}}$	(0.19)0.19, **0.60**
3055.32	5	32720.31	$a\ ^2G_{4\frac{1}{2}} - y\ ^4H^0_{4\frac{1}{2}}$ $a\ ^2P_{0\frac{1}{2}} - y\ ^4F^0_{1\frac{1}{2}}$	
3053.65	10	32738.20	$a\ ^2H_{4\frac{1}{2}} - y\ ^4G^0_{3\frac{1}{2}}$	
3052.97	3	32745.49		
3051.60	6	32760.20		(0.00)0.48*A*†
3051.37	2	32762.67	$a\ ^2H_{4\frac{1}{2}} - y\ ^4F^0_{3\frac{1}{2}}$	
3050.74	6	32769.43	$b\ ^2H_{5\frac{1}{2}} - z\ ^2H^0_{4\frac{1}{2}}$	(0.00)1.34†
3050.14	100	32775.88	$a\ ^2H_{5\frac{1}{2}} - z\ ^2I^0_{6\frac{1}{2}}$	(0.00)1.05
3049.49	10*w*, *l*	32782.86	$z\ ^4F^0_{4\frac{1}{2}} - e\ ^4D_{3\frac{1}{2}}$	(0.00*w*)1.13*w*†
3047.77	25	32801.36	$a\ ^4P_{1\frac{1}{2}} - z\ ^4D^0_{2\frac{1}{2}}$	P–B
3047.62	20	32802.98	$a\ ^4P_{2\frac{1}{2}} - z\ ^4D^0_{2\frac{1}{2}}$	P–B
3046.27	1	32817.51	$a\ ^2H_{4\frac{1}{2}} - y\ ^4F^0_{4\frac{1}{2}}$	

TABLE 1. *Wavelengths of* Cr II *in air*—Continued

Wavelength	Intensity	Wave No.	Term combination	Zeeman effect
3045. 62	3	32824. 52	$c\ ^2G_{4\frac{1}{2}} - x\ ^2G^0_{3\frac{1}{2}}$	
3045. 52	4*l*	32825. 49	$z\ ^4F^0_{3\frac{1}{2}} - e\ ^4D_{2\frac{1}{2}}$ $b\ ^4F_{4\frac{1}{2}} - z\ ^2G^0_{4\frac{1}{2}}$	(0.36*B*)1.18*C*†
3044. 23	10	32839. 51	$c\ ^2F_{3\frac{1}{2}} - x\ ^2G^0_{3\frac{1}{2}}$	(0.00w_2)1.30w_1
3043. 89	18	32843. 17	$b\ ^4F_{3\frac{1}{2}} - z\ ^2G^0_{3\frac{1}{2}}$	(0.00)0.91†
3042. 79	25	32855. 04	$b\ ^4F_{4\frac{1}{2}} - z\ ^4G^0_{3\frac{1}{2}}$	(0.12)1.12
3041. 73	50	32866. 49	$b\ ^2H_{4\frac{1}{2}} - z\ ^2H^0_{3\frac{1}{2}}$	(0.00)0.93
3040. 91	70	32875. 36	$a\ ^2H_{4\frac{1}{2}} - z\ ^2I^0_{5\frac{1}{2}}$	(0.00)0.97
3040. 18	8*d*?	32883. 25		(0.00)1.00†
3039. 32	4	32892. 55	$c\ ^2G_{4\frac{1}{2}} - x\ ^2G^0_{4\frac{1}{2}}$	(0.00)1.19
3038. 80	4	32898. 18	$a\ ^2G_{4\frac{1}{2}} - y\ ^4H^0_{5\frac{1}{2}}$	
3038. 51	4	32901. 32	$a\ ^2F_{3\frac{1}{2}} - z\ ^4G^0_{3\frac{1}{2}}$	
3038. 04	8	32906. 42	$c\ ^2F_{3\frac{1}{2}} - x\ ^2G^0_{3\frac{1}{2}}$	(0.00)0.96†
3034. 99	20	32939. 48	$a\ ^2F_{2\frac{1}{2}} - z\ ^2G^0_{3\frac{1}{2}}$	(0.00)0.91
3034. 54	25	32944. 37	$a\ ^4F_{3\frac{1}{2}} - y\ ^4D^0_{1\frac{1}{2}}$	(**0.09,** 0.26)0.78
3034. 06	5	32949. 58	$a\ ^2P_{1\frac{1}{2}} - z\ ^4S^0_{1\frac{1}{2}}$	
3032. 94	50	32961. 74	$a\ ^4P_{2\frac{1}{2}} - z\ ^4D^0_{3\frac{1}{2}}$	P–B
3032. 65	4	32964. 90	$c\ ^2G_{3\frac{1}{2}} - x\ ^2G^0_{3\frac{1}{2}}$	
3031. 63	3	32975. 98	$b\ ^2F_{3\frac{1}{2}} - z\ ^2F^0_{2\frac{1}{2}}$	
3028. 12	75	33014. 21	$b\ ^2F_{3\frac{1}{2}} - z\ ^2F^0_{3\frac{1}{2}}$	(0.00)0.86
3026. 86	20	33027. 95	$a\ ^2F_{3\frac{1}{2}} - z\ ^4G^0_{4\frac{1}{2}}$	(0.00)1.09
3026. 64	100	33030. 35	$b\ ^2H_{5\frac{1}{2}} - z\ ^2H^0_{5\frac{1}{2}}$	(0.00)1.10
3026. 38	7	33033. 19	$c\ ^2G_{3\frac{1}{2}} - x\ ^2G^0_{4\frac{1}{2}}$	
3024. 90	3	33049. 35		
3017. 78	10*w*	33127. 32	$z\ ^6D^0_{1\frac{1}{2}} - e\ ^6D_{0\frac{1}{2}}$ $b\ ^2H_{4\frac{1}{2}} - z\ ^2H^0_{5\frac{1}{2}}$	
3015. 51	50	33152. 26	$b\ ^2F_{3\frac{1}{2}} - z\ ^2F^0_{3\frac{1}{2}}$	(0.00)1.15
3012. 47	5	33185. 71		
3012. 33	3	33187. 25	$a\ ^2F_{3\frac{1}{2}} - z\ ^2G^0_{3\frac{1}{2}}$	
3012. 01	2	33190. 78	$b\ ^2F_{2\frac{1}{2}} - z\ ^2F^0_{3\frac{1}{2}}$	
3011. 42	7	33197. 28	$b\ ^4P_{2\frac{1}{2}} - y\ ^4D^0_{1\frac{1}{2}}$	(**0.20,** 0.59)1.38, 1.80, **2.18**
3010. 92	4*w*, *l*	33202. 79	$z\ ^6D^0_{3\frac{1}{2}} - e\ ^6D_{0\frac{1}{2}}$ $z\ ^6D^0_{1\frac{1}{2}} - e\ ^6D_{2\frac{1}{2}}$	
3010. 64	10	33205. 88	$b\ ^4G_{3\frac{1}{2}} - y\ ^4P^0_{2\frac{1}{2}}$	(0.00)1.32
3008. 67	4	33227. 62	$a\ ^2P_{1\frac{1}{2}} - z\ ^2F^0_{2\frac{1}{2}}$	
3008. 30	6	33231. 71	$b\ ^4G_{2\frac{1}{2}} - z\ ^2D^0_{1\frac{1}{2}}$	(0.00 *w*)0.00 *W*†
3007. 98	6*w*, *l*	33235. 25	$b\ ^2F_{3\frac{1}{2}} - y\ ^4H^0_{3\frac{1}{2}}$ $z\ ^6D^0_{3\frac{1}{2}} - e\ ^6D_{2\frac{1}{2}}$	
3004. 77	2*w*, *l*	33270. 75	$z\ ^6D^0_{0\frac{1}{2}} - e\ ^6D_{1\frac{1}{2}}$	
3004. 47	3	33274. 07	$b\ ^2F_{2\frac{1}{2}} - y\ ^4H^0_{3\frac{1}{2}}$	(0.00)0.40†
3003. 92	35	33280. 16	$a\ ^4F_{3\frac{1}{2}} - y\ ^4D^0_{3\frac{1}{2}}$	(**0.07,** 0.22, 0.35)**0.88,** 1.02, 1.18
3000. 65	2*w*, *l*	33316. 43	$z\ ^6D^0_{1\frac{1}{2}} - e\ ^6D_{2\frac{1}{2}}$	
2999. 96	25	33324. 09	$a\ ^2F_{3\frac{1}{2}} - z\ ^2G^0_{4\frac{1}{2}}$	(0.00)0.95
2999. 30	8	33331. 42	$a\ ^4F_{2\frac{1}{2}} - y\ ^4D^0_{3\frac{1}{2}}$	(0.86 *B*)1.38 *C*†
2999. 00	1*w*, *l*	33334. 66	$z\ ^6D^0_{3\frac{1}{2}} - e\ ^6D_{3\frac{1}{2}}$	
2994. 74	20	33382. 17	$a\ ^4H_{4\frac{1}{2}} - z\ ^4H^0_{3\frac{1}{2}}$	(0.00 *WD*)2.09 *B*†
2993. 54	7*w*, *l*	33395. 55	$z\ ^6D^0_{3\frac{1}{2}} - e\ ^6D_{3\frac{1}{2}}$	
2992. 96	10*w*, *l*	33402. 03	$z\ ^6D^0_{4\frac{1}{2}} - e\ ^6D_{4\frac{1}{2}}$	
2992. 59	7	33406. 16	$b\ ^2S_{0\frac{1}{2}} - x\ ^2P^0_{1\frac{1}{2}}$	
2992. 42	10	33408. 05	$a\ ^4H_{5\frac{1}{2}} - z\ ^4H^0_{4\frac{1}{2}}$	(**0.09,** 0.23, 0.42, 0.59, 0.73)1.74, **1.85**
2989. 18	70	33444. 26	$a\ ^4H_{3\frac{1}{2}} - z\ ^4H^0_{3\frac{1}{2}}$	(0.00)0.68
2988. 04	12	33457. 02	$a\ ^4H_{4\frac{1}{2}} - z\ ^4H^0_{3\frac{1}{2}}$	(0.00 w_2 *D*)1.73 *B*
2987. 52	3	33462. 84	$b\ ^2H_{5\frac{1}{2}} - y\ ^4H^0_{5\frac{1}{2}}$	
2986. 87	8	33470. 13	$b\ ^2S_{0\frac{1}{2}} - x\ ^2P^0_{0\frac{1}{2}}$	(0.60)1.28†
2985. 32	75	33487. 50	$a\ ^4H_{4\frac{1}{2}} - z\ ^4H^0_{4\frac{1}{2}}$	(0.00)0.98
2985. 01	7	33490. 98	$b\ ^4G_{3\frac{1}{2}} - z\ ^2D^0_{2\frac{1}{2}}$	
2984. 69	10	33494. 57	$b\ ^4P_{1\frac{1}{2}} - y\ ^4D^0_{0\frac{1}{2}}$	(0.87)0.87, **2.56**†
2982. 69	2	33517. 03		(0.00)1.27†
2979. 73	80	33550. 32	$a^4H_{5\frac{1}{2}} - z\ ^4H^0_{5\frac{1}{2}}$	(0.00)1.13
2977. 65	2	33573. 76	$a\ ^2D_{2\frac{1}{2}} - y\ ^4D^0_{3\frac{1}{2}}$	
2976. 70	35	33584. 47	$b\ ^4P_{2\frac{1}{2}} - y\ ^4D^0_{2\frac{1}{2}}$	(0.34, **0.59**)1.03, 1.27, **1.50,** 1.73, 1.89
2975. 80	4*w*	33594. 63	$z\ ^6D^0_{3\frac{1}{2}} - e\ ^6D_{3\frac{1}{2}}$	
2974. 83	4*w*, *l*	33605. 58		
2973. 10	12	33625. 14	$a\ ^2D_{1\frac{1}{2}} - z\ ^4G^0_{2\frac{1}{2}}$	(**0.11,** 0.31)**0.26,** 0.50, 0.79

TABLE 1. *Wavelengths of* Cr II *in air*—Continued

Wavelength	Intensity	Wave No.	Term combination	Zeeman effect
2972.67	7*w*	33630.00	*a* $^4H_{4\frac{1}{2}} - z\ ^4H^0_{3\frac{1}{2}}$	
2972.57	8	33631.13	*a* $^2G_{4\frac{1}{2}} - y\ ^2G^0_{3\frac{1}{2}}$	
2971.90	75	33638.71	*a* $^4H_{6\frac{1}{2}} - z\ ^4H^0_{5\frac{1}{2}}$	(0.00)1.23
2970.65	2	33652.87	*b* $^4G_{2\frac{1}{2}} - z\ ^2P^0_{1\frac{1}{2}}$	
2969.67	15	33663.97	*a* $^2H_{5\frac{1}{2}} - z\ ^2H^0_{6\frac{1}{2}}$	(0.28)1.75 *B*†
29 . t 8	15	33675.20	*b* $^4G_{3\frac{1}{2}} - y\ ^4G^0_{3\frac{1}{2}}$	(0.00)1.29
2968.20	3	33680.64	*b* $^2H_{5\frac{1}{2}} - y\ ^4H^0_{5\frac{1}{2}}$	
2966.03	40	33705.28	*a* $^4F_{4\frac{1}{2}} - y\ ^4D^0_{3\frac{1}{2}}$	(0.00 w_3 *D*)1.00 *A*
2965.18	2	33714.94	*b* $^4G_{4\frac{1}{2}} - y\ ^4G^0_{3\frac{1}{2}}$	
2963.46	20	33734.51	*b* $^4G_{4\frac{1}{2}} - y\ ^4G^0_{4\frac{1}{2}}$	(0.00)1.18
2961.72	50	33754.35	*b* $^4G_{3\frac{1}{2}} - y\ ^4F^0_{4\frac{1}{2}}$	(0.00 w_2)1.13 w_2
2961.70		33754.56	*b* $^4P_{1\frac{1}{2}} - y\ ^4D^0_{1\frac{1}{2}}$	(0.27, **0.80**)0.95, **1.47**, 2.00
2959.95	18	33774.52	*b* $^4G_{4\frac{1}{2}} - y\ ^4F^0_{3\frac{1}{2}}$	(0.00)1.17
2959.54	18	33779.19	*b* $^2F_{2\frac{1}{2}} - x\ ^4F^0_{1\frac{1}{2}}$	(0.00 *w*)1.19†
2958.51	2	33790.95	*b* $^2H_{5\frac{1}{2}} - x\ ^4F^0_{4\frac{1}{2}}$	
2958.17	1	33794.84	*b* $^4F_{2\frac{1}{2}} - z\ ^2D^0_{1\frac{1}{2}}$	
2958.04	4	33796.32		(0.00)1.32†
2957.55	5	33801.92	*a* $^2G_{2\frac{1}{2}} - y\ ^2G^0_{3\frac{1}{2}}$	
2957.26	4	33805.24	*b* $^4F_{1\frac{1}{2}} - z\ ^2D^0_{1\frac{1}{2}}$; *a* $^2D_{2\frac{1}{2}} - z\ ^4G^0_{2\frac{1}{2}}$	
2956.60	10	33812.78	*b* $^4G_{2\frac{1}{2}} - y\ ^4G^0_{3\frac{1}{2}}$	(0.00 w_1)0.99
2955.68	2	33823.30	*b* $^4G_{3\frac{1}{2}} - y\ ^4G^0_{2\frac{1}{2}}$	
2955.12	10	33829.72	*b* $^4G_{4\frac{1}{2}} - y\ ^4F^0_{4\frac{1}{2}}$	(0.54 *B*)1.22 *C*†
2954.65	10	33835.10	*a* $^2G_{4\frac{1}{2}} - y\ ^2G^0_{4\frac{1}{2}}$	(0.00*d*?)1.09 w_1
2953.70	45	33845.98	*a* $^2H_{4\frac{1}{2}} - z\ ^2H^0_{5\frac{1}{2}}$	(0.00)0.92
2953.34	35	33850.11	*b* $^4P_{0\frac{1}{2}} - y\ ^4D^0_{0\frac{1}{2}}$	(1.33)1.33
2952.45	12	33860.31	*d* $^2D_{1\frac{1}{2}} - v\ ^2F^0_{2\frac{1}{2}}$	(0.00)0.93
2951.94	10	33866.16	*b* $^4G_{2\frac{1}{2}} - y\ ^4F^0_{2\frac{1}{2}}$	(00.00)0.94†
2951.39	10	33872.47	*b* $^4G_{2\frac{1}{2}} - y\ ^4F^0_{3\frac{1}{2}}$; *b* $^4F_{2\frac{1}{2}} - y\ ^4P^0_{2\frac{1}{2}}$	(0.59)1.50†
2950.69	7	33880.50	*a* $^2I_{6\frac{1}{2}} - z\ ^4H^0_{5\frac{1}{2}}$	(0.88)1.13†
2950.10	10	33887.28	*a* $^2I_{5\frac{1}{2}} - z\ ^4H^0_{4\frac{1}{2}}$; *b* $^4G_{4\frac{1}{2}} - z\ ^2I^0_{5\frac{1}{2}}$	
2949.79	10	33890.84	*b* $^2F_{3\frac{1}{2}} - x\ ^4F^0_{4\frac{1}{2}}$; *b* $^4F_{3\frac{1}{2}} - y\ ^4P^0_{2\frac{1}{2}}$	(0.00)1.89†
2949.44	20	33894.86	*b* $^4G_{5\frac{1}{2}} - z\ ^2I^0_{6\frac{1}{2}}$	(0.00*W*)0.00*W*†
2949.07	2	33899.11	*b* $^2F_{3\frac{1}{2}} - x\ ^4F^0_{3\frac{1}{2}}$	
2948.47	3	33906.11	*a* $^2D_{2\frac{1}{2}} - z\ ^4G^0_{3\frac{1}{2}}$	(0.00)0.67†
2948.20	3	33909.12	*b* $^2F_{2\frac{1}{2}} - x\ ^4F^0_{2\frac{1}{2}}$	(0.00)0.87†
2947.50	25	33917.17	*d* $^2F_{2\frac{1}{2}} - u\ ^2F^0_{2\frac{1}{2}}$	(0.00)0.90
2946.81	50	33925.11	*a* $^2H_{5\frac{1}{2}} - z\ ^2H^0_{5\frac{1}{2}}$	(0.00)1.09
2946.70	15*w*, *l*	33926.38	*z* $^4D^0_{1\frac{1}{2}} - e\ ^4P^0_{0\frac{1}{2}}$	
2945.74	7*w*	33937.43	*d* $^2F_{3\frac{1}{2}} - u\ ^2F^0_{3\frac{1}{2}}$; *b* $^2F_{2\frac{1}{2}} - x\ ^4F^0_{3\frac{1}{2}}$	(0.00*w*)1.61*B*†
2943.64	4	33961.75	*b* $^4G_{2\frac{1}{2}} - y\ ^4F^0_{1\frac{1}{2}}$	(0.00)0.67†
2942.99	3	33969.14	*b* $^4G_{3\frac{1}{2}} - y\ ^4F^0_{3\frac{1}{2}}$	
2941.96	35	33981.04	*b* $^2D_{2\frac{1}{2}} - w\ ^2F^0_{3\frac{1}{2}}$	(0.00w_1D)1.04*A*
2941.32	3	33988.43	*a* $^4F_{3\frac{1}{2}} - z\ ^4G^0_{2\frac{1}{2}}$	(0.00)0.88
2940.97	7	33992.47	*a* $^2P_{1\frac{1}{2}} - x\ ^4F^0_{1\frac{1}{2}}$	(0.40, **1.09**)0.21, **1.00**,1.70†
2940.42	2	33998.83	*a* $^4F_{4\frac{1}{2}} - z\ ^4I^0_{4\frac{1}{2}}$	
2940.22	25	34001.15	*b* $^2D_{1\frac{1}{2}} - w\ ^2F^0_{2\frac{1}{2}}$	(0.00w_1)0.88
2939.78	3	34006.24	*a* $^2G_{3\frac{1}{2}} - y\ ^2G^0_{4\frac{1}{2}}$	
2939.44	20	34010.17	*d* $^2F_{3\frac{1}{2}} - u\ ^2F^0_{3\frac{1}{2}}$	(0.00)1.13
2938.24	3	34024.05		
2936.92	25	34039.35	*a* $^4F_{2\frac{1}{2}} - z\ ^4G^0_{2\frac{1}{2}}$	(0.19, 0.69, **1.15**)0.34,**0.80**, 1.24, 1.72
2936.05	3	34049.43	*a* $^4F_{3\frac{1}{2}} - z\ ^4I^0_{4\frac{1}{2}}$	
2935.58	4	34054.88		
2935.12	60	34060.22	*b* $^4P_{2\frac{1}{2}} - y\ ^4D^0_{2\frac{1}{2}}$	**0.09**, 0.30, 0.45)**0.97**, 1.16, 1.36, **1.54**, 1.70, 185
2934.30	20	34069.74	*b* $^2F_{2\frac{1}{2}} - y\ ^2D^0_{1\frac{1}{2}}$	
2934.13	10	34071.72		(0.00)1.02†

TABLE 1. *Wavelengths of* Cr II *in air*—Continued

Wavelength	Intensity	Wave No.	Term combination	Zeeman effect
2933. 95	35	34073. 80	$a\ ^4F_{1\frac{1}{2}} - z\ ^4G^0_{2\frac{1}{2}}$	(**0.07,** 0.26)0.33, 0.49, 0.64, **0.83**
2933. 60	12	34077. 87	$d\ ^2D_{2\frac{1}{2}} - v\ ^2F^0_{3\frac{1}{2}}$	(0.00)1.13†
2932. 69	30	34088. 45	$a\ ^4F_{3\frac{1}{2}} - z\ ^4G^0_{3\frac{1}{2}}$	[1.63, 1.90 (0.15, 0.40, 0.67, **0.96**)0.30, 0.55, 0.82, **1.09,** 1.37,
2931. 07	4	34107. 29	$a\ ^2H_{4\frac{1}{2}} - z\ ^2H^0_{5\frac{1}{2}}$	
2930. 83	35	34110. 07	$b\ ^4P_{0\frac{1}{2}} - y\ ^4D^0_{1\frac{1}{2}}$	(0.73)**0.45,** 1.96
2929. 78	4	34122. 30	$a\ ^2P_{1\frac{1}{2}} - x\ ^4F^0_{2\frac{1}{2}}$	(0.28)0.99†
2929. 44	18	34126. 26	$a\ ^2G_{4\frac{1}{2}} - y\ ^2H^0_{5\frac{1}{2}}$	(0.00*w*)1.51†
2929. 18	2	34129. 29	$a\ ^2H_{4\frac{1}{2}} - z\ ^2F^0_{3\frac{1}{2}}$	
2928. 32	50	34139. 31	$b\ ^2G_{3\frac{1}{2}} - x\ ^2G^0_{3\frac{1}{2}}$ $a\ ^4F_{2\frac{1}{2}} - z\ ^4G^0_{3\frac{1}{2}}$	(0.00)0.90†
2928. 12	40	34141. 65	$b\ ^4P_{1\frac{1}{2}} - y\ ^4D^0_{2\frac{1}{2}}$	(**0.19,** 0.55)**0.82,** 1.21, 1.57
2927. 09	50	34153. 66	$b\ ^2G_{4\frac{1}{2}} - x\ ^2G^0_{4\frac{1}{2}}$	(0.00)1.10
2926. 15	18	34164. 62	$a\ ^4F_{4\frac{1}{2}} - z\ ^4G^0_{4\frac{1}{2}}$	(0.28, 0.51, 0.73, **0.95**)0.82, 1.03, **1.25,** 1.43, 1.66, 1.88, 2.09
2925. 90	3	34167. 55	$b\ ^4F_{1\frac{1}{2}} - z\ ^2D^0_{2\frac{1}{2}}$	
2925. 22	3	34175. 48	$b\ ^4F_{3\frac{1}{2}} - z\ ^2D^0_{2\frac{1}{2}}$	(0.00)1.22†
2924. 86	2	34179. 69	$a\ ^2H_{5\frac{1}{2}} - y\ ^4H^0_{4\frac{1}{2}}$	
2923. 80	8	34192. 08	$a\ ^2D_{2\frac{1}{2}} - z\ ^2G^0_{3\frac{1}{2}}$	
2923. 67	40	34193. 60	$b\ ^2I_{5\frac{1}{2}} - y\ ^2I^0_{6\frac{1}{2}}$	(0.26)0.97†
2923. 46	30	34196. 06	$b\ ^2I_{5\frac{1}{2}} - y\ ^2I^0_{5\frac{1}{2}}$	(0.00*w*)1.45†
2922. 46	5	34207. 76	$b\ ^2G_{3\frac{1}{2}} - x\ ^2G^0_{4\frac{1}{2}}$	
2921. 81	40	34215. 37	$a\ ^4F_{3\frac{1}{2}} - z\ ^4G^0_{4\frac{1}{2}}$	(0.00*w*)0.85*A*†
2921. 23	50	34222. 17	$b\ ^2I_{6\frac{1}{2}} - y\ ^2I^0_{6\frac{1}{2}}$	(0.28)1.06†
2921. 10	5	34223. 69		(0.00)0.32
2920. 90	4	34226. 03		
2919. 93	2*w*	34237. 40	$c\ ^2F_{3\frac{1}{2}} - x\ ^2F^0_{3\frac{1}{2}}$	
2918. 93	1*w, l*	34249. 13	$z\ ^6P^0_{3\frac{1}{2}} - e\ ^6D_{2\frac{1}{2}}$	
2918. 29	3	34256. 64	$b\ ^4G_{4\frac{1}{2}} - x\ ^4D^0_{3\frac{1}{2}}$	
2917. 40	1*w, l*	34267. 09		
2916. 94	2*w, l*	34272. 49	$z\ ^6P^0_{3\frac{1}{2}} - e\ ^6D_{1\frac{1}{2}}$	
2916. 07	10	34282. 72	$a\ ^2P_{1\frac{1}{2}} - y\ ^2D^0_{1\frac{1}{2}}$	(0.40, **1.16**)0.21, **0.99,** 1.72†
2915. 46	30	34289. 89	$c\ ^2G_{4\frac{1}{2}} - x\ ^2F^0_{3\frac{1}{2}}$	(0.00)1.06†
2915. 28	15	34292. 01	$a\ ^2G_{3\frac{1}{2}} - y\ ^2H^0_{4\frac{1}{2}}$	(0.00)1.46
2915. 22	10	34292. 71	$b\ ^2H_{4\frac{1}{2}} - y\ ^2G^0_{3\frac{1}{2}}$	(0.00)1.33
2914. 38	2	34302. 60	$a\ ^2S_{0\frac{1}{2}} - x\ ^4P^0_{1\frac{1}{2}}$	(0.00)1.52
2913. 50	10	34312. 96		(0.00)0.72
2912. 53	1	34324. 38	$a\ ^4F_{4\frac{1}{2}} - z\ ^2G^0_{3\frac{1}{2}}$	
2911. 69	35	34334. 29	$b\ ^2F_{2\frac{1}{2}} - y\ ^2G^0_{3\frac{1}{2}}$	(0.00)0.98†
2910. 64	30	34346. 67	$b\ ^4G_{3\frac{1}{2}} - x\ ^4D^0_{3\frac{1}{2}}$ $b\ ^2F_{2\frac{1}{2}} - y\ ^2D^0_{2\frac{1}{2}}$	(0.00 w_1 *D*)1.06*A*
2909. 13	2*w, l*	34364. 50	$z\ ^6P^0_{1\frac{1}{2}} - e\ ^6D_{1\frac{1}{2}}$	
2908. 29	10	34374. 42	$a\ ^4F_{2\frac{1}{2}} - z\ ^2G^0_{3\frac{1}{2}}$	(0.78, **1.14**) 0.70, **1.08,** 1.38, 1.73, 2.02
2907. 00	4*w*	34389. 68	$z\ ^6P^0_{2\frac{1}{2}} - e\ ^6D_{2\frac{1}{2}}$	
2906. 76	2	34392. 52	$b\ ^4P_{2\frac{1}{2}} - z\ ^4G^0_{3\frac{1}{2}}$	
2906. 17	10	34399. 50	$b\ ^2H_{5\frac{1}{2}} - y\ ^2G^0_{5\frac{1}{2}}$	(0.00) 1.50†
2905. 57	3	34406. 60	$a\ ^2G_{4\frac{1}{2}} - x\ ^4G^0_{5\frac{1}{2}}$	
2903. 97	20	34425. 56	$a^4F_{2\frac{1}{2}} - z\ ^2G^0_{3\frac{1}{2}}$	(0.00 *D*) 0.58*A*
2903. 58	15	34430. 18		(0.00) 1.80
2902. 86	10	34438. 72	$a\ ^2S_{0\frac{1}{2}} - y\ ^2P^0_{0\frac{1}{2}}$	(0.12)1.88
2902. 60	7	34441. 81	$c\ ^2F_{3\frac{1}{2}} - w\ ^4F^0_{3\frac{1}{2}}$	(0.00)1.20
2901. 00	12	34460. 80	$a\ ^4F_{4\frac{1}{2}} - z\ ^2G^0_{4\frac{1}{2}}$	(0.76*B*)1.27*C*†
2900. 50	4	34466. 74	$a\ ^2F_{2\frac{1}{2}} - z\ ^2P^0_{1\frac{1}{2}}$	
2899. 48	35	34478. 86	$b\ ^4F_{2\frac{1}{2}} - y\ ^4G^0_{3\frac{1}{2}}$	(0.00)0.99†
2899. 15	25	34482. 79	$a\ ^2G_{3\frac{1}{2}} - y\ ^2F^0_{3\frac{1}{2}}$	(0.00)0.97†
2898. 53	50	34490. 16	$a\ ^4F_{4\frac{1}{2}} - z\ ^4G^0_{5\frac{1}{2}}$	(0.00 w_3*D*)1.02*A*
2897. 82	10	34498. 61	$b\ ^4F_{4\frac{1}{2}} - y\ ^4G^0_{4\frac{1}{2}}$	
2897. 73	20	34499. 68	$b\ ^4F_{1\frac{1}{2}} - y\ ^4G^0_{2\frac{1}{2}}$	(0.00)1.08
2897. 67	30	34500. 40	$b\ ^2F_{3\frac{1}{2}} - y\ ^2G^0_{3\frac{1}{2}}$	(0.00)1.10†

TABLE 1. *Wavelengths of* Cr II *in air*—Continued

Wavelength	Intensity	Wave No.	Term combination	Zeeman effect
2897. 24	10	34505. 52	$b\ ^2I_{8\frac{1}{2}} - x\ ^2H^{\circ}_{7\frac{1}{2}}$ $a\ ^2S_{0\frac{1}{2}} - x\ ^4P^{\circ}_{1\frac{1}{2}}$	(0.00*w*) 1.17, **1.91**†
2896. 74	35	34511. 47	$a\ ^4F_{3\frac{1}{2}} - z\ ^2G^{\circ}_{4\frac{1}{2}}$	(0.00w_3D) 0.82*A*
2896. 45	40	34514. 93	$b\ ^2I_{8\frac{1}{2}} - z\ ^2K^{\circ}_{8\frac{1}{2}}$ $b\ ^4F_{4\frac{1}{2}} - y\ ^4G^{\circ}_{5\frac{1}{2}}$	(0.00w_3D) 0.99, **1.26**
2896. 31	30	34516. 60	$b\ ^4F_{3\frac{1}{2}} - y\ ^4G^{\circ}_{4\frac{1}{2}}$	(0.00) 1.07†
2895. 66	5	34524. 35	$b\ ^4F_{2\frac{1}{2}} - y\ ^4F^{\circ}_{1\frac{1}{2}}$	(0.38) 1.76†
2895. 02	18	34531. 98	$c\ ^2F_{3\frac{1}{2}} - w\ ^4F^{\circ}_{3\frac{1}{2}}$ $b\ ^4F_{2\frac{1}{2}} - y\ ^4F^{\circ}_{2\frac{1}{2}}$	(0.00) 1.04†
2894. 81	18	34534. 48	$b\ ^4F_{1\frac{1}{2}} - y\ ^4F^{\circ}_{1\frac{1}{2}}$	(0.00) 0.47†
2894. 40	10	34539. 38	$b\ ^4F_{4\frac{1}{2}} - y\ ^4F^{\circ}_{3\frac{1}{2}}$	
2894. 24	25	34541. 28	$b\ ^2I_{8\frac{1}{2}} - z\ ^2K^{\circ}_{9\frac{1}{2}}$	(0.61) 1.01
2893. 50	4*w*, *l*	34550. 12	$z\ ^6P^{\circ}_{3\frac{1}{2}} - e\ ^6D_{3\frac{1}{2}}$ $b\ ^4F_{2\frac{1}{2}} - y\ ^4F^{\circ}_{2\frac{1}{2}}$	(0.00*w*) 1.70†
2892. 95	20	34556. 68	$b\ ^4F_{3\frac{1}{2}} - y\ ^4F^{\circ}_{3\frac{1}{2}}$	(0.16) 1.25†
2892. 74	18	34559. 20		(0.00) 1.28†
2891. 87	20	34569. 59	$a\ ^2S_{0\frac{1}{2}} - y\ ^2P^{\circ}_{1\frac{1}{2}}$	(0.33) **1.04**, 1.76
2891. 40	20	34575. 21	$a\ ^2H_{9\frac{1}{2}} - y\ ^4H^{\circ}_{9\frac{1}{2}}$	(0.00*w*) 1.40†
2891. 20	20	34577. 60	$a\ ^2G_{9\frac{1}{2}} - x\ ^4G^{\circ}_{9\frac{1}{2}}$	(0.00*w*) 1.36†
2891. 06	25	34579. 27	$a\ ^2G_{4\frac{1}{2}} - y\ ^2F^{\circ}_{3\frac{1}{2}}$	(0.00w_1) 1.03w_1
2889. 82	25	34594. 11	$b\ ^4F_{4\frac{1}{2}} - y\ ^4F^{\circ}_{4\frac{1}{2}}$	(0.00) 1.32
2889. 50	35	34597. 94	$a\ ^2P_{1\frac{1}{2}} - y\ ^2D^{\circ}_{2\frac{1}{2}}$	(0.00) 1.10†
2889. 19	35	34601. 66	$a\ ^4D_{2\frac{1}{2}} - z\ ^4D^{\circ}_{2\frac{1}{2}}$	(0.00w_1) 1.49
2888. 73	40	34607. 16	$a\ ^2G_{4\frac{1}{2}} - x\ ^4G^{\circ}_{5\frac{1}{2}}$	(0.14*C*) 1.34*B*
2888. 33	2*w*, *l*	34611. 98	$z\ ^6D^{\circ}_{3\frac{1}{2}} - e\ ^4D_{1\frac{1}{2}}$	
2887. 77	20	34618. 67	$c\ ^2D_{1\frac{1}{2}} - w\ ^2D^{\circ}_{1\frac{1}{2}}$	(0.00) 0.79
2886. 38	7	34635. 34	$c\ ^2G_{3\frac{1}{2}} - w\ ^4F^{\circ}_{3\frac{1}{2}}$	(0.00) 0.96
2885. 29	10	34648. 42		(0.00) 1.12
2884. 98	2	34652. 15	$b\ ^4F_{4\frac{1}{2}} - z\ ^2I^{\circ}_{5\frac{1}{2}}$	
2884. 61	1	34656. 59	$a\ ^2F_{3\frac{1}{2}} - z\ ^2D^{\circ}_{2\frac{1}{2}}$	
2881. 91	45	34689. 06	$a\ ^2P_{0\frac{1}{2}} - x\ ^4F^{\circ}_{1\frac{1}{2}}$	(0.00) 0.64†
2881. 86	55	34689. 65	$c\ ^2D_{2\frac{1}{2}} - w\ ^2D^{\circ}_{2\frac{1}{2}}$	(0.00) 1.18†
2880. 86	75	34701. 70	$a\ ^4D_{2\frac{1}{2}} - z\ ^4D^{\circ}_{1\frac{1}{2}}$	(**0.11**, 0.25) 1.26, 1.46, **1.64**
2880. 08	2*w*, *l*	34711. 10		
2879. 68	3*w*, *l*	34715. 92	$z\ ^6D^{\circ}_{4\frac{1}{2}} - e\ ^4D_{3\frac{1}{2}}$	
2879. 17	10	34722. 07	$b\ ^4P_{1\frac{1}{2}} - z\ ^2S^{\circ}_{0\frac{1}{2}}$	(0.00*d*) 1.64†
2878. 45	50	34730. 75	$a\ ^6D_{4\frac{1}{2}} - z\ ^6F^{\circ}_{5\frac{1}{2}}$	(**0.07**, 0.20, 0.34, 0.48) 1.52, 1.73, 1.93, **2.12**
2877. 97	60	34736. 55	$a\ ^6D_{3\frac{1}{2}} - z\ ^6F^{\circ}_{4\frac{1}{2}}$	(**0.13**, 0.41, 0.69) 1.17, 1.45, 1.73, 2.00, **2.27**
2876. 66	20	34752. 36	$c\ ^2G_{3\frac{1}{2}} - x\ ^2F^{\circ}_{3\frac{1}{2}}$	(0.00) 1.05†
2876. 30	40	34756. 71	$b\ ^2I_{8\frac{1}{2}} - z\ ^2K^{\circ}_{9\frac{1}{2}}$	(0.00) 1.01
2876. 24	60	34757. 44	$a\ ^6D_{2\frac{1}{2}} - z\ ^6F^{\circ}_{1\frac{1}{2}}$	(**0.30**, 0.88) 1.37, 1.95, **2.56**
2875. 97	100	34760. 70	$a\ ^4D_{3\frac{1}{2}} - z\ ^4D^{\circ}_{3\frac{1}{2}}$	(0.00) 1.43
2875. 03	30	34772. 07	$c\ ^2G_{3\frac{1}{2}} - x\ ^2H^{\circ}_{4\frac{1}{2}}$	(0.00w_1D) 0.68*A*
2874. 51	10	34778. 36		(0.00) 1.15†
2874. 07	8	34783. 68	$b\ ^2H_{4\frac{1}{2}} - y\ ^2H^{\circ}_{4\frac{1}{2}}$	
2873. 81	50	34786. 83	$a\ ^4D_{1\frac{1}{2}} - z\ ^4D^{\circ}_{0\frac{1}{2}}$	(0.62) 0.62, **1.78**
2873. 46	65	34791. 06	$b\ ^2D_{1\frac{1}{2}} - x\ ^2P^{\circ}_{0\frac{1}{2}}$ $a\ ^4D_{1\frac{1}{2}} - z\ ^6F^{\circ}_{2\frac{1}{2}}$	(1.26) 0.61, **3.14**
2871. 45	20	34815. 41	$b\ ^2D_{2\frac{1}{2}} - x\ ^2P^{\circ}_{1\frac{1}{2}}$	(0.00w_1) 1.10
2870. 43	100	34827. 79	$a\ ^4D_{2\frac{1}{2}} - z\ ^4D^{\circ}_{2\frac{1}{2}}$	(0.00) 1.38
2869. 72	3*w*, *l*	34836. 41	$z\ ^4D^{\circ}_{3\frac{1}{2}} - f\ ^4D_{3\frac{1}{2}}$	
2869. 61	3*w*, *l*	34837. 74	$z\ ^4D^{\circ}_{1\frac{1}{2}} - f\ ^4D_{1\frac{1}{2}}$	
2868. 63	4*w*, *l*	34849. 64	$z\ ^4D^{\circ}_{2\frac{1}{2}} - f\ ^4D_{2\frac{1}{2}}$ $b\ ^4P_{1\frac{1}{2}} - z\ ^4G^{\circ}_{2\frac{1}{2}}$	
2868. 47	2*w*, *l*	34851. 59	$z\ ^4D^{\circ}_{0\frac{1}{2}} - f\ ^4D_{0\frac{1}{2}}$	
2867. 94	4*w*	34858. 03	$b\ ^2F_{2\frac{1}{2}} - x\ ^4G^{\circ}_{3\frac{1}{2}}$ $b\ ^4G_{4\frac{1}{2}} - z\ ^2H^{\circ}_{5\frac{1}{2}}$	
2867. 65	100	34861. 55	$a\ ^6D_{0\frac{1}{2}} - z\ ^6F^{\circ}_{1\frac{1}{2}}$	(2.00) 1.28
2867. 09	65	34868. 36	$a\ ^4D_{1\frac{1}{2}} - z\ ^4D^{\circ}_{1\frac{1}{2}}$	(0.00) 1.16
2866. 72	100	34872. 86	$a\ ^6D_{1\frac{1}{2}} - z\ ^6F^{\circ}_{1\frac{1}{2}}$	(0.40, **1.18**) 0.70, **1.53**, 2.29
2865. 87	50	34883. 19	$c\ ^2G_{4\frac{1}{2}} - x\ ^2H^{\circ}_{5\frac{1}{2}}$	(0.00) 0.87†
2865. 65	20	34885. 88	$d\ ^2F_{2\frac{1}{2}} - v\ ^2G^{\circ}_{3\frac{1}{2}}$	(0.00) 0.96†

TABLE 1. *Wavelengths of* Cr II *in air*—Continued

Wavelength	Intensity	Wave No.	Term combination	Zeeman effect
2865. 34	30	34889. 65	$a\ ^4D_{3\frac{1}{2}} - z\ ^4D^0_{3\frac{1}{2}}$	(0.00)**0.00**†
2865. 10	150	34892. 58	$a\ ^6D_{2\frac{1}{2}} - z\ ^6F^0_{3\frac{1}{2}}$	(0.16, 0.50, **0.88**)1.14, **1.50,** 1.84, 2.18
2862. 57	125	34923. 41	$a\ ^6D_{3\frac{1}{2}} - z\ ^6F^0_{3\frac{1}{2}}$	[2.08 (0.27, 0.49, **0.69**)0.92, 1.11, 1.30, **1.50,** 1.70, 1.89,
2860. 92	85	34943. 55	$a\ ^6D_{3\frac{1}{2}} - z\ ^6F^0_{4\frac{1}{2}}$	(1.13)**0.06,** 2.18
2858. 91	75	34968. 12	$a\ ^6D_{4\frac{1}{2}} - z\ ^6F^0_{4\frac{1}{2}}$	(0.57*B*)1.49
2858. 64	30	34971. 42	$a\ ^4D_{3\frac{1}{2}} - z\ ^4D^0_{3\frac{1}{2}}$	(0.60)0.60, **1.80**†
2857. 99	20	34979. 38	$a\ ^2P_{1\frac{1}{2}} - y\ ^2D^0_{2\frac{1}{2}}$	(0.00)0.60†
2857. 40	40	34986. 60	$a\ ^4D_{2\frac{1}{2}} - z\ ^4D^0_{2\frac{1}{2}}$	(0.00)1.52†
2856. 77	40	34994. 31	$a\ ^4D_{1\frac{1}{2}} - z\ ^4D^0_{2\frac{1}{2}}$	(0.00)1.50*B*†
2856. 42	4	34998. 60	$a\ ^4H_{4\frac{1}{2}} - z\ ^4I^0_{5\frac{1}{2}}$	
2856. 32	20	34999. 82	$a\ ^4H_{3\frac{1}{2}} - z\ ^4G^0_{3\frac{1}{2}}$	(0.00w_1)0.94
2855. 67	100	35007. 79	$a\ ^6D_{1\frac{1}{2}} - z\ ^6F^0_{2\frac{1}{2}}$	(**0.30,** 0.84)**0.53,** 1.07, 1.58, 2.15
2855. 43	8	35010. 73	$c\ ^4D_{0\frac{1}{2}} - w\ ^4D^0_{1\frac{1}{2}}$	
2855. 05	35	35015. 39	$b\ ^4F_{2\frac{1}{2}} - x\ ^4D^0_{1\frac{1}{2}}$ $b\ ^4F_{1\frac{1}{2}} - x\ ^4D^0_{1\frac{1}{2}}$ $b\ ^2F_{2\frac{1}{2}} - y\ ^2F^0_{3\frac{1}{2}}$	(0.00)0.86†
2854. 65	3	35020. 30		
2854. 58	5	35021. 16	$b\ ^4F_{4\frac{1}{2}} - x\ ^4D^0_{3\frac{1}{2}}$	(0.00)1.29†
2854. 23	3	35025. 45	$b\ ^4F_{1\frac{1}{2}} - x\ ^4D^0_{1\frac{1}{2}}$	
2854. 14	20*w, d*?	35026. 56		(0.00)0.94†
2853. 76	8	35031. 22	$b\ ^4F_{3\frac{1}{2}} - x\ ^4D^0_{2\frac{1}{2}}$	
2853. 26	30	35037. 36	$b\ ^2D_{2\frac{1}{2}} - x\ ^2D^0_{2\frac{1}{2}}$	(0.00)1.22
2853. 18	30	35038. 34	$a\ ^4H_{4\frac{1}{2}} - z\ ^4G^0_{5\frac{1}{2}}$	(0.00)1.00
2852. 75	7	35043. 62	$b\ ^4G_{5\frac{1}{2}} - z\ ^2H^0_{6\frac{1}{2}}$	
2852. 67	20	35044. 61	$c\ ^4D_{1\frac{1}{2}} - w\ ^4D^0_{0\frac{1}{2}}$	
2852. 27	25	35049. 52	$c\ ^4D_{1\frac{1}{2}} - w\ ^4D^0_{1\frac{1}{2}}$	(0.00)1.16†
2851. 35	60	35060. 83	$a\ ^4H_{3\frac{1}{2}} - z\ ^4I^0_{4\frac{1}{2}}$	(0.00w_3D)1.03*B*
2850. 72	7	35068. 58	$b\ ^2H_{4\frac{1}{2}} - x\ ^4G^0_{4\frac{1}{2}}$	
2850. 29	3	35073. 87	$c\ ^4D_{1\frac{1}{2}} - w\ ^4D^0_{2\frac{1}{2}}$	
2849. 83	100	35079. 53	$a\ ^6D_{2\frac{1}{2}} - z\ ^6F^0_{3\frac{1}{2}}$	(**0.12,** 0.37, 0.67)**0.68,** 1.00, 1.27, 1.54, 1.81, 2.07
2849. 33	18	35085. 68	$a\ ^4H_{3\frac{1}{2}} - z\ ^4G^0_{4\frac{1}{2}}$	(0.00)1.14
2848. 40	20*d*?	35097. 14	$c\ ^4D_{2\frac{1}{2}} - w\ ^4D^0_{1\frac{1}{2}}$	
2848. 15	4*w*	35098. 99	$a\ ^4H_{3\frac{1}{2}} - z\ ^4G^0_{3\frac{1}{2}}$	
2846. 70	15	35118. 10	$a\ ^2D_{1\frac{1}{2}} - z\ ^2D^0_{1\frac{1}{2}}$	(0.18*B*)0.90*C*
2846. 44	30	35121. 31	$c\ ^4D_{2\frac{1}{2}} - w\ ^4D^0_{2\frac{1}{2}}$ $a\ ^4H_{3\frac{1}{2}} - z\ ^4I^0_{3\frac{1}{2}}$	(0.00)1.37
2846. 32	25	35122. 78	$b\ ^2D_{1\frac{1}{2}} - x\ ^2D^0_{1\frac{1}{2}}$	(0.05*B*)0.86*C*
2844. 83	3	35141. 18	$b\ ^4G_{4\frac{1}{2}} - z\ ^2F^0_{3\frac{1}{2}}$	
2843. 24	100	35160. 83	$a\ ^6D_{3\frac{1}{2}} - z\ ^6F^0_{4\frac{1}{2}}$	[1.95 (0.00w_3D)**0.88,** 1.05, 1.19, 1.35, 1.51, 1.67, 1.82,
2842. 78	20	35166. 52	$c\ ^4D_{3\frac{1}{2}} - w\ ^4D^0_{3\frac{1}{2}}$	(0.00)1.54†
2842. 43	5	35170. 85	$c\ ^4D_{2\frac{1}{2}} - w\ ^4D^0_{3\frac{1}{2}}$	(0.00)1.56†
2842. 32	5	35172. 21	$b\ ^2H_{5\frac{1}{2}} - x\ ^4G^0_{4\frac{1}{2}}$	
2841. 15	2*w, l*	35186. 69		
2840. 43	12	35195. 61	$a\ ^2D_{1\frac{1}{2}} - y\ ^4P^0_{2\frac{1}{2}}$	
2840. 01	85	35200. 82	$a\ ^4H_{4\frac{1}{2}} - z\ ^4I^0_{5\frac{1}{2}}$	(0.00)0.96
2839. 23	12	35210. 49		(0.00)1.06†
2838. 78	65	35216. 07	$c\ ^4D_{3\frac{1}{2}} - w\ ^4D^0_{3\frac{1}{2}}$	(0.00)1.44
2837. 96	4	35226. 24	$a\ ^4H_{6\frac{1}{2}} - z\ ^4I^0_{5\frac{1}{2}}$	
2837. 88	20	35227. 24	$a\ ^4H_{3\frac{1}{2}} - z\ ^4G^0_{4\frac{1}{2}}$	(**0.24,** 0.68, 1.14, 1.61)0.90, 1.35, 1.83, 2.26, **2.67**
2836. 47	30	35244. 75	$b\ ^2F_{3\frac{1}{2}} - y\ ^2F^0_{3\frac{1}{2}}$	(0.00)1.16
2835. 63	200	35255. 19	$a\ ^6D_{4\frac{1}{2}} - z\ ^6F^0_{4\frac{1}{2}}$	(0.00w_3D) 1.03*A*
2834. 28	35	35271. 98	$d\ ^2F_{3\frac{1}{2}} - z\ ^2G^0_{4\frac{1}{2}}$	(0.00)1.13†
2834. 24	60	35272. 48	$a\ ^2H_{4\frac{1}{2}} - y\ ^2G^0_{5\frac{1}{2}}$	(0.00)0.94†
2833. 37	8	35283. 31	$b\ ^2F_{2\frac{1}{2}} - y\ ^2F^0_{3\frac{1}{2}}$	(0.00*w*)1.64*B*†
2832. 45	60	35294. 76	$a\ ^2H_{5\frac{1}{2}} - y\ ^2G^0_{4\frac{1}{2}}$	(0.00)1.03
2830. 60	60	35317. 83	$a\ ^4H_{4\frac{1}{2}} - z\ ^4G^0_{5\frac{1}{2}}$	(0.00w_1D)1.06*A*
2830. 46	100	35319. 58	$a\ ^4H_{5\frac{1}{2}} - z\ ^4I^0_{6\frac{1}{2}}$	(0.00w_1D)1.06*A*
2830. 24	10	35322. 32	$b\ ^4G_{2\frac{1}{2}} - y\ ^4H^0_{3\frac{1}{2}}$	
2830. 08	8	35324. 32	$a\ ^4H_{4\frac{1}{2}} - z\ ^2G^0_{3\frac{1}{2}}$	(0.00)0.84†
2828. 79	15	35340. 43	$a\ ^2D_{1\frac{1}{2}} - z\ ^2P^0_{0\frac{1}{2}}$	(0.00)0.76
2827. 95	15	35350. 93		(0.00)1.24†
2826. 42	7	35370. 06		(0.41)1.52†
2826. 15	10	35373. 44	$b\ ^4G_{4\frac{1}{2}} - y\ ^4H^0_{5\frac{1}{2}}$	(0.72)1.09†

TABLE 1. *Wavelengths of* Cr II *in air*—Continued

Wavelength	Intensity	Wave No.	Term combination	Zeeman effect
2825.95	7	35375.94	$a\ ^2D_{2\frac{1}{2}} - y\ ^4P^0_{2\frac{1}{2}}$	
2825.73	4	35378.70		(0.73)1.33†
2825.50	20	35381.58	$a\ ^4H_{3\frac{1}{2}} - z\ ^2G^0_{3\frac{1}{2}}$	(0.00)1.12
2824.54	12	35393.60		(0.17)0.44†
2822.38	100	35420.69	$a\ ^4H_{6\frac{1}{2}} - z\ ^4I^0_{7\frac{1}{2}}$	(0.00w_2D)1.06A
2822.01	65	35425.33	$b\ ^4G_{2\frac{1}{2}} - y\ ^4H^0_{3\frac{1}{2}}$	(0.00w_2D)0.87B
2819.16	2	35461.11	$a\ ^4H_{4\frac{1}{2}} - z\ ^2G^0_{4\frac{1}{2}}$	
2818.66	5	35467.43	$a\ ^2I_{5\frac{1}{2}} - z\ ^4I^0_{5\frac{1}{2}}$	
2818.36	75	35471.21	$b\ ^4G_{2\frac{1}{2}} - y\ ^4H^0_{3\frac{1}{2}}$	(0.00)0.96
2818.08	3	35474.73	$a\ ^2I_{5\frac{1}{2}} - z\ ^4I^0_{5\frac{1}{2}}$	
2817.96	12	35476.24	$b\ ^4G_{3\frac{1}{2}} - y\ ^4H^0_{3\frac{1}{2}}$	(0.63)0.98†
2817.57	8	35481.15	$a\ ^2D_{1\frac{1}{2}} - z\ ^2D^0_{2\frac{1}{2}}$ $d\ ^2D_{1\frac{1}{2}} - w\ ^2P^0_{1\frac{1}{2}}$	
2817.00	15w, l	35488.33	$z\ ^6F^0_{5\frac{1}{2}} - e\ ^6D^0_{4\frac{1}{2}}$	
2816.83	30	35490.47	$a\ ^4H_{4\frac{1}{2}} - z\ ^4G^0_{4\frac{1}{2}}$ $b\ ^4P_{2\frac{1}{2}} - y\ ^4P^0_{1\frac{1}{2}}$	(0.00d?)1.51
2814.22	5	35523.38	$a\ ^4H_{3\frac{1}{2}} - z\ ^2G^0_{4\frac{1}{2}}$	
2813.53	5	35532.10	$a\ ^4F_{2\frac{1}{2}} - z\ ^2D^0_{1\frac{1}{2}}$	(0.00)1.14†
2812.31	2	35547.51	$d\ ^2D_{1\frac{1}{2}} - w\ ^2P^0_{1\frac{1}{2}}$	
2812.00	85	35551.43	$b\ ^2G_{4\frac{1}{2}} - x\ ^2F^0_{3\frac{1}{2}}$ $b\ ^4G_{4\frac{1}{2}} - y\ ^4H^0_{5\frac{1}{2}}$	(0.00D)1.02A
2811.45	10	35558.38	$a\ ^4F_{3\frac{1}{2}} - y\ ^4P^0_{2\frac{1}{2}}$ $a\ ^2I_{6\frac{1}{2}} - z\ ^4G^0_{5\frac{1}{2}}$	
2811.05	15	35563.45	$c\ ^2D_{1\frac{1}{2}} - v\ ^2F^0_{2\frac{1}{2}}$	(0.00d?)0.92
2810.89	6	35565.47	$d\ ^2D_{2\frac{1}{2}} - w\ ^2P^0_{1\frac{1}{2}}$ $a\ ^2I_{5\frac{1}{2}} - z\ ^4G^0_{5\frac{1}{2}}$	(0.00)1.15
2810.78	5	35566.86	$a\ ^4F_{1\frac{1}{2}} - z\ ^2D^0_{1\frac{1}{2}}$	
2810.03	20w, l	35576.35	$z\ ^6F^0_{4\frac{1}{2}} - e\ ^6D^0_{3\frac{1}{2}}$	(0.00)1.12†
2809.62	2	35581.54	$b\ ^2I_{5\frac{1}{2}} - w\ ^2G^0_{4\frac{1}{2}}$	
2809.56	5	35582.30	$a\ ^2H_{5\frac{1}{2}} - y\ ^2H^0_{4\frac{1}{2}}$	
2809.27	6	35585.98	$a\ ^2H_{5\frac{1}{2}} - y\ ^2H^0_{5\frac{1}{2}}$	(0.57)1.18†
2808.02	20	35601.81		(0.00)1.25†
2807.63	5	35606.76		
2806.34	3w	35623.13		
2803.96	10w, l	35653.37	$z\ ^6F^0_{5\frac{1}{2}} - e\ ^6D^0_{4\frac{1}{2}}$	
2803.35	20	35661.12	$a\ ^2D_{2\frac{1}{2}} - z\ ^2D^0_{2\frac{1}{2}}$	(0.27B)1.23C
2803.22	8	35662.77	$a\ ^2I_{6\frac{1}{2}} - z\ ^4I^0_{7\frac{1}{2}}$	
2802.40	2w, l	35673.21		
2800.77	85	35693.97	$b\ ^4G_{3\frac{1}{2}} - y\ ^4H^0_{4\frac{1}{2}}$	(0.00w_2D)1.07A
2800.16	20	35701.75	$c\ ^2D_{2\frac{1}{2}} - v\ ^2F^0_{3\frac{1}{2}}$	(0.00)1.07†
2798.77	30	35719.47	$a\ ^2D_{2\frac{1}{2}} - z\ ^2P^0_{1\frac{1}{2}}$	(0.00w_1)1.08
2798.65	35	35721.00		(0.00)1.33†
2798.48	4w, l	35723.07	$z\ ^6F^0_{3\frac{1}{2}} - e\ ^6D^0_{3\frac{1}{2}}$	
2795.32	2	35763.56	$a\ ^2H_{4\frac{1}{2}} - y\ ^2H^0_{4\frac{1}{2}}$	
2794.39	5w, l	35775.47	$z\ ^6F^0_{4\frac{1}{2}} - e\ ^6D^0_{4\frac{1}{2}}$	
2793.63	10	35785.20	$b\ ^4P_{2\frac{1}{2}} - z\ ^2D^0_{2\frac{1}{2}}$	(**0.29**,1.03) 1.16, 2.00, **2.76**†
2793.51	3w, l	35786.73	$z\ ^6F^0_{5\frac{1}{2}} - e\ ^6D^0_{5\frac{1}{2}}$	
2792.79	4	35795.95	$a\ ^2H_{4\frac{1}{2}} - x\ ^4G^0_{5\frac{1}{2}}$	(0.00)0.89†
2792.49	4	35799.80	$c\ ^4D_{2\frac{1}{2}} - x\ ^2F^0_{3\frac{1}{2}}$	
2792.16	80	35804.04	$b\ ^4G_{3\frac{1}{2}} - x\ ^4F^0_{4\frac{1}{2}}$	(0.00w_2)1.04A
2791.70	7	35809.93	$b\ ^2G_{3\frac{1}{2}} - w\ ^4F^0_{3\frac{1}{2}}$	
2791.45	5	35813.14	$a\ ^2D_{1\frac{1}{2}} - y\ ^4G^0_{2\frac{1}{2}}$	(0.00)1.24
2791.37	3w	35814.16	$e\ ^6F^0_{3\frac{1}{2}} - e\ ^6D^0_{3\frac{1}{2}}$	
2790.94	5	35819.68	$d\ ^2F_{2\frac{1}{2}} - v\ ^2D^0_{2\frac{1}{2}}$	
2790.64	1	35823.53	$d\ ^2F_{2\frac{1}{2}} - v\ ^2D^0_{1\frac{1}{2}}$	
2789.39	40	35839.58	$d\ ^2F_{3\frac{1}{2}} - v\ ^2D^0_{2\frac{1}{2}}$ $c\ ^2F_{3\frac{1}{2}} - w\ ^2G^0_{3\frac{1}{2}}$	(0.50B)1.03C
2789.08	8	35843.57	$a\ ^4F_{3\frac{1}{2}} - z\ ^2D^0_{2\frac{1}{2}}$	(0.00)1.23
2788.74	5	35847.94	$a\ ^2D_{1\frac{1}{2}} - y\ ^4F^0_{1\frac{1}{2}}$	
2787.90	25	35858.74	$b\ ^2G_{4\frac{1}{2}} - y\ ^2I^0_{5\frac{1}{2}}$	(0.22)0.00W†
2787.61	55	35862.47	$b\ ^4P_{2\frac{1}{2}} - y\ ^4P^0_{2\frac{1}{2}}$	(0.21B)1.57C

TABLE 1. *Wavelengths of* Cr II *in air*—Continued

Wavelength	Intensity	Wave No.	Term combination	Zeeman effect
2787. 30	5	35866. 46	$a\ ^2H_{3\frac{1}{2}} - x\ ^4G^0_{4\frac{1}{2}}$	
2787. 13	2*w*	35868. 64	$z\ ^6F^0_{5\frac{1}{2}} - e\ ^6D_{3\frac{1}{2}}$	
2786. 46	10	35877. 27	$c\ ^4D_{2\frac{1}{2}} - w\ ^4F^0_{1\frac{1}{2}}$	(0.20)0.20, **0.61**
2786. 30	2	35879. 33	$b\ ^4G_{4\frac{1}{2}} - x\ ^4F^0_{3\frac{1}{2}}$	
2785. 69	65	35887. 18	$b\ ^4G_{4\frac{1}{2}} - x\ ^4F^0_{3\frac{1}{2}}$	(0.00)1.17
2785. 32	2	35891. 95	$c\ ^2G_{4\frac{1}{2}} - w\ ^2G^0_{3\frac{1}{2}}$	
2785. 10	10	35894. 79	$a\ ^4F_{2\frac{1}{2}} - z\ ^2D^0_{2\frac{1}{2}}$	(0.50*B*)1.09*C*†
2784. 30	4*w*	35905. 10		(0.00)0.45
2783. 84	20	35911. 03	$c\ ^4D_{1\frac{1}{2}} - w\ ^4F^0_{1\frac{1}{2}}$	(0.50, **1.20**)0.00, **0.78**, 1.60†
2782. 59	25	35927. 16	$b\ ^2G_{3\frac{1}{2}} - x\ ^2F^0_{3\frac{1}{2}}$	(0.00)0.86
2782. 44	3	35929. 10	$a\ ^4F_{1\frac{1}{2}} - z\ ^2D^0_{2\frac{1}{2}}$	
2782. 36	40	35930. 13	$b\ ^4G_{2\frac{1}{2}} - x\ ^4F^0_{1\frac{1}{2}}$	(0.00)0.57
2782. 13	4	35933. 10	$c\ ^2F_{3\frac{1}{2}} - w\ ^2G^0_{4\frac{1}{2}}$	
2781. 55	4*w*, *l*	35940. 60	$z\ ^4D^0_{3\frac{1}{2}} - e\ ^4F_{3\frac{1}{2}}$	
2781. 07	25	35946. 80	$b\ ^2G_{3\frac{1}{2}} - x\ ^2H^0_{4\frac{1}{2}}$	(0.00)0.94†
2780. 89	25	35949. 12	$b\ ^4P_{1\frac{1}{2}} - y\ ^4P^0_{2\frac{1}{2}}$	(0.43)**1.34**, 2.22†
2780. 30	85	35956. 75	$c\ ^4D_{1\frac{1}{2}} - w\ ^4F^0_{2\frac{1}{2}}$ $b\ ^4G_{3\frac{1}{2}} - x\ ^4F^0_{3\frac{1}{2}}$	(0.00)0.94†
2778. 94	10	35974. 35	$c\ ^2F_{2\frac{1}{2}} - w\ ^2G^0_{3\frac{1}{2}}$	(0.00)0.95
2778. 51	5	35979. 92	$a\ ^2F_{2\frac{1}{2}} - z\ ^2F^0_{2\frac{1}{2}}$	
2778. 27	4	35983. 02	$a\ ^2D_{2\frac{1}{2}} - y\ ^4G^0_{3\frac{1}{2}}$	
2778. 06	70	35985. 74	$c\ ^2G_{4\frac{1}{2}} - w\ ^2G^0_{4\frac{1}{2}}$	(0.00)1.11
2776. 65	20	36004. 01	$c\ ^4D_{2\frac{1}{2}} - w\ ^4F^0_{3\frac{1}{2}}$	(0.85)1.19†
2776. 00	3*w*, *l*	36012. 45	$z\ ^4D^0_{1\frac{1}{2}} - e\ ^4F_{1\frac{1}{2}}$	
2774. 44	50	36032. 70	$c\ ^2G_{3\frac{1}{2}} - w\ ^2G^0_{3\frac{1}{2}}$	(0.34*B*)0.96*C*
2773. 30	30	36047. 50	$b\ ^4P_{1\frac{1}{2}} - y\ ^4P^0_{1\frac{1}{2}}$	(0.07)1.71
2772. 33	8	36060. 12	$b\ ^4G_{2\frac{1}{2}} - x\ ^4F^0_{2\frac{1}{2}}$	(1.00) . . .?†
2771. 89	20*w*, *l*	36065. 84	$z\ ^4D^0_{3\frac{1}{2}} - e\ ^4F_{4\frac{1}{2}}$	(0.00*D*)1.15*C*
2771. 27	12	36073. 90	$c\ ^4D_{1\frac{1}{2}} - x\ ^2F^0_{2\frac{1}{2}}$	0.00 *w*)0.56*A*†
2769. 92	10*w*, *l*	36091. 49	$z\ ^4D^0_{2\frac{1}{2}} - e\ ^4F_{2\frac{1}{2}}$	(0.00 *w*)0.96*A*†
2769. 70	3*w*, *l*	36094. 36	$z\ ^4D^0_{0\frac{1}{2}} - e\ ^4F_{1\frac{1}{2}}$	
2769. 29	8*w*, *l*	36099. 70	$z\ ^4D^0_{3\frac{1}{2}} - e\ ^4F_{3\frac{1}{2}}$	(0.00)1.18†
2768. 59	50	36108. 82	$c\ ^4D_{2\frac{1}{2}} - w\ ^4F^0_{3\frac{1}{2}}$	(0.00 w_3D)0.93*A*
2768. 16	10	36114. 43	$a\ ^4F_{4\frac{1}{2}} - y\ ^4G^0_{3\frac{1}{2}}$	
2767. 92	3	36117. 56		
2767. 62	20	36121. 48	$c\ ^4D_{1\frac{1}{2}} - x\ ^4P^0_{2\frac{1}{2}}$	(0.00*D*)2.01*B*†
2767. 26	10	36126. 18	$c\ ^2G_{3\frac{1}{2}} - w\ ^2G^0_{4\frac{1}{2}}$	(0.00)1.49† [1.79, 1.95
2766. 55	150	36135. 45	$a\ ^4D_{3\frac{1}{2}} - z\ ^6P^0_{3\frac{1}{2}}$	(**0.08**, 0.24, 0.38, 0.55)**1.00**, 1.15, 1.31, 1.48, 1.63,
2765. 86	20	36144. 46	$b\ ^2G_{4\frac{1}{2}} - x\ ^2H^0_{5\frac{1}{2}}$	(0.00)0.87†
2765. 62	12	36147. 60	$b\ ^4P_{2\frac{1}{2}} - z\ ^2D^0_{2\frac{1}{2}}$	(0.74) . . .?†
2765. 46	20	36149. 69	$a\ ^4F_{4\frac{1}{2}} - y\ ^4G^0_{4\frac{1}{2}}$	(0.00)1.11†
2765. 13	4	36154. 01	$c\ ^4D_{2\frac{1}{2}} - w\ ^4F_{3\frac{1}{2}}$	
2764. 96	10	36156. 23	$a\ ^2F_{2\frac{1}{2}} - z\ ^2F^0_{3\frac{1}{2}}$	
2764. 28	15	36165. 12	$a\ ^4F_{3\frac{1}{2}} - y\ ^4G^0_{3\frac{1}{2}}$	(0.60*B*)1.11*C*†
2763. 97	12	36169. 18	$c\ ^4D_{2\frac{1}{2}} - x\ ^4P^0_{2\frac{1}{2}}$	(0.44*B*)1.40*C*†
2763. 59	20	36174. 15	$a\ ^4F_{4\frac{1}{2}} - y\ ^4F^0_{3\frac{1}{2}}$	(0.00)1.67†
2762. 78	10	36184. 76	$a\ ^4F_{3\frac{1}{2}} - y\ ^4G^0_{3\frac{1}{2}}$	
2762. 58	140	36187. 38	$a\ ^6D_{3\frac{1}{2}} - z\ ^6P^0_{3\frac{1}{2}}$	(**0.17**, 0.46, 0.75)**0.82**, 1.15, 1.45, 1.74, 2.04, 2.34
2761. 16	5	36205. 99	$b\ ^4P_{2\frac{1}{2}} - z\ ^2P^0_{1\frac{1}{2}}$	
2760. 83	15	36210. 31		(0.00)0.86†
2760. 53	25	36214. 25	$c\ ^4D_{3\frac{1}{2}} - x\ ^4P^0_{2\frac{1}{2}}$	(0.00)1.22†
2760. 36	20	36216. 47	$a\ ^4F_{3\frac{1}{2}} - y\ ^4G^0_{3\frac{1}{2}}$	(0.00)1.11†
2760. 20	12	36218. 58	$a\ ^4F_{3\frac{1}{2}} - y\ ^4F^0_{3\frac{1}{2}}$	
2760. 04	20	36220. 67	$b\ ^4G_{3\frac{1}{2}} - y\ ^2D^0_{2\frac{1}{2}}$	(0.00)0.67
2759. 73	30	36224. 74	$a\ ^4F_{3\frac{1}{2}} - y\ ^4F^0_{2\frac{1}{2}}$	(0.22)1.05
2759. 40	50	36229. 08	$a\ ^4F_{4\frac{1}{2}} - y\ ^4F^0_{4\frac{1}{2}}$	(0.00)1.32
2759. 23	7	36231. 31		
2758. 99	40	36234. 46	$c\ ^4D_{3\frac{1}{2}} - w\ ^4F^0_{4\frac{1}{2}}$	(0.00*D*)1.01*A*
2758. 61	15	36239. 45	$a\ ^2F_{3\frac{1}{2}} - y\ ^4H^0_{4\frac{1}{2}}$	(0.00)1.10†
2757. 72	80	36251. 14	$a\ ^6D_{2\frac{1}{2}} - z\ ^6P^0_{1\frac{1}{2}}$	(**0.36**, 1.09)**0.60**, 1.33, 2.04, 2.76
2756. 96	20	36261. 14	$a\ ^4F_{1\frac{1}{2}} - y\ ^4G^0_{2\frac{1}{2}}$	(0.00)0.79†

TABLE 1. *Wavelengths of* Cr II *in air*—Continued

Wavelength	Intensity	Wave No.	Term combination	Zeeman effect
2756.89	15	36262.06	$a\ ^4F_{2\frac{1}{2}} - y\ ^4F^\circ_{1\frac{1}{2}}$	
2756.30	40	36269.82	$a\ ^4F_{2\frac{1}{2}} - y\ ^4F^\circ_{2\frac{1}{2}}$	(0.00)1.01
2755.81	10	36276.27	$a\ ^4F_{2\frac{1}{2}} - y\ ^4F^\circ_{3\frac{1}{2}}$	(0.00)1.59†
2755.53	15	36279.95	$a\ ^4F_{2\frac{1}{2}} - y\ ^4F^\circ_{4\frac{1}{2}}$	(0.00)1.49†
2755.18	2	36284.57	$b\ ^4G_{4\frac{1}{2}} - y\ ^2G^\circ_{3\frac{1}{2}}$	
2754.66	2*w*, *l*	36291.41		
2754.28	30	36296.42	$a\ ^4F_{1\frac{1}{2}} - y\ ^4F^\circ_{1\frac{1}{2}}$	(0.00)0.49†
2753.90	15	36301.43		(0.00)0.86†
2753.66	20	36304.59	$a\ ^4F_{1\frac{1}{2}} - y\ ^4F^\circ_{2\frac{1}{2}}$ $b\ ^4P_{2\frac{1}{2}} - y\ ^4P^\circ_{2\frac{1}{2}}$	(0.00)2.59†
2752.37	10	36321.61	$c\ ^4D_{0\frac{1}{2}} - x\ ^4P^\circ_{1\frac{1}{2}}$	
2751.85	85	36328.47	$a\ ^4D_{2\frac{1}{2}} - z\ ^4P^\circ_{2\frac{1}{2}}$	(0.43*B*)1.67†
2751.52	3	36332.83		
2751.22	4	36336.79	$a\ ^2D_{1\frac{1}{2}} - x\ ^4D^\circ_{2\frac{1}{2}}$	
2751.04	4	36339.17	$a\ ^2D_{1\frac{1}{2}} - x\ ^4D^\circ_{1\frac{1}{2}}$	
2750.72	100	36343.39	$a\ ^6D_{2\frac{1}{2}} - z\ ^6P^\circ_{2\frac{1}{2}}$	(0.11, 0.33, **0.57**)1.35, 1.56, **1.78**, 1.98, 2.20
2749.82	20	36355.29	$c\ ^4D_{1\frac{1}{2}} - x\ ^4P^\circ_{1\frac{1}{2}}$	(0.74*B*)1.45*C*†
2748.98	100	36366.39	$a\ ^6D_{1\frac{1}{2}} - z\ ^6P^\circ_{1\frac{1}{2}}$	(0.27, **0.77**)1.60, **2.13**, 2.64
2748.33	4	36375.00		
2747.94	12	36380.16		(0.00)1.04†
2747.76	7	36382.54	$b\ ^4G_{2\frac{1}{2}} - y\ ^2G^\circ_{1\frac{1}{2}}$	(0.00)0.89†
2746.21	50	36403.07	$c\ ^4D_{2\frac{1}{2}} - x\ ^4P^\circ_{1\frac{1}{2}}$ $b\ ^4P_{2\frac{1}{2}} - y\ ^4P^\circ_{1\frac{1}{2}}$	(0.20)0.87 (0.51)**1.20**, 2.19
2746.15	15	36403.87	$a\ ^2F_{3\frac{1}{2}} - z\ ^2F^\circ_{3\frac{1}{2}}$	(0.00)1.17
2745.41	12	36413.68	$b\ ^4G_{2\frac{1}{2}} - y\ ^2G^\circ_{4\frac{1}{2}}$	
2744.97	40	36419.52	$b\ ^4P_{1\frac{1}{2}} - y\ ^4P^\circ_{2\frac{1}{2}}$	(**0.11**, 0.34)**1.17**, 1.42, 1.68
2744.59	25	36424.56	$e\ ^2G_{4\frac{1}{2}} - v\ ^2G^\circ_{4\frac{1}{2}}$	(0.00)1.16†
2743.94	6	36433.19	$b\ ^4G_{3\frac{1}{2}} - y\ ^2D^\circ_{2\frac{1}{2}}$	
2743.63	70	36437.31	$a\ ^6D_{3\frac{1}{2}} - z\ ^6P^\circ_{2\frac{1}{2}}$	(0.47)**1.92**, 2.86
2742.02	70	36458.70	$a\ ^6D_{1\frac{1}{2}} - z\ ^6P^\circ_{2\frac{1}{2}}$	(0.00)1.90
2741.07	8	36471.33		(0.00)0.99
2740.09	35	36484.38	$a\ ^6D_{2\frac{1}{2}} - z\ ^6P^\circ_{3\frac{1}{2}}$	(0.00*d*?)1.83
2739.74	7	36489.04	$b\ ^4G_{4\frac{1}{2}} - y\ ^2G^\circ_{4\frac{1}{2}}$	(0.00)1.03†
2738.67	2	36503.29	$b\ ^4F_{1\frac{1}{2}} - x\ ^4F^\circ_{1\frac{1}{2}}$	
2738.51	1	36505.43		
2737.66	3	36516.76	$a\ ^2D_{2\frac{1}{2}} - x\ ^4D^\circ_{2\frac{1}{2}}$	
2737.47	4	36519.29	$a\ ^2D_{2\frac{1}{2}} - x\ ^4D^\circ_{1\frac{1}{2}}$	
2737.19	3	36523.03	$b\ ^4P_{2\frac{1}{2}} - y\ ^4F^\circ_{2\frac{1}{2}}$	
2737.09	15	36524.36	$c\ ^4D_{0\frac{1}{2}} - x\ ^4P^\circ_{0\frac{1}{2}}$ $a\ ^2D_{2\frac{1}{2}} - x\ ^4D^\circ_{3\frac{1}{2}}$	
2736.73	5	36529.17	$b\ ^4P_{2\frac{1}{2}} - y\ ^4F^\circ_{3\frac{1}{2}}$	
2736.20	2	36536.24	$b\ ^4G_{2\frac{1}{2}} - y\ ^2D^\circ_{3\frac{1}{2}}$	
2735.76	12	36542.12	$e\ ^2G_{2\frac{1}{2}} - v\ ^2G^\circ_{3\frac{1}{2}}$	(0.00)0.94†
2734.57	15	36558.02	$c\ ^4D_{1\frac{1}{2}} - x\ ^4P^\circ_{2\frac{1}{2}}$	(0.21)**1.01**, 1.40
2734.07	3	36564.70	$b\ ^4P_{1\frac{1}{2}} - z\ ^2P^\circ_{0\frac{1}{2}}$	
2733.93	2	36566.58		
2732.41	2	36586.92	$b\ ^4G_{2\frac{1}{2}} - y\ ^2G^\circ_{4\frac{1}{2}}$	
2731.40	4*w*, *l*	36600.45		
2731.04	3*w*, *l*	36605.27		
2730.25	2*w*, *l*	36615.86		
2729.73	6	36622.84	$b\ ^4F_{2\frac{1}{2}} - x\ ^4F^\circ_{2\frac{1}{2}}$	(0.00)1.07†
2729.15	1*w*	36630.62		
2728.93	2	36633.58	$b\ ^4F_{1\frac{1}{2}} - x\ ^4F^\circ_{2\frac{1}{2}}$	
2728.17	15	36643.78	$b\ ^4F_{4\frac{1}{2}} - x\ ^4F^\circ_{4\frac{1}{2}}$	(0.00)1.33
2727.59	1	36651.57	$b\ ^4F_{4\frac{1}{2}} - x\ ^4F^\circ_{3\frac{1}{2}}$ $b\ ^4F_{2\frac{1}{2}} - x\ ^4F^\circ_{2\frac{1}{2}}$	
2727.25	85	36656.14	$a\ ^4F_{4\frac{1}{2}} - x\ ^4D^\circ_{3\frac{1}{2}}$	(0.00)1.19†
2726.26	15	36669.44	$b\ ^4F_{2\frac{1}{2}} - x\ ^4F^\circ_{3\frac{1}{2}}$	(0.00)1.22†
2724.76	1*w*, *l*	36688.64		

TABLE 1. *Wavelengths of* Cr II *in air*—Continued

Wavelength	Intensity	Wave No.	Term combination	Zeeman effect
2724.55	1	36692.46		
2724.04	65	36699.33	$a\ ^4F_{3\frac{1}{2}} - x\ ^4D^0_{3\frac{1}{2}}$	
2723.64	60	36704.72	$b\ ^4P_{1\frac{1}{2}} - z\ ^2D^0_{2\frac{1}{2}}$	
2723.48	30	36706.87	$a\ ^4F_{3\frac{1}{2}} - x\ ^4D^0_{2\frac{1}{2}}$	
2722.74	70	36716.85	$a\ ^6D_{1\frac{1}{2}} - z\ ^6P^0_{2\frac{1}{2}}$	(0.50)**1.38**, 2.36
2720.69	15	36744.51	$a\ ^2F_{2\frac{1}{2}} - x\ ^4F^0_{1\frac{1}{2}}$	
2720.25	40	36750.46	$a\ ^4F_{2\frac{1}{2}} - x\ ^4D^0_{2\frac{1}{2}}$	P–B
2720.06	50	36753.03	$a\ ^4F_{2\frac{1}{2}} - x\ ^4D^0_{1\frac{1}{2}}$	P–B
2719.68	3	36758.16	$a\ ^4F_{2\frac{1}{2}} - x\ ^4D^0_{3\frac{1}{2}}$	P–B
2719.31	3	36763.16	$b\ ^4P_{1\frac{1}{2}} - z\ ^2P^0_{1\frac{1}{2}}$	
2718.43	55	36775.06	$a\ ^2D_{1\frac{1}{2}} - z\ ^6S^0_{1\frac{1}{2}}$	
2718.32	40	36776.55	$a\ ^4F_{1\frac{1}{2}} - x\ ^4D^0_{0\frac{1}{2}}$	
2718.08	12	36779.80	$b\ ^4G_{4\frac{1}{2}} - y\ ^2H^0_{5\frac{1}{2}}$	
2717.51	40	36787.51	$a\ ^4F_{1\frac{1}{2}} - x\ ^4D^0_{1\frac{1}{2}}$ $a\ ^6D_{0\frac{1}{2}} - z\ ^6P^0_{0\frac{1}{2}}$	
2717.05	7	36793.74	$b\ ^4F_{1\frac{1}{2}} - y\ ^2D^0_{1\frac{1}{2}}$	
2716.89	6	36795.90	$b\ ^4G_{3\frac{1}{2}} - x\ ^4G^0_{2\frac{1}{2}}$	
2715.97	3	36808.36	$b\ ^4G_{4\frac{1}{2}} - x\ ^4G^0_{3\frac{1}{2}}$	
2715.61	5*w*, *l*	36813.25		
2715.03	5*w*, *l*	36821.11		
2712.85	10	36850.70	$b\ ^2I_{5\frac{1}{2}} - w\ ^2H^0_{5\frac{1}{2}}$	
2712.30	80	36858.17	$a\ ^6D_{2\frac{1}{2}} - z\ ^4P^0_{1\frac{1}{2}}$	(0.23)1.45*A*
2711.19	20	36873.26	$b\ ^4G_{3\frac{1}{2}} - y\ ^2H^0_{4\frac{1}{2}}$	
2710.92	65	36876.93	$b\ ^2I_{6\frac{1}{2}} - w\ ^2H^0_{5\frac{1}{2}}$	(0.00)1.04
2709.31	60	36898.85	$b\ ^4G_{2\frac{1}{2}} - x\ ^4G^0_{2\frac{1}{2}}$	(0.00)0.60
2708.78	65	36906.06	$b\ ^4G_{3\frac{1}{2}} - x\ ^4G^0_{3\frac{1}{2}}$	(0.00)0.98
2706.06	8*w*, *l*	36943.15	$z\ ^6D^0_{3\frac{1}{2}} - e\ ^6P_{3\frac{1}{2}}$	
2704.73	4	36961.32		(0.00)1.21
2703.85	30	36973.35	$a\ ^6D_{1\frac{1}{2}} - z\ ^4P^0_{1\frac{1}{2}}$	(0.11)1.81
2703.56	75	36977.32	$a\ ^4H_{4\frac{1}{2}} - y\ ^4G^0_{3\frac{1}{2}}$	(0.00)1.14
2702.96	4*w*, *l*	36985.52	$z\ ^6D^0_{2\frac{1}{2}} - e\ ^6P_{2\frac{1}{2}}$ $b\ ^4G_{3\frac{1}{2}} - x\ ^4G^0_{3\frac{1}{2}}$	(0.00)1.30†
2702.89	5	36986.48		
2701.75	12	37002.09	$c\ ^2F_{3\frac{1}{2}} - w\ ^2F^0_{3\frac{1}{2}}$	(0.00)1.17†
2701.65	15	37003.46	$b\ ^4P_{2\frac{1}{2}} - x\ ^4D^0_{3\frac{1}{2}}$	(0.57)1.07†
2701.24	20	37009.07	$b\ ^2H_{5\frac{1}{2}} - x\ ^2G^0_{4\frac{1}{2}}$ $b\ ^4G_{2\frac{1}{2}} - x\ ^4G^0_{3\frac{1}{2}}$	(0.00)1.11†
2701.10	30	37010.99	$b\ ^4P_{2\frac{1}{2}} - x\ ^4D^0_{2\frac{1}{2}}$	(0.00*w*)0.99*A*†
2699.84	2*w*, *l*	37028.26		
2699.34	20	37035.12	$a\ ^2F_{2\frac{1}{2}} - y\ ^2D^0_{2\frac{1}{2}}$	(0.00)1.05†
2698.85	30	37041.85	$b\ ^2I_{6\frac{1}{2}} - w\ ^2H^0_{5\frac{1}{2}}$	(0.00)0.95†
2698.68	35	37044.18	$a\ ^6D_{0\frac{1}{2}} - z\ ^4P^0_{1\frac{1}{2}}$	(0.78)**1.07**, 2.57†
2698.40	100	37048.02	$a\ ^6D_{3\frac{1}{2}} - z\ ^4P^0_{2\frac{1}{2}}$	(0.00)1.50
2698.11	8	37052.00	$a\ ^2D_{1\frac{1}{2}} - z\ ^2F^0_{2\frac{1}{2}}$	
2697.90	30	37054.89	$c\ ^2G_{4\frac{1}{2}} - w\ ^2F^0_{3\frac{1}{2}}$ $a\ ^4H_{5\frac{1}{2}} - y\ ^4G^0_{4\frac{1}{2}}$	(0.00)0.98†
2697.51	25	37060.25	$b\ ^4G_{4\frac{1}{2}} - x\ ^4G^0_{4\frac{1}{2}}$	(0.57*B*)1.13*C*†
2696.76	20	37070.55	$a\ ^4H_{3\frac{1}{2}} - y\ ^4G^0_{3\frac{1}{2}}$	(0.63*B*)1.32*C*
2696.10	4	37079.63	$b\ ^4P_{1\frac{1}{2}} - y\ ^4F^0_{2\frac{1}{2}}$ $b\ ^2F_{2\frac{1}{2}} - x\ ^2G^0_{3\frac{1}{2}}$	
2694.70	7	37098.89	$b\ ^4F_{2\frac{1}{2}} - y\ ^2D^0_{2\frac{1}{2}}$	(0.38) 1.15†
2694.43	4*w*,*l*	37102.60	$z\ ^6D^0_{1\frac{1}{2}} - e\ ^6P_{1\frac{1}{2}}$	
2693.87	7*w*	37110.32	$c\ ^2F_{2\frac{1}{2}} - w\ ^2F^0_{2\frac{1}{2}}$ $b\ ^2F_{2\frac{1}{2}} - x\ ^2G^0_{3\frac{1}{2}}$	
2693.53	45	37115.00	$a\ ^4H_{4\frac{1}{2}} - y\ ^4G^0_{3\frac{1}{2}}$	(0.00)0.84†
2693.00	4	37122.31	$a\ ^2F_{3\frac{1}{2}} - x\ ^4F^0_{3\frac{1}{2}}$	(0.00)1.36†
2692.64	1*w*	37127.27	$z\ ^6D^0_{3\frac{1}{2}} - e\ ^6P_{2\frac{1}{2}}$	
2692.11	25	37134.58	$a\ ^4H_{4\frac{1}{2}} - y\ ^4G^0_{4\frac{1}{2}}$	(0.79*B*)1.07*C*†
2691.99	3*w*	37136.23	$z\ ^6D^0_{3\frac{1}{2}} - e\ ^6P_{3\frac{1}{2}}$ $c\ ^2F_{2\frac{1}{2}} - w\ ^2F^0_{3\frac{1}{2}}$	
2691.03	90	37149.48	$a\ ^6D_{4\frac{1}{2}} - z\ ^6D^0_{3\frac{1}{2}}$ $a\ ^4H_{5\frac{1}{2}} - y\ ^4F^0_{4\frac{1}{2}}$	(0.00)1.53*A*
2690.41	2*w*	37158.04	$b\ ^4G_{3\frac{1}{2}} - x\ ^4G^0_{3\frac{1}{2}}$	(0.00*w*)1.16†

TABLE 1. *Wavelengths of* Cr II *in air*—Continued

Wavelength	Intensity	Wave No.	Term combination	Zeeman effect
2690.34	8*w*	37159.01		
2689.79	10	37166.61	*b* $^6G_{3\frac{1}{2}}$ — *y* $^7F^0_{2\frac{1}{2}}$	
2689.20	35	37174.76	*a* $^6H_{4\frac{1}{2}}$ — *y* $^6F^0_{3\frac{1}{2}}$	(0.00*w*) 0.46*A*†
2689.03	20	37177.11	*a* $^6H_{3\frac{1}{2}}$ — *y* $^6G^0_{3\frac{1}{2}}$	
2688.41	45	37185.68	*b* $^6G_{3\frac{1}{2}}$ — *x* $^6G^0_{3\frac{1}{2}}$	(0.50*B*)1.20*C*†
2688.28	55	37187.48	*a* $^6H_{3\frac{1}{2}}$ — *y* $^6G^0_{2\frac{1}{2}}$	(0.00)0.75†
2688.14	5	37189.42	*c* $^2D_{2\frac{1}{2}}$ — *w* $^2P^0_{1\frac{1}{2}}$	
2687.60	3	37196.89	*a* $^6H_{3\frac{1}{2}}$ — *y* $^6G^0_{4\frac{1}{2}}$	
2687.09	65	37203.95	*a* $^6D_{2\frac{1}{2}}$ — *z* $^6P^0_{2\frac{1}{2}}$	(0.00)1.64
2686.66	4	37209.90	*a* $^2I_{5\frac{1}{2}}$ — *y* $^6G^0_{4\frac{1}{2}}$	
2686.40	6	37213.50	*a* $^2G_{4\frac{1}{2}}$ — *w* $^6D^0_{3\frac{1}{2}}$	
2686.00	8	37219.05	*a* $^2I_{6\frac{1}{2}}$ — *y* $^6G^0_{5\frac{1}{2}}$	
2685.66	2*w*, *l*	37223.76		
2685.19	18	37230.27	*a* $^6H_{4\frac{1}{2}}$ — *y* $^6F^0_{4\frac{1}{2}}$ *a* $^6H_{3\frac{1}{2}}$ — *y* $^6F^0_{3\frac{1}{2}}$	(0.00*w*)0.00*w*†
2685.04	18	37232.35	*a* $^2D_{2\frac{1}{2}}$ — *z* $^2F^0_{2\frac{1}{2}}$	(0.57)0.94
2684.72	7	37236.79	*a* $^6H_{3\frac{1}{2}}$ — *y* $^6F^0_{2\frac{1}{2}}$	
2684.09	8	37245.53	*c* $^2F_{2\frac{1}{2}}$ — *w* $^2F^0_{2\frac{1}{2}}$	(0.00)0.82
2683.73	4	37250.53	*c* $^2D_{1\frac{1}{2}}$ — *w* $^2P^0_{1\frac{1}{2}}$	(0.00)0.82†
2683.45	20	37254.41	*c* $^2G_{4\frac{1}{2}}$ — *w* $^2H^0_{5\frac{1}{2}}$	(0.00)1.06
2682.95	1	37261.35	*b* $^6G_{4\frac{1}{2}}$ — *x* $^6G^0_{3\frac{1}{2}}$	
2682.50	2*w*, *l*	37267.60		
2682.25	2*w*, *l*	37271.08		
2681.07	3	37287.48	*a* $^6H_{4\frac{1}{2}}$ — *z* $^2I^0_{5\frac{1}{2}}$	(0.00)0.79†
2680.85	5	37290.54	*a* $^6H_{3\frac{1}{2}}$ — *z* $^2I^0_{4\frac{1}{2}}$	(0.00)0.92†
2680.32	15	37297.91	*a* $^8S_{3\frac{1}{2}}$ — *x* $^6P^0_{3\frac{1}{2}}$	(0.33)**0.92,** 1.70†
2680.16	8	37300.14	*a* $^2F_{2\frac{1}{2}}$ — *y* $^2G^0_{3\frac{1}{2}}$	(0.00)0.82†
2679.89	15	37303.90	*c* $^2G_{3\frac{1}{2}}$ — *w* $^2F^0_{2\frac{1}{2}}$	(0.00*w*)1.25†
2678.79	100	37319.22	*a* $^6D_{4\frac{1}{2}}$ — *z* $^6P^0_{3\frac{1}{2}}$	(**0.15,** 0.34) **1.28,** 1.48, 1.76, 1.97
2677.19	125	37341.52	*a* $^6D_{4\frac{1}{2}}$ — *z* $^6D^0_{3\frac{1}{2}}$	(0.00)1.58
2677.13	100	37342.36	*a* $^6D_{3\frac{1}{2}}$ — *z* $^6D^0_{2\frac{1}{2}}$	(0.00)1.58
2676.53	5	37350.73	*a* $^2F_{2\frac{1}{2}}$ — *y* $^2D^0_{2\frac{1}{2}}$	(0.64)0.96†
2675.74	15	37361.75	*a* $^2S_{0\frac{1}{2}}$ — *x* $^2P^0_{0\frac{1}{2}}$	
2675.67	20	37362.73	*a* $^2I_{5\frac{1}{2}}$ — *z* $^2I^0_{5\frac{1}{2}}$	(0.00)0.93
2675.25	6	37368.60		(0.00)1.22†
2674.26	7*w*	37382.42	*z* $^6F^0_{4\frac{1}{2}}$ — *e* $^6G_{4\frac{1}{2}}$	
2674.07	8*w*	37385.08	*z* $^6F^0_{3\frac{1}{2}}$ — *e* $^6G_{3\frac{1}{2}}$	
2673.97	8*w*	37386.48	*z* $^6F^0_{2\frac{1}{2}}$ — *e* $^6G_{2\frac{1}{2}}$	
2673.49	3	37393.19	*c* $^2F_{3\frac{1}{2}}$ — *w* $^2H^0_{4\frac{1}{2}}$	
2672.83	90	37402.43	*a* $^6D_{3\frac{1}{2}}$ — *z* $^6D^0_{2\frac{1}{2}}$	(0.00*d*)1.55
2672.37	15	37408.86	*a* $^2D_{2\frac{1}{2}}$ — *z* $^2F^0_{3\frac{1}{2}}$	(0.00)1.17
2671.80	80	37416.84	*a* $^6D_{2\frac{1}{2}}$ — *z* $^6D^0_{1\frac{1}{2}}$	(0.00, **0.25**) **1.41,** 1.66, 1.83
2671.02	2	37427.77	*b* $^4P_{0\frac{1}{2}}$ — *y* $^4F^0_{1\frac{1}{2}}$	
2670.90	3*w*	37429.45		
2670.24	25	37438.70	*a* $^2I_{6\frac{1}{2}}$ — *z* $^2I^0_{5\frac{1}{2}}$	(0.00)1.12
2670.06	30	37441.23	*b* $^4P_{2\frac{1}{2}}$ — *z* $^4S^0_{1\frac{1}{2}}$	(**0.19,** 0.56)**1.03,** 1.41, 1.78, 2.15
2669.07	3*w*	37455.12		
2668.71	70	37460.16	*a* $^6D_{1\frac{1}{2}}$ — *z* $^6D^0_{0\frac{1}{2}}$	(0.63)**1.24,** 2.51
2667.89	25*w*, *l*	37471.68	*z* $^6F^0_{1\frac{1}{2}}$ — *e* $^6G_{2\frac{1}{2}}$ *b* $^6F_{1\frac{1}{2}}$ — *x* $^6G^0_{2\frac{1}{2}}$	(0.00*w*)0.77*w*†
2667.21	4	37481.23		
2666.02	80	37497.96	*a* $^6D_{2\frac{1}{2}}$ — *z* $^6D^0_{3\frac{1}{2}}$	(0.13)**1.43,** 1.65
2665.58	30*w*, *l*	37504.15	*z* $^6F^0_{3\frac{1}{2}}$ — *e* $^6G_{3\frac{1}{2}}$	(0.00)1.02†
2664.28	2	37522.45	*b* $^2D_{2\frac{1}{2}}$ — *w* $^2D^0_{2\frac{1}{2}}$	
2663.67	45	37531.04	*a* $^6D_{0\frac{1}{2}}$ — *z* $^6D^0_{0\frac{1}{2}}$	(0.00)3.25
2663.42	75	37534.56	*a* $^6D_{3\frac{1}{2}}$ — *z* $^6D^0_{4\frac{1}{2}}$	(0.08)1.51
2663.28	30*w*, *l*	37536.53	*z* $^6F^0_{3\frac{1}{2}}$ — *e* $^6G_{4\frac{1}{2}}$	
2663.02	10	37540.20	*b* $^6F_{4\frac{1}{2}}$ — *y* $^2H^0_{5\frac{1}{2}}$	
2662.72	7	37544.43	*b* $^6F_{4\frac{1}{2}}$ — *y* $^2H^0_{5\frac{1}{2}}$	(0.00*d*?)1.04†
2662.15	4	37552.47	*b* $^4P_{1\frac{1}{2}}$ — *x* $^6D^0_{0\frac{1}{2}}$	
2661.73	50	37558.39	*a* $^6D_{2\frac{1}{2}}$ — *z* $^6D^0_{2\frac{1}{2}}$	((0.09)1.65
2661.59	10	37560.37	*b* $^4P_{1\frac{1}{2}}$ — *x* $^6D^0_{2\frac{1}{2}}$	

TABLE 1. *Wavelengths of* Cr II *in air*—Continued

Wavelength	Intensity	Wave No.	Term combination	Zeeman effect
2661. 41	7	37562. 91	$b\ ^4P_{1\frac{1}{2}} - x\ ^4D_{1\frac{1}{2}}$	
2661. 22	50*w*	37565. 59	$z\ ^4F_{3\frac{1}{2}} - e\ ^6G_{3\frac{1}{2}}$	(0.00)1.16†
2660. 77	8	37571. 94	$b\ ^4F_{2\frac{1}{2}} - x\ ^4G_{3\frac{1}{2}}$	(0.00)1.00†
2659. 73	8	37586. 64	$c\ ^2G_{3\frac{1}{2}} - w\ ^2H_{4\frac{1}{2}}$	(0.00)0.76
2659. 47	10*w*, *d*?	37590. 31	$b\ ^4F_{2\frac{1}{2}} - x\ ^4G_{3\frac{1}{2}}$ $a\ ^4F_{3\frac{1}{2}} - z\ ^2F_{3\frac{1}{2}}$	
2658. 91	40	37598. 22	$a\ ^2F_{3\frac{1}{2}} - y\ ^2D_{2\frac{1}{2}}$	(0.00w_1)1.08
2658. 59	100	37602. 75	$a\ ^4D_{0\frac{1}{2}} - z\ ^6D_{1\frac{1}{2}}$	(0.74)**1.10,** 2.58
2658. 34	2*w*	37606. 28		
2657. 53	15*w*, *l*	37617. 74		(0.00)1.09*A*†
2657. 13	8	37623. 41		(0.00)1.17†
2655. 78	10	37642. 53	$a\ ^4F_{2\frac{1}{2}} - z\ ^2F_{3\frac{1}{2}}$	(0.00)1.36†
2654. 84	1	37655. 86	$a\ ^4H_{4\frac{1}{2}} - x\ ^4D_{3\frac{1}{2}}$	
2654. 02	4*w*, *l*	37667. 50	$z\ ^4F_{3\frac{1}{2}} - f\ ^4D_{1\frac{1}{2}}$	
2653. 57	85	37673. 88	$a\ ^4D_{1\frac{1}{2}} - z\ ^6D_{2\frac{1}{2}}$	(**0.14,** 0.38)**1.26,** 1.51, 1.77, 2.02
2653. 25	4*w*, *l*	37678. 42	$z\ ^4F_{3\frac{1}{2}} - f\ ^4D_{2\frac{1}{2}}$	
2652. 78	3*w*, *l*	37685. 10	$z\ ^4F_{3\frac{1}{2}} - f\ ^4D_{2\frac{1}{2}}$ $z\ ^4F_{1\frac{1}{2}} - f\ ^4D_{0\frac{1}{2}}$	
2652. 29	4*w*	37692. 06		
2652. 00	30*w*, *l*	37696. 18		(0.00)1.03†
2651. 42	4*w*, *l*	37704. 43	$z\ ^6D_{3\frac{1}{2}} - f\ ^6D_{2\frac{1}{2}}$	
2651. 15	1*w*	37708. 27		
2650. 80	7	37713. 25	$a\ ^2F_{2\frac{1}{2}} - x\ ^4G_{3\frac{1}{2}}$	
2650. 57	1*w*	37716. 52		
2650. 38	2	37719. 22	$b\ ^4P_{2\frac{1}{2}} - z\ ^2F_{3\frac{1}{2}}$	
2649. 89	1	37726. 20	$a\ ^4F_{3\frac{1}{2}} - y\ ^4H_{4\frac{1}{2}}$	
2649. 66	7	37729. 47	$b\ ^4F_{3\frac{1}{2}} - y\ ^2F_{3\frac{1}{2}}$	(0.00)0.89†
2648. 95	2	37739. 59	$b\ ^4F_{1\frac{1}{2}} - y\ ^2F_{2\frac{1}{2}}$	
2648. 30	8*w*, *l*	37748. 85	$z\ ^6D_{1\frac{1}{2}} - f\ ^6D_{0\frac{1}{2}}$	
2648. 08	15	37752. 27	$a\ ^2F_{3\frac{1}{2}} - y\ ^2G_{3\frac{1}{2}}$	(0.00)1.09
2647. 22	2*w*	37764. 24		
2647. 04	2*w*	37766. 81	$z\ ^6D_{3\frac{1}{2}} - f\ ^6D_{2\frac{1}{2}}$	
2646. 60	2	37773. 09	$a\ ^4F_{0\frac{1}{2}} - y\ ^4H_{1\frac{1}{2}}$	
2645. 74	2*w*	37785. 37		
2645. 18	2*w*	37793. 37		
2644. 80	2*w*	37798. 80		
2644. 19	3*w*	37807. 52		
2643. 54	12	37816. 81	$a\ ^2D_{1\frac{1}{2}} - x\ ^4F_{1\frac{1}{2}}$	(0.27)0.70
2643. 31	1*w*	37820. 10	$z\ ^6D_{3\frac{1}{2}} - f\ ^6D_{3\frac{1}{2}}$	
2643. 02	5	37824. 25	$b\ ^4F_{1\frac{1}{2}} - x\ ^4G_{2\frac{1}{2}}$ $a\ ^4F_{3\frac{1}{2}} - y\ ^4H_{4\frac{1}{2}}$ $a\ ^2F_{2\frac{1}{2}} - x\ ^4G_{3\frac{1}{2}}$	
2642. 60	2*w*	37830. 26	$z\ ^4F_{3\frac{1}{2}} - f\ ^4D_{2\frac{1}{2}}$	
2641. 80	25	37841. 86	$a\ ^2G_{4\frac{1}{2}} - x\ ^2F_{3\frac{1}{2}}$ $b\ ^4F_{3\frac{1}{2}} - x\ ^4G_{3\frac{1}{2}}$	(0.00)1.04
2641. 30	15*w*, *l*	37848. 88	$z\ ^6D_{4\frac{1}{2}} - f\ ^6D_{4\frac{1}{2}}$ $z\ ^6D_{1\frac{1}{2}} - f\ ^6D_{2\frac{1}{2}}$	(0.00)1.55
2641. 09	3	37851. 89		
2640. 45	2*w*	37861. 07	$z\ ^6D_{3\frac{1}{2}} - f\ ^6D_{3\frac{1}{2}}$	
2640. 00	7	37867. 52	$b\ ^2F_{3\frac{1}{2}} - w\ ^4D_{2\frac{1}{2}}$	
2639. 91	7*w*, *l*	37868. 81	$z\ ^6D_{2\frac{1}{2}} - f\ ^6D_{2\frac{1}{2}}$	(0.00)1.68†
2639. 32	8	37877. 27	$b\ ^2F_{3\frac{1}{2}} - w\ ^4D_{1\frac{1}{2}}$	
2639. 05	8*w*, *l*	37881. 15		(0.00)1.39†
2638. 53	3*w*, *l*	37888. 62	$z\ ^6D_{2\frac{1}{2}} - e\ ^6F_{1\frac{1}{2}}$	
2638. 05	5	37895. 50	$b\ ^4P_{2\frac{1}{2}} - z\ ^2F_{3\frac{1}{2}}$	
2637. 92	2*w*	37897. 37		
2637. 48	20	37903. 70	$a\ ^2H_{3\frac{1}{2}} - x\ ^2G_{3\frac{1}{2}}$	(0.00)1.02
2637. 20	10	37907. 86	$b\ ^4P_{0\frac{1}{2}} - x\ ^4D_{0\frac{1}{2}}$	(1.35)1.35†
2636. 70	3*w*, *l*	37914. 91		
2636. 46	10	37918. 35	$b\ ^4P_{0\frac{1}{2}} - x\ ^4D_{1\frac{1}{2}}$	(0.70)**0.48,** 1.73†
2635. 75	10*w*	37928. 57		

TABLE 1. *Wavelengths of* Cr II *in air*—Continued

Wavelength	Intensity	Wave No.	Term combination	Zeeman effect
2634.84	2*w*	37941.67		
2634.27	12*w*	37950.31		(0.00)1.28†
2633.59	10*w*	37959.68	$z\ ^6D^0_{3½} - e\ ^6F_{2½}$	
2632.77	5	37971.50	$c\ ^2F_{2½} - x\ ^2P^0_{1½}$	
2632.54	15*w*, *l*	37974.82	$y\ ^4F^0_{4½} - f\ ^4G_{5½}$ $y\ ^4F^0_{3½} - f\ ^4G_{4½}$	
2632.36	20*w*, *l*	37977.42	$z\ ^6D^0_{1½} - e\ ^6F_{0½}$	
2632.10	3	37981.17	$a\ ^2F_{2½} - y\ ^2F^0_{2½}$	
2631.87	3*w*	37984.48		
2630.93	50	37998.06	$b\ ^4P_{1½} - z\ ^4S^0_{1½}$	(0.35)1.61, **1.87**, 2.13
2629.81	2*w*	38014.24		
2629.58	8	38017.56	$a\ ^2H_{4½} - x\ ^2G^0_{3½}$	(0.00)0.94†
2629.42	4*w*, *l*	38019.88	$z\ ^6D^0_{3½} - e\ ^6F_{2½}$	
2629.04	5	38025.37	$b\ ^4F_{4½} - x\ ^4G^0_{3½}$	
2628.88	2, Fe II?	38027.68		
2628.72	2*w*	38030.00	$z\ ^6D^0_{1½} - e\ ^6F_{1½}$	
2627.95	35*w*, *l*	38041.15	$z\ ^6D^0_{5½} - f\ ^6D_{4½}$	(0.00w_1)1.37*A*
2627.17	3*w*	38052.43	$z\ ^6D^0_{3½} - e\ ^6F_{3½}$	
2626.78	20	38058.08	$c\ ^2F_{3½} - x\ ^2D^0_{3½}$	(0.00*w*)0.80*w*†
2626.69	15*w*	38059.39	$z\ ^6P^0_{3½} - e\ ^6P_{2½}$	
2626.30	2*w*	38065.04		
2625.87	2	38071.27	$a\ ^2F_{3½} - x\ ^4G^0_{3½}$	
2625.00	2*w*, *l*	38083.89		
2624.66	4*w*, *l*	38088.82		
2623.82	10*w*, *l*	38101.02	$z\ ^6D^0_{0½} - e\ ^6F_{1½}$ $z\ ^6D^0_{1½} - e\ ^6F_{2½}$	
2623.39	30	38107.26	$a\ ^2D_{1½} - y\ ^2D^0_{1½}$	(0.00*d*?)0.70†
2623.20	40*w*, *l*	38110.02	$z\ ^6D^0_{4½} - e\ ^6F_{4½}$	
2623.00	5*w*, *l*	38112.93	$z\ ^6D^0_{3½} - e\ ^6F_{3½}$	
2622.64	4*w*, *l*	38118.16		
2622.03	3	38127.02	$a\ ^2D_{2½} - x\ ^4F^0_{2½}$	
2621.80	4*w*, *l*	38130.37		
2621.18	2*w*, *l*	38139.39		
2620.86	5	38144.05		
2620.48	50*w*, *l*	38149.58	$z\ ^6P^0_{3½} - e\ ^6P_{3½}$	(0.00)1.73
2620.10	1*w*	38155.11	$a\ ^2D_{2½} - x\ ^4F^0_{3½}$	
2619.59	75*w*, *l*	38162.53	$z\ ^6D^0_{4½} - e\ ^6F_{3½}$	(0.00w_3)1.09*A*
2618.77	12*w*	38174.48		
2618.63	15*w*, *l*	38176.52	$z\ ^6P^0_{3½} - e\ ^6P_{1½}$	(0.00)1.85†
2618.49	7	38178.57	$a\ ^4H_{3½} - z\ ^2H^0_{4½}$	
2617.50	3*w*	38193.01	$c\ ^2F_{2½} - x\ ^2D^0_{2½}$	
2617.03	1*w*	38199.86	$z\ ^6P^0_{2½} - e\ ^6P_{2½}$	
2616.18	50*w*, *l*	38212.28		(0.00)1.34†
2615.85	1	38217.09	$a\ ^2G_{3½} - w\ ^4F^0_{3½}$	
2614.90	10	38230.98	$a\ ^4F_{2½} - x\ ^4F^0_{1½}$	
2614.57	50*w*, *l*	38235.80		(0.00)1.48
2613.82	3, + FeII	38246.77	$b\ ^2D_{1½} - v\ ^2F^0_{2½}$	
2613.51	12	38251.31	$c\ ^2G_{3½} - x\ ^2D^0_{2½}$	
2613.14	10*w*, *l*	38256.73		(0.00)1.61*w*†
2612.56	15	38265.22	$a\ ^4F_{1½} - x\ ^4F^0_{1½}$	(0.00*d*?)0.52†
2612.34	7*w*	38268.44	$z\ ^6P^0_{1½} - e\ ^6P_{1½}$	(0.00)2.41†
2612.08	8	38272.26		
2611.62	20	38278.99	$a\ ^4F_{4½} - x\ ^4F^0_{4½}$	(0.00)1.15
2611.04	30	38287.49	$a\ ^4F_{4½} - x\ ^4F^0_{3½}$ $a\ ^2D_{2½} - y\ ^2D^0_{1½}$	(0.00)1.77†
2610.81	50*w*, *l*	38290.87	$z\ ^6P^0_{3½} - e\ ^6P_{3½}$	(0.00w_2)1.29*A*
2610.70	40*w*, *l*	38292.48	$z\ ^6P^0_{1½} - e\ ^6P_{2½}$	
2610.04	20*w*, *l*	38302.16	$z\ ^6D^0_{3½} - e\ ^6F_{4½}$	(0.00)1.14†

TABLE 1. *Wavelengths of* Cr II *in air*—Continued

Wavelength	Intensity	Wave No.	Term combination	Zeman effect
2609. 55	3	38309. 35	$a\ ^4F_{3\frac{1}{2}} - x\ ^4F^{\circ}_{2\frac{1}{2}}$	
2609. 24	4*w*, *l*	38313. 90		
2609. 11	1	38315. 81	$b\ ^2G_{4\frac{1}{2}} - w\ ^2F^{\circ}_{3\frac{1}{2}}$	
2608. 80	8	38320. 37	$a\ ^4H_{3\frac{1}{2}} - z\ ^2H^{\circ}_{3\frac{1}{2}}$	(0.00)1.41†
2608. 60	1	38323. 30	$a\ ^2F_{3\frac{1}{2}} - x\ ^4G^{\circ}_{3\frac{1}{2}}$	
2608. 29	3*w*	38327. 86		
2608. 17	20	38329. 62	$a\ ^4F_{3\frac{1}{2}} - x\ ^4F^{\circ}_{3\frac{1}{2}}$	(0.00)1.38†
2607. 90	50	38333. 59	$a\ ^2I_{5\frac{1}{2}} - z\ ^2H^{\circ}_{4\frac{1}{2}}$	(0.00)1.00
2607. 85	10	38334 32	$a\ ^2G_{3\frac{1}{2}} - x\ ^2F^{\circ}_{3\frac{1}{2}}$	
2607. 64	10	38337. 56	$a\ ^4F_{3\frac{1}{2}} - x\ ^4F^{\circ}_{3\frac{1}{2}}$	(0.00)1.38†
2607. 06	12	38345. 93	$a\ ^4H_{5\frac{1}{2}} - z\ ^2H^{\circ}_{5\frac{1}{2}}$	(**0.13,** 0.30) . . .?
2606. 65	4*w*, *l*	38351. 97		
2606. 53	25	38353. 74	$a\ ^2G_{3\frac{1}{2}} - x\ ^2H^{\circ}_{4\frac{1}{2}}$ $b\ ^4P_{2\frac{1}{2}} - z\ ^4S^{\circ}_{1\frac{1}{2}}$	(0.36)**1.65.** . . .?
2606. 07	12	38360. 51	$a\ ^4F_{2\frac{1}{2}} - x\ ^4F^{\circ}_{3\frac{1}{2}}$	(0.00)1.07†
2605. 63	15	38366. 98	$c\ ^2F_{2\frac{1}{2}} - x\ ^2D^{\circ}_{2\frac{1}{2}}$	(0.00)0.86†
2604. 16	20	38388. 64	$a\ ^4F_{2\frac{1}{2}} - x\ ^4F^{\circ}_{2\frac{1}{2}}$	(0.00)1.60†
2603. 73	10	38394. 98	$a\ ^4F_{1\frac{1}{2}} - x\ ^4F^{\circ}_{2\frac{1}{2}}$	(0.00)1.92†
2603. 25	2*w*	38402. 05		
2603. 00	10*w*	38405. 74		
2602. 04	3*w*	38419. 91		
2601. 85	10	38422. 72	$a\ ^2D_{1\frac{1}{2}} - y\ ^2D^{\circ}_{2\frac{1}{2}}$	(0.00)1.61†
2601. 58	6	38426. 71	$a\ ^4H_{2\frac{1}{2}} - z\ ^2F^{\circ}_{3\frac{1}{2}}$	(0.00)0.40†
2601. 30	3*w*	38430. 84		
2601. 04	8	38434. 68	$a\ ^2G_{4\frac{1}{2}} - x\ ^2H^{\circ}_{5\frac{1}{2}}$	(0.00)0.90†
2600. 73	5*w*	38439. 27	$a\ ^4H_{3\frac{1}{2}} - z\ ^2H^{\circ}_{3\frac{1}{2}}$	
2599. 65	1*w*	38455. 23		
2599. 04	2*w*	38464. 26		
2598. 73	2*w*	38468. 85		
2598. 48	3*w*	38472. 55		
2598. 06	3	38478. 76	$b\ ^2G_{3\frac{1}{2}} - w\ ^2F^{\circ}_{2\frac{1}{2}}$	
2597. 44	2*w*, *l*	38487. 95		
2596. 87	8	38496. 40	$a\ ^2F_{3\frac{1}{2}} - y\ ^2F^{\circ}_{3\frac{1}{2}}$	(0.00)1.24
2596. 17	40	38506. 77	$b\ ^2F_{2\frac{1}{2}} - x\ ^2F^{\circ}_{3\frac{1}{2}}$	(0.00)1.17†
2596. 03	25	38508. 85		(0.00)1.17
2595. 55	25	38515. 97	$b\ ^2G_{4\frac{1}{2}} - w\ ^2H^{\circ}_{5\frac{1}{2}}$	(0.00)1.03†
2595. 34	4*w*, *l*	38519. 09	$a\ ^4H_{4\frac{1}{2}} - z\ ^2H^{\circ}_{5\frac{1}{2}}$	
2594. 80	1*w*	38527. 10		
2594. 51	1*w*	38531. 41		
2594. 32	7	38534. 23	$b\ ^2D_{2\frac{1}{2}} - v\ ^2F^{\circ}_{3\frac{1}{2}}$	(0.00)1.10†
2594. 10	4*w*, *l*	38537. 50		
2593. 92	3	38540. 17	$a\ ^4H_{4\frac{1}{2}} - z\ ^2F^{\circ}_{3\frac{1}{2}}$	
2593. 49	8	38546. 56	$b\ ^2S_{0\frac{1}{2}} - w\ ^2P^{\circ}_{1\frac{1}{2}}$	
2593. 10	1	38552. 36	$a\ ^2D_{2\frac{1}{2}} - y\ ^2G^{\circ}_{3\frac{1}{2}}$	
2592. 86	3	38555. 93	$a\ ^4F_{1\frac{1}{2}} - y\ ^2D^{\circ}_{1\frac{1}{2}}$	
2592. 42	3*w*, *l*	38562. 47		
2592. 32	2	38563. 96	$c\ ^4D_{2\frac{1}{2}} - w\ ^2F^{\circ}_{3\frac{1}{2}}$	
2590. 72	75	38587. 78	$a\ ^2I_{6\frac{1}{2}} - z\ ^2H^{\circ}_{5\frac{1}{2}}$	(0.00)1.03
2590. 37	20*w*, *l*	38592. 99		
2589. 70	30	38602. 97	$a\ ^2D_{2\frac{1}{2}} - y\ ^2D^{\circ}_{2\frac{1}{2}}$	(0.13)1.17
2589. 44	1	38606. 85		
2589. 05	15	38612. 66	$b\ ^2S_{0\frac{1}{2}} - w\ ^2P^{\circ}_{1\frac{1}{2}}$	(0.30)**0.98,** 1.60†
2588. 25	12	38624. 60	$a\ ^4H_{4\frac{1}{2}} - y\ ^4H^{\circ}_{3\frac{1}{2}}$	
2587. 92	4*w*, *l*	38630. 12		
2587. 42	35	38636. 99		(0.00)1.18
2586. 98	3	38643. 56		
2586. 69	4	38647. 89		
2585. 89	2*w*	38659. 85		
2585. 60	15	38664. 33		(0.00)1.25†
2584. 83	10*w*, *l*	38675. 70		
2584. 10	50	38686. 47	$a\ ^4H_{3\frac{1}{2}} - y\ ^4H^{\circ}_{3\frac{1}{2}}$	(0.00)0.67†

TABLE 1. *Wavelengths of* Cr II *in air*—Continued

Wavelength	Intensity	Wave No.	Term combination	Zeeman effect
2583.61	12	38693.96	$a\ ^4H_{3\frac{1}{2}} - y\ ^4H^0_{3\frac{1}{2}}$	(0.00)1.74†
2582.91	5*w*	38704.45	$b\ ^2F_{2\frac{1}{2}} - w\ ^4F^0_{1\frac{1}{2}}$	
2582.76	7*w*, *l*	38706.69		
2582.27	15	38714.04	$b\ ^2H_{5\frac{1}{2}} - y\ ^2I^0_{5\frac{1}{2}}$	(0.65)1.13†
2582.10	20	38716.59	$b\ ^2H_{5\frac{1}{2}} - y\ ^2I^0_{4\frac{1}{2}}$	(0.00)0.82†
2581.80	5*w*, *l*	38721.08		
2581.13	1*w*, *h*	38731.14		
2580.88	1*w*	38734.89	$a\ ^4F_{3\frac{1}{2}} - y\ ^2G^0_{3\frac{1}{2}}$	
2580.72	10	38737.14		(0.00)0.90†
2580.35	4*w*, *l*	38742.84		(0.00)1.19†
2579.88	4	38749.90	$b\ ^2F_{2\frac{1}{2}} - w\ ^4F^0_{2\frac{1}{2}}$	
2579.63	7*w*, *l*	38753.65		
2579.30	1	38758.61	$b\ ^4D_{3\frac{1}{2}} - u\ ^4D^0_{3\frac{1}{2}}$	
2579.12	15	38761.32	$b\ ^2G_{3\frac{1}{2}} - w\ ^2H^0_{3\frac{1}{2}}$	(0.00)0.95†
2578.70	7*w*, *l*	38767.63	$b\ ^4D_{3\frac{1}{2}} - y\ ^4D^0_{3\frac{1}{2}}$	
2578.31	40	38773.34	$a\ ^4H_{4\frac{1}{2}} - y\ ^4H^0_{3\frac{1}{2}}$	(0.00)0.97
2577.97	5	38778.46	$a\ ^4H_{4\frac{1}{2}} - y\ ^4H^0_{5\frac{1}{2}}$	
2577.74	10*w*	38782.07	$z\ ^4F^0_{4\frac{1}{2}} - e\ ^4F_{3\frac{1}{2}}$ $z\ ^6P^0_{3\frac{1}{2}} - f\ ^6D_{2\frac{1}{2}}$	(0.00)1.25†
2577.48	4	38785.98	$a\ ^4F_{2\frac{1}{2}} - y\ ^2G^0_{3\frac{1}{2}}$ $a\ ^2D_{1\frac{1}{2}} - x\ ^4G^0_{2\frac{1}{2}}$	
2577.34	5	38788.09		
2576.45	2*w*	38801.49	$z\ ^4F^0_{3\frac{1}{2}} - e\ ^4F_{2\frac{1}{2}}$	
2575.81	20	38811.12	$b\ ^2H_{4\frac{1}{2}} - y\ ^2I^0_{5\frac{1}{2}}$	(0.00)1.15†
2575.47	3	38816.25	$b\ ^2F_{2\frac{1}{2}} - w\ ^4F^0_{3\frac{1}{2}}$	
2575.24	4*w*	38819.71		
2574.35	2*w*, *l*	38833.13		
2574.18	7	38835.70	$a\ ^4H_{3\frac{1}{2}} - y\ ^4H^0_{4\frac{1}{2}}$	
2573.54	50	38845.35	$b\ ^2H_{4\frac{1}{2}} - x\ ^2H^0_{5\frac{1}{2}}$	(0.00)0.92
2573.32	4	38848.68	$a\ ^2I_{5\frac{1}{2}} - y\ ^4H^0_{4\frac{1}{2}}$	
2572.40	12*w*, *l*	38862.57	$z\ ^6P^0_{3\frac{1}{2}} - f\ ^6D_{1\frac{1}{2}}$	
2572.11	15	38866.95	$b\ ^2F_{2\frac{1}{2}} - x\ ^2F^0_{2\frac{1}{2}}$	(0.12)0.88
2571.78	50	38871.94	$a\ ^4H_{5\frac{1}{2}} - y\ ^4H^0_{5\frac{1}{2}}$	(0.00)1.13
2571.10	3*w*, *l*	38882.22	$z\ ^6P^0_{4\frac{1}{2}} - f\ ^6D_{3\frac{1}{2}}$	
2570.70	7	38888.27	$a\ ^4F_{4\frac{1}{2}} - y\ ^2G^0_{4\frac{1}{2}}$	
2569.83	5	38901.43		
2569.40	15*w*, *l*	38907.94	$z\ ^4F^0_{4\frac{1}{2}} - e\ ^4F_{4\frac{1}{2}}$	(0.00)1.36†
2568.86	4*w*	38916.12	$z\ ^6P^0_{4\frac{1}{2}} - f\ ^6D_{3\frac{1}{2}}$	
2568.51	20*w*, *l*	38921.42	$z\ ^6P^0_{3\frac{1}{2}} - f\ ^6D_{2\frac{1}{2}}$ $z\ ^4F^0_{3\frac{1}{2}} - e\ ^4F_{2\frac{1}{2}}$	(0.00*w*)1.07†
2568.07	3*w*	38928.09	$z\ ^4F^0_{1\frac{1}{2}} - e\ ^4F_{1\frac{1}{2}}$	
2567.80	4	38932.18		
2567.59	8	38935.37	$c\ ^2D_{1\frac{1}{2}} - u\ ^2F^0_{2\frac{1}{2}}$	(0.00)0.99†
2567.50	5*w*	38936.73	$z\ ^4F^0_{3\frac{1}{2}} - e\ ^4F_{3\frac{1}{2}}$	
2567.34	10	38939.16	$a\ ^4F_{3\frac{1}{2}} - y\ ^2G^0_{4\frac{1}{2}}$	(0.00*w*)1.02†
2566.85	10	38946.59	$c\ ^2D_{2\frac{1}{2}} - u\ ^2F^0_{3\frac{1}{2}}$	(0.00*w*)1.16†
2566.52	8	38951.60	$a\ ^4H_{4\frac{1}{2}} - y\ ^4H^0_{3\frac{1}{2}}$	(0.00)1.69†
2566.27	8*w*, *l*	38956.92	$z\ ^6P^0_{1\frac{1}{2}} - f\ ^6D_{1\frac{1}{2}}$	(0.35)1.66†
2565.59	1	38965.72	$a\ ^2D_{2\frac{1}{2}} - x\ ^4G^0_{2\frac{1}{2}}$	
2564.76	7	38978.32		(0.00*w*)1.07†
2564.27	3*w*	38985.78		
2563.58	50	38996.27	$a\ ^4H_{6\frac{1}{2}} - y\ ^4H^0_{5\frac{1}{2}}$	(0.00)1.23
2563.35	40	38999.76	$b\ ^2H_{5\frac{1}{2}} - x\ ^2H^0_{5\frac{1}{2}}$	(0.00)0.90†
2562.37	25*w*, *l*	39014.68	$b\ ^4D_{2\frac{1}{2}} - y\ ^4D^0_{1\frac{1}{2}}$ $z\ ^6P^0_{1\frac{1}{2}} - f\ ^6D_{2\frac{1}{2}}$	(0.00)1.55†
2561.81	15*w*	39023.21	$z\ ^6P^0_{2\frac{1}{2}} - f\ ^6D_{3\frac{1}{2}}$	
2561.59	7*w*	39026.56	$a\ ^2I_{5\frac{1}{2}} - y\ ^4H^0_{5\frac{1}{2}}$ $b\ ^4D_{0\frac{1}{2}} - y\ ^4D^0_{1\frac{1}{2}}$	
2560.99	20	39035.71	$b\ ^2H_{5\frac{1}{2}} - z\ ^2K^0_{6\frac{1}{2}}$	(0.00)0.73†
2559.76	15	39054.45	$a\ ^2D_{1\frac{1}{2}} - y\ ^2F^0_{2\frac{1}{2}}$	

TABLE 1. *Wavelengths of* Cr II *in air*—Continued

Wavelength	Intensity	Wave No.	Term combination	Zeeman effect
2559.71	50*w*, *l*	39055.22	$z\ ^6P^0_{3½} - f\ ^6D_{4½}$ $z\ ^6F^0_{3½} - e\ ^6F_{3½}$	(0.00) 1.20†
2558.68	4*w*, *l*	39070.94		
2558.35	4	39075.98	$a\ ^2D_{2½} - x\ ^4G^0_{3½}$	
2558.28	3	39077.05		
2557.45	10	39089.74	$a\ ^4H_{3½} - y\ ^4H^0_{3½}$	(0.00) 1.48†
2556.97	7	39097.06	$b\ ^2H_{4½} - x\ ^2H^0_{5½}$	(0.00) 1.20†
2555.47	75*w*, *l*	39120.02		(0.00) 1.00†
2555.07	4*w*, *h*	39126.14	$z\ ^6P^0_{3½} - e\ ^6F_{3½}$	
2554.23	4*w*, *h*	39139.01	$d\ ^2D^0_{1½} - p\ ^2D^0_{1½}$	
2553.62	3	39148.35	$a\ ^4F_{3½} - x\ ^4G^0_{3½}$	
2553.33	3	39152.80	$d\ ^2D^0_{2½} - p\ ^2D^0_{2½}$	
2552.15	2	39170.90		
2551.88	7	39175.05	$a\ ^4F_{4½} - y\ ^2H^0_{5½}$	
2551.58	50	39179.65	$a\ ^4F_{4½} - y\ ^2H^0_{5½}$	(0.00w_3) 0.65*A*
2551.25	2	39184.72		
2550.54	1*w*	39195.63	$z\ ^6P^0_{3½} - e\ ^6F_{1½}$	
2550.28	15	39199.62	$a\ ^4F_{2½} - x\ ^4G^0_{2½}$ $a\ ^4H_{3½} - x\ ^4F^0_{3½}$	
2549.72	1	39208.23	$a\ ^4F_{4½} - x\ ^4G^0_{3½}$	
2548.58	40	39225.77	$a\ ^4F_{3½} - y\ ^2H^0_{4½}$	(0.00w_3) 0.86*A*
2548.42	5*w*	39228.23	$z\ ^6F^0_{3½} - e\ ^6G_{3½}$	
2548.04	25	39234.08	$a\ ^4F_{1½} - x\ ^4G^0_{2½}$	(0.00w_3) 0.81*B*
2547.76	10	39238.39	$a\ ^2I_{6½} - y\ ^4H^0_{5½}$	
2547.50	20*w*, *l*	39242.40		(0.00*w*) 0.87†
2547.04	1*w*	39249.49		
2546.45	20	39258.57	$a\ ^4F_{3½} - x\ ^4G^0_{3½}$	(0.74) 1.17†
2545.87	7*w*, *l*	39267.52	$z\ ^6P^0_{2½} - e\ ^6F_{1½}$ $z\ ^6P^0_{1½} - e\ ^6F_{2½}$	
2545.51	1*w*	39273.23	$z\ ^6F^0_{4½} - e\ ^6G_{3½}$	
2544.58	2	39287.42	$a\ ^4H_{4½} - x\ ^4F^0_{3½}$	
2544.26	15	39292.37	$a\ ^6D_{4½} - z\ ^4F^0_{3½}$	(0.00) 1.06†
2543.14	30	39309.67	$a\ ^4F_{2½} - x\ ^4G^0_{3½}$	(0.00) 0.95
2542.73	10*w*, *l*	39316.01	$z\ ^6P^0_{3½} - e\ ^6F_{4½}$	
2542.38	3	39321.42	$a\ ^4H_{3½} - x\ ^4F^0_{2½}$	
2541.74	2	39331.32	$b\ ^4P_{1½} - y\ ^2D^0_{1½}$	
2540.48	2*w*	39350.82	$c\ ^4D_{1½} - x\ ^2P^0_{1½}$	
2540.22	3	39354.85	$a\ ^2I_{5½} - x\ ^4F^0_{4½}$	
2539.52	15	39365.70	$a\ ^6D_{3½} - z\ ^4F^0_{3½}$	
2538.54	2	39380.90	$c\ ^4D_{0½} - x\ ^2P^0_{0½}$	
2538.45	20*w*, *l*	39382.30	$z\ ^6F^0_{5½} - e\ ^6G_{4½}$	
2538.31	100*w*, *l*	39384.46	$z\ ^6F^0_{3½} - e\ ^6G_{3½}$	(0.00w_2) 1.13*A*
2537.19	2	39401.85	$b\ ^4D_{2½} - y\ ^4D^0_{2½}$	
2536.93	3	39405.89	$b\ ^4D_{1½} - y\ ^4D^0_{2½}$	
2536.35	5	39414.90	$b\ ^4D_{3½} - y\ ^4D^0_{3½}$	
2536.02	2*w*	39420.03	$z\ ^4P^0_{½} - e\ ^4P_{0½}$	
2535.60	1*w*, *h*	39426.55	$z\ ^6F^0_{½} - e\ ^6G_{2½}$	
2535.42	3	39429.35		
2534.96	3	39436.51	$a\ ^6D_{2½} - z\ ^4F^0_{1½}$	
2534.49	5	39443.82	$a\ ^2G_{4½} - w\ ^2G^0_{3½}$	
2534.33	40	39446.31	$a\ ^6D_{4½} - z\ ^4F^0_{4½}$	(0.57, 0.80, **1.01**) 0.80, 1.01, 1.23. **1.45**, 1.67, 1.89
2533.45	10	39460.01	$a\ ^4F_{4½} - x\ ^4G^0_{4½}$	(0.00) 1.16†
2532.99	6	39467.18	$a\ ^4F_{3½} - y\ ^2F^0_{3½}$	
2532.65	20*w*	39472.47		(0.00*w*) 1.14†
2531.84	25	39485.10	$a\ ^6D_{3½} - z\ ^4F^0_{3½}$	(0.91, **1.21**) 1.47
2530.78	20	39501.64	$a\ ^4F_{1½} - y\ ^2F^0_{2½}$ $a\ ^2D_{2½} - y\ ^2F^0_{2½}$	
2530.20	150*w*, *l*	39510.69	$z\ ^6F^0_{3½} - e\ ^6G_{2½}$	
2530.18		39511.01	$a\ ^4F_{3½} - x\ ^4G^0_{4½}$	

TABLE 1. *Wavelengths of* Cr II *in air*—Continued

Wavelength	Intensity	Wave No.	Term combination	Zeeman effect
2529.90	75*w*, *l*	39515.38	$z\ {}^6F^\circ_{4\frac{1}{2}} - e\ {}^6G_{3\frac{1}{2}}$	(0.00w_3)1.08*A*
2529.48	25	39521.94	$a\ {}^6D^\circ_{2\frac{1}{2}} - z\ {}^6F^\circ_{2\frac{1}{2}}$	
2527.57	7	39551.80	$a\ {}^6D^\circ_{1\frac{1}{2}} - z\ {}^4F^\circ_{1\frac{1}{2}}$	
2527.40	2*w*, *l*	39554.46	$z\ {}^6F^\circ_{3\frac{1}{2}} - e\ {}^6G_{1\frac{1}{2}}$	(0.00)1.56†
2526.30	15*w*, *l*	39571.68	$z\ {}^4P^\circ_{2\frac{1}{2}} - e\ {}^4P_{2\frac{1}{2}}$	(0.00)1.67†
2525.35	20*w*, *l*	39586.57		(0.00)1.33†
2524.55	15*w*, *l*	39599.11		
2523.93	15	39608.84	$a\ {}^2H_{5\frac{1}{2}} - y\ {}^2I^\circ_{5\frac{1}{2}}$	
2523.76	15*w*, *l*	39611.50	$a\ {}^2H_{5\frac{1}{2}} - y\ {}^2I^\circ_{6\frac{1}{2}}$	
2523.62	30*w*, *l*	39613.70	$z\ {}^6F^\circ_{2\frac{1}{2}} - e\ {}^6G_{2\frac{1}{2}}$	
2523.24	150*w*, *l*	39619.67	$z\ {}^6F^\circ_{3\frac{1}{2}} - e\ {}^6G_{4\frac{1}{2}}$	(0.00w_3)0.98*A*
2522.55	20*w*	39630.51	$z\ {}^4P^\circ_{1\frac{1}{2}} - e\ {}^4P_{1\frac{1}{2}}$	(0.00)1.73†
2522.01	4	39638.99	$a\ {}^6D^\circ_{3\frac{1}{2}} - z\ {}^4F^\circ_{4\frac{1}{2}}$	
2521.76	5	39642.92	$a\ {}^2H_{5\frac{1}{2}} - x\ {}^2H^\circ_{6\frac{1}{2}}$	
2521.50	1	39647.01	$b\ {}^4P_{1\frac{1}{2}} - y\ {}^2D^\circ_{2\frac{1}{2}}$	
2520.83	20*w*, *l*	39657.55	$z\ {}^4G^\circ_{5\frac{1}{2}} - f\ {}^4G_{4\frac{1}{2}}$	
2520.65	40	39660.38	$a\ {}^4F_{4\frac{1}{2}} - x\ {}^4G^\circ_{3\frac{1}{2}}$	(0.00*w*)0.66*A*†
2520.28	5	39666.20		
2519.61	15*w*, *l*	39676.75	$z\ {}^4P^\circ_{0\frac{1}{2}} - e\ {}^4P_{0\frac{1}{2}}$	
2519.08	25	39685.10	$a\ {}^4H_{4\frac{1}{2}} - y\ {}^2G^\circ_{4\frac{1}{2}}$	
2518.84	30*w*, *l*	39688.87	$z\ {}^6F^\circ_{1\frac{1}{2}} - e\ {}^6G_{1\frac{1}{2}}$	
2518.29	100*w*, *l*	39697.54	$z\ {}^6F^\circ_{2\frac{1}{2}} - e\ {}^6G_{2\frac{1}{2}}$	(0.00)0.79†
2517.86	7*w*	39704.32		
2517.36	20*w*	39712.21	$z\ {}^4G^\circ_{3\frac{1}{2}} - f\ {}^4G_{3\frac{1}{2}}$	
2516.57	40*w*, *l*	39724.67		(0.00)1.09†
2515.89	4	39735.41	$a\ {}^4F_{2\frac{1}{2}} - y\ {}^2F^\circ_{3\frac{1}{2}}$	
2515.06	55*w*, *l*	39748.52	$z\ {}^6F^\circ_{1\frac{1}{2}} - e\ {}^6G_{2\frac{1}{2}}$	(0.00)0.75†
2513.66	50*w*, *l*	39770.65	$z\ {}^6F^\circ_{0\frac{1}{2}} - e\ {}^6G_{1\frac{1}{2}}$	(0.34)0.35†
2512.80	5*w*	39784.27		
2512.38	10	39790.92	$a\ {}^2H_{4\frac{1}{2}} - y\ {}^2I^\circ_{5\frac{1}{2}}$	(0.00)1.02†
2512.22	8	39793.45	$b\ {}^4F_{2\frac{1}{2}} - x\ {}^2G^\circ_{3\frac{1}{2}}$	
2511.22	20	39809.30	$a\ {}^4H_{5\frac{1}{2}} - y\ {}^2G^\circ_{4\frac{1}{2}}$	(0.00)1.20†
2510.24	20	39824.83	$a\ {}^2H_{4\frac{1}{2}} - x\ {}^2H^\circ_{4\frac{1}{2}}$	(0.00)0.95†
2509.10	12*w*, *l*	39842.93		(0.00)1.59†
2507.57	10	39867.24	$b\ {}^2D_{1\frac{1}{2}} - w\ {}^2P^\circ_{0\frac{1}{2}}$	(0.00)0.88†
2506.93	4	39877.42	$b\ {}^4D_{2\frac{1}{2}} - y\ {}^4D^\circ_{3\frac{1}{2}}$	
2506.76	5*w*	39880.12	$b\ {}^4F_{3\frac{1}{2}} - x\ {}^2G^\circ_{4\frac{1}{2}}$	
2506.11	8	39890.46	$b\ {}^4D_{3\frac{1}{2}} - y\ {}^4D^\circ_{3\frac{1}{2}}$	
2505.86	20	39894.44	$a\ {}^2H_{5\frac{1}{2}} - x\ {}^2H^\circ_{5\frac{1}{2}}$	(0.00)1.07†
2505.45	2*w*, *h*	39900.97		
2504.55	3*w*	39915.30	$z\ {}^4P^\circ_{1\frac{1}{2}} - e\ {}^4P_{2\frac{1}{2}}$	
2503.89	4*w*	39925.83		
2503.62	3	39930.13	$a\ {}^2H_{5\frac{1}{2}} - z\ {}^2K^\circ_{4\frac{1}{2}}$	
2503.41	2	39933.48	$b\ {}^2D_{1\frac{1}{2}} - w\ {}^2P^\circ_{1\frac{1}{2}}$	
2502.96	2*w*	39940.66		
2502.16	12*w*	39953.43		
2501.48	25	39964.29	$a\ {}^2I_{5\frac{1}{2}} - y\ {}^2G^\circ_{4\frac{1}{2}}$	(0.00 *w*)0.00 *w* †
2500.21	7 *w*	39984.59	$z\ {}^4G^\circ_{5\frac{1}{2}} - f\ {}^4G_{4\frac{1}{2}}$	(0.00)1.11 †
2500.07	5	39986.83	$b\ {}^4D_{1\frac{1}{2}} - z\ {}^2S^\circ_{0\frac{1}{2}}$	
2499.63	5	39993.87	$b\ {}^4D_{0\frac{1}{2}} - z\ {}^2S^\circ_{0\frac{1}{2}}$	
2499.35	8 *w*	39998.34		
2498.80	40	40007.15	$a\ {}^4H_{3\frac{1}{2}} - y\ {}^2H^\circ_{3\frac{1}{2}}$	(0.00)1.34 †
2498.23	2 *w*	40016.28		
2497.87	10	40022.04	$b\ {}^2D_{2\frac{1}{2}} - w\ {}^2P^\circ_{1\frac{1}{2}}$	(0.00)1.10 †
2496.81	40*w*, *l*	40039.03	$z\ {}^4G^\circ_{3\frac{1}{2}} - f\ {}^4G_{3\frac{1}{2}}$	(0.00)1.15 †
2496.60	15*w*	40042.40		
2496.44	10	40044.97	$a\ {}^2F_{2\frac{1}{2}} - x\ {}^2G^\circ_{3\frac{1}{2}}$	(0.00)0.87 †
2495.20	7*w*, *l*	40064.87		
2495.10	7*w*, *l*	40066.47		
2494.26	10*w*	40079.96		

TABLE 1. *Wavelengths of* Cr II *in air*—Continued

Wavelength	Intensity	Wave No.	Term combination	Zeeman effect
2493.60	5*w*, *d*?	40090.57		
2493.28	25	40095.71	$a\ ^4H_{3\frac{1}{2}} - y\ ^2H^0_{3\frac{1}{2}}$	(0.00)1.26 †
2493.08	15*w*	40098.93		
2492.86	30	40102.46	$b\ ^2H_{3\frac{1}{2}} - w\ ^2G^0_{4\frac{1}{2}}$	(0.00)1.03
2492.62	40	40106.33	$b\ ^2H_{4\frac{1}{2}} - w\ ^2G^0_{3\frac{1}{2}}$	(0.00 w_1)0.97
2490.75	25*w*, *l*	40136.44		(0.00)0.98 †
2490.07	20	40147.40	$b\ ^2F_{2\frac{1}{2}} - w\ ^2G^0_{3\frac{1}{2}}$	(0.00)0.95 †
2489.67	20*w*, *l*	40153.85		
2489.46	15*w*	40157.24		
2489.28	50	40160.14	$a\ ^4H_{3\frac{1}{2}} - x\ ^4G^0_{2\frac{1}{2}}$	(0.00 *d*)0.78
2488.30	12*w*	40175.96		(0.00)1.08 †
2487.03	12*w*, *l*	40196.47	$z\ ^6F^0_{3\frac{1}{2}} - e\ ^6F_{4\frac{1}{2}}$	(0.00)1.17 †
2486.86	1	40199.22	$b\ ^2H_{4\frac{1}{2}} - w\ ^2G^0_{4\frac{1}{2}}$	
2486.66	20	40202.45	$b\ ^2F_{3\frac{1}{2}} - w\ ^2G^0_{4\frac{1}{2}}$	(0.00)1.00
2486.29	30	40208.43	$a\ ^4H_{4\frac{1}{2}} - x\ ^4G^0_{3\frac{1}{2}}$	(0.00)0.91
2485.41	15*w*	40222.67	$z\ ^6F^0_{3\frac{1}{2}} - f\ ^6D_{4\frac{1}{2}}$	(0.28)1.54 †
2483.79	40	40248.90	$a\ ^2I_{6\frac{1}{2}} - y\ ^2H^0_{5\frac{1}{2}}$	
2483.74	40*w*, *l*	40249.71	$z\ ^6F^0_{5\frac{1}{2}} - e\ ^6F_{5\frac{1}{2}}$	
2483.67	25	40250.85	$a\ ^2I_{5\frac{1}{2}} - y\ ^2H^0_{4\frac{1}{2}}$	
2483.25	4*w*, *d*?	40257.65		
2482.48	10	40270.14	$a\ ^4H_{3\frac{1}{2}} - x\ ^4G^0_{3\frac{1}{2}}$	
2481.09	4	40292.70	$a\ ^2F_{3\frac{1}{2}} - x\ ^2G^0_{3\frac{1}{2}}$	
2479.57	20*w*, *l*	40317.39		(0.00)1.02 †
2478.78	20*w*, *l*	40330.24		(0.00)1.66 †
2477.70	15*w*, *l*	40347.82		(0.00)0.67 †
2477.00	12*w*, *l*	40359.22		
2476.90	20	40360.85	$a\ ^2F_{3\frac{1}{2}} - x\ ^2G^0_{4\frac{1}{2}}$	(0.00)1.04 †
2475.69	30	40380.58	$a\ ^4H_{5\frac{1}{2}} - x\ ^4G^0_{4\frac{1}{2}}$	(0.00)1.38 †
2474.90	20*w*, *l*	40393.47		(0.00)1.45 †
2470.87	12*w*, *l*	40459.34	$z\ ^6F^0_{3\frac{1}{2}} - f\ ^6D_{4\frac{1}{2}}$	
2470.81	8	40460.32	$a\ ^4H_{4\frac{1}{2}} - x\ ^4G^0_{4\frac{1}{2}}$	
2469.95	10*w*, *l*	40474.41	$z\ ^6F^0_{5\frac{1}{2}} - f\ ^6D_{5\frac{1}{2}}$	(0.00)1.65 †
2469.40	20*w*, *l*	40483.43	$z\ ^6F^0_{4\frac{1}{2}} - e\ ^6F_{4\frac{1}{2}}$	(0.00)1.30 †
2469.13	20	40487.85	$a\ ^4H_{6\frac{1}{2}} - x\ ^4G^0_{5\frac{1}{2}}$	(0.00)1.44 †
2468.67	1	40495.40	$b\ ^4G_{4\frac{1}{2}} - x\ ^2F^0_{3\frac{1}{2}}$	
2468.12	2*w*, *l*	40504.43		
2466.64	5*w*, *h*	40528.72		
2466.48	25*w*, *l*	40531.35	$z\ ^6F^0_{3\frac{1}{2}} - e\ ^6F_{3\frac{1}{2}}$	(0.00)1.32†
2466.22	10	40535.62	$a\ ^2I_{5\frac{1}{2}} - x\ ^4G^0_{3\frac{1}{2}}$	(0.00)0.71†
2465.78	18	40542.86	$c\ ^2F_{3\frac{1}{2}} - w\ ^2D^0_{2\frac{1}{2}}$	(0.00).075†
2465.61	18	40545.65	$c\ ^2F_{2\frac{1}{2}} - w\ ^2D^0_{1\frac{1}{2}}$	(0.00)0.90†
2464.94	8	40556.67	$b\ ^4F_{2\frac{1}{2}} - w\ ^4D^0_{1\frac{1}{2}}$	(0.00)0.79†
2464.62	7	40561.93	$b\ ^4F_{1\frac{1}{2}} - w\ ^4D^0_{0\frac{1}{2}}$	
2464.48	3*w*	40564.24		
2464.31	4	40567.04	$b\ ^4F_{1\frac{1}{2}} - w\ ^4D^0_{1\frac{1}{2}}$	
2463.46	8	40581.03	$b\ ^4F_{2\frac{1}{2}} - w\ ^4D^0_{2\frac{1}{2}}$ $a\ ^4H_{5\frac{1}{2}} - x\ ^4G^0_{5\frac{1}{2}}$	
2462.82	1	40591.58	$b\ ^4F_{1\frac{1}{2}} - w\ ^4D^0_{2\frac{1}{2}}$	
2462.35	15	40599.32	$b\ ^4F_{3\frac{1}{2}} - w\ ^4D^0_{3\frac{1}{2}}$	(0.00)1.08†
2461.93	5	40606.25	$a\ ^2G_{4\frac{1}{2}} - w\ ^2F^0_{3\frac{1}{2}}$	(0.00)0.96†
2461.75	2*w*	40609.22		
2460.77	15*w*, *h*	40625.39	$z\ ^6F^0_{3\frac{1}{2}} - e\ ^6F_{2\frac{1}{2}}$	(0.00)1.44†
2460.55	10*w*	40629.02		
2460.42	30	40631.18	$b\ ^4F_{4\frac{1}{2}} - w\ ^4D^0_{3\frac{1}{2}}$	(0.00)1.17†
2459.58	3*w*	40645.05		
2459.35	8	40648.85	$b\ ^4F_{2\frac{1}{2}} - w\ ^4D^0_{2\frac{1}{2}}$	
2457.59	2	40677.95	$c\ ^2F_{2\frac{1}{2}} - w\ ^2D^0_{2\frac{1}{2}}$	
2456.94	8*w*	40688.72	$z\ ^6F^0_{1\frac{1}{2}} - e\ ^6F_{1\frac{1}{2}}$	
2456.23	3*w*	40700.48		
2455.15	12*w*	40718.38	$z\ ^6F^0_{3\frac{1}{2}} - e\ ^6F_{3\frac{1}{2}}$ $z\ ^6F^0_{5\frac{1}{2}} - e\ ^6F_{5\frac{1}{2}}$	(0.00)1.63†
2455.00	2*w*	40720.87	$z\ ^6F^0_{3\frac{1}{2}} - e\ ^6F_{3\frac{1}{2}}$	

TABLE 1. *Wavelengths of* Cr II *in air*—Continued

Wavelength	Intensity	Wave No.	Term combination	Zeeman effect
2454.47	30	40729.66	$a\ ^2I_{6\frac{1}{2}} - x\ ^4G^0_{5\frac{1}{2}}$	(0.00)0.83†
2454.06	15	40736.46	$a\ ^2I_{5\frac{1}{2}} - x\ ^4G^0_{4\frac{1}{2}}$	(0.00)0.75†
2453.90	1	40738.62	$d\ ^2F_{3\frac{1}{2}} - u\ ^2D^0_{2\frac{1}{2}}$	
2452.71	18	40758.88	$d\ ^2F_{3\frac{1}{2}} - u\ ^2D^0_{3\frac{1}{2}}$	(0.00)1.04†
2452.04	4*w*	40770.02	$z\ ^6F^0_{5\frac{1}{2}} - e\ ^6F_{4\frac{1}{2}}$	
2451.63	7	40776.84	$c\ ^2D_{2\frac{1}{2}} - v\ ^2D^0_{2\frac{1}{2}}$ $a\ ^2G_{3\frac{1}{2}} - w\ ^2F^0_{3\frac{1}{2}}$	
2450.80	5*w*	40790.64		
2450.37	20	40797.80	$b\ ^4G_{3\frac{1}{2}} - w\ ^4F^0_{2\frac{1}{2}}$	(0.00)0.93†
2449.95	25	40804.80	$b\ ^4G_{4\frac{1}{2}} - w\ ^4F^0_{3\frac{1}{2}}$	(0.00)1.02†
2449.63	25	40810.13	$b\ ^4G_{5\frac{1}{2}} - w\ ^4F^0_{4\frac{1}{2}}$	(0.00)1.13†
2447.76	3*w*	40841.30	$c\ ^2D_{1\frac{1}{2}} - v\ ^2D^0_{1\frac{1}{2}}$	
2446.91	15	40855.49	$b\ ^4G_{2\frac{1}{2}} - w\ ^4F^0_{1\frac{1}{2}}$	(0.00)0.66†
2446.11	10	40868.85	$d\ ^2F_{2\frac{1}{2}} - u\ ^2D^0_{1\frac{1}{2}}$	
2445.14	7	40885.06		
2445.09	10	40885.90	$a\ ^2G_{3\frac{1}{2}} - w\ ^2F^0_{2\frac{1}{2}}$ $b\ ^4G_{4\frac{1}{2}} - w\ ^4F^0_{4\frac{1}{2}}$	
2444.20	7	40900.78	$b\ ^4G_{2\frac{1}{2}} - w\ ^4F^0_{2\frac{1}{2}}$	
2444.08	7	40902.79	$b\ ^4G_{3\frac{1}{2}} - w\ ^4F^0_{3\frac{1}{2}}$	
2443.35	5	40915.01	$b\ ^4G_{3\frac{1}{2}} - x\ ^2F^0_{2\frac{1}{2}}$	
2440.48	2	40963.12	$b\ ^4G_{3\frac{1}{2}} - x\ ^4P^0_{2\frac{1}{2}}$	
2439.88	4*w*	40973.19		
2438.87	5*w*	40990.16		
2438.46	35	40997.05	$a\ ^2H_{5\frac{1}{2}} - w\ ^2G^0_{4\frac{1}{2}}$	(0.00)1.07†
2437.50	1	41013.20	$b\ ^4G_{3\frac{1}{2}} - x\ ^2H^0_{3\frac{1}{2}}$	
2433.72	2	41076.89		
2433.20	25	41085.67	$a\ ^2H_{4\frac{1}{2}} - w\ ^2G^0_{3\frac{1}{2}}$	(0.00)0.94†
2430.59	1	41129.78	$a\ ^2F_{3\frac{1}{2}} - w\ ^4D^0_{3\frac{1}{2}}$	
2428.29	2	41168.74	$a\ ^2G_{3\frac{1}{2}} - w\ ^2H^0_{4\frac{1}{2}}$	
2427.68	4	41179.08	$a\ ^2H_{4\frac{1}{2}} - w\ ^2G^0_{4\frac{1}{2}}$	
2427.12	1	41188.58		
2425.66	15	41213.37	$b\ ^4D_{1\frac{1}{2}} - y\ ^4P^0_{0\frac{1}{2}}$	
2425.21	18	41221.02	$b\ ^4D_{0\frac{1}{2}} - y\ ^4P^0_{0\frac{1}{2}}$	(1.30)1.30†)
2423.53	4	41249.59		
2422.93	2	41259.80	$b\ ^4F_{4\frac{1}{2}} - x\ ^2F^0_{3\frac{1}{2}}$	
2421.90	3	41277.35	$b\ ^4F_{3\frac{1}{2}} - x\ ^2F^0_{3\frac{1}{2}}$	
2420.73	2	41297.30	$a\ ^2D_{2\frac{1}{2}} - x\ ^2G^0_{3\frac{1}{2}}$	
2420.11	25	41307.88	$b\ ^4D_{2\frac{1}{2}} - y\ ^4P^0_{1\frac{1}{2}}$	(0.00)0.96†
2419.87	15	41311.98	$b\ ^4D_{1\frac{1}{2}} - y\ ^4P^0_{1\frac{1}{2}}$	
2419.38	15	41320.34	$b\ ^4D_{0\frac{1}{2}} - y\ ^4P^0_{1\frac{1}{2}}$	
2417.31	2	41355.72	$c\ ^2F_{3\frac{1}{2}} - v\ ^2F^0_{2\frac{1}{2}}$	
2416.40	40	41371.29	$b\ ^2H_{3\frac{1}{2}} - w\ ^2H^0_{3\frac{1}{2}}$	(0.00)1.07†
2415.23	5*W*	41391.34	$z\ ^4H^0_{5\frac{1}{2}} - f\ ^4G_{3\frac{1}{2}}$	
2413.64	15*W*	41418.60	$b\ ^4F_{2\frac{1}{2}} - w\ ^4F^0_{1\frac{1}{2}}$	
2413.06	8	41428.56	$b\ ^4F_{1\frac{1}{2}} - w\ ^4F^0_{1\frac{1}{2}}$	
2411.01	15	41463.78	$b\ ^4F_{2\frac{1}{2}} - w\ ^4F^0_{2\frac{1}{2}}$	(0.00)1.21†
2410.75	2	41468.25	$b\ ^2H_{4\frac{1}{2}} - w\ ^2H^0_{3\frac{1}{2}}$	
2410.43	3	41473.75	$b\ ^4F_{1\frac{1}{2}} - w\ ^4F^0_{2\frac{1}{2}}$	
2409.96	5	41481.84	$b\ ^4F_{3\frac{1}{2}} - w\ ^4F^0_{2\frac{1}{2}}$	
2409.45	1	41490.61,	$c\ ^2F_{2\frac{1}{2}} - v\ ^2F^0_{2\frac{1}{2}}$	
2408.02	3*W*	41515.25	$z\ ^4H^0_{5\frac{1}{2}} - f\ ^4G_{4\frac{1}{2}}$	
2405.72	1	41554.94	$c\ ^2F_{3\frac{1}{2}} - v\ ^2F^0_{3\frac{1}{2}}$	
2405.28	10	41562.55	$b\ ^2H_{5\frac{1}{2}} - w\ ^2H^0_{4\frac{1}{2}}$	
2404.92	8	41568.76	$b\ ^4F_{2\frac{1}{2}} - w\ ^4F^0_{3\frac{1}{2}}$	(0.00)1.10†
2404.72	2*W*	41572.22	$z\ ^4H^0_{5\frac{1}{2}} - f\ ^4G_{5\frac{1}{2}}$	
2404.22	3	41580.87	$b\ ^4F_{2\frac{1}{2}} - x\ ^2F^0_{2\frac{1}{2}}$	
2403.87	10	41586.92	$b\ ^4F_{3\frac{1}{2}} - w\ ^4F^0_{3\frac{1}{2}}$	(0.00)1.19†
2403.62	3	41591.24	$b\ ^4F_{1\frac{1}{2}} - x\ ^2F^0_{1\frac{1}{2}}$	
2403.54	2*W*	41592.63		
2402.98	4*W*	41602.33	$b\ ^4D_{2\frac{1}{2}} - z\ ^2D^0_{1\frac{1}{2}}$ $b\ ^4F_{4\frac{1}{2}} - x\ ^2H^0_{5\frac{1}{2}}$	
2402.73	3	41606.65	$b\ ^4D_{1\frac{1}{2}} - z\ ^2D^0_{1\frac{1}{2}}$	
2402.31	2	41613.92	$b\ ^4D_{0\frac{1}{2}} - z\ ^2D^0_{1\frac{1}{2}}$	

TABLE 1. *Wavelengths of* Cr II *in air*—Continued

Wavelength	Intensity	Wave No.	Term combination	Zeeman effect
2402.07	5	41618.09	$b\ ^2D_{1\frac{1}{2}} - u\ ^2F^\circ_{2\frac{1}{2}}$	
2401.33	2	41630.90	$a\ ^2P_{1\frac{1}{2}} - w\ ^2F^\circ_{2\frac{1}{2}}$	
2400.24	15	41649.81	$b\ ^4F_{4\frac{1}{2}} - w\ ^4F^\circ_{4\frac{1}{2}}$	(0.00)1.30†
2399.67	30	41659.70	$b\ ^2H_{4\frac{1}{2}} - w\ ^2H^\circ_{4\frac{1}{2}}$	(0.00)0.90†
2399.21	3	41667.69	$b\ ^4F_{3\frac{1}{2}} - w\ ^4F^\circ_{4\frac{1}{2}}$	
2398.51	15	41679.85	$b\ ^4D_{2\frac{1}{2}} - y\ ^4P^\circ_{2\frac{1}{2}}$	
2398.28	1	41683.84	$b\ ^4D_{1\frac{1}{2}} - y\ ^4P^\circ_{2\frac{1}{2}}$	
2397.75	40	41693.06	$b\ ^4D_{3\frac{1}{2}} - y\ ^4P^\circ_{3\frac{1}{2}}$	(0.00)1.32†
2396.48	10	41715.15	$a\ ^2F_{2\frac{1}{2}} - w\ ^4F^\circ_{3\frac{1}{2}}$	
2393.99	50	41758.53	$a\ ^2F_{3\frac{1}{2}} - x\ ^2F^\circ_{3\frac{1}{2}}$	(0.00)1.16†
2393.35	4	41769.70		
2392.80	4	41779.30	$b\ ^2D_{2\frac{1}{2}} - u\ ^2F^\circ_{3\frac{1}{2}}$	
2392.55	5	41783.67		
2389.75	40	41832.62	$a\ ^2F_{2\frac{1}{2}} - x\ ^2F^\circ_{3\frac{1}{2}}$	(0.00)0.88†
2387.03	4	41880.28	$a\ ^2D_{1\frac{1}{2}} - w\ ^4D^\circ_{1\frac{1}{2}}$	
2386.08	3	41896.96		
2382.20	5	41965.19	$b\ ^4D_{2\frac{1}{2}} - z\ ^2D^\circ_{2\frac{1}{2}}$	
2381.97	2	41969.24	$b\ ^4D_{1\frac{1}{2}} - z\ ^2D^\circ_{2\frac{1}{2}}$	
2381.48	50	41977.88	$a\ ^4P_{0\frac{1}{2}} - y\ ^4D^\circ_{0\frac{1}{2}}$ $a\ ^4P_{1\frac{1}{2}} - y\ ^4D^\circ_{0\frac{1}{2}}$	P–B
2378.90	3	42023.40	$b\ ^4D_{2\frac{1}{2}} - z\ ^2P^\circ_{1\frac{1}{2}}$	
2378.68	5	42027.29	$b\ ^4D_{1\frac{1}{2}} - z\ ^2P^\circ_{1\frac{1}{2}}$	
2378.28	3	42034.36	$b\ ^4D_{0\frac{1}{2}} - z\ ^2P^\circ_{1\frac{1}{2}}$	
2377.32	2	42051.32		
2376.40	5	42067.60	$a\ ^2F_{3\frac{1}{2}} - w\ ^4F^\circ_{3\frac{1}{2}}$	
2375.69	4	42080.17	$a\ ^2F_{3\frac{1}{2}} - x\ ^2F^\circ_{2\frac{1}{2}}$	
2374.57	1	42100.02	$a\ ^2F_{3\frac{1}{2}} - x\ ^2H^\circ_{4\frac{1}{2}}$	
2373.70	2	42115.45	$a\ ^2F_{2\frac{1}{2}} - x\ ^4P^\circ_{1\frac{1}{2}}$	
2372.63	2	42134.44	$a\ ^2D_{2\frac{1}{2}} - w\ ^4D^\circ_{3\frac{1}{2}}$	
2371.23	4	42159.32		
2366.84	35*w*	42237.50	$a\ ^4P_{0\frac{1}{2}} - y\ ^4D^\circ_{1\frac{1}{2}}$ $a\ ^4P_{1\frac{1}{2}} - y\ ^4D^\circ_{1\frac{1}{2}}$	P–B
2366.75	5	42239.12	$a\ ^4P_{2\frac{1}{2}} - y\ ^4D^\circ_{1\frac{1}{2}}$	
2366.28	1	42248.04	$a\ ^2H_{4\frac{1}{2}} - w\ ^2F^\circ_{3\frac{1}{2}}$	
2365.26	20*w*	42265.72	$a\ ^2H_{3\frac{1}{2}} - w\ ^2H^\circ_{4\frac{1}{2}}$ $a\ ^4F_{4\frac{1}{2}} - w\ ^4D^\circ_{3\frac{1}{2}}$	(0.00)1.13†
2365.15	4	42267.68	$a\ ^4F_{3\frac{1}{2}} - w\ ^4D^\circ_{2\frac{1}{2}}$	
2364.98	2	42270.72		
2364.02	10	42287.89	$a\ ^6D_{4\frac{1}{2}} - z\ ^4D^\circ_{3\frac{1}{2}}$	
2363.65	3	42294.50	$a\ ^4F_{2\frac{1}{2}} - w\ ^4D^\circ_{1\frac{1}{2}}$	
2363.32	1*w*	42300.41		
2362.26	2	42319.39	$a\ ^4F_{2\frac{1}{2}} - w\ ^4D^\circ_{2\frac{1}{2}}$	
2362.00	1	42324.05	$a\ ^4F_{1\frac{1}{2}} - w\ ^4D^\circ_{0\frac{1}{2}}$	
2361.79	3	42327.81	$b\ ^2F_{3\frac{1}{2}} - x\ ^2D^\circ_{2\frac{1}{2}}$	
2361.31	1	42336.41	$b\ ^4D_{1\frac{1}{2}} - y\ ^4F^\circ_{1\frac{1}{2}}$	
2361.09	1	42340.35	$b\ ^4D_{2\frac{1}{2}} - y\ ^4F^\circ_{2\frac{1}{2}}$	
2360.89	6*l*	42343.94	$b\ ^4D_{0\frac{1}{2}} - y\ ^4F^\circ_{1\frac{1}{2}}$ $b\ ^4D_{1\frac{1}{2}} - y\ ^4F^\circ_{2\frac{1}{2}}$	
2360.75	8	42346.46	$b\ ^4D_{2\frac{1}{2}} - y\ ^4F^\circ_{3\frac{1}{2}}$	
2360.14	10	42357.40	$a\ ^2P_{1\frac{1}{2}} - x\ ^2P^\circ_{1\frac{1}{2}}$	
2358.82	5	42381.10	$a\ ^2F_{2\frac{1}{2}} - y\ ^2P^\circ_{1\frac{1}{2}}$	
2356.96	5	42414.54	$b\ ^4D_{3\frac{1}{2}} - y\ ^4F^\circ_{3\frac{1}{2}}$	
2356.58	4	42421.38	$a\ ^2P_{1\frac{1}{2}} - x\ ^2P^\circ_{0\frac{1}{2}}$	
2355.62	3	42438.67	$a\ ^2S_{0\frac{1}{2}} - w\ ^2P^\circ_{0\frac{1}{2}}$	
2355.10	3	42448.04	$a\ ^2H_{4\frac{1}{2}} - w\ ^2H^\circ_{5\frac{1}{2}}$	
2354.64	3	42456.33	$a\ ^6D_{0\frac{1}{2}} - z\ ^4D^\circ_{0\frac{1}{2}}$	
2354.59	3	42457.23	$a\ ^2H_{5\frac{1}{2}} - w\ ^2H^\circ_{5\frac{1}{2}}$	
2354.05	3	42466.97	$a\ ^6D_{1\frac{1}{2}} - z\ ^4D^\circ_{1\frac{1}{2}}$	
2353.54	1	42476.17		
2353.44	3	42477.98	$a\ ^6D_{2\frac{1}{2}} - z\ ^4D^\circ_{2\frac{1}{2}}$	
2353.29	3	42480.68	$a\ ^6D_{3\frac{1}{2}} - z\ ^4D^\circ_{3\frac{1}{2}}$	
2351.96	4	42504.71	$a\ ^2S_{0\frac{1}{2}} - w\ ^2P^\circ_{1\frac{1}{2}}$	
2350.14	1	42537.62	$a\ ^6D_{0\frac{1}{2}} - z\ ^4D^\circ_{1\frac{1}{2}}$	
2350.00	2	42540.15	$b\ ^2F_{2\frac{1}{2}} - x\ ^2D^\circ_{1\frac{1}{2}}$	

TABLE 1. *Wavelengths of* Cr II *in air*—Continued

Wavelength	Intensity	Wave No.	Term combination	Zeeman effect
2348.25	3	42571.86	$b\ ^4P_{2\frac{1}{2}} - w\ ^4D^o_{2\frac{1}{2}}$	
2347.08	2	42593.07	$a\ ^6D_{1\frac{1}{2}} - z\ ^4D^o_{2\frac{1}{2}}$	
2345.53	2	42621.21	$b\ ^4P_{2\frac{1}{2}} - w\ ^4D^o_{3\frac{1}{2}}$	
2345.35	25	42624.48	$a\ ^4P_{1\frac{1}{2}} - y\ ^4D^o_{2\frac{1}{2}}$	P–B
2345.25	15	42626.30	$a\ ^4P_{2\frac{1}{2}} - y\ ^4D^o_{2\frac{1}{2}}$	P–B
2344.54	20	42639.21	$a\ ^2H_{4\frac{1}{2}} - w\ ^2H^o_{5\frac{1}{2}}$	(0.00)0.91†
2339.90	1	42723.76	$b\ ^2G_{3\frac{1}{2}} - v\ ^2F^o_{3\frac{1}{2}}$	
2338.27	1	42753.54	$a\ ^2P_{1\frac{1}{2}} - x\ ^2D^o_{1\frac{1}{2}}$	
2337.74	20	42763.22	$a\ ^2D_{2\frac{1}{2}} - x\ ^2F^o_{3\frac{1}{2}}$	(0.00)1.19†
2336.42	3	42787.38	$a\ ^2D_{1\frac{1}{2}} - w\ ^4F^o_{2\frac{1}{2}}$	
2334.83	10	42816.52	$b\ ^4D_{1\frac{1}{2}} - x\ ^4D^o_{0\frac{1}{2}}$	
2334.62	5	42820.37		
2334.58	10	42821.10	$b\ ^4D_{2\frac{1}{2}} - x\ ^4D^o_{2\frac{1}{2}}$	
2334.45	5	42823.49	$b\ ^4D_{2\frac{1}{2}} - x\ ^4D^o_{1\frac{1}{2}}$	
2334.41	2	42824.23	$b\ ^4D_{0\frac{1}{2}} - x\ ^4D^o_{0\frac{1}{2}}$	
2334.37	8	42824.95	$b\ ^4D_{1\frac{1}{2}} - x\ ^4D^o_{2\frac{1}{2}}$	
2334.24	7	42827.34	$b\ ^4D_{1\frac{1}{2}} - x\ ^4D^o_{1\frac{1}{2}}$	
2334.17	8	42828.62	$b\ ^4D_{2\frac{1}{2}} - x\ ^4D^o_{3\frac{1}{2}}$	
2333.87	7	42834.13	$b\ ^4D_{3\frac{1}{2}} - x\ ^4D^o_{2\frac{1}{2}}$	
2333.84	12	42834.68	$b\ ^4D_{0\frac{1}{2}} - x\ ^4D^o_{1\frac{1}{2}}$	
2333.46	25	42841.65	$b\ ^4D_{3\frac{1}{2}} - x\ ^4D^o_{3\frac{1}{2}}$	(0.00)1.45†
2332.39	3	42861.30	$b\ ^4F_{2\frac{1}{2}} - w\ ^2G^o_{3\frac{1}{2}}$	
2330.03	10	42904.72	$a\ ^2D_{1\frac{1}{2}} - x\ ^2F^o_{2\frac{1}{2}}$	
2326.61	3	42967.78	$a\ ^2D_{2\frac{1}{2}} - w\ ^4F^o_{2\frac{1}{2}}$	
2326.26	3	42974.24		
2325.04	1	42996.79	$a\ ^4F_{2\frac{1}{2}} - x\ ^2F^o_{3\frac{1}{2}}$	
2321.95	4	43054.00	$a\ ^2P_{0\frac{1}{2}} - x\ ^2P^o_{1\frac{1}{2}}$	
2320.94	1	43072.74	$a\ ^2D_{2\frac{1}{2}} - w\ ^4F^o_{3\frac{1}{2}}$	
2320.39	10	43082.94	$a\ ^4G_{3\frac{1}{2}} - z\ ^4H^o_{3\frac{1}{2}}$	P–B
2320.29	5	43084.80	$a\ ^2D_{2\frac{1}{2}} - x\ ^2F^o_{3\frac{1}{2}}$	
2320.08	30	43088.70	$a\ ^4G_{2\frac{1}{2}} - z\ ^4H^o_{3\frac{1}{2}}$	P–B
2319.38	50	43101.71	$a\ ^4P_{2\frac{1}{2}} - y\ ^4D^o_{3\frac{1}{2}}$	
2318.77	10	43113.05	$a\ ^2F_{3\frac{1}{2}} - w\ ^2G^o_{3\frac{1}{2}}$	(0.00)0.99†
2318.49	2	43118.24	$a\ ^2P_{0\frac{1}{2}} - x\ ^2P^o_{0\frac{1}{2}}$	
2314.81	8	43186.80	$a\ ^4G_{4\frac{1}{2}} - z\ ^4H^o_{4\frac{1}{2}}$	P–B
2314.71	40	43188.66	$a\ ^4G_{3\frac{1}{2}} - z\ ^4H^o_{3\frac{1}{2}}$	P–B
2313.82	3	43205.27	$a\ ^4P_{1\frac{1}{2}} - z\ ^2S^o_{0\frac{1}{2}}$ $a\ ^4P_{0\frac{1}{2}} - z\ ^2S^o_{0\frac{1}{2}}$	
2310.96	2	43258.73	$b\ ^4D_{2\frac{1}{2}} - z\ ^4S^o_{1\frac{1}{2}}$	
2310.75	1	43262.47	$b\ ^4D_{1\frac{1}{2}} - z\ ^4S^o_{1\frac{1}{2}}$	
2307.56	10*w*, *l*	43322.46	$z\ ^6P^o_{3\frac{1}{2}} - e\ ^6S_{2\frac{1}{2}}$ $a\ ^2D_{1\frac{1}{2}} - y\ ^2P^o_{0\frac{1}{2}}$	
2307.19	35	43329.41	$a\ ^4G_{4\frac{1}{2}} - z\ ^4H^o_{5\frac{1}{2}}$	P–B
2306.81	10	43336.55	$a\ ^4G_{5\frac{1}{2}} - z\ ^4H^o_{4\frac{1}{2}}$	P–B
2305.94	1	43352.90	$a\ ^4F_{1\frac{1}{2}} - x\ ^2F^o_{2\frac{1}{2}}$	
2305.52	2	43360.79	$a\ ^2F_{3\frac{1}{2}} - w\ ^2G^o_{3\frac{1}{2}}$	
2304.02	4	43388.83	$a\ ^2D_{1\frac{1}{2}} - x\ ^4P^o_{0\frac{1}{2}}$	
2300.58	30	43453.89	$a\ ^2F_{3\frac{1}{2}} - w\ ^2G^o_{4\frac{1}{2}}$	(0.00)1.17†
2300.08	8*w*, *l*	43463.35	$z\ ^6P^o_{2\frac{1}{2}} - e\ ^6S_{2\frac{1}{2}}$	
2299.52	5	43473.92		
2297.17	50	43518.39	$a\ ^4G_{5\frac{1}{2}} - z\ ^4H^o_{5\frac{1}{2}}$	(0.00)1.12†
2296.22	2	43536.39	$b\ ^4D_{3\frac{1}{2}} - z\ ^2F^o_{3\frac{1}{2}}$	
2295.20	4*w*, *l*	43555.74	$z\ ^6P^o_{1\frac{1}{2}} - e\ ^6S_{2\frac{1}{2}}$	
2294.46	8	43569.78	$b\ ^4G_{2\frac{1}{2}} - w\ ^2F^o_{2\frac{1}{2}}$	
2291.85	4	43619.40	$b\ ^4P_{2\frac{1}{2}} - x\ ^4P^o_{2\frac{1}{2}}$	
2291.11	10	43633.49	$a\ ^2D_{2\frac{1}{2}} - y\ ^2P^o_{1\frac{1}{2}}$	
2286.27	8	43725.84	$b\ ^4D_{2\frac{1}{2}} - z\ ^2F^o_{3\frac{1}{2}}$	
2284.13	10	43766.81		
2279.64	1	43853.01	$b\ ^4P_{2\frac{1}{2}} - x\ ^4P^o_{1\frac{1}{2}}$	
2271.01	3	44019.63		
2268.34	4	44071.44	$d\ ^2D_{2\frac{1}{2}} - u\ ^2D^o_{2\frac{1}{2}}$	

TABLE 1. *Wavelengths of* Cr II *in air*—Continued

Wavelength	Intensity	Wave number	Term combination
2262.93	1	44176.79	$b\ ^4P_{1\frac{1}{2}} - x\ ^4P^0_{2\frac{1}{2}}$
2262.58	2	44183.62	$d\ ^2D_{1\frac{1}{2}} - u\ ^2D^0_{1\frac{1}{2}}$
2258.09	40	44271.47	$a\ ^2I_{4\frac{1}{2}} - y\ ^2I^0_{3\frac{1}{2}}$
2257.96	50	44274.02	$a\ ^2I_{4\frac{1}{2}} - y\ ^2I^0_{4\frac{1}{2}}$
			$a\ ^6D_{0\frac{1}{2}} - y\ ^4D^0_{0\frac{1}{2}}$
2257.76	45	44277.94	$a\ ^2I_{3\frac{1}{2}} - y\ ^2I^0_{3\frac{1}{2}}$
2257.62	35	44280.69	$a\ ^2I_{3\frac{1}{2}} - y\ ^2I^0_{2\frac{1}{2}}$
2256.56	2	44301.49	$b\ ^4D_{2\frac{1}{2}} - x\ ^4F^0_{1\frac{1}{2}}$
2256.38	12	44305.02	$b\ ^4D_{1\frac{1}{2}} - x\ ^4F^0_{1\frac{1}{2}}$
2256.01	50	44312.28	$a\ ^2I_{3\frac{1}{2}} - x\ ^2H^0_{4\frac{1}{2}}$
			$b\ ^4D_{0\frac{1}{2}} - x\ ^4F^0_{1\frac{1}{2}}$
2253.29	1	44365.76	$a\ ^2D_{2\frac{1}{2}} - w\ ^2G^0_{3\frac{1}{2}}$
2252.37	4	44383.89	$a\ ^2F_{2\frac{1}{2}} - w\ ^2F^0_{2\frac{1}{2}}$
2249.98	20	44431.03	$a\ ^4D_{1\frac{1}{2}} - y\ ^4D^0_{1\frac{1}{2}}$
			$b\ ^4D_{2\frac{1}{2}} - x\ ^4F^0_{2\frac{1}{2}}$
2249.91	8	44432.41	$a\ ^4P_{0\frac{1}{2}} - y\ ^4P^0_{0\frac{1}{2}}$
			$a\ ^4P_{1\frac{1}{2}} - y\ ^4P^0_{0\frac{1}{2}}$
2249.78	30	44434.98	$b\ ^4D_{1\frac{1}{2}} - x\ ^4F^0_{2\frac{1}{2}}$
2249.32	2	44444.06	$b\ ^4D_{3\frac{1}{2}} - x\ ^4F^0_{3\frac{1}{2}}$
2248.56	40	44459.09	$b\ ^4D_{2\frac{1}{2}} - x\ ^4F^0_{3\frac{1}{2}}$
2248.30	50	44464.23	$b\ ^4D_{3\frac{1}{2}} - x\ ^4F^0_{4\frac{1}{2}}$
2247.91	18	44471.94	$b\ ^4D_{3\frac{1}{2}} - x\ ^4F^0_{3\frac{1}{2}}$
2245.33	7	44523.04	$a\ ^2F_{3\frac{1}{2}} - w\ ^2F^0_{3\frac{1}{2}}$
2244.90	20	44531.56	$a\ ^4P_{0\frac{1}{2}} - y\ ^4P^0_{1\frac{1}{2}}$
			$a\ ^4P_{1\frac{1}{2}} - y\ ^4P^0_{1\frac{1}{2}}$
2244.83	10	44532.95	$a\ ^4P_{2\frac{1}{2}} - y\ ^4P^0_{1\frac{1}{2}}$
2243.62	50	44556.96	$a\ ^2I_{4\frac{1}{2}} - x\ ^2H^0_{5\frac{1}{2}}$
2243.50	8	44559.35	
2243.28	40	44563.72	$a\ ^2I_{5\frac{1}{2}} - x\ ^2H^0_{6\frac{1}{2}}$
2241.80	30	44593.14	$a\ ^2I_{6\frac{1}{2}} - z\ ^2K^0_{8\frac{1}{2}}$
2241.69	15	44595.32	$b\ ^4D_{1\frac{1}{2}} - y\ ^2D^0_{1\frac{1}{2}}$
2241.47	3	44599.70	$a\ ^2I_{5\frac{1}{2}} - z\ ^2K^0_{8\frac{1}{2}}$
2241.30	15	44603.08	$b\ ^4D_{0\frac{1}{2}} - y\ ^2D^0_{1\frac{1}{2}}$
2239.51	4	44638.73	$a\ ^4G_{3\frac{1}{2}} - z\ ^4G^0_{3\frac{1}{2}}$
2239.24	8	44644.11	$a\ ^4G_{2\frac{1}{2}} - z\ ^4G^0_{3\frac{1}{2}}$
2238.87	1	44651.48	$a\ ^4D_{2\frac{1}{2}} - y\ ^4D^0_{2\frac{1}{2}}$
2236.47	3	44699.40	$a\ ^4G_{3\frac{1}{2}} - z\ ^4I^0_{4\frac{1}{2}}$
2234.58	12	44737.20	$a\ ^4G_{4\frac{1}{2}} - z\ ^4G^0_{5\frac{1}{2}}$
2234.50	7	44738.80	$a\ ^4G_{3\frac{1}{2}} - z\ ^4G^0_{3\frac{1}{2}}$
2234.22	5	44744.41	$a\ ^4G_{2\frac{1}{2}} - z\ ^4G^0_{3\frac{1}{2}}$
2231.45	15	44799.95	$c\ ^2F_{3\frac{1}{2}} - u\ ^2F^0_{3\frac{1}{2}}$
2231.02	12	44808.58	$a\ ^2I_{6\frac{1}{2}} - z\ ^2K^0_{7\frac{1}{2}}$
2230.57	2	44817.63	$a\ ^4D_{1\frac{1}{2}} - y\ ^4D^0_{2\frac{1}{2}}$
2230.18	1	44825.46	$a\ ^4P_{0\frac{1}{2}} - z\ ^2D^0_{1\frac{1}{2}}$
2228.82	5	44852.60	$c\ ^2G_{4\frac{1}{2}} - u\ ^2F^0_{3\frac{1}{2}}$
2228.34	15	44862.47	$c\ ^2F_{2\frac{1}{2}} - u\ ^2F^0_{2\frac{1}{2}}$
2228.26	12	44864.08	$a\ ^4G_{4\frac{1}{2}} - z\ ^4G^0_{5\frac{1}{2}}$
2228.18	8	44865.69	$a\ ^4G_{3\frac{1}{2}} - z\ ^4G^0_{4\frac{1}{2}}$
2227.88	10	44871.73	$a\ ^4G_{3\frac{1}{2}} - z\ ^4G^0_{4\frac{1}{2}}$
2226.47	7	44900.14	$a\ ^4G_{4\frac{1}{2}} - z\ ^4I^0_{5\frac{1}{2}}$
			$a\ ^4D_{3\frac{1}{2}} - y\ ^4D^0_{3\frac{1}{2}}$
2226.35	15	44902.56	$a\ ^4P_{1\frac{1}{2}} - y\ ^4P^0_{2\frac{1}{2}}$
2226.27	15	44904.18	$a\ ^4P_{2\frac{1}{2}} - y\ ^4P^0_{2\frac{1}{2}}$
2225.93	1	44911.03	$b\ ^4D_{1\frac{1}{2}} - y\ ^2D^0_{2\frac{1}{2}}$
2225.44	3	44920.92	$c\ ^2G_{3\frac{1}{2}} - u\ ^2F^0_{2\frac{1}{2}}$
2224.87	1	44932.43	$a\ ^2P_{1\frac{1}{2}} - w\ ^2D^0_{1\frac{1}{2}}$
			$b\ ^4F_{1\frac{1}{2}} - x\ ^2P^0_{0\frac{1}{2}}$
2221.86	12	44993.30	$c\ ^2G_{3\frac{1}{2}} - u\ ^2F^0_{3\frac{1}{2}}$
2220.31	1	45024.70	$a\ ^4G_{3\frac{1}{2}} - z\ ^2G^0_{3\frac{1}{2}}$
2220.01	2	45030.78	$a\ ^4G_{2\frac{1}{2}} - z\ ^2G^0_{3\frac{1}{2}}$
2219.17	1	45047.83	$a\ ^4P_{1\frac{1}{2}} - z\ ^2P^0_{0\frac{1}{2}}$
			$a\ ^4P_{0\frac{1}{2}} - z\ ^2P^0_{0\frac{1}{2}}$
2219.05	2	45050.26	
2218.36	6	45064.27	$a\ ^2P_{1\frac{1}{2}} - w\ ^2D^0_{2\frac{1}{2}}$
2217.89	7	45073.82	$b\ ^4D_{2\frac{1}{2}} - y\ ^2G^0_{3\frac{1}{2}}$
2216.32	4	45105.75	$a\ ^4G_{3\frac{1}{2}} - z\ ^4I^0_{4\frac{1}{2}}$
2215.30	5	45126.51	$a\ ^4D_{2\frac{1}{2}} - y\ ^4D^0_{2\frac{1}{2}}$
2215.08	20	45130.99	$a\ ^2G_{3\frac{1}{2}} - v\ ^2F^0_{2\frac{1}{2}}$
2213.68	30	45159.53	$a\ ^2G_{4\frac{1}{2}} - v\ ^2F^0_{3\frac{1}{2}}$
2213.56	10	45161.98	$a\ ^4G_{3\frac{1}{2}} - z\ ^2G^0_{4\frac{1}{2}}$
2212.30	3	45187.70	$a\ ^4P_{1\frac{1}{2}} - z\ ^2D^0_{2\frac{1}{2}}$
2212.21	15	45189.54	$a\ ^4G_{4\frac{1}{2}} - z\ ^4G^0_{5\frac{1}{2}}$
2211.85	20	45196.90	$a\ ^4G_{3\frac{1}{2}} - z\ ^4G^0_{3\frac{1}{2}}$
2209.43	10	45246.39	$a\ ^4P_{0\frac{1}{2}} - z\ ^2P^0_{1\frac{1}{2}}$
			$a\ ^4P_{1\frac{1}{2}} - z\ ^2P^0_{1\frac{1}{2}}$
2209.37	8	45247.62	$a\ ^4P_{2\frac{1}{2}} - z\ ^2P^0_{1\frac{1}{2}}$
2208.27	2	45270.16	$b\ ^4D_{2\frac{1}{2}} - x\ ^4G^0_{3\frac{1}{2}}$
2208.08	3	45274.05	$b\ ^4D_{1\frac{1}{2}} - x\ ^4G^0_{2\frac{1}{2}}$
2205.34	4	45330.30	$a\ ^2G_{3\frac{1}{2}} - v\ ^2F^0_{3\frac{1}{2}}$
2203.89	10	45360.12	$a\ ^4D_{3\frac{1}{2}} - z\ ^4G^0_{4\frac{1}{2}}$
2202.93	7	45379.88	$b\ ^4D_{2\frac{1}{2}} - x\ ^4G^0_{3\frac{1}{2}}$
2202.30	3	45392.86	$b\ ^4D_{3\frac{1}{2}} - x\ ^4G^0_{4\frac{1}{2}}$
2202.04	3	45398.22	$a\ ^4D_{1\frac{1}{2}} - z\ ^2S^0_{0\frac{1}{2}}$
2200.50	8	45429.99	
2199.23	5	45456.22	$a\ ^2D_{1\frac{1}{2}} - w\ ^2F^0_{2\frac{1}{2}}$
2199.09	2	45459.11	$a\ ^4D_{2\frac{1}{2}} - z\ ^4G^0_{3\frac{1}{2}}$
2197.06	2	45501.11	$a\ ^4D_{0\frac{1}{2}} - z\ ^2S^0_{0\frac{1}{2}}$
2196.84	15	45505.67	$a\ ^2F_{2\frac{1}{2}} - z\ ^2D^0_{2\frac{1}{2}}$
2195.78	4	45527.63	$a\ ^2D_{2\frac{1}{2}} - w\ ^2F^0_{3\frac{1}{2}}$
2193.30	20	45579.11	$a\ ^2F_{3\frac{1}{2}} - x\ ^2D^0_{2\frac{1}{2}}$
2193.11	10	45583.05	
2191.08	2	45625.29	$b\ ^2F_{3\frac{1}{2}} - v\ ^2F^0_{3\frac{1}{2}}$
2190.92	5	45628.62	$a\ ^2P_{0\frac{1}{2}} - w\ ^2D^0_{1\frac{1}{2}}$
2190.52	2	45636.95	$a\ ^2D_{2\frac{1}{2}} - w\ ^2F^0_{2\frac{1}{2}}$
2190.13	4	45645.07	$b\ ^4D_{3\frac{1}{2}} - x\ ^4G^0_{4\frac{1}{2}}$
2189.62	4	45655.70	$a\ ^4D_{3\frac{1}{2}} - z\ ^2G^0_{4\frac{1}{2}}$
2189.24	3	45663.62	$b\ ^2F_{2\frac{1}{2}} - v\ ^2F^0_{2\frac{1}{2}}$
2187.70	2	45695.77	$c\ ^2D_{2\frac{1}{2}} - u\ ^2D^0_{2\frac{1}{2}}$
2181.54	4	45824.78	$b\ ^2F_{3\frac{1}{2}} - v\ ^2F^0_{3\frac{1}{2}}$
2179.72	2	45863.04	$b\ ^2F_{2\frac{1}{2}} - v\ ^2F^0_{3\frac{1}{2}}$
2179.39	1	45869.98	$a\ ^4F_{2\frac{1}{2}} - w\ ^2F^0_{2\frac{1}{2}}$
2178.46	3	45889.56	$c\ ^2G_{3\frac{1}{2}} - v\ ^2G^0_{3\frac{1}{2}}$
2171.55	20	46035.57	$a\ ^4P_{0\frac{1}{2}} - x\ ^4D^0_{0\frac{1}{2}}$
			$a\ ^4P_{1\frac{1}{2}} - x\ ^4D^0_{0\frac{1}{2}}$
2171.18	30	46043.41	$a\ ^4P_{1\frac{1}{2}} - x\ ^4D^0_{2\frac{1}{2}}$
2171.06	40	46045.95	$a\ ^4P_{0\frac{1}{2}} - x\ ^4D^0_{1\frac{1}{2}}$
			$a\ ^4P_{1\frac{1}{2}} - x\ ^4D^0_{1\frac{1}{2}}$
2170.97	10	46047.86	$a\ ^4P_{2\frac{1}{2}} - x\ ^4D^0_{1\frac{1}{2}}$
2170.71	50	46053.38	$a\ ^4P_{2\frac{1}{2}} - x\ ^4D^0_{2\frac{1}{2}}$
2167.81	3	46114.98	$c\ ^2G_{4\frac{1}{2}} - v\ ^2G^0_{4\frac{1}{2}}$
			$b\ ^2G_{4\frac{1}{2}} - u\ ^2F^0_{3\frac{1}{2}}$
2166.75	10	46137.54	$a\ ^4G_{2\frac{1}{2}} - z\ ^2D^0_{2\frac{1}{2}}$
2164.67	7	46182.51	$a\ ^2D_{1\frac{1}{2}} - x\ ^2P^0_{1\frac{1}{2}}$
2163.40	3	46208.97	$a\ ^4G_{3\frac{1}{2}} - y\ ^4P^0_{2\frac{1}{2}}$
2161.66	10	46246.59	$a\ ^2D_{1\frac{1}{2}} - x\ ^2P^0_{0\frac{1}{2}}$
2156.22	20	46362.83	$a\ ^2D_{2\frac{1}{2}} - x\ ^2P^0_{1\frac{1}{2}}$
2150.74	30	46480.95	$a\ ^4P_{1\frac{1}{2}} - z\ ^4S^0_{1\frac{1}{2}}$
			$a\ ^4P_{0\frac{1}{2}} - z\ ^4S^0_{1\frac{1}{2}}$
2150.65	20	46482.89	$a\ ^4P_{2\frac{1}{2}} - z\ ^4S^0_{1\frac{1}{2}}$
2150.10	15	46494.78	$a\ ^4G_{3\frac{1}{2}} - z\ ^2D^0_{2\frac{1}{2}}$
2147.19	30	46557.78	$a\ ^4D_{2\frac{1}{2}} - y\ ^4P^0_{1\frac{1}{2}}$
2146.23	10	46578.58	$a\ ^2D_{1\frac{1}{2}} - x\ ^2D^0_{1\frac{1}{2}}$
2145.97	15	46584.25	$a\ ^2D_{2\frac{1}{2}} - x\ ^2D^0_{2\frac{1}{2}}$

TABLE 1. *Wavelengths of* Cr II *in air*—Continued

Wavelength	Intensity	Wave number	Term combination
2144.05	15	46625.96	$a\ ^4D_{1\frac{1}{2}} - y\ ^4P^0_{2\frac{1}{2}}$
2143.86	5	46630.09	$c\ ^2F_{3\frac{1}{2}} - v\ ^2D^0_{2\frac{1}{2}}$
2140.50	20	46703.28	$a\ ^4D_{3\frac{1}{2}} - y\ ^4P^0_{2\frac{1}{2}}$
2139.54	10	46724.01	$a\ ^4D_{1\frac{1}{2}} - y\ ^4P^0_{1\frac{1}{2}}$
2139.33	7	46728.82	$a\ ^4D_{0\frac{1}{2}} - y\ ^4P^0_{0\frac{1}{2}}$
2137.96	15	46758.76	$a\ ^2D_{2\frac{1}{2}} - x\ ^2D^0_{2\frac{1}{2}}$
2137.50	7	46768.82	$c\ ^2F_{2\frac{1}{2}} - v\ ^2D^0_{1\frac{1}{2}}$
2135.42	50	46814.37	$a\ ^4G_{4\frac{1}{2}} - y\ ^4G^0_{3\frac{1}{2}}$
2135.34	50	46816.12	$a\ ^4G_{3\frac{1}{2}} - y\ ^4G^0_{3\frac{1}{2}}$
2135.09	15	46821.60	$a\ ^4G_{2\frac{1}{2}} - y\ ^4G^0_{3\frac{1}{2}}$
2134.88	25	46826.21	$a\ ^4G_{3\frac{1}{2}} - y\ ^4G^0_{2\frac{1}{2}}$ $a\ ^4D_{0\frac{1}{2}} - y\ ^4P^0_{1\frac{1}{2}}$
2134.62	75	46831.91	$a\ ^4G_{2\frac{1}{2}} - y\ ^4G^0_{3\frac{1}{2}}$
2134.52	100	46833.89	$a\ ^4G_{4\frac{1}{2}} - y\ ^4G^0_{4\frac{1}{2}}$
2134.20	40	46841.13	$a\ ^4G_{5\frac{1}{2}} - y\ ^4G^0_{4\frac{1}{2}}$
2133.81	18	46849.47	$a\ ^4G_{4\frac{1}{2}} - y\ ^4G^0_{3\frac{1}{2}}$
2133.49	100	46856.49	$a\ ^4G_{3\frac{1}{2}} - y\ ^4G^0_{3\frac{1}{2}}$
2133.03	30	46866.60	$a\ ^4G_{2\frac{1}{2}} - y\ ^4F^0_{1\frac{1}{2}}$
2132.93	40	46869.01	$a\ ^4G_{3\frac{1}{2}} - y\ ^4F^0_{2\frac{1}{2}}$
2132.71	35	46873.85	$a\ ^4G_{4\frac{1}{2}} - y\ ^4F^0_{3\frac{1}{2}}$
2132.62	40	46875.83	$a\ ^4G_{2\frac{1}{2}} - y\ ^4F^0_{2\frac{1}{2}}$ $a\ ^4G_{3\frac{1}{2}} - y\ ^4F^0_{3\frac{1}{2}}$
2132.38	8	46880.88	$a\ ^4G_{2\frac{1}{2}} - y\ ^4F^0_{3\frac{1}{2}}$
2130.22	50	46928.41	$a\ ^2I_{6\frac{1}{2}} - w\ ^2H^0_{5\frac{1}{2}}$ $a\ ^4G_{4\frac{1}{2}} - y\ ^4F^0_{4\frac{1}{2}}$ $a\ ^4D_{2\frac{1}{2}} - y\ ^4P^0_{2\frac{1}{2}}$
2129.89	50	46935.69	$a\ ^4G_{5\frac{1}{2}} - y\ ^4F^0_{4\frac{1}{2}}$ $a\ ^2I_{5\frac{1}{2}} - w\ ^2H^0_{5\frac{1}{2}}$
2127.53	8	46987.96	$a\ ^4G_{4\frac{1}{2}} - z\ ^2I^0_{5\frac{1}{2}}$
2127.26	7	46993.92	$a\ ^4G_{5\frac{1}{2}} - z\ ^2I^0_{5\frac{1}{2}}$
2121.50	1	47121.50	$a\ ^4D_{0\frac{1}{2}} - z\ ^2D^0_{1\frac{1}{2}}$
2121.26	30	47126.83	$a\ ^2I_{5\frac{1}{2}} - w\ ^2H^0_{4\frac{1}{2}}$
2116.17	1	47240.16	$a\ ^4D_{1\frac{1}{2}} - z\ ^2P^0_{0\frac{1}{2}}$
2113.04	8	47310.14	$a\ ^4D_{3\frac{1}{2}} - y\ ^4G^0_{3\frac{1}{2}}$
2112.16	10	47329.84	$a\ ^4D_{3\frac{1}{2}} - y\ ^4G^0_{4\frac{1}{2}}$
2111.57	3	47343.07	$a\ ^4D_{0\frac{1}{2}} - z\ ^2P^0_{0\frac{1}{2}}$
2111.26	4	47350.02	$a\ ^4G_{3\frac{1}{2}} - x\ ^4D^0_{2\frac{1}{2}}$
2110.98	10	47356.30	$a\ ^4G_{2\frac{1}{2}} - x\ ^4D^0_{2\frac{1}{2}}$
2110.92	5	47357.64	$a\ ^4G_{2\frac{1}{2}} - x\ ^4D^0_{1\frac{1}{2}}$
2110.68	4	47363.02	$a\ ^4G_{4\frac{1}{2}} - x\ ^4D^0_{3\frac{1}{2}}$
2110.37	5	47369.99	$a\ ^4D_{3\frac{1}{2}} - y\ ^4F^0_{3\frac{1}{2}}$
2109.85	6	47381.66	$a\ ^4D_{1\frac{1}{2}} - z\ ^2D^0_{2\frac{1}{2}}$
2107.92	15	47425.03	$a\ ^4D_{2\frac{1}{2}} - y\ ^4F^0_{2\frac{1}{2}}$
2107.28	2	47439.44	$a\ ^4D_{1\frac{1}{2}} - z\ ^2P^0_{1\frac{1}{2}}$
2102.97	25	47536.65	$a\ ^4D_{2\frac{1}{2}} - y\ ^4G^0_{3\frac{1}{2}}$
2102.72	7	47542.30	$a\ ^4D_{0\frac{1}{2}} - z\ ^2P^0_{1\frac{1}{2}}$
2102.55	5	47546.13	$a\ ^4D_{2\frac{1}{2}} - y\ ^4G^0_{2\frac{1}{2}}$
2101.69	4	47565.60	
2100.96	2	47582.13	$a\ ^4D_{2\frac{1}{2}} - y\ ^4F^0_{1\frac{1}{2}}$
2100.61	10	47590.05	$a\ ^4D_{2\frac{1}{2}} - y\ ^4F^0_{2\frac{1}{2}}$
2100.34	15	47596.16	$a\ ^4D_{2\frac{1}{2}} - y\ ^4F^0_{3\frac{1}{2}}$
2096.42	6	47684.70	$a\ ^2F_{2\frac{1}{2}} - w\ ^2D^0_{1\frac{1}{2}}$
2093.62	2	47748.92	$a\ ^4D_{1\frac{1}{2}} - y\ ^4F^0_{1\frac{1}{2}}$
2093.29	8	47756.45	$a\ ^4D_{1\frac{1}{2}} - y\ ^4F^0_{2\frac{1}{2}}$
2090.70	20	47815.60	$a\ ^4P_{1\frac{1}{2}} - y\ ^2D^0_{1\frac{1}{2}}$
2089.12	12	47851.76	$a\ ^4D_{0\frac{1}{2}} - y\ ^4F^0_{1\frac{1}{2}}$ $a\ ^4D_{2\frac{1}{2}} - x\ ^4D^0_{2\frac{1}{2}}$
2084.43	4	47959.41	$a\ ^4G_{4\frac{1}{2}} - z\ ^2H^0_{4\frac{1}{2}}$ $a\ ^4G_{3\frac{1}{2}} - z\ ^2H^0_{4\frac{1}{2}}$
2079.86	10	48064.78	$a\ ^2F_{3\frac{1}{2}} - w\ ^2D^0_{2\frac{1}{2}}$
2079.65	2	48069.63	$a\ ^4D_{2\frac{1}{2}} - x\ ^4D^0_{2\frac{1}{2}}$
2079.27	20	48078.41	$a\ ^4D_{2\frac{1}{2}} - x\ ^4D^0_{3\frac{1}{2}}$
2076.96	30	48131.88	$a\ ^4P_{2\frac{1}{2}} - y\ ^2D^0_{2\frac{1}{2}}$
2073.21	4	48218.93	$a\ ^4G_{4\frac{1}{2}} - z\ ^2H^0_{5\frac{1}{2}}$
2072.90	5	48226.14	$a\ ^4G_{3\frac{1}{2}} - z\ ^2H^0_{5\frac{1}{2}}$
2072.56	2	48234.05	$a\ ^4D_{1\frac{1}{2}} - x\ ^4D^0_{2\frac{1}{2}}$ $a\ ^4D_{1\frac{1}{2}} - x\ ^4D^0_{0\frac{1}{2}}$
2068.63	1	48325.67	$a\ ^4G_{3\frac{1}{2}} - y\ ^4H^0_{4\frac{1}{2}}$
2068.38	8	48331.51	$a\ ^4G_{2\frac{1}{2}} - y\ ^4H^0_{3\frac{1}{2}}$
2068.22	1	48335.25	$a\ ^4D_{0\frac{1}{2}} - x\ ^4D^0_{1\frac{1}{2}}$
2066.96	3	48364.71	$b\ ^4D_{1\frac{1}{2}} - w\ ^4D^0_{0\frac{1}{2}}$
2066.75	3	48369.62	$b\ ^4D_{1\frac{1}{2}} - w\ ^4D^0_{1\frac{1}{2}}$
2066.66	2	48371.73	$b\ ^4D_{0\frac{1}{2}} - w\ ^4D^0_{0\frac{1}{2}}$
2066.44	2	48376.88	$b\ ^4D_{0\frac{1}{2}} - w\ ^4D^0_{1\frac{1}{2}}$
2065.89	10	48389.75	$b\ ^4D_{2\frac{1}{2}} - w\ ^4D^0_{2\frac{1}{2}}$
2065.46	150	48399.83	$a\ ^6S_{2\frac{1}{2}} - z\ ^6P^0_{1\frac{1}{2}}$
2063.76	4	48439.69	$b\ ^4D_{2\frac{1}{2}} - w\ ^4D^0_{3\frac{1}{2}}$
2063.21	10	48452.60	$b\ ^4D_{3\frac{1}{2}} - w\ ^4D^0_{3\frac{1}{2}}$
2062.25	10	48475.14	$a\ ^4G_{3\frac{1}{2}} - y\ ^4H^0_{4\frac{1}{2}}$
2061.54	175	48491.85	$a\ ^6S_{2\frac{1}{2}} - z\ ^6P^0_{2\frac{1}{2}}$
2061.03	3	48503.84	$a\ ^2G_{3\frac{1}{2}} - u\ ^2F^0_{2\frac{1}{2}}$
2057.95	1	48576.43	$a\ ^2G_{3\frac{1}{2}} - u\ ^2F^0_{3\frac{1}{2}}$
2055.59	200	48632.19	$a\ ^6S_{2\frac{1}{2}} - z\ ^6P^0_{3\frac{1}{2}}$
2054.75	10	48652.07	$a\ ^4G_{4\frac{1}{2}} - y\ ^4H^0_{5\frac{1}{2}}$
2054.44	4	48659.41	$a\ ^4G_{5\frac{1}{2}} - y\ ^4H^0_{5\frac{1}{2}}$
2050.32	10	48757.17	$a\ ^2D_{1\frac{1}{2}} - w\ ^2D^0_{1\frac{1}{2}}$
2047.32	2	48828.61	$a\ ^2F_{2\frac{1}{2}} - v\ ^2F^0_{2\frac{1}{2}}$
2046.98	8	48836.72	$a\ ^4G_{2\frac{1}{2}} - x\ ^4F^0_{1\frac{1}{2}}$
2045.30	12	48876.83	$a\ ^2F_{3\frac{1}{2}} - v\ ^2F^0_{2\frac{1}{2}}$ $a\ ^4G_{5\frac{1}{2}} - y\ ^4H^0_{5\frac{1}{2}}$
2044.76	1	48889.73	$a\ ^2D_{1\frac{1}{2}} - w\ ^2D^0_{2\frac{1}{2}}$
2043.93	3	48909.58	
2042.78	5	48937.12	$a\ ^2D_{2\frac{1}{2}} - w\ ^2D^0_{1\frac{1}{2}}$
2041.80	7	48960.60	$a\ ^4G_{3\frac{1}{2}} - x\ ^4F^0_{2\frac{1}{2}}$
2041.57	6	48966.11	$a\ ^4G_{2\frac{1}{2}} - x\ ^4F^0_{2\frac{1}{2}}$
2041.02	8	48979.30	$a\ ^4G_{4\frac{1}{2}} - x\ ^4F^0_{3\frac{1}{2}}$
2040.68	20*d*	48987.47	$a\ ^4G_{3\frac{1}{2}} - x\ ^4F^0_{4\frac{1}{2}}$ $a\ ^4G_{4\frac{1}{2}} - x\ ^4F^0_{3\frac{1}{2}}$
2040.42	4	48993.71	$a\ ^4G_{3\frac{1}{2}} - x\ ^4F^0_{3\frac{1}{2}}$
2039.90	10	49006.20	$a\ ^6S_{2\frac{1}{2}} - z\ ^4P^0_{1\frac{1}{2}}$
2038.64	2	49036.46	$b\ ^2F_{2\frac{1}{2}} - u\ ^2F^0_{2\frac{1}{2}}$
2037.26	4	49069.69	$a\ ^2D_{2\frac{1}{2}} - w\ ^2D^0_{2\frac{1}{2}}$ $b\ ^2F_{3\frac{1}{2}} - u\ ^2F^0_{3\frac{1}{2}}$
2036.98	3	49076.44	$a\ ^2F_{3\frac{1}{2}} - v\ ^2F^0_{3\frac{1}{2}}$
2034.88	15	49127.08	$a\ ^4G_{3\frac{1}{2}} - y\ ^2D^0_{1\frac{1}{2}}$
2029.84	1	49249.04	$a\ ^2P_{1\frac{1}{2}} - u\ ^2F^0_{2\frac{1}{2}}$
2028.86	5	49272.82	$b\ ^4D_{2\frac{1}{2}} - w\ ^4F^0_{2\frac{1}{2}}$
2028.69	5	49276.95	$b\ ^4D_{1\frac{1}{2}} - w\ ^4F^0_{2\frac{1}{2}}$
2027.69	8	49301.25	$a\ ^2G_{4\frac{1}{2}} - v\ ^2G^0_{4\frac{1}{2}}$
2025.58	5	49352.60	$a\ ^6S_{2\frac{1}{2}} - z\ ^4P^0_{2\frac{1}{2}}$
2024.20	2	49386.24	$a\ ^4G_{2\frac{1}{2}} - y\ ^2G^0_{3\frac{1}{2}}$
2024.02	2	49390.63	$b\ ^4D_{3\frac{1}{2}} - w\ ^4F^0_{3\frac{1}{2}}$
2022.10	12	49437.52	$b\ ^4D_{2\frac{1}{2}} - x\ ^4P^0_{2\frac{1}{2}}$ $a\ ^4G_{3\frac{1}{2}} - y\ ^2D^0_{2\frac{1}{2}}$
2021.89	5	49442.66	$a\ ^4G_{2\frac{1}{2}} - y\ ^2D^0_{2\frac{1}{2}}$
2021.56	20	49450.73	$b\ ^4D_{3\frac{1}{2}} - x\ ^4P^0_{2\frac{1}{2}}$
2020.69	10	49472.01	$b\ ^4D_{3\frac{1}{2}} - w\ ^4F^0_{4\frac{1}{2}}$ $a\ ^4D_{2\frac{1}{2}} - x\ ^4F^0_{2\frac{1}{2}}$ $a\ ^2G_{3\frac{1}{2}} - v\ ^2G^0_{3\frac{1}{2}}$
2020.31	1	49481.32	$a\ ^4D_{3\frac{1}{2}} - x\ ^4F^0_{3\frac{1}{2}}$
2019.88	2	49491.85	
2017.48	2	49550.72	$a\ ^4D_{2\frac{1}{2}} - x\ ^4F^0_{3\frac{1}{2}}$
2016.90	7	49564.96	$a\ ^6S_{2\frac{1}{2}} - z\ ^6D^0_{3\frac{1}{2}}$
2016.27	7	49580.45	

TABLE 1. *Wavelengths of* Cr II *in air*—Continued

Wavelength	Intensity	Wave number	Term combination	Wavelength	Intensity	Wave No.	Term combination
2015.87	15	49590.29	$a\ ^4G_{2\frac{1}{2}} - y\ ^2G^0_{3\frac{1}{2}}$	2004.24	10	49878.00	$b\ ^4D_{1\frac{1}{2}} - x\ ^4P^0_{0\frac{1}{2}}$
2013.65	40	49644.95	$a\ ^6S_{2\frac{1}{2}} - z\ ^6D^0_{3\frac{1}{2}}$	2004.03	5	49883.22	$a\ ^4G_{3\frac{1}{2}} - y\ ^2H^0_{4\frac{1}{2}}$
2012.74	10	49667.39	$a\ ^2G_{4\frac{1}{2}} - v\ ^2G^0_{3\frac{1}{2}}$	2003.88	35	49886.96	$a\ ^4G_{3\frac{1}{2}} - y\ ^2H^0_{5\frac{1}{2}}$
2012.58	20	49671.34	$b\ ^4D_{2\frac{1}{2}} - x\ ^4P^0_{1\frac{1}{2}}$	2002.99	30	49909.12	$a\ ^4G_{3\frac{1}{2}} - x\ ^4G^0_{3\frac{1}{2}}$
2012.43	10	49675.04	$b\ ^4D_{1\frac{1}{2}} - x\ ^4P^0_{1\frac{1}{2}}$	2002.71	10	49916.10	$a\ ^4G_{2\frac{1}{2}} - x\ ^4G^0_{3\frac{1}{2}}$
2012.21	25	49680.47	$a\ ^4D_{2\frac{1}{2}} - x\ ^4F^0_{3\frac{1}{2}}$	2001.65	4	49942.53	$b\ ^4D_{1\frac{1}{2}} - y\ ^2P^0_{1\frac{1}{2}}$
2012.12	4	49682.69	$b\ ^4D_{0\frac{1}{2}} - x\ ^4P^0_{1\frac{1}{2}}$	2001.36	3	49949.76	$b\ ^4D_{0\frac{1}{2}} - y\ ^2P^0_{1\frac{1}{2}}$
2011.13	20	49707.14	$a\ ^6S_{2\frac{1}{2}} - z\ ^6D^0_{2\frac{1}{2}}$ $a\ ^4D_{2\frac{1}{2}} - x\ ^4F^0_{3\frac{1}{2}}$	2000.76	5	49964.74	$b\ ^2H_{4\frac{1}{2}} - v\ ^2G^0_{3\frac{1}{2}}$
2007.39	10	49799.74	$a\ ^4G_{3\frac{1}{2}} - x\ ^4G^0_{3\frac{1}{2}}$				
2007.18	20	49804.95	$a\ ^4G_{2\frac{1}{2}} - x\ ^4G^0_{2\frac{1}{2}}$				
2006.91	10	49811.65	$b\ ^4D_{1\frac{1}{2}} - y\ ^2P^0_{0\frac{1}{2}}$				
2006.61	10	49819.10	$b\ ^4D_{0\frac{1}{2}} - y\ ^2P^0_{0\frac{1}{2}}$ $a\ ^4D_{0\frac{1}{2}} - x\ ^4F^0_{1\frac{1}{2}}$				
2005.50	4	49846.67	$a\ ^4D_{1\frac{1}{2}} - x\ ^4F^0_{2\frac{1}{2}}$				
2005.19	3	49854.37					
2004.34	35	49875.51	$a\ ^4G_{4\frac{1}{2}} - y\ ^2H^0_{5\frac{1}{2}}$ $a\ ^4G_{3\frac{1}{2}} - y\ ^2H^0_{4\frac{1}{2}}$				

TABLE 2. *Wavelengths of* Cr II *in vacuum*

Wavelength	Intensity	Wave number	Term combination	Wavelength	Intensity	Wave number	Term combination
1998.14	2	50046.54	$a\ ^2H_{4\frac{1}{2}} - u\ ^2F^0_{3\frac{1}{2}}$	1866.32	15	53581.26	$a\ ^2F_{2\frac{1}{2}} - v\ ^2G^0_{4\frac{1}{2}}$
1996.62	3	50084.54	$a\ ^4D_{3\frac{1}{2}} - y\ ^2G^0_{4\frac{1}{2}}$	1865.80	1	53596.31	$a\ ^4G_{4\frac{1}{2}} - x\ ^2F^0_{3\frac{1}{2}}$ $a\ ^4G_{3\frac{1}{2}} - x\ ^2F^0_{3\frac{1}{2}}$
1993.63	25	50159.81	$a\ ^4G_{4\frac{1}{2}} - x\ ^4G^0_{5\frac{1}{2}}$	1860.12	12	53759.85	$a\ ^4G_{2\frac{1}{2}} - w\ ^4F^0_{1\frac{1}{2}}$
1993.37	15	50166.40	$a\ ^4G_{3\frac{1}{2}} - x\ ^4G^0_{4\frac{1}{2}}$	1858.72	15	53800.52	$a\ ^4G_{3\frac{1}{2}} - w\ ^4F^0_{2\frac{1}{2}}$
1990.79	10	50231.22	$b\ ^2H_{3\frac{1}{2}} - v\ ^2G^0_{4\frac{1}{2}}$	1858.44	20	53808.43	$a\ ^4G_{2\frac{1}{2}} - w\ ^4F^0_{2\frac{1}{2}}$
1987.43	5	50316.24	$a\ ^2F_{2\frac{1}{2}} - w\ ^2P^0_{1\frac{1}{2}}$				
1985.67	12	50360.92	$a\ ^4G_{4\frac{1}{2}} - x\ ^4G^0_{4\frac{1}{2}}$	1855.14	20	53904.35	$a\ ^4G_{4\frac{1}{2}} - w\ ^4F^0_{3\frac{1}{2}}$ $a\ ^4G_{3\frac{1}{2}} - w\ ^4F^0_{3\frac{1}{2}}$
1985.52	22	50364.69	$a\ ^4G_{3\frac{1}{2}} - x\ ^4G^0_{4\frac{1}{2}}$	1854.68	3	53917.75	$a\ ^4G_{3\frac{1}{2}} - x\ ^2F^0_{3\frac{1}{2}}$
1963.00	15	50942.56	$a\ ^2H_{4\frac{1}{2}} - v\ ^2G^0_{3\frac{1}{2}}$	1854.46	1	53924.05	$a\ ^4G_{2\frac{1}{2}} - x\ ^2F^0_{3\frac{1}{2}}$
1955.93	15	51126.52	$a\ ^2H_{3\frac{1}{2}} - v\ ^2G^0_{3\frac{1}{2}}$	1852.37	3	53984.96	$a\ ^4G_{4\frac{1}{2}} - w\ ^4F^0_{4\frac{1}{2}}$
1950.06	50	51280.39	$c\ ^2G_{4\frac{1}{2}} - u\ ^2G^0_{4\frac{1}{2}}$	1852.13	25	53991.80	$a\ ^4G_{3\frac{1}{2}} - w\ ^4F^0_{4\frac{1}{2}}$
1949.22	35	51302.57	$c\ ^2G_{3\frac{1}{2}} - u\ ^2G^0_{3\frac{1}{2}}$				
1949.00	40	51308.42	$a\ ^2H_{4\frac{1}{2}} - v\ ^2G^0_{4\frac{1}{2}}$	1836.23	12	54459.44	$a\ ^4D_{3\frac{1}{2}} - x\ ^4P^0_{2\frac{1}{2}}$
1948.51	10	51321.32	$a\ ^2D_{1\frac{1}{2}} - w\ ^2P^0_{0\frac{1}{2}}$	1830.61	5	54626.66	$a\ ^6S_{2\frac{1}{2}} - z\ ^4D^0_{3\frac{1}{2}}$
1945.98	10	51388.49	$a\ ^2D_{1\frac{1}{2}} - w\ ^2P^0_{1\frac{1}{2}}$	1828.62	3	54686.05	$a\ ^4D_{2\frac{1}{2}} - x\ ^4P^0_{2\frac{1}{2}}$
1939.96	5	51549.02	$c\ ^2F_{3\frac{1}{2}} - u\ ^2D^0_{3\frac{1}{2}}$	1825.34	3	54784.16	$a\ ^6S_{2\frac{1}{2}} - z\ ^4D^0_{2\frac{1}{2}}$
1939.15	6	51568.99	$a\ ^2D_{2\frac{1}{2}} - w\ ^2P^0_{1\frac{1}{2}}$	1823.07	1	54852.53	$a\ ^4D_{1\frac{1}{2}} - x\ ^4P^0_{2\frac{1}{2}}$
1938.42	3	51588.51	$a\ ^4P_{0\frac{1}{2}} - w\ ^4D^0_{1\frac{1}{2}}$	1821.58	8	54897.25	$a\ ^6D_{4\frac{1}{2}} - y\ ^4F^0_{3\frac{1}{2}}$
1937.56	20	51611.30	$a\ ^4P_{1\frac{1}{2}} - w\ ^4D^0_{2\frac{1}{2}}$	1820.84	4	54919.83	$a\ ^4D_{2\frac{1}{2}} - x\ ^4P^0_{1\frac{1}{2}}$
1935.58	25	51664.02	$a\ ^4P_{2\frac{1}{2}} - w\ ^4D^0_{3\frac{1}{2}}$	1819.81	5	54950.79	$a\ ^6D_{4\frac{1}{2}} - y\ ^4F^0_{4\frac{1}{2}}$
				1818.89	1	54978.53	$a\ ^2D_{1\frac{1}{2}} - v\ ^2D^0_{2\frac{1}{2}}$
1932.64	5	51742.66	$c\ ^2G_{3\frac{1}{2}} - u\ ^2D^0_{2\frac{1}{2}}$	1815.32	3	55086.56	$a\ ^4D_{1\frac{1}{2}} - x\ ^4P^0_{1\frac{1}{2}}$
1929.96	12	51814.65	$c\ ^2F_{2\frac{1}{2}} - u\ ^2D^0_{1\frac{1}{2}}$				
1923.02	8	52001.43	$a\ ^2F_{3\frac{1}{2}} - u\ ^2F^0_{3\frac{1}{2}}$	1813.50	1	55141.99	$a\ ^6D_{3\frac{1}{2}} - y\ ^4F^0_{4\frac{1}{2}}$
1918.30	4	52129.39	$a\ ^4G_{4\frac{1}{2}} - z\ ^2G^0_{4\frac{1}{2}}$	1812.95	1	55158.60	$a\ ^2D_{2\frac{1}{2}} - v\ ^2D^0_{2\frac{1}{2}}$
1911.36	7	52318.88	$a\ ^2F_{3\frac{1}{2}} - u\ ^2F^0_{3\frac{1}{2}}$	1810.08	5	55246.10	$a\ ^4D_{2\frac{1}{2}} - y\ ^4F^0_{3\frac{1}{2}}$
				1808.66	2	55289.68	$a\ ^4D_{1\frac{1}{2}} - x\ ^4P^0_{0\frac{1}{2}}$
1907.36	3	52428.49	$a\ ^6D_{4\frac{1}{2}} - y\ ^4D^0_{3\frac{1}{2}}$	1791.51	2	55818.86	$b\ ^2F_{3\frac{1}{2}} - u\ ^2D^0_{2\frac{1}{2}}$
1898.92	35	52661.51	$a\ ^4P_{2\frac{1}{2}} - x\ ^4P^0_{2\frac{1}{2}}$	1786.07	2	55988.99	$b\ ^2F_{2\frac{1}{2}} - u\ ^2D^0_{1\frac{1}{2}}$
1890.55	30	52894.72	$a\ ^4P_{1\frac{1}{2}} - x\ ^4P^0_{1\frac{1}{2}}$				
1887.96	6	52967.30	$a\ ^2F_{2\frac{1}{2}} - v\ ^2G^0_{3\frac{1}{2}}$				
1884.12	1	53075.18	$a\ ^2D_{1\frac{1}{2}} - u\ ^2F^0_{2\frac{1}{2}}$				
1883.35	10	53096.88	$a\ ^4P_{0\frac{1}{2}} - x\ ^4P^0_{0\frac{1}{2}}$				
1881.06	6	53161.41	$a\ ^4P_{2\frac{1}{2}} - y\ ^2P^0_{1\frac{1}{2}}$				
1879.05	10	53218.38	$a\ ^2F_{3\frac{1}{2}} - v\ ^2G^0_{3\frac{1}{2}}$				
1875.22	3	53327.08	$a\ ^2D_{2\frac{1}{2}} - u\ ^2F^0_{3\frac{1}{2}}$				
1870.46	1	53462.64	$a\ ^4D_{3\frac{1}{2}} - w\ ^4D^0_{3\frac{1}{2}}$				

TABLE 3. *Even terms of* Cr II

Electron configuration	Term symbol	Level	$\Delta\nu$	Observed g
$3d^5$	$a\ ^6S_{2\frac{1}{2}}$	0. 00		
$3d^4(a\ ^5D)4s$	$a\ ^6D_{0\frac{1}{2}}$	11962. 00	70. 72	3. 323
	$^6D_{1\frac{1}{2}}$	12032. 72	115. 28	1. 867
	$^6D_{2\frac{1}{2}}$	12148. 00	155. 98	1. 669
	$^6D_{3\frac{1}{2}}$	12303. 98	192. 81	1. 578
	$^6D_{4\frac{1}{2}}$	12496. 79		1. 554
$3d^4(a\ ^5D)4s$	$a\ ^4D_{0\frac{1}{2}}$	19528. 38	102. 90	0. 000
	$^4D_{1\frac{1}{2}}$	19631. 28	166. 73	1. 192
	$^4D_{2\frac{1}{2}}$	19798. 01	226. 17	1. 370
	$^4D_{3\frac{1}{2}}$	20024. 18		1. 427
$3d^5$	$a\ ^4G_{2\frac{1}{2}}$	20512. 62	5. 71	0. 599
	$^4G_{3\frac{1}{2}}$	20518. 33	1. 52	0. 994
	$^4G_{4\frac{1}{2}}$	20519. 85	−7. 10	1. 161
	$^4G_{5\frac{1}{2}}$	20512. 75		1. 278
$3d^5$	$a\ ^4P_{0\frac{1}{2}}$	21824. 25	0. 57	2. 693
	$^4P_{1\frac{1}{2}}$	21824. 82	−1. 96	1. 717
	$^4P_{2\frac{1}{2}}$	21822. 86		1. 590
$3d^5$	$b\ ^4D_{0\frac{1}{2}}$	25035. 64	7. 46	−0. 045
	$^4D_{1\frac{1}{2}}$	25043. 10	3. 94	1. 207
	$^4D_{2\frac{1}{2}}$	25047. 04	−13. 09	1. 381
	$^4D_{3\frac{1}{2}}$	25033. 95		1. 432
$3d^5$	$a\ ^2I_{5\frac{1}{2}}$	30143. 72	6. 44	
	$^2I_{6\frac{1}{2}}$	30150. 16		
$3d^4(a\ ^3H)4s$	$a\ ^4H_{3\frac{1}{2}}$	30156. 94	62. 10	0. 667
	$^4H_{4\frac{1}{2}}$	30219. 04	79. 73	0. 978
	$^4H_{5\frac{1}{2}}$	30298. 77	93. 17	1. 162
	$^4H_{6\frac{1}{2}}$	30391. 94		1. 234
$3d^4(a\ ^3P)4s$	$b\ ^4P_{0\frac{1}{2}}$	29952. 08	355. 52	2. 685
	$^4P_{1\frac{1}{2}}$	30307. 60	557. 01	1. 756
	$^4P_{2\frac{1}{2}}$	30864. 61		1. 572
$3d^4(a\ ^3F)4s$	$a\ ^4F_{1\frac{1}{2}}$	31083. 11	34. 48	0. 418
	$^4F_{2\frac{1}{2}}$	31117. 59	51. 19	1. 032
	$^4F_{3\frac{1}{2}}$	31168. 78	50. 71	1. 246
	$^4F_{4\frac{1}{2}}$	31219. 49		1. 340
$3d^5$	$a\ ^2D_{2\frac{1}{2}}$	31351. 15	−180. 47	
	$^2D_{1\frac{1}{2}}$	31531. 62		
$3d^5$	$a\ ^2F_{3\frac{1}{2}}$	32355. 94	−247. 79	
	$^2F_{2\frac{1}{2}}$	32603. 73		
$3d^5$	$b\ ^4F_{1\frac{1}{2}}$	32844. 92	10. 17	
	$^4F_{2\frac{1}{2}}$	32855. 09	−18. 25	
	$^4F_{3\frac{1}{2}}$	32836. 84	17. 62	
	$^4F_{4\frac{1}{2}}$	32854. 46		
$3d^4(a\ ^3G)4s$	$b\ ^4G_{2\frac{1}{2}}$	33418. 11	103. 12	0. 588
	$^4G_{3\frac{1}{2}}$	33521. 23	97. 90	1. 024
	$^4G_{4\frac{1}{2}}$	33619. 13	75. 34	1. 185
	$^4G_{5\frac{1}{2}}$	33694. 47		1. 276
$3d^4(a\ ^3H)4s$	$a\ ^2H_{4\frac{1}{2}}$	34631. 14	181. 92	
	$^2H_{5\frac{1}{2}}$	34813. 06		
$3d^4(a\ ^3P)4s$	$a\ ^2P_{0\frac{1}{2}}$	34659. 48	696. 58	0. 670
	$^2P_{1\frac{1}{2}}$	35356. 06		1. 331
$3d^4(a\ ^3F)4s$	$b\ ^2F_{2\frac{1}{2}}$	35569. 02	38. 58	0. 867
	$^2F_{3\frac{1}{2}}$	35607. 60		1. 144
$3d^5$	$b\ ^2H_{4\frac{1}{2}}$	35610. 50	97. 16	
	$^2H_{5\frac{1}{2}}$	35707. 66		
$3d^5$	$a\ ^2G_{3\frac{1}{2}}$	36101. 82	170. 84	
	$^2G_{4\frac{1}{2}}$	36272. 66		
$3d^4(a\ ^3D)4s$	$c\ ^4D_{3\frac{1}{2}}$	38269. 67	−45. 33	
	$^4D_{2\frac{1}{2}}$	38315. 00	−47. 56	
	$^4D_{1\frac{1}{2}}$	38362. 56	−33. 80	
	$^4D_{0\frac{1}{2}}$	38396. 36		
$3d^4(a\ ^1G)4s$	$b\ ^2G_{3\frac{1}{2}}$	38509. 07	54. 08	0. 910
	$^2G_{4\frac{1}{2}}$	38563. 15		1. 100
$3d^4(a\ ^3G)4s$	$c\ ^2G_{3\frac{1}{2}}$	39684. 00	140. 52	
	$^2G_{4\frac{1}{2}}$	39824. 52		
$3d^5$	$c\ ^2F_{2\frac{1}{2}}$	39742. 36	134. 92	
	$^2F_{3\frac{1}{2}}$	39877. 28		
$3d^4(a\ ^1I)4s$	$b\ ^2I_{6\frac{1}{2}}$	40202. 14	−26. 30	
	$^2I_{5\frac{1}{2}}$	40228. 44		
$3d^4(a\ ^1S)4s$	$a\ ^2S_{0\frac{1}{2}}$	40415. 34		
$3d^4(a\ ^3D)4s$	$b\ ^2D_{2\frac{1}{2}}$	42898. 12	−88. 61	
	$^2D_{1\frac{1}{2}}$	42986. 73		
$3d^5$	$b\ ^2S_{0\frac{1}{2}}$	44307. 44		
$3d^4(a\ ^1D)4s$	$c\ ^2D_{1\frac{1}{2}}$	45669. 54	61. 20	
	$^2D_{2\frac{1}{2}}$	45730. 74		
$3d^5$	$d\ ^2D_{2\frac{1}{2}}$	47354. 63	−18. 12	
	$^2D_{1\frac{1}{2}}$	47372. 75		
$3d^4(a\ ^1F)4s$	$d\ ^2F_{3\frac{1}{2}}$	50667. 33	−20. 30	
	$^2F_{2\frac{1}{2}}$	50687. 63		
$3d^5$	$d\ ^2G_{3\frac{1}{2}}$	52298. 12	23. 18	
	$^2G_{4\frac{1}{2}}$	52321. 30		
$3d^3\ 4s^2$	$c\ ^4F_{1\frac{1}{2}}$	53051. 55	219. 52	
	$^4F_{2\frac{1}{2}}$	53271. 07	295. 15	
	$^4F_{3\frac{1}{2}}$	53566. 22	357. 35	
	$^4F_{4\frac{1}{2}}$	53923. 57		
$3d^3\ 4s^2$	$e\ ^2G_{3\frac{1}{2}}$	54444. 19	234. 76	
	$^2G_{4\frac{1}{2}}$	54678. 95		
$3d^3\ 4s^2$	$c\ ^4P_{0\frac{1}{2}}$	. . . .		
	$^4P_{1\frac{1}{2}}$	55081. 77	−58. 4	
	$^4P_{2\frac{1}{2}}$	55023. 30		
$3d^3\ 4s^2$	$b\ P_{0\frac{1}{2}}$	. . . .		
	$^2P_{1\frac{1}{2}}$	59130. 51		
$3d^3\ 4s^2$	$e\ ^2D_{1\frac{1}{2}}$	59527. 05	43. 18	
	$^2D_{2\frac{1}{2}}$	59570. 23		
$3d^4(a^5D)5s$	$e\ ^6D_{0\frac{1}{2}}$	82692. 26	71. 19	
	$^6D_{1\frac{1}{2}}$	82763. 45	117. 85	
	$^6D_{2\frac{1}{2}}$	82881. 30	159. 90	
	$^6D_{3\frac{1}{2}}$	83041. 20	199. 00	
	$^6D_{4\frac{1}{2}}$	83240. 20		
$3d^4(a\ ^5D)5s$	$e\ ^4D_{0\frac{1}{2}}$	84208. 28	110. 26	
	$^4D_{1\frac{1}{2}}$	84318. 54	175. 66	
	$^4D_{2\frac{1}{2}}$	84494. 20	231. 76	
	$^4D_{3\frac{1}{2}}$	84725. 96		

TABLE 3. *Even terms of* Cr II—Continued

Electron configuration	Term symbol	Level	Δν	Observed g
$3d^4(a\ ^5D)4d$	$e\ ^6G_{11/2}$	86594. 82	59. 61	
	$^6G_{9/2}$	86654. 43	83. 93	
	$^6G_{7/2}$	86738. 36	108. 94	
	$^6G_{5/2}$	86847. 30	133. 12	
	$^6G_{3/2}$	86980. 42	156. 92	
	$^6G_{1/2}$	87137. 34		
$3d^4(a\ ^5D)4d$	$e\ ^6P_{7/2}$	86667. 95	23. 82	
	$^6P_{5/2}$	86691. 77	90. 30	
	$^6P_{3/2}$	86782. 07		
$3d^4(a\ ^5D)4d$	$f\ ^6D_{9/2}$	87314. 0	40. 6	
	$^6D_{7/2}$	87354. 62	58. 65	
	$^6D_{5/2}$	87413. 27	101. 83	
	$^6D_{3/2}$	85715. 10	172. 56	
	$^6D_{1/2}$	87687. 66		
$3d^4(a\ ^5D)4d$	$e\ ^6F_{11/2}$	87542. 12	52. 48	
	$^6F_{9/2}$	87594. 60	71. 40	
	$^6F_{7/2}$	87666. 00	92. 88	
	$^6F_{5/2}$	87758. 88	189. 82	
	$^6F_{3/2}$	87948. 70	52. 62	
	$^6F_{1/2}$	88001. 32		
$3d^4(a\ ^5D)4d$	$e\ ^6G_{9/2}$	89056. 10	118. 00	
	$^6G_{7/2}$	89174. 10	151. 50	
	$^6G_{5/2}$	89325. 60	183. 03	
	$^6G_{3/2}$	89508. 63		
$3d^4(a\ ^5D)4d$	$e\ ^4P_{5/2}$	88426. 2	210. 5	
	$^4P_{3/2}$	88636. 7	286. 5	
	$^4P_{1/2}$	88923. 2		
$3d^4(a\ ^5D)4d$	$f\ ^4D_{7/2}$	89269. 88	67. 82	
	$^4D_{5/2}$	89337. 70	137. 38	
	$^4D_{3/2}$	89475. 08	146. 17	
	$^4D_{1/2}$	89621. 25		
$3d^4(a\ ^5D)4d$	$e\ ^4F_{5/2}$	90512. 50	78. 60	
	$^4F_{3/2}$	90591. 10	134. 40	
	$^4F_{7/2}$	90725. 50	125. 50	
	$^4F_{9/2}$	90851. 00		
$3d^4(a\ ^5D)4d$	$e\ ^6S_{5/2}$	91954. 78		
$3d^4(a\ ^3G)5s$	$f\ ^4G_{7/2}$	------		
	$^4G_{9/2}$	------		
	$^4G_{11/2}$	105365. 2	56. 7	
	$^4G_{13/2}$	105421. 9		

TABLE 4. *Odd terms of Cr* II

Electron configuration	Term symbol	Level	Δν	Observed g
$3d^4(a\ ^5D)4p$	$z\ ^6F^0_{11/2}$	46823. 64	81. 88	−0. 689
	$^6F^0_{9/2}$	46905. 52	135. 02	1. 124
	$^6F^0_{7/2}$	47040. 54	186. 96	1. 314
	$^6F^0_{5/2}$	47227. 50	237. 44	1. 378
	$^6F^0_{3/2}$	47464. 94	287. 04	1. 416
	$^6F^0_{1/2}$	47751. 98		
$3d^4(a\ ^5D)4p$	$z\ ^6P^0_{7/2}$	48399. 19	92. 20	2. 382
	$^6P^0_{5/2}$	48491. 39	140. 97	1. 875
	$^6P^0_{3/2}$	48632. 36		1. 710
$3d^4(a\ ^5D)4p$	$z\ ^4P^0_{5/2}$	48749. 57	256. 58	2. 844
	$^4P^0_{3/2}$	49006. 15	345. 81	1. 802
	$^4P^0_{1/2}$	49351. 96		1. 628
$3d^4(a\ ^5D)4p$	$z\ ^6D^0_{9/2}$	49493. 00	71. 80	3. 155
	$^6D^0_{7/2}$	49564. 80	141. 67	1. 824
	$^6D^0_{5/2}$	49706. 47	−60. 22	1. 624
	$^6D^0_{3/2}$	49646. 25	192. 18	1. 577
	$^6D^0_{1/2}$	49838. 43		1. 570
$3d^4(a\ ^5D)4p$	$z\ ^4F^0_{7/2}$	51584. 44	85. 31	0. 406
	$^4F^0_{5/2}$	51669. 75	119. 46	1. 025
	$^4F^0_{3/2}$	51789. 21	153. 83	1. 248
	$^4F^0_{1/2}$	51943. 04		1. 338
$3d^4(a\ ^5D)4p$	$z\ ^4D^0_{5/2}$	54418. 08	81. 62	0. 007
	$^4D^0_{7/2}$	54499. 70	126. 06	1. 178
	$^4D^0_{3/2}$	54625. 76	158. 91	1. 376
	$^4D^0_{1/2}$	54784. 67		1. 430
$3d^4(a\ ^3H)4p$	$z\ ^4H^0_{13/2}$	63601. 20	105. 42	0. 680
	$^4H^0_{11/2}$	63706. 62	142. 49	1. 030
	$^4H^0_{9/2}$	63849. 11	181. 74	1. 138
	$^4H^0_{7/2}$	64030. 85		1. 234
$3d^4(a\ ^3P)4p$	$y\ ^4D^0_{5/2}$	63802. 41	259. 41	0. 000
	$^4D^0_{7/2}$	64061. 82	387. 02	1. 199
	$^4D^0_{3/2}$	64448. 84	475. 46	1. 380
	$^4D^0_{1/2}$	64924. 30		1. 411
$3d^4(a^3P)4p$	$z\ ^2S^0_{1/2}$	65029. 67		
$3d^4(a\ ^3H)4p$	$z\ ^4G^0_{11/2}$	65156. 84	100. 19	0. 593
	$^4G^0_{9/2}$	65257. 03	127. 01	0. 920
	$^4G^0_{7/2}$	65384. 04	325. 49	1. 120
	$^4G^0_{5/2}$	65709. 53		1. 265
$3d^4(a\ ^3H)4p$	$z\ ^4I^0_{13/2}$	65217. 61	202. 34	
	$^4I^0_{11/2}$	65419. 95	198. 46	
	$^4I^0_{9/2}$	65618. 41	194. 22	
	$^4I^0_{7/2}$	65812. 63		
$3d^4(a\ ^3H)4p$	$z\ ^2G^0_{9/2}$	65543. 06	137. 09	
	$^2G^0_{7/2}$	65680. 15		
$3d^4(a\ ^3P)4p$	$y\ ^4P^0_{5/2}$	66256. 77	98. 36	2. 545
	$^4P^0_{3/2}$	66355. 13	372. 03	1. 671
	$^4P^0_{1/2}$	66277. 16		1. 502
$3d^4(a\ ^3P)4p$	$z\ ^2D^0_{5/2}$	66649. 71	362. 57	
	$^2D^0_{3/2}$	67012. 28		

TABLE 4. *Odd terms of* Cr II—Continued

Electron configuration	Term symbol	Level	$\Delta\nu$	Observed g
$3d^4(a\ ^3P)4p$	$z\ ^2P^0_{3/2}$	66872. 12	198. 36	
	$z\ ^2P^0_{1/2}$	67070. 48		
$3d^4(a\ ^3F)4p$	$y\ ^4G^0_{5/2}$	67344. 42	−10. 22	
	$^4G^0_{3/2}$	67334. 20	19. 40	
	$^4G^0_{11/2}$	67353. 60	15. 73	
	$^4G^0_{9/2}$	67369. 33		
$3d^4(a\ ^3F)4p$	$y\ ^4F^0_{7/2}$	67379. 92	7. 38	
	$^4F^0_{5/2}$	67387. 30	6. 50	
	$^4F^0_{3/2}$	67393. 80	55. 02	
	$^4F^0_{9/2}$	67448. 82		
$3d^4(a\ ^3H)4p$	$z\ ^2I^0_{11/2}$	67506. 34	82. 72	
	$^2I^0_{13/2}$	67589. 06		
$3d^4(a\ ^3F)4p$	$x\ ^4D^0_{3/2}$	67859. 91	10. 59	
	$^4D^0_{7/2}$	67870. 50	−2. 45	
	$^4D^0_{5/2}$	67868. 05	7. 63	
	$^4D^0_{1/2}$	67875. 68		
$3d^4(a\ ^3P)4p$	$z\ ^4S^0_{3/2}$	68305. 73	1. 978	
$3d^4(a\ ^1H)4p$	$z\ ^2H^0_{9/2}$	68477. 11	260. 88	
	$^2H^0_{11/2}$	68737. 99		
$3d^4(a\ ^3F)4p$	$z\ ^2F^0_{5/2}$	68583. 44	176. 56	
	$^2F^0_{7/2}$	68760. 00		
$3d^4(a\ ^3G)4p$	$y\ ^4H^0_{13/2}$	68843. 51	149. 04	
	$^4H^0_{11/2}$	68992. 55	178. 05	
	$^4H^0_{7/2}$	69170. 60	217. 80	
	$^4H^0_{9/2}$	69388. 40		
$3d^4(a\ ^3G)4p$	$x\ ^4F^0_{7/2}$	69348. 36	129. 70	
	$^4F^0_{9/2}$	69478. 06	28. 10	
	$^4F^0_{5/2}$	69506. 16	−7. 89	
	$^4F^0_{3/2}$	69498. 27		
$3d^4(a\ ^3F)4p$	$y\ ^2D^0_{5/2}$	69638. 77	315. 43	
	$^2D^0_{3/2}$	69954. 20		
$3d^4(a\ ^3F)4p$	$y\ G^0_{7/2}$	69903. 46	204. 37	
	$^2G^0_{9/2}$	70107. 83		
$3d^4(a\ ^5G)4p$	$x\ ^4G^0_{7/2}$	70317. 04	110. 18	
	$^4G^0_{5/2}$	70427. 22	252. 00	
	$^4G^0_{11/2}$	70679. 22	200. 73	
	$^4G^0_{9/2}$	70879. 95		
$3d^4(a\ ^3G)4p$	$y\ ^2H^0_{11/2}$	70394. 46	4. 58	
	$^2H^0_{9/2}$	70399. 04		
$3d^4(a\ ^3G)4p$	$y\ ^2F^0_{7/2}$	70584. 64	267. 60	
	$^2F^0_{5/2}$	70852. 24		
$3d^4(a\ ^3G)4p$	$x\ ^2G^0_{9/2}$	72648. 79	68. 12	
	$^2G^0_{7/2}$	72716. 91		
$3d^4(a\ ^3D)4p$	$w\ ^4D^0_{3/2}$	73406. 68	5. 26	
	$^4D^0_{7/2}$	73411. 94	24. 33	
	$^4D^0_{5/2}$	73436. 27	49. 33	
	$^4D^0_{1/2}$	73485. 60		
$3d^4(a\ ^3D)4p$	$x\ ^2F^0_{5/2}$	74114. 48	−321. 66	
	$^2F^0_{7/2}$	74436. 14		
$3d^4(a\ ^3D)4p$	$w\ ^4F^0_{7/2}$	74273. 48	45. 38	
	$^4F^0_{5/2}$	74318. 86	104. 98	
	$^4F^0_{3/2}$	74423. 84	80. 67	
	$^4F^0_{9/2}$	74504. 51		
$3d^4(a\ ^1I)4p$	$y\ ^2I^0_{13/2}$	74421. 76	2. 59	
	$^2I^0_{11/2}$	74424. 35		
$3d^4(a\ ^1I)4p$	$x\ ^2H^0_{9/2}$	74455. 90	251. 52	
	$^2H^0_{11/2}$	74707. 42		
$3d^4(a\ ^3D)4p$	$x\ ^4P^0_{5/2}$	74484. 25	−233. 80	
	$^4P^0_{3/2}$	74718. 05	−202. 75	
	$^4P^0_{1/2}$	74920. 80		
$3d^4(a\ ^1I)4p$	$z\ ^2K^0_{15/2}$	74743. 33	215. 47	
	$^2K^0_{13/2}$	74958. 80		
$3d^4(a\ ^3D)4p$	$y\ ^2P^0_{3/2}$	74854. 08	130. 85	
	$^2P^0_{1/2}$	74984. 93		
$3d^4(a\ ^1G)4p$	$w\ ^2G^0_{9/2}$	75716. 74	93. 36	
	$^2G^0_{7/2}$	75810. 10		
$3d^4(a\ ^1G)4p$	$w\ ^2F^0_{5/2}$	76879. 03	−108. 75	
	$^2F^0_{7/2}$	76987. 78		
$3d^4(a\ ^1G)4p$	$w\ ^2H^0_{11/2}$	77078. 96	−191. 44	
	$^2H^0_{9/2}$	77270. 40		
$3d^4(a\ ^1S)4p$	$x\ ^2P^0_{1/2}$	77713. 66	−63. 92	
	$^2P^0_{3/2}$	77777. 58		
$3d^4(a\ ^3D)4p$	$x\ ^2D^0_{3/2}$	77935. 24	−174. 40	
	$^2D^0_{1/2}$	78109. 64		
$3d^4(a\ ^1D)4p$	$w\ ^2D^0_{5/2}$	80288. 25	132. 18	
	$^2D^0_{3/2}$	80420. 43		
$3d^4(a\ ^1D)4p$	$v\ ^2F^0_{5/2}$	81232. 91	199. 45	
	$^2F^0_{7/2}$	81432. 36		
$3d^4(a\ ^1D)4p$	$w\ ^2P^0_{3/2}$	82854. 00	66. 03	
	$^2P^0_{1/2}$	82920. 03		
$3d^4(a\ ^1F)4p$	$u\ ^2F^0_{7/2}$	84604. 99	72. 40	
	$^2F^0_{5/2}$	84677. 39		
$3d^4(a\ ^1F)4p$	$v\ ^2G^0_{9/2}$	85573. 43	366. 08	
	$^2G^0_{7/2}$	85939. 50		
$3d^4(a\ ^1F)4p$	$v\ ^2D^0_{3/2}$	86507. 38	−3. 70	
	$^2D^0_{1/2}$	86511. 08		
$3d^4(b\ ^3F)4p$	$u\ ^2G^0_{9/2}$	90986. 31	117. 05	
	$^2G^0_{7/2}$	91103. 36		
$3d^4(b\ ^3F)4p$	$u\ ^2D^0_{5/2}$	91426. 31	−130. 23	
	$^2D^0_{3/2}$	91556. 54		

TABLE 5. *Theoretical terms of* Cr II

Electron configuration $1s^2\ 2s^2\ 2p^6\ 3s^2\ 3p^6+$	Theoretical terms
$3d^5$	^{6}**S** ^{4}(**G D**) ^{2}(**IGFDS**) ^{4}(**FP**) ^{2}(**HGFDP**) ^{2}D
$3d^4\ 4s$	^{6,4}**D** ^{4,2}(**HGFDP**) ^{2}(**IGFDS**) ^{4,2}(FP) ^{2}(DGS)
$3d^3\ 4s^2$	^{4}(**FP**) ^{2}(HGF**DP**) ^{2}D
$3d^3\ 4p$	^{6,4}(**FDP**)° ^{4,2}(**IHG**)° ^{4,2}(**HGF**)° ^{4,2}(**GFD**)° ^{4,2}(**FDP**)° ^{4,2}(**DPS**)° ^{2}(**KIH**)° ^{2}(**HGF**)° ^{2}(**GFD**)° ^{2}(**FDP**)° ^{2}P° ^{4,2}(GFD)° ^{4,2}(DPS)° ^{2}(FDP)° ^{2}(HGF)° ^{2}P°
$3d^4\ 4d$	^{6,4}(**GFDPS**) ^{4,2}(KIHGF) ^{4,2}(IHGFD) ^{4,2}(HGFDP) ^{4,2}(GFDPS), etc.
$3d^4\ 5s$	^{6,4}**D** ^{4,2}(HGFDP) etc.

TABLE 6. *Series terms of* Cr II

Terms	Electron configuration		Terms	Electron configuration	
	$3d^5$	$3d^4\ 4d$		$3d^4\ 4s$	$3d^4\ 5s$
$^6S_{2½}$	0. 00	91954. 78	$^6D_{4½}$	12496. 79	83240. 20
$^4G_{5½}$	20512. 75	89508. 63	$^4D_{3½}$	20024. 18	84725. 96
$^4P_{2½}$	21822. 86	88923. 2	$^4G_{5½}$	33694. 47	105421. 9
$^4D_{3½}$	25033. 95	89621. 25			
$^4F_{4½}$	32854. 46	90851. 00			

4. References

[1] M. A. Catalán, Phil. Trans. Roy. Soc. London A **223,** 127 (1922).
[2] H. Giesecler, Ann. Physik [IV] **69,** 147 (1922).
[3] C. C. and H. K. Kiess, Science **56,** 666 (1922).
[4] H. Kayser, Handbuch der Spectroscopie. S. Hirzel, Leipzig (1910) and (1934)
[5] C. C. Kiess, BS J. Research **5,** 775 (1930) RP229.
[6] E. Krömer, Z. Physik **52,** 531 (1928).
[7] M. A. Catalán, An. Espan. Soc. Fis. Quim. **28,** 611 (1930).
[8] C. C. Kiess and O. Laporte, Science **63,** 234 (1926).
[9] R. W. Wood, Nature **140,** 723 (1937).
[10] H. D. Curtis, J. Opt. Soc. Am. **8,** 697 (1924).
[11] A. S. King, Astrophys. J. **41,** 86 (1915); **60,** 282 (1924).
[12] J. S. V. Allen and C. E. Hesthal, Phys. Rev. **47,** 926 (1935).
[13] H. N. Russell, Proc. Nat. Acad. Sci. **11,** 322 (1925).
[14] C. C. Kiess and G. Shortley, J. Research NBS **42,** 183 (1949) RP1961.
[15] O. Laporte, Phys. Rev. **61,** 302 (1942).
[16] O. Laporte and J. R. Platt, Phys. Rev. **61,** 305 (1942).
[17] G. Racah, Phys. Rev. **63,** 367 (1943).
[18] A. A. Schweizer, Phys. Rev. **80,** 1080 (1950).
[19] H. N. Russell, Astrophys. J. **66,** 233 (1927).
[20] A. G. Shenstone, Phil. Trans. Roy. Soc. London [A] **335,** 195 (1936).
[21] H. N. Russell, J. Opt. Soc. Am. **40,** 618 (1950).

WASHINGTON, February 23, 1951.

Journal of Research of the National Bureau of Standards Vol. 47, No. 5, November 1951 Research Paper 2267

Harmonic Output of the Synchronous Rectifier

Paul Selgin

If a sine-wave current or voltage of generic frequency f is admitted into a switching device that inverts its polarity with frequency F, the output will contain all the positive frequencies $\pm f + NF$, with N an odd integer. This fact, as well as the amplitude and phase of each component, results from the expansion of the output in a complex Fourier series. Application to particular cases illustrates the behavior of the synchronous rectifier in cases when the input contains nonsynchronous components. In particular, the selectivity and damping associated with the synchronous rectifier are made the object of comparative considerations.

1. Use of the Synchronous Rectifier [1]

Rectification based on the unilateral conductivity of semi conductors, of gas or vapor discharges, and of vacuum tubes, is a comparatively recent development. Rectification based on mechanical switching, timed to coincide with the inversion in polarity, is much older: its first example was the two-pole commutator used in the early permanent magnet dynamos. Mechanically operated synchronous rectifiers present a problem when they are required to handle considerable power because of the difficulty in mechanically commutating large currents, although there are ways of overcoming this by interrupting the circuit at the instants when the current is at a minimum; so-called "contact rectifiers", studied and used chiefly in Germany, are based on this principle.

In the measurement field [2] synchronous rectifiers are useful chiefly in combination with "choppers", to permit the use of a-c amplifiers to handle a d-c signal. Ordinary unidirectional rectifiers, such as diodes, do not discriminate between the desired signal and noise, and the only way to reduce the noise present in the output is to insert a selective band-pass filter somewhere in the system. The output of synchronous rectifiers, on the other hand, contains d-c only when the input contains the synchronous frequency itself or an odd multiple thereof. Therefore only discrete infinitesimal portions of the noise spectrum will contribute to the d-c level, and because of the random phase the net total of an infinite number of these infinitesimal contributions will be zero. In other words, the synchronous rectifier d-c output is unaffected by noise. While this is a very desirable feature, it does not eliminate the need for filtering; a-c components of the output have to be reduced to prevent them from masking the d-c component. This is easier to achieve than the selective transmission of a narrow band; however, if the a-c components are cut down below a certain point the system becomes very sluggish and slow to respond to changes in the d-c level. Basically, the difficulty is the same whatever the system used; it is impossible to eliminate noise entirely without sacrificing the ability to follow arbitrary variations in d-c level.

Aside from the specific application mentioned above, it is of some interest to investigate the behavior of the synchronous rectifier generally, taking as the starting point the Fourier analysis of the output when a sine-wave input of arbitrary frequency, phase and amplitude, is impressed upon the rectifier, which is assumed to do nothing more than invert periodically the polarity of the input at a given fixed frequency F.

2. Initial Steps in the Fourier Analysis

Consider a harmonic time function whose phase is changed by π at uniform time intervals. The phase inversion may be regarded as the effect of multiplication of the harmonic function by a "square wave" function of value ± 1, the sign changing periodically. Let f be the frequency of the harmonic function, hereafter called the "input", and F that of the square wave; let F be designated as the "synchronous frequency".

In general, f and F will be incommensurable. We will suppose, however, that their ratio is rational. This does not, in effect, limit the scope of the analysis, since it will appear that the components of the output approach a limit as the input frequency approaches any arbitrary value through a sequence of rational numbers (with reference to the synchronous frquency taken as unity).

We can therefore write

$$\frac{f}{F}=\frac{m}{M}, \tag{1}$$

and, in setting up the Fourier analysis, we can ignore the actual frequencies in the interest of simplicity in writing, and use instead the two numbers m and M, assuming that within the time interval 2π the input function goes through m complete periods, and the square wave function through M periods. The situation is illustrated in figure 1. We can see that the output will be periodic, of period 2π. This time interval is, in fact, the least common multiple of both the input and synchronous periods.

Our substitutions enable us to write the input function in the form:

[1] "Synchronous rectifiers", as discussed here, include types wherein the rectification is due to mechanical interruption of a circuit at the synchronizing frequency. The analysis applies only approximately to synchronous detectors, where a synchronizing voltage is applied, together with the signal voltage, to suitable points of a diode or vacuum tube circuit.

[2] Walter, Zeitschrift f. Tech. Physik **13**, 363 and 436 (1932). Morton, Trans. Faraday Soc. **46**, 818 (1934); Astbury, J. Sci. Inst. **17**, 25 (1940). Michaels and Curtis, Rev. Sci. Instr. **12**, 444 (Sept. 1941).

$$v_i(t) = V_i \cos(mt+\Phi) = a \cos mt + b \sin mt \qquad (2)$$

$$\left[V_i = \sqrt{a^2+b^2};\ \tan\phi = \frac{b}{a}\right]$$

and the output in the form of a complex Fourier series: [3]

$$v_0(t) = \sum_{n=-\infty}^{\infty} C_n e^{-int}, \qquad (3)$$

which is equivalent to the more familiar, but less convenient in this case, Fourier series with real coefficients:

$$v_0(t) = \sum_{n=0}^{\infty} (a_n \cos nt + b_n \sin nt), \qquad (4)$$

provided the complex coefficients C_n in (3) and the real coefficients a_n and b_n in (4) are mutually bound by the equations:

$$\left.\begin{aligned} C_n &= \frac{1}{2}(a_n - ib_n) \\ C_{-n} &= \frac{1}{2}(a_n + ib_n) \end{aligned}\right\} \qquad (5)$$

The square-wave synchronous function of figure 1 may be designated provisionally by $S(t)$. The output may, therefore, be written also in the form of a factor:

$$v_0(t) = S(t)v_i(t) = S(t)(a \cos mt + b \sin mt), \qquad (6)$$

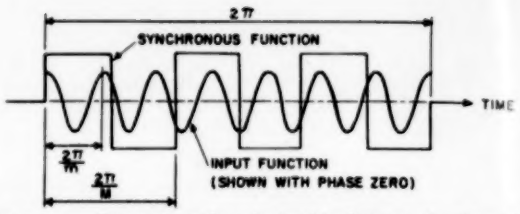

FIGURE 1. *Illustrating the relationship between the "input" and "square wave" functions.*

hence the coefficients C_n of eq 3 take the form:

$$C_n = \frac{1}{2\pi}\int_{-\pi}^{\pi} v_0(t)e^{-int}dt = \frac{1}{2\pi}\int_{-\pi}^{\pi} S(t)(a \cos mt + b \sin mt)e^{-int}dt, \qquad (7)$$

and, expanding:

$$C_n = \frac{a-ib}{4\pi}\int_{-\pi}^{\pi} S(t)e^{i(m-n)t}dt + \frac{a+ib}{4\pi}\int_{-\pi}^{\pi} S(t)e^{-i(m+n)t}dt \qquad (8)$$

3. Complex Fourier Coefficients

The function $S(t)$ simply resolves itself into a + or − sign if we divide each of the above integrals into partial integrals, each extending over a half period of the synchronous frequency. Thus

$$\int_{-\pi}^{\pi} S(t)e^{i(m-n)t}dt = \int_{-\pi}^{-\pi+\frac{\pi}{M}} e^{i(m-n)t}dt - \int_{-\pi+\frac{\pi}{M}}^{-\pi+\frac{2\pi}{M}} e^{i(m-n)t}dt + \ldots + \int_{\pi-\frac{2\pi}{M}}^{\pi-\frac{\pi}{M}} e^{i(m-n)t}dt - \int_{\pi-\frac{\pi}{M}}^{\pi} e^{i(m-n)t}dt$$

$$= \frac{-i}{m-n}\left\{\left[e^{i(m-n)t}\right]_{-\pi}^{-\pi+\frac{\pi}{M}} - \left[e^{i(m-n)t}\right]_{-\pi+\frac{\pi}{M}}^{-\pi+\frac{2\pi}{M}} + \ldots + \left[e^{i(m-n)t}\right]_{\pi-\frac{2\pi}{M}}^{\pi-\frac{\pi}{M}} - \left[e^{i(m-n)t}\right]_{\pi-\frac{\pi}{M}}^{\pi}\right\}$$

$$= \frac{-i}{m-n}\left\{e^{\pi i(m-n)\frac{1-M}{M}} - e^{-\pi i(m-n)} - e^{\pi i(m-n)\frac{2-M}{M}} + e^{\pi i(m-n)\frac{1-M}{M}} + \ldots + e^{\pi i(m-n)\frac{M-1}{M}} - e^{\pi i(m-n)\frac{M-2}{M}} - e^{\pi i(m-n)} + e^{\pi i(m-n)\frac{M-1}{M}}\right\}$$

$$= \frac{-i}{m-n}e^{-\pi i(m-n)}\left\{2e^{\pi i\frac{m-n}{M}} - 2e^{2\pi i\frac{m-n}{M}} + 2e^{3\pi i\frac{m-n}{M}} - \ldots + 2e^{(2M-1)\pi i\frac{m-n}{M}} - 1 - e^{2\pi i(m-n)}\right\} \qquad (9)$$

Let us temporarily, for convenience, write:

$$e^{\pi i\frac{m-n}{M}} = \alpha \qquad (10)$$

and rearrange (9) as follows:

$$\int_{-\pi}^{\pi} S(t)e^{i(m-n)t} = \frac{2i}{m-n}\alpha^{-M}\left\{1 - \alpha + \alpha^2 - \alpha^3 + \alpha^4 - \ldots - \alpha^{2M-1} - \frac{1-\alpha^{2M}}{2}\right\} \qquad (11)$$

[3] See for example, Churchill, Fourier series and boundary value problems (McGraw-Hill Book Co., Inc., New York, N. Y., 1941).

Recalling the identity:

$$1-\alpha+\alpha^2-\alpha^3+\alpha^4-\ \ldots\ -\alpha^{2M-1}=\frac{1-\alpha^{2M}}{1+\alpha} \quad (12)$$

equation (9) becomes

$$\int_{-\tau}^{\tau} S(t)e^{i(m-n)t}=\frac{i}{m-n}(\alpha^{-M}-\alpha^{M})\frac{1-\alpha}{1+\alpha} \quad (13)$$

and restoring the original notation for α:

$$\int_{-\tau}^{\tau} S(t)e^{i(m-n)t}=\frac{-2i[\sin\pi(m-n)]\left[\tan\frac{\pi}{2}\frac{m-n}{M}\right]}{m-n} \quad (14)$$

We can now write an expression for C_n, the complex Fourier coefficient, from equations (8) and (14): for brevity we will use the notation

$$\left.\begin{aligned}\frac{[\sin\pi(m+n)]\left[\tan\frac{\pi}{2}\frac{m+n}{M}\right]}{\pi(m+n)}&=p_n\\ \frac{[\sin\pi(m-n)]\left[\tan\frac{\pi}{2}\frac{m-n}{M}\right]}{\pi(m-n)}&=q_n\end{aligned}\right\} \quad (15)$$

thus obtaining

$$C_n=\frac{i}{2}[a(p_n-q_n)+ib(p_n+q_n)]. \quad (16)$$

4. Harmonic Spectrum

The real Fourier coefficients, giving the phase and amplitude of each harmonic in the synchronous rectifier output, may now be written, using eq 16 and the relationships (5). The steps simplify because of the identities:

$$\left.\begin{aligned}p_{-n}&=q_n\\ q_{-n}&=p_n\end{aligned}\right\} \quad (17)$$

implicit in eq 15. Using these, and eq 5, we have:

$$\begin{aligned}a_n=C_n+C_{-n}&=\frac{i}{2}[a(p_n-q_n+q_n-p_n)\\ &\quad+ib(p_n+q_n+q_n+p_n)]\\ &=-b(p_n-q_n)\end{aligned} \quad (18)$$

$$\begin{aligned}b_n=i(C_n-C_{-n})&=-\frac{1}{2}[a(p_n-q_n-q_n+p_n)\\ &\quad+ib(p_n+q_n-q_n-p_n)]\\ &=-a(p_n-q_n),\end{aligned} \quad (18a)$$

where a_n and b_n are the Fourier coefficients relative to the nth harmonic; the nth harmonic, that is, not of the input frequency nor of the synchronous frequency but of that frequency whose period is the least common multiple of the two; or, in other words, the nth harmonic of the frequency at which there is a recurrence of phase coincidence between the input and square-wave functions.

We can readily express the amplitude and phase of this nth harmonic: (see eqn 2):

$$\begin{aligned}V_n=\sqrt{a_n^2+b_n^2}&=\sqrt{(p_n^2+q_n^2)(a^2+b^2)-2p_nq_n(a^2-b^2)}\\ &=V_i\sqrt{p_n^2+q_n^2-2p_nq_n\cos 2\phi}\end{aligned} \quad (19)$$

$$\tan\phi_n=(\cot\phi)\frac{p_n-q_n}{p_n+q_n}, \quad (20)$$

where V_i and φ are the amplitude and phase of the input. The analysis of the harmonic spectrum is simplified by the fact that for a given harmonic of order n, the coefficients p_n and q_n do not generally exist together, one or the other being zero except in the particular case when f and F, input and synchronous frequencies, are commensurable.

Considering, in fact, eq 15, we see that, since both m and n are integers by definition, both p_n and q_n are zero, because of the vanishing of the sines except when $(m+n)/M$ or $(m-n)/M$ are odd integers, in which case the tangents are infinite and p_n, or q_n, respectively, takes an interderminate form that has finite nonzero value.

Consequently, p_n and q_n can coexist only when both $(m+n)/M$ and $(m-n)/M$ are odd integers. But if this is true, the sum and difference of these numbers must be even integers, from which we conclude that both ratios m/M and n/M are integers; which means that the input frequency f must be a multiple of the synchronous frequency F, which then becomes the fundamental frequency.

This special case will be considered later. Let us first assume that f is not a multiple of F. The harmonic spectrum then divides into two families: (a) harmonics corresponding to $(m+n)/M=N$ with N an odd integer; (b) harmonics corresponding to $(m-n)/M=N$ with N an odd integer. In terms of actual frequencies, the frequency of a particular harmonic of order n will be

$$f_n=n\frac{F}{M}, \quad (21)$$

since F/M is the fundamental frequency (fig. 1). Hence the frequencies of family (a):

$$f_n'=(NM-m)\frac{F}{M}=-f+NF, \quad (22)$$

where N must be an odd integer greater than f/F.

For the frequencies of family (b) we have, likewise:

$$f_n''=f+NF, \quad (23)$$

where N must be an odd integer greater than $-f/F$.

The grouping of the two families is illustrated in

figure 2. As for the amplitude and phase values: for family (a) we have

$$\left.\begin{aligned} p_n' &= \frac{(\sin \pi NM)\left(\tan \frac{\pi}{2} N\right)}{\pi NM} \\ q_n' &= 0 \end{aligned}\right\} \tag{24}$$

and for family (b):

$$\left.\begin{aligned} p_n'' &= 0 \\ q_n'' &= \frac{(\sin \pi NM)\left(\tan \frac{\pi}{2} N\right)}{\pi NM} \end{aligned}\right\} \tag{25}$$

The common value of p_n' and q_n'' is given in indeterminate form and must be evaluated. This can be done by L'Hopital's rule; the result is

$$p_n' = \frac{2}{\pi N} \qquad q_n'' = \frac{2}{\pi N} \tag{26}$$

We can now tabulate the frequency, amplitude and phase values for the two families in the general case when the input and synchronous frequencies are incommensurable:

	Family (a)	Family (b)
Frequency:	$f_n' = -f + NF$	$f_n'' = f + NF$
	$\left(N > \frac{f}{F};\ N \text{ odd}\right)$	$\left(N > -\frac{f}{F};\ N \text{ odd}\right)$
Amplitude:	$V_n' = \frac{2Vi}{\pi N}$	$V_n'' = \frac{2Vi}{\pi N}$
Phase:	$\phi_n' = \frac{\pi}{2} - \phi$	$\phi_n'' = \begin{cases} \phi - \frac{\pi}{2};\ (N < 0) \\ \phi + \frac{\pi}{2};\ (N > 0) \end{cases}$

The following deductions can be drawn from an examination of the data of figure 2:

1. The amplitude of the harmonics does not depend on the phase of the input.

2. Family (a) may be regarded as a "reflection" of family (b) at the axis of zero frequency, accompanied by a reversal in phase.

3. The two harmonics of greatest amplitude are symmetrically spaced about the frequency f if $f > F$, about F if $f < F$.

4. The conclusions reached may be extended to the case when f is not rational. If, in fact, the input frequency approaches a value f irrationally related to F in such a manner that its subsequent values $f_1, f_2, f_3, \ldots$, are all rationally related to F, the nth harmonic of the output will take on values $\pm f_1 + NF$, $\pm f_2 + NF$, $\pm f_3 + NF, \ldots$ which tend to $\pm f + NF$ as a limit. The restriction imposed at the start of the analysis, that f/F be a rational number, may therefore be removed.

5. There is no d-c output in the general case when f is not a multiple of F. This can be deduced from figure 2 by inspection. Only frequencies that are odd multiples of the synchronous frequencies contribute to the d-c output.

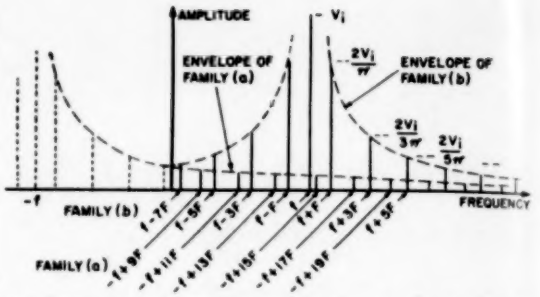

FIGURE 2. *Harmonic spectrum in a generic case, showing the presence of two distinct "families".*

5. Commensurable Case

In the particular case when $f = mF$, F becomes the fundamental frequency, and M is equal to unity. The expressions for p_n and q_n (eq 15) then become:

$$\left.\begin{aligned} p_n &= \frac{[\sin \pi(m+n)]\left[\tan \frac{\pi}{2}(m+n)\right]}{\pi(m+n)} \\ q_n &= \frac{[\sin \pi(m-n)]\left[\tan \frac{\pi}{2}(m-n)\right]}{\pi(m-n)} \end{aligned}\right\} \tag{27}$$

and we find that both p_n and q_n exist for the same values of n: specifically, if m is *odd*, p_n and q_n exist together for every *even* value of n; if m is *even*, for every *odd* value.

We therefore have only one family of harmonics: those of frequency:

$$f_n = nF \tag{28}$$

with the understanding that n can be any positive odd integer when $m = f/F$ is even, and any positive even integer, or zero, when m is odd.

The evaluation of p_n and q_n can be carried out as before; we obtain:

$$\left.\begin{aligned} p_n &= \frac{2}{\pi(m+n)} \\ q_n &= \frac{2}{\pi(m-n)} \end{aligned}\right\} \tag{29}$$

hence the amplitude of the nth harmonic (eq 19):

$$V_n = \frac{4V_i\sqrt{m^2 \sin^2 \phi + n^2 \cos^2 \phi}}{\pi(m^2 - n^2)} \tag{30}$$

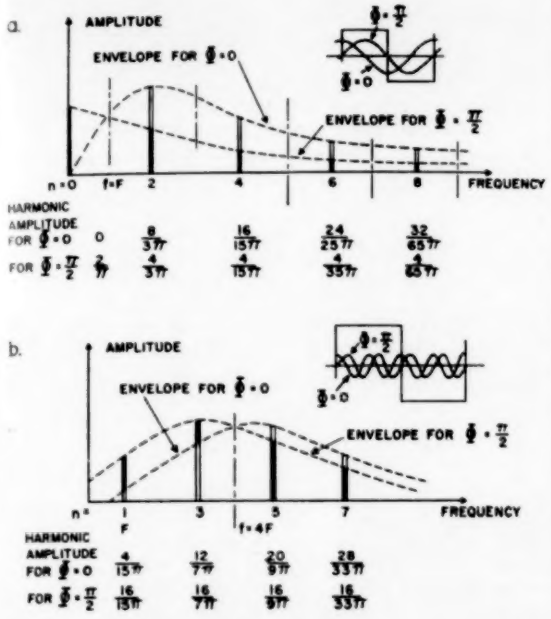

FIGURE 3. *a, Harmonic spectrum for the case $m=1$; b, harmonic spectrum for the case $m=4$.*

and its phase (eq 20):

$$\phi_n = -\frac{n}{m}\tan\phi. \tag{31}$$

Figure 3 illustrates the harmonic spectrum in the two cases of $m=1$ and $m=4$. It is worthy of note that the amplitude of each harmonic is now dependent on the phase of the input, which is not true in the general case. This apparent contradiction may be explained if we think of the two families (a) and (b), which exist separately in the general case, as merging into one in the particular case when f is a multiple of F (the commensurable case). Depending on the relative phase of the two families (hence on the phase of the input, fig. 2) the resultant of each pair of merging harmonics will vary in amplitude.

In particular, note that the d-c component appears in the case of m odd *except* when the phase of the input is zero or a multiple of π (that is, when the input goes through a maximum, or minimum at each reversal of polarity). This may be verified by making $n=0$ and $\sin\phi=0$ in eq. 30; V_n vanishes under these conditions.

6. Correlation between Time Constant and Selectivity

One feature of the synchronous detector is of particular importance; its rejection of nonsynchronous input components. To achieve this, however,

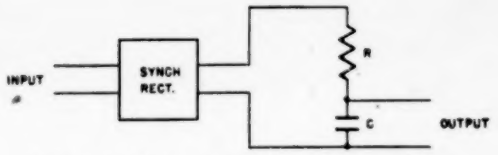

FIGURE 4. *Output circuit of synchronous rectifier.*

it becomes necessary to eliminate the a-c output of the synchronous detector. The foregoing analysis shows, in fact, that if the input contains, for example, the frequency $F+\Delta F$, slightly higher than the synchronous frequency, the output will contain all the frequencies $F+\Delta F\pm NF$ and $-f-\Delta F\pm NF$, and in particular, the frequency ΔF, which, being low, cannot be eliminated without a network which will also delay amplitude changes in the synchronous signal.

In order to study this situation quantitatively, let us assume that the input frequency is capable of varying within a range and let us ask what time constant will be required, if we use a synchronous rectifier in conjunction with a resistance-capacitance (R-C) network, to achieve the same degree of selectivity as would be obtained with an ordinary rectifier preceded by a band-pass filter or the equivalent of selectivity Q_0. What we are looking for specifically is a correlation between τ, the time constant of the R-C network, and Q_0, the selectivity [4] of the equivalent band-pass filter. Suppose the input signal, of amplitude V_i, changes from the frequency F to $F+\Delta F$. Assume, on the one hand, a band-pass filter such that this frequency deviation is accompanied by a reduction in half of the input energy. This filter will have selectivity of value:

$$Q_0 = \frac{F}{2\Delta F}. \tag{32}$$

On the other hand, consider the synchronous rectifier. Before the shift this produced a d-c output of amplitude:

$$V_0 = \frac{2V_i}{\pi}. \tag{33}$$

After the shift there will no longer be a d-c component, but there will be a component of frequency ΔF (the harmonic of family (b), fig. 2, for $N=-1$). This will have amplitude:

$$V_0 = \frac{2V_i}{2\pi}. \tag{34}$$

Now suppose the synchronous rectifier is connected to the circuit of figure 4. The change in peak voltage across the condenser due to the frequency shift will be due entirely to the discriminating action of the R-C circuit, because aside from this the d-c and a-c peak values, as given by eq. 34 and 35, are the same.

[4] Selgin, Electrical transmission in steady state, pp. 180 and 295 (McGraw-Hill Book Co., Inc. New York, N. Y., 1946).

The peak voltage will therefore change in the ratio:

$$r=\frac{1}{\sqrt{1+4\pi^2\Delta f^2\tau^2}}, \tag{35}$$

where τ is the time constant of the R-C circuit. We are assuming that the condenser is not shunted by an appreciable load.

If we require the synchronous rectifier, with its R-C circuit, to be as selective as the band-pass filter previously considered, the above ratio must be equal to $1/\sqrt{2}$, resulting in the equation:

$$4\pi^2\Delta f^2\tau^2=1 \tag{36}$$

which, combined with (33), gives

$$Q_0=\pi F\tau \tag{36}$$

or, expressing the period T of the synchronous frequency:

$$Q_0=\pi\frac{\tau}{T}. \tag{37}$$

We therefore achieve, with the synchronous rectifier, an equivalent Q_0 equal to the ratio between the time constant and the period, multiplied by π. This result may serve to correlate selectivity with what we might call the "damping" of the synchronous rectifier: if instead of changing frequency we were to suddenly drop the amplitude of the input, the capacitor voltage (fig. 4) would fall exponentially, and the decrement (neglecting the source impedance of the input circuit which we assume to be small) would be

$$\delta=\frac{1}{\tau}=\frac{\pi}{Q_0T}. \tag{38}$$

It is significant to compare with this the decrement associated with the build-up or decay of energy within the resonant circuit of selectivity Q_0 which, coupled to a nonsynchronous rectifier, was considered as an equivalent device. This second value of decrement may be derived from the equation

$$Q_0=\frac{1}{2}\frac{\omega_0}{\alpha_0},$$

which relates selectivity to the real and imaginary parts of the oscillation constant (decrement and angular frequency of the free oscillation). (See footnote 4). The decrement α_0 is therefore given, identically, by

$$\alpha_0=\frac{\pi}{Q_0T}.$$

What this means in practice is that the length of time required before the system reaches a new equilibrium after a change in input amplitude is the same whether we use a synchronous rectifier with R-C network filtering or a nonsynchronous rectifier with a selective band-pass filter.

The gain in selectivity made possible by the use of synchronous rectifiers is largely due to the fact that very selective stable filters are difficult to realize, particularly at very low frequencies.

WASHINGTON, September 20, 1950